NASA CONTRACTOR REPORT

NASA CR-2029

IMPROVED GUIDANCE HARDWARE STUDY FOR THE SCOUT LAUNCH VEHICLE

by Roger T. Schappell, Michael L. Salis, Ray Mueller, Lloyd E. Best, Albert J. Bradt, Robert Harrison, and John H. Burrell

Prepared by
MARTIN MARIETTA CORPORATION
Denver, Colo. 80201
for Langley Research Center

NATIONAL AERONAUTICS AND SPACE ADMINISTRATION • WASHINGTON, D. C. • JUNE 1972

1. Report No. NASA CR-2029	2. Government Accession No.	3. Recipient's Catalog No.
4. Title and Subtitle IMPROVED GUIDANCE HARDWARE STUDY FOR THE SCOUT LAUNCH VEHICLE		5. Report Date June 1972
		6. Performing Organization Code
7. Author(s) Roger T. Schappell, Michael L. Salis, Ray Mueller, Lloyd E. Best, Dr. Albert J. Bradt, Robert Harrison, and John H. Burrell		8. Performing Organization Report No. MCR-71-158
9. Performing Organization Name and Address Martin Marietta Corporation Denver, Colo.		10. Work Unit No.
		11. Contract or Grant No. NAS1-10504
12. Sponsoring Agency Name and Address National Aeronautics and Space Administration Washington, D.C. 20546		13. Type of Report and Period Covered Contractor Report
		14. Sponsoring Agency Code
15. Supplementary Notes		

16. Abstract

A market survey and evaluation of inertial guidance systems (Inertial Measurement Units and Digital Computers) were made. Comparisons were made to determine the candidate systems for use in the Scout Launch Vehicle. Error analysis were made using typical Scout trajectories. A Reaction Control System was sized for the fourth stage. The guidance hardware to Scout vehicle interface was listed.

17. Key Words (Suggested by Author(s)) Guidance Hardware Survey Computer Sizing Reaction Control System Sizing Trajectory Error Analysis	18. Distribution Statement Unclassified - Unlimited

19. Security Classif. (of this report) Unclassified	20. Security Classif. (of this page) Unclassified	21. No. of Pages 245	22. Price* $3.00

*For sale by the National Technical Information Service, Springfield, Virginia 22151

FOREWORD

This report presents the results of nine-month *Improved Guidance Hardware Study for the Scout Launch Vehicle.* It includes a survey of inertial measurement units and computers, closed-loop trajectory error analysis results, open-loop perturbation analysis results, lunar mission analysis results, and a preliminary sizing of a fourth-stage reaction control system and an orbital correction system for the Scout launch vehicle. As a result of this effort, a reference guidance system configuration was selected and detailed for further analysis.

CONTENTS

Figure

Table

IMPROVED GUIDANCE HARDWARE STUDY FOR THE SCOUT LAUNCH VEHICLE

By Roger T. Schappell, Michael L. Salis, Ray Mueller,
Lloyd E. Best, Dr. Albert J. Bradt, Robert Harrison,
and John H. Burrell
Martin Marietta Corporation

SUMMARY

This report documents the results of the *Improved Guidance Hardware Study for the Scout Launch Vehicle*, Contract NAS1-10504.

The Scout launch vehicle requirements, constraints, and goals are summarized. They are based on the Scout D configuration, which consists of the Algol III first stage, Castor II second stage, Antares II third stage without the existing guidance hardware, and the fourth stage consisting of the FW-4S motor, the improved guidance system, the reaction control system (RCS), and the required telemetry system and batteries.

Ninety-eight gimbaled and strapdown guidance systems were investigated for possible application to the Scout vehicle. This included inertial platforms and attitude reference units. Also the nine proposed Viking ARUs, IMUs, and VRUs were considered and are summarized. As a result of this evaluation, 8 systems were selected for further evaluation and are summarized in matrix format and individually. (See section entitled *Guidance Hardware Survey and Candidate Selection*.) As a function of performance, cost, risk, and weight, three systems were selected for further evaluation and their relative merits are discussed. They consist of the strapdown DIGS, the gimbaled KT-70 missile system, and the LN-30 navigation system. Due to the emphasis on cost and weight savings, the KT-70 missile system was selected as the reference guidance platform for the improved Scout configuration.

Of 100 computers surveyed, 35 were selected for further evaluation. A computer sizing effort was then initiated for controlling the reference closed-loop guidance and control configuration. As a result of this sizing effort, several computers were selected as candidates for integration with the reference guidance platforms. It should be noted that since the guidance and control logic has not been designed, the computer sizing results represent worst case requirements, but do not constitute the final computer requirements.

The fourth-stage reaction control system has been sized for three types of fuel -- hydrazine, hydrogen peroxide, and nitrogen. The torque disturbances were calculated and the thrust levels were established for a bilevel system resulting in a 26-pound hydrazine reaction control system, a 27-pound hydrogen peroxide system, or a 42-pound nitrogen system. Through subsequent weight tradeoffs, a 20-pound hydrogen peroxide bilevel system was ultimately selected. An orbital correction system requiring 4.3 extra pounds was also sized using the RCS jets to add or subtract velocity after fourth-stage burn. This sizing was based on providing a 1σ post-boost velocity vernier capability of 53 fps for a 322-pound fourth stage. The total RCS weight required for attitude stabilization and postboost velocity correction is therefore 24.3 pounds.

Four Martin Marietta simulation programs were used for error analysis studies:

1) The trajectory error analysis program (TEAP) was checked out for both gimbaled and strapdown systems, and was modified to accept the NASA-furnished Scout trajectory data. Both gimbaled and strapdown inertial systems as well as attitude reference systems have been flown for hardware performance evaluation. The selected hardware resulted in 1σ dispersions on the order of 16 fps and 4500-foot position uncertainties. These errors are due to guidance hardware only;

2) The simulated trajectory error analysis program (STEAP) was used to target five lunar trajectories and to calculate the ΔV maneuvers for midcourse and lunar orbit insertion. The results indicate that, based on the assumptions in the section entitled *Lunar Mission Analysis*, the Scout vehicle is potentially capable of placing 80% of its payload weight after translunar injection into lunar orbit;

3) The UD213 trajectory simulation program, a point mass, 3-degree-of-freedom program, was used to run perturbation analysis for the open-loop attitude-stabilized Scout vehicle. The results of this simulation indicate that the spin-stabilized fourth-stage tipoff errors are the primary source of mission error for open-loop guidance. By using a 3-axis rate package mounted on a nonspinning fourth stage, the errors will be reduced by a factor greater than 2;

4) An isoprobability contouring program written for this study was implemented on the 1130 computer with a Cal Comp plotter. These isoprobability contours show the distribution of possible combinations of apogee/perigee deviations consistent with a specified probability value. Confidence regions were thus contoured for each candidate guidance system for the present Scout configuration, for the gyro-attitude-stabilized fourth-stage configuration, and for the closed-loop guidance configuration. When superimposed, as shown in figure 1, it is apparent that the closed-loop guidance configuration is optimum from the performance point of view.

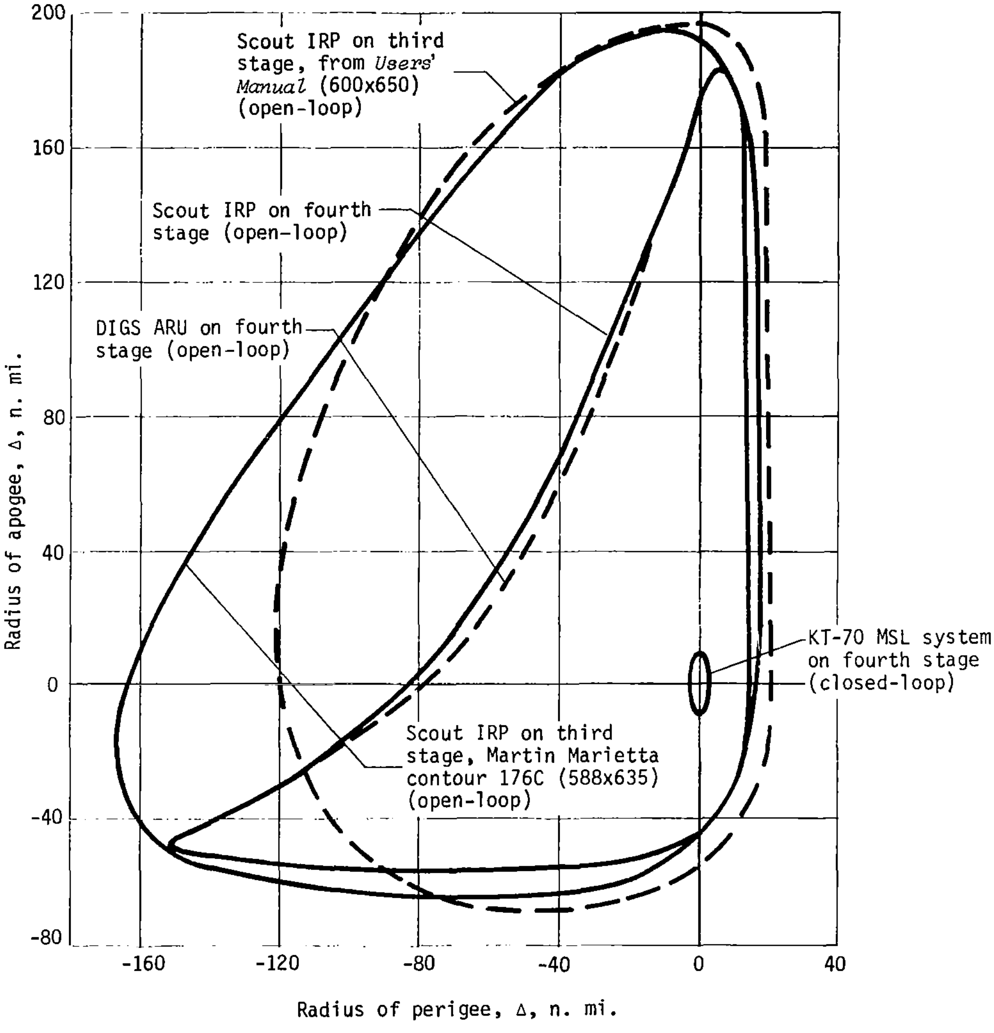

FIGURE 1.- ISOPROBABILITY CONTOURS

Based on the results of this study, Martin Marietta recommends that:

1) State-of-the-art guidance and control technology be applied to the Scout launch vehicle. This would result in a significant improvement in performance and mission flexibility. Available miniature guidance hardware can be adapted to the Scout vehicle as shown in this report;

2) A form of closed-loop guidance be implemented in the fourth stage, along with a hot gas attitude control system with a postboost velocity correction capability;

3) Several other areas be studied prior to hardware implementation,

   a) Investigating future mission requirements for the next 10 years,

   b) Selecting a guidance and control logic for Scout,

   c) Investigating redundancy and reliability requirements,

   d) Investigating the relative merits of a digital autopilot for Scout,

   e) Conducting a detailed computer timing and sizing study,

   f) Investigating ground support electronics requirements,

   g) Preparing an IMU and computer RFQ,

   h) Ultimately performing a guidance hardware laboratory evaluation.

An approach for achieving improved guidance for Scout is summarized in the *Guidance Integration Program Summary* section. Although guidance logic selection was beyond the scope of this study, the considerations and tradeoffs are discussed in the *Guidance Software* section of this report.

INTRODUCTION

The primary objective of this study was to investigate the use of improved guidance and control hardware in the Scout launch vehicle that would provide improved performance and future growth. This was accomplished through hardware surveys, computer simulation, and numerous technical discussions with NASA, LTV-MSD, and the inertial components manufacturers.

This report contains the results of a multitude of surveys, sizing, and analysis tasks performed in the evaluation of improved guidance for the Scout launch vehicle. To aid in gaining a better understanding of the report content and to place the various tasks in perspective, a summary of the sequential sections follows.

The *Summary* section summarizes the results of the individual tasks and includes the study recommendations.

As a point of reference, this *Introduction* describes the current Scout launch vehicle and its open-loop guidance system. This is followed by a summary of the study approach and ultimate goals.

The *Scout Launch Vehicle Characteristics and Constraints* section establishes the vehicle physical and environmental characteristics and guidance system constraints as provided by NASA and based on the current Scout vehicle.

The next section, *Guidance Hardware Survey and Candidate Selection* summarizes the candidate guidance hardware considered in this study. The physical and performance characteristics are tabulated and the selection rationale is presented.

The *Computer Sizing Survey and Selection* section provides the data and rationale for establishing the computer requirements. The results of a market survey are given and a candidate selection is presented based on the established requirements.

The *Instrumentation System* section summarizes the preliminary characteristics of a new PCM instrumentation system for Scout.

Since the present Scout vehicle employs spin stabilization for the fourth stage, a new control system is required. The next two sections, *Reaction Control System Sizing* and *Orbital Correction System*, consist of sizing analysis of a control system for fourth-stage attitude control and for postboost orbital correction capability.

The three analysis sections present error analysis results for (1) a closed-loop evaluation of the candidate guidance system errors, (2) mission errors associated with an open-loop guidance approach (present Scout as well as an improved version featuring an attitutde reference package on a nonspinning fourth stage), and (3) analytical results of a deep-space error analysis describing the lunar mission capabilities of an improved Scout vehicle in terns of the trajectories involved, targeting that can be achieved, and additional fuel required.

These sections consist of the *Closed-Loop Error Analysis, Open-Loop Error Analysis,* and *Lunar Mission Analysis.*

The next section summarizes the *Recommended Guidance and Control System.* Although guidance logic design was beyond the scope of this study, the *Guidance Software* section discusses guidance logic considerations and tradeoffs to be considered in subsequent studies. This section includes a discussion of system requirements, the guidance concepts and logic that require analysis, and a summary of present closed-loop guidance techniques.

Having selected a reference configuration, the system modifications, along with a preliminary interfacing definition, are outlined in the *Guidance Hardware/Scout Vehicle Interfacing* section.

The next two sections include a definitive *Guidance Integration Program Summary* that consists of an overall plan for arriving at improved guidance for Scout. This is followed by the study *Recommendations* section.

The first four appendixes include a detailed description of the computer simulation programs used in the performance of this study. Appendix E presents a cross-section survey of guidance equations for various launch vehicles. Appendix F discusses a centralized executive system as a future consideration.

Scout Launch Vehicle

The Scout launch vehicle was developed by the National Aeronautics and Space Administration to provide an efficient means of boosting a payload into space on a planned trajectory. Scout became operational in July 1960 and has been used for launching a variety of payloads, including orbital, probe, and reentry missions that encompassed inclined, equatorial, and polar orbits. It is a four- or five-stage solid-propellant booster system, 72 feet long with a launch weight of 46,000 pounds and a liftoff thrust of 141,900 pounds. The fifth stage, though not considered in this study, is used for highly elliptical and solar orbit missions. The reference vehicle used in this study is the Scout D (Algol III/Castor IIA/Antares II/Alair III) with a 34-inch-diameter heat shield and enlarged jet valves and fin tips. The Scout configurations are summarized in Table 1, with configurations B, C, D, and E in current use. The Scout vehicle is equipped with a preprogrammed open-loop guidance system where each expended stage separates on a timed sequence. The fourth stage is spin-stabilized with no provisions for thrust termination or vernier control. This is a limiting factor in terms of performance and flexibility. A two-piece heat shield is used to protect the payload from high temperatures during ascent and is ejected just before third-stage ignition.

Launch facilities for Scout are presently available at Wallops Island, Virginia; Vandenberg Air Force Base, California; and Formosa Bay, Africa. The latter launch site is located on platforms in the Indian Ocean about three miles off the coast of Kenya, Africa. Wallops Station is used primarily for easterly launches, the Vandenberg AFB for polar and high-inclination orbital launches, and the San Marco equatorial range for low-inclination orbital launches. The launch site coordinates used in this study are:

1) Wallops Island, Virginia - 37.8479° North latitude, 75.4739° West longitude;

2) Vandenberg Air Force Base, California - 34,6081° North latitude, 120.6233° West longitude;

3) San Marco Tower (off-shore, Kenya) - 2.2057° South latitude, 40.2128° East longitude.

TABLE 1.- DESIGNATION OF SCOUT CONFIGURATIONS*

CONFIGURATION	FIRST-STAGE	SECOND-STAGE	THIRD-STAGE	FOURTH-STAGE	FIFTH-STAGE
X	Algol I	Dummy	Antares I	None	None
X-1	Algol I	Castor I	Antares I	Altair I	None
X-1A	Algol I	Castor I	Antares I	Altair I	NOTS-17
X-2	Algol I	Castor I	Antares II	Altair I	None
X-2B	Algol I	Castor I	Antares II	Altair II	None
X-2M	Algol I	Castor I	Antares II	M-2	None
X-3	Algol II	Castor I	Antares II	Altair I	None
X-3A	Algol II	Castor I	Antares II	Altair I	NOTS-17
X-3C X-3A	Algol II	Castor I	Antares II	None	None
X-3M	Algol II	Castor I	Antares II	M-2	None
X-4	Algol II	Castor I	Antares II	Altair II	None
X-4A	Algol II	Castor I	Antares II	Altair II	NOTS-17
A	Algol II	Castor II	Antares II	Altair II	None
B	Algol II	Castor II	Antares II	Altair III	None
C	Algol II	Castor II	Antares II	Altair III	BE-3
D	Algol III	Castor II	Antares II	Altair III	None
E	Algol III	Castor II	Antares II	Altair III	BE-3

*OTHER REFERENCE DESIGNATIONS:

Algol I - Aerojet Senior, 33KS-120,000
Algol II - 45KS-100,000

Castor I - XM33E5, XM-75, 27KS-55,000
Castor II - TX354

Antares I - X254, XM-70, 38DS-14,000
Antares II - X259, 33DS-21,540

Altair I - X248, XM-69, 40DS-3100
Altair II - X258, XM-94, 24DS-5850
Altair III - FW4S, XSR-57-UT

NOTS-17, XM-78, NOTS100-17, 43K-882

BE-3, 9.15-DS-5770

Current Guidance and Control System

Since this study is concerned with improved guidance hardware for the Scout vehicle, the current guidance and control concept is briefly described.

The Scout launch vehicle has been flying a trajectory defined by a preprogrammed time/attitude profile. Since the guidance system is in effect an attitude control system, the time/attitude profile is achieved by torquing the appropriate rate integrating gyros in discrete steps. The gyros are operated in a rate feedback loop and function as an attitude reference system. They respond to vehicle rates and are also torqued in response to signals from the programmer. The guidance hardware is located in the third stage as shown in figure 2 and consists of a noncomputational three-gyro strapped-down attitude reference unit (IRP), a rate gyro package for sensing vehicle rates, a relay unit for power and ignition switching, an intervalometer to provide precise scheduling of events during flight, a programmer to provide voltages for torquing the pitch and yaw gyros for changing vehicle orientation in flight, and the associated inverter and battery power supplies. An electronic switching unit (PVE) is included for controlling the valves of the reaction jet system according to the error signals received from the attitude reference unit.

A proportional control system consisting of jet vanes and aerodynamic control surfaces is used to control the vehicle during the first-stage burn. The jet vanes provide the major portion of the control force during the thrust pulse, whereas the aerodynamic tip controls provide all the control force during the coast phase following first-stage burnout. Second- and third-stage control forces are provided by hydrogen peroxide reaction jet motors. The fourth stage, including the payload, is spin-stabilized, with spinning being initiated approximately 6 seconds before fourth-stage ignition.

Study Approach and Goals

The guidance hardware study approach was to (1) establish the improved Scout vehicle goals, (2) determine the existing vehicle constraints, (3) conduct a survey of guidance and control system hardware and miniature airborne computers, and (4) conduct a hardware evaluation by performance analysis and computer simulation. Although guidance logic selection was beyond the scope of this study, guidance logic considerations are discussed in the section entitled *Guidance Software*. A description of the simulation programs used in this study for performance analysis can be found in Appendices A thru D.

As a guideline, the guidance and control system goals were established as discussed in the following paragraphs.

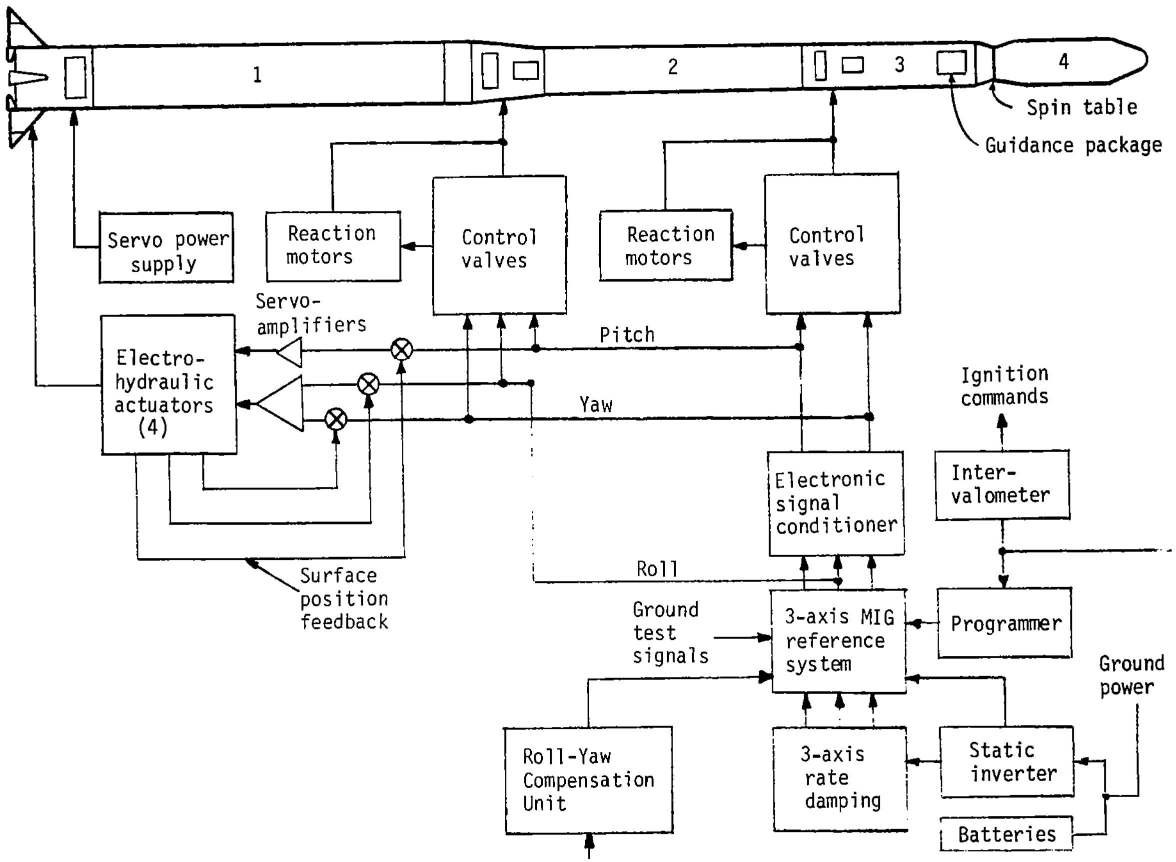

FIGURE 2.- SCOUT GUIDANCE AND CONTROL BLOCK DIAGRAM

Performance.- The present Scout launch vehicle is sufficiently accurate to perform its assigned missions. It employs a spin-stabilized fourth stage that makes final insertion accuracy a function of tipoff rates, total FW-4S impulse deviation, unbalance, and other errors characteristic of a solid-motor spin-stabilized vehicle. Typical performance deviations are shown in figure 3. However, to provide for future mission requirements and greater flexibility, a performance capability in line with current technology is desirable as well as achievable, as shown in figure 1. Therefore the following performance goals were established:

1) Velocity - 12 fps, 1 σ all axes;

2) Position - 10 000 ft, 1 σ all axes;

3) Attitude - <0.5 deg, 1 σ all axes at end of coast.

It must be remembered that these accuracy numbers are goals and did not negate the evaluation of lower performance guidance hardware. An order of magnitude improvement in Scout performance is desirable to provide for improved mission capability, added payload life, and a higher probability of mission success. Expanded mission capability can be achieved by lowering velocity and position uncertainties, by providing an attitude-stabilized fourth stage and payload, by providing a vernier control for correcting velocity errors after insertion, and by being able to orient and point the payload after cutoff. Error analysis results have shown these goals to be achievable.

Rate capability.- The maximum rate capability is:

1) Pitch and yaw - 10 deg/s;

2) Roll - 30 deg/s.

Checkout and stabilization time.- Although warmup time is not a critical parameter, most candidate guidance systems will be stabilized within 20 to 60 minutes after turn-on from ambient. Ready time, which includes warmup, alignment, and checkout, may require as much as 60 to 90 minutes.

Calibration frequency.- Although a calibration cycle of 90 days is a desired goal, the potential for cost reduction and/or accuracy improvement with automatic onpad prelaunch calibration can be significant.

Weight.- Since the improved guidance and reaction control systems will be located in the fourth stage, weight must be minimized to maximize the payload capability. The entire guidance and control system weight goal is 75 pounds.

Volume.- The available volume for the guidance system, telemetry system, and batteries is as shown in the E-section in figure 4. However, instead of a conical E-section, it will be cylindrical with an 18-inch diameter and a length of 9 to 12 inches. A layout of the fourth stage with the improved guidance and control hardware can be found in the section entitled *Guidance Hardware/Scout Vehicle Interfacing*.

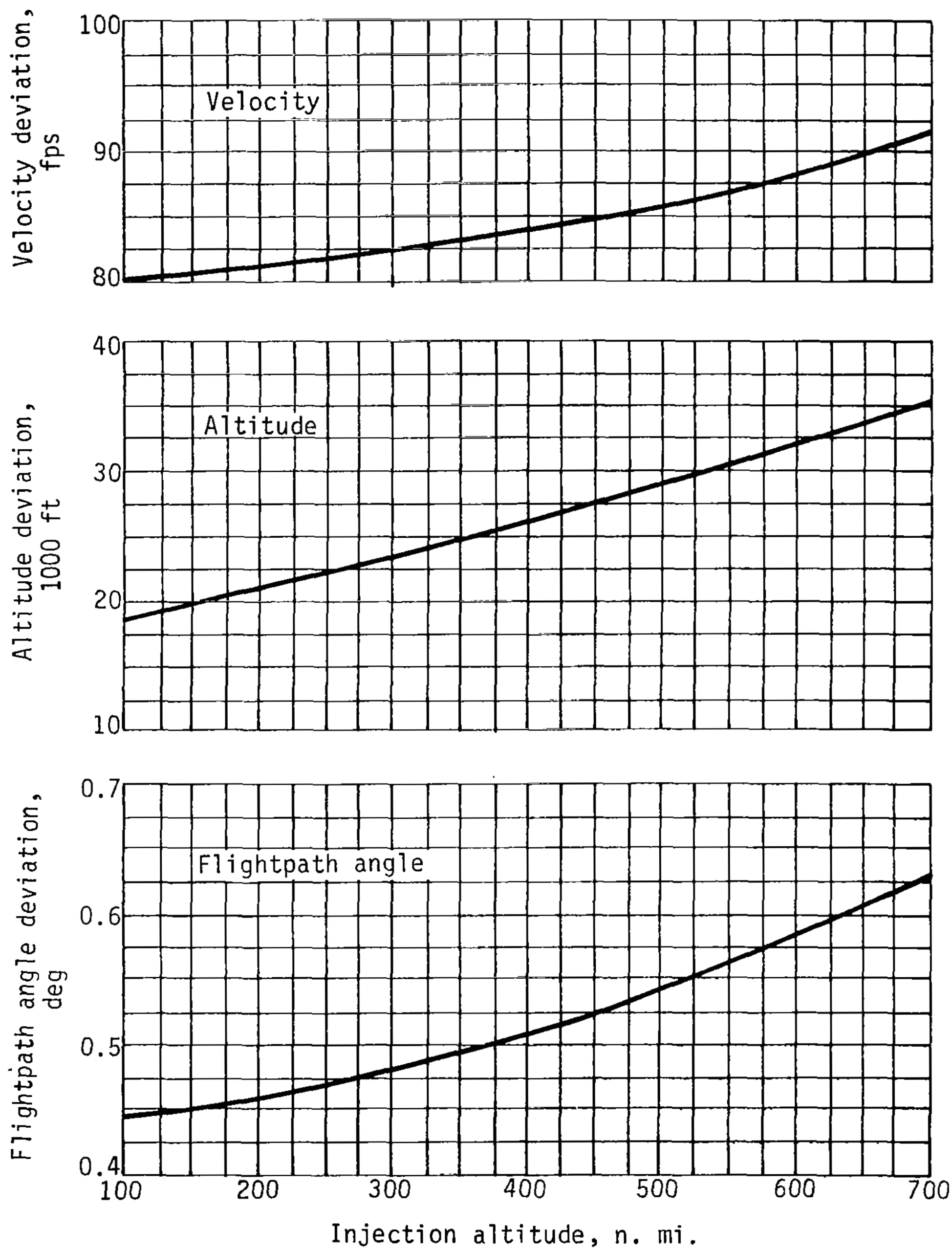

FIGURE 3.- STANDARD DEVIATION IN INJECTION CONDITIONS

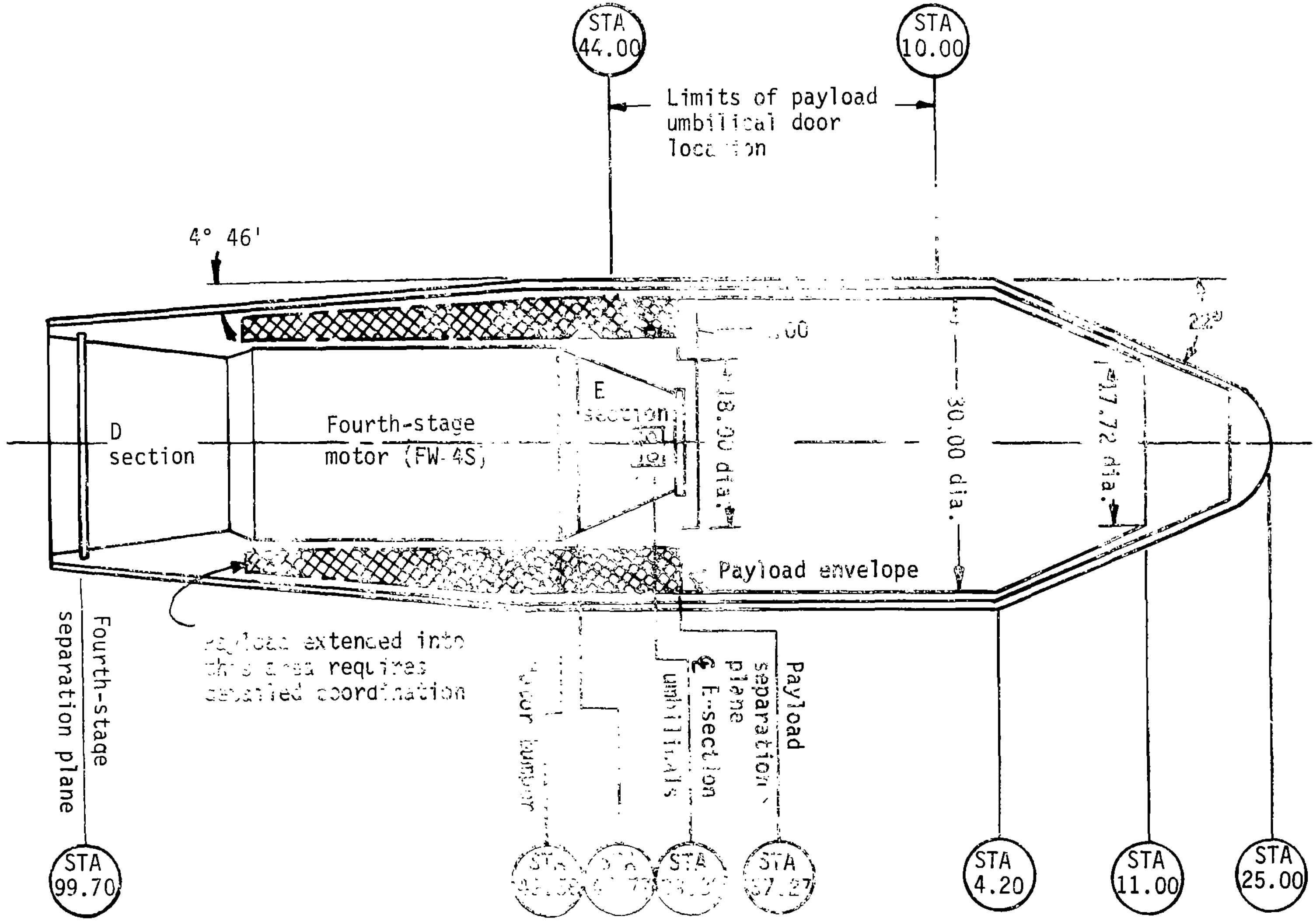

FIGURE 4.- SCOUT FOURTH-STAGE ENVELOPE

SCOUT LAUNCH VEHICLE CHARACTERISTICS AND CONSTRAINTS

Since the Scout launch vehicle has been flying for over a decade, its performance and physical characteristics for the current configuration are well defined. However, upon removing the current guidance and control system hardware from the third stage and the spin stabilization hardware from the third and fourth stages, and then installing the improved guidance and control system hardware in the fourth stage, a number of parameters must be redefined and estimated. Typically, a temperature profile is required for the fourth stage guidance system compartment, a new vehicle weight breakdown will result providing different fourth stage inertias, prelaunch vehicle environmental characteristics must be determined, and boost environmental requirements must be defined. Several of these pertinent vehicle characteristics and constraints are summarized in this section. These data were used in establishing a reference for hardware evaluation and budgetary pricing for the improved fourth stage guidance configuration.

Reference Trajectories

The following trajectories provided by NASA were used in Martin Marietta's trajectory error analysis programs for guidance system performance comparison and vehicle accuracy prediction:

1) Circular orbit 176C,
    a) Apogee = 630 n. mi.,
    b) Perigee = 580 n. mi.,
    c) Inclination = 89.9 deg;
2) Elliptical orbit 169C,
    a) Apogee = 1742.98 n. mi.,
    b) Perigee = 211.1 n. mi.,
    c) Inclination = 102.67 deg;
3) Injection conditions for direct lunar injection trajectory from San Marco,
    a) Velocity = 35,880 fps,
    b) Position = 21,535,198 ft,
    c) Eccentricity = 0.9695.

Performance

Typical performance curves for the Scout D configuration with a 34-inch-diameter heat shield are shown in figure 5. These curves illustrate payload weight capability for circular orbits.

The current Scout orbital injection deviations in altitude, velocity, and flightpath angle at fourth-stage burnout are shown in figure 3 as a function of injection altitude. These deviations can be either plus or minus and thus define the deviation on each side of the nominal values. One standard deviation in azimuth at injection is + or -0.625 degrees and is independent of injection altitude.

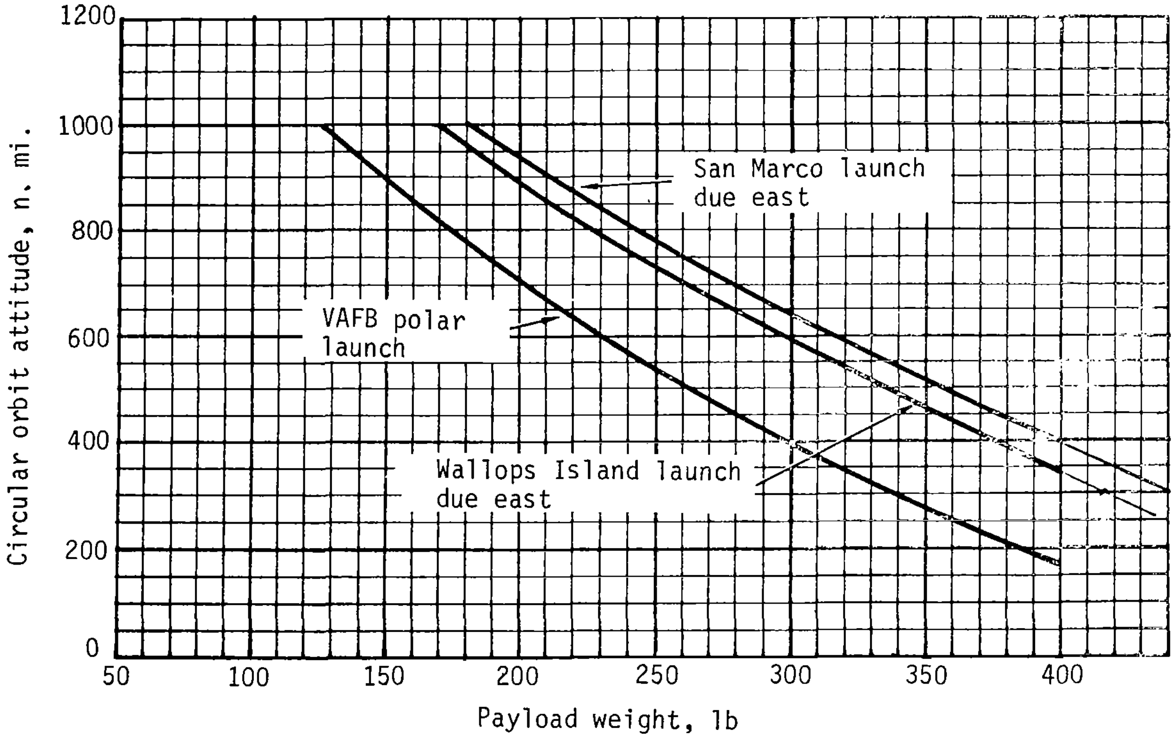

Note: These curves only valid for 34-inch-diameter heat shields. 42-inch-diameter heat shield reduces payload weight capability 25 lb for a 400 n. mi. circular orbit.

FIGURE 5.- PAYLOAD WEIGHT CAPABILITY, SCOUT D

Cooling and Thermal Control

Prelaunch environmental control is provided by purging the fourth stage payload and guidance compartment (Section E, figure 4) with cooled, or heated, oil-free air that has been filtered and dried by the launcher environmental system. This system can supply air with a maximum humidity of 20 percent. The heating and cooling capability of the environmental system, based on a standard temperature of 70°F and pressure of 14.7 psia, is defined by the shaded areas of figure 6. These conditions apply to the air as it is supplied to the heat shield.

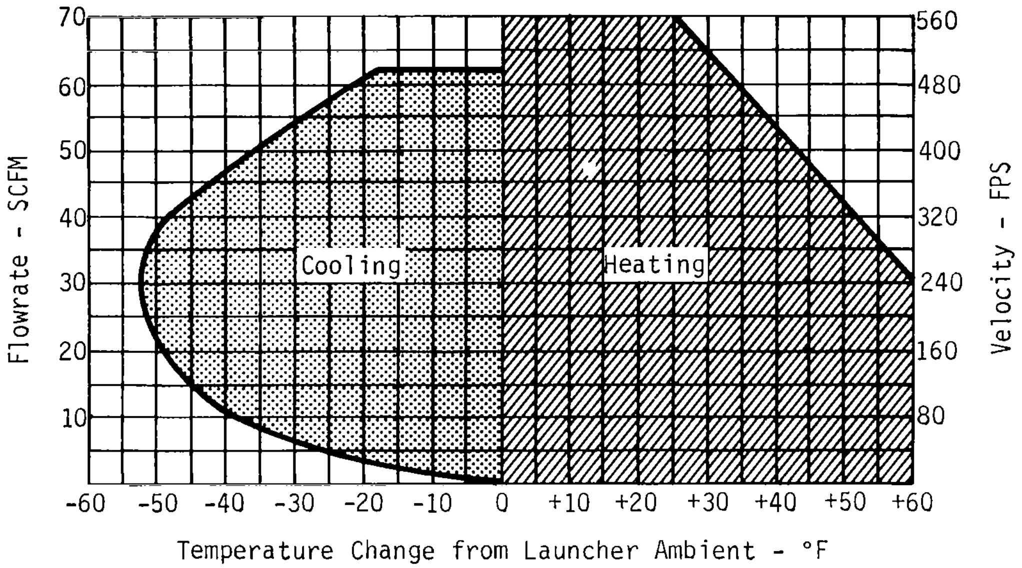

FIGURE 6.- LAUNCHER AIR-COOLING AND HEATING

Preflight Heater Power

Since guidance system warmup will occur on the launch pad, external power from the AGE power supplies will be used during this prelaunch period.

Storage Life

A storage life of five years is required.

Cooling and Thermal Control

Prelaunch environmental control is provided by purging the fourth stage payload and guidance compartment (Section E, figure 4) with cooled, or heated, oil-free air that has been filtered and dried by the launcher environmental system. This system can supply air with a maximum humidity of 20 percent. The heating and cooling capability of the environmental system, based on a standard temperature of 70°F and pressure of 14.7 psia, is defined by the shaded areas of figure 6. These conditions apply to the air as it is supplied to the heat shield.

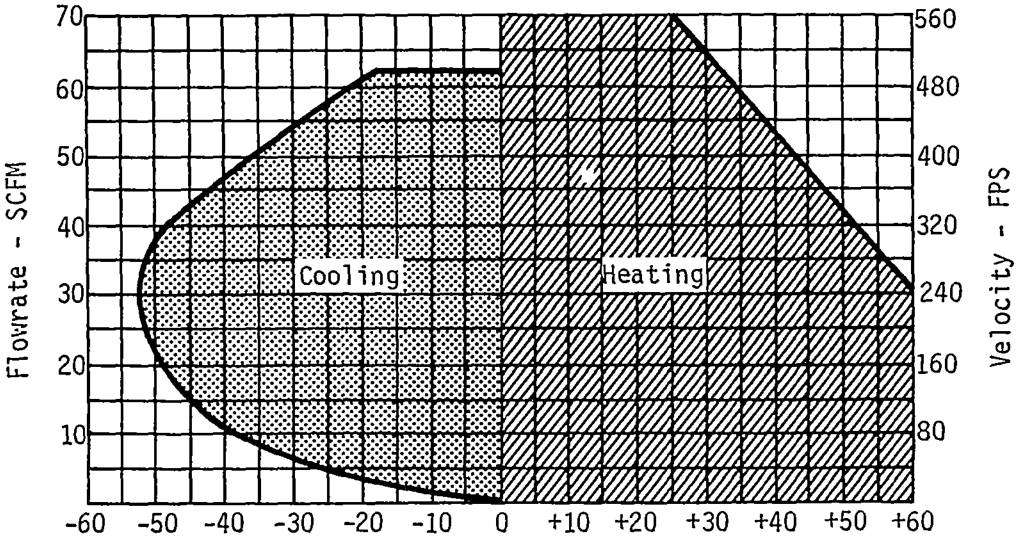

FIGURE 6.- LAUNCHER AIR-COOLING AND HEATING

Preflight Heater Power

Since guidance system warmup will occur on the launch pad, external power from the AGE power supplies will be used during this prelaunch period.

Storage Life

A storage life of five years is required.

Environmental

The following environmental requirements represent the minimum test levels for a system in a vehicle transition section and do not necessarily represent the improved guidance hardware qualification levels.

Pressure characteriatics.- The pressure within the payload heat shield and therefore the guidance compartment is as shown in figure 7.

Longitudinal accelerations.- The Scout acceleration profile for the fourth-stage is shown in figure 8. Only the fourth-stage profile is shown since it is the most severe. These data are based on a payload of approximately 45 pounds and represent the maximum acceleration experienced throughout the flight. Figu... shows the effects of various payload weights.

Shock.- The shock requirement for the payload which is located directly above the guidance compartment, is three half-sine pulses of 30 g peak amplitude and 7 to 13 milliseconds total duration. This represents the input to the supporting structure where the guidance hardware will be located.

Vibration.- The required vibration test levels are shown in figures 10, 11, and 12. These are system operating test levels and apply at the interface of the forward shoulder of the fourth-stage motor, which is where the guidance hardware will be located. The sinusoidal vibration tests and the required levels are as follows:

1) Qualification test - Apply one sweep in each of three axes at a logarithmic sweep rate not greater than 2 octaves per minute;

2) Flight acceptance test - Apply one sweep in each of three axes at a logarithmic sweep rate not greater than 4 octaves per minute.

The random vibration test and the required levels are as follows:

1) Qualification test - Apply gaussian random in each of three axes for 2 minutes;

2) Flight acceptance test - Apply gaussian random in each of three axes for one minute.

Temperature environment.- The temperature environment will be based on the curves shown in figures 13, 14, and 15. These curves represent time-varying temperature extremes at the indicated points in the fourth stage. The guidance hardware will be located just forward of station 49 shown in figure 14. The typical external temperature curves of the fourth-stage motor due to motor operation are shown in figure 15, and represent FW-4S temperatures on the forward dome, motor case middle, and aft motor case from time of ignition to 700 seconds. These curves represent case radial locations where the most severe heating occurs.

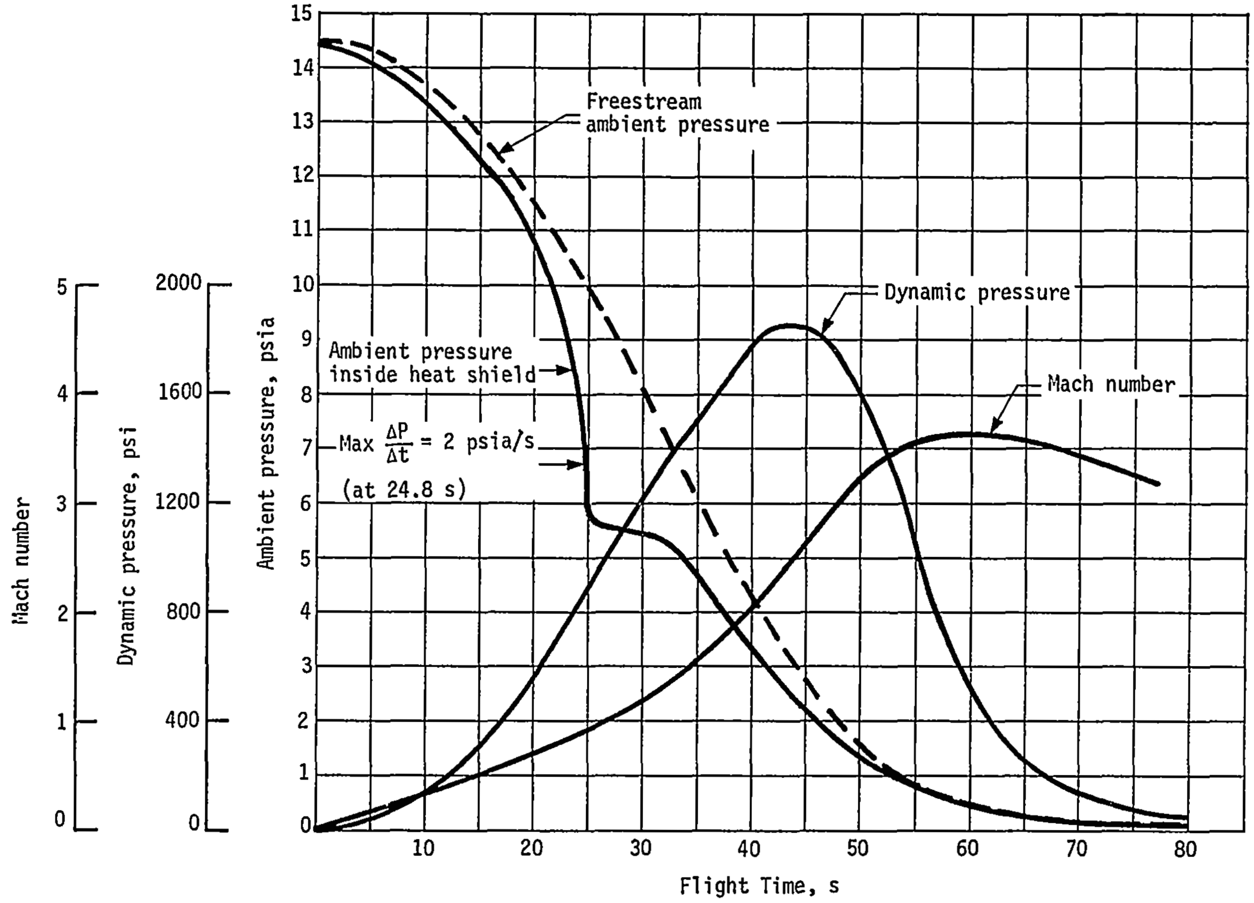

FIGURE 7.- SCOUT VEHICLE S-172C AMBIENT PRESSURE INSIDE HEAT SHIELD

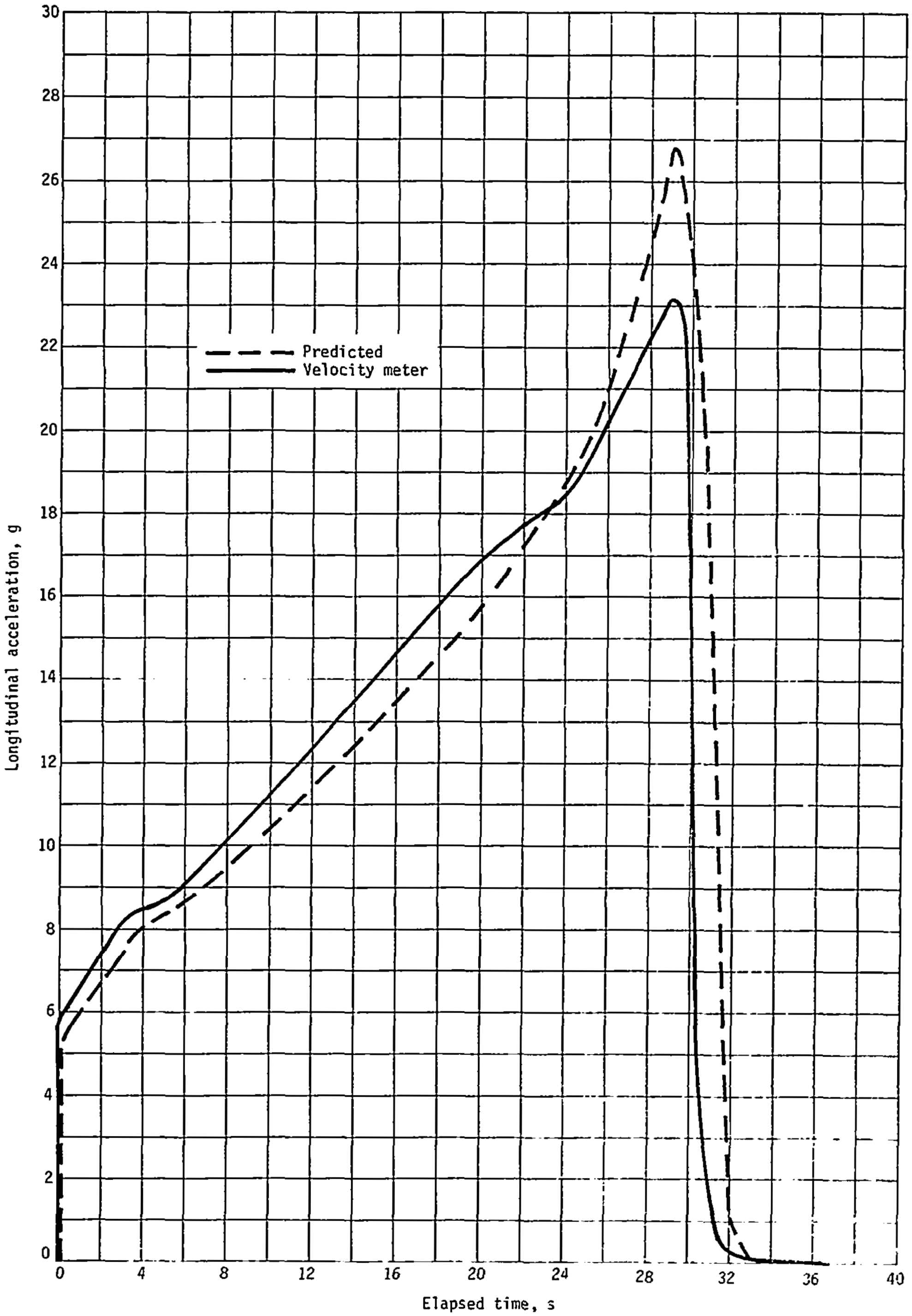

FIGURE 8.- SCOUT VEHICLE S-131 LONGITUDINAL ACCELERATION VS TIME, FOURTH STAGE

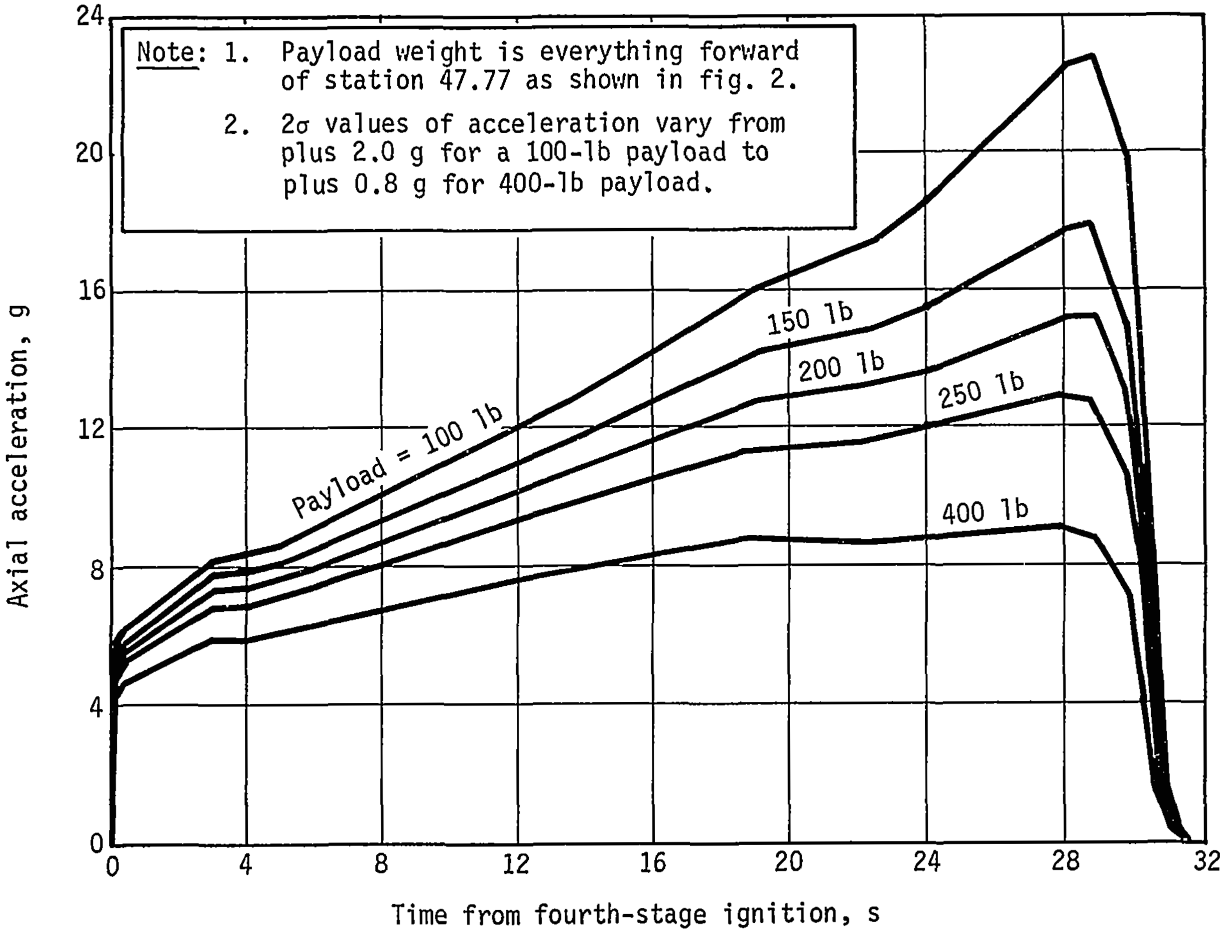

FIGURE 9.- AXIAL ACCELERATION DURING FOURTH-STAGE THRUSTING FOR VARIOUS PAYLOADS

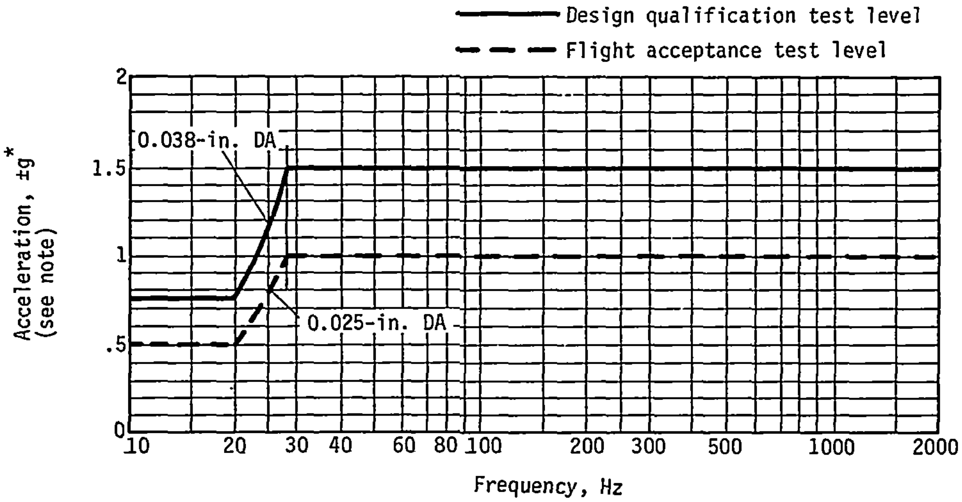

Note:	During sinusoidal vibration test in the lateral axis, the acceleration at the spacecraft center of gravity shall be limited to ±3 g from one-half the first resonant frequency of the spacecraft to one-and-one-half the frequency when vibrated in either of the lateral axes.

FIGURE 10.- SINUSOIDAL VIBRATION, LATERAL AXIS

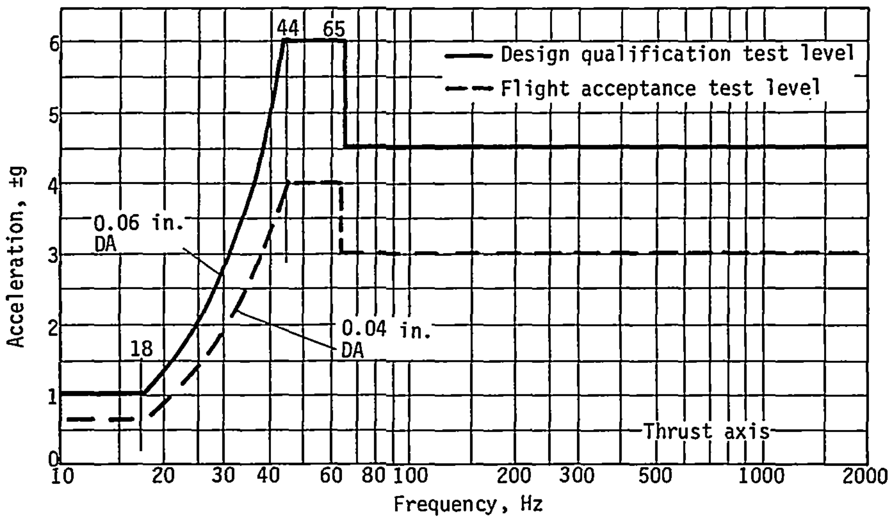

FIGURE 11.- SINUSOIDAL VIBRATION, THRUST AXIS

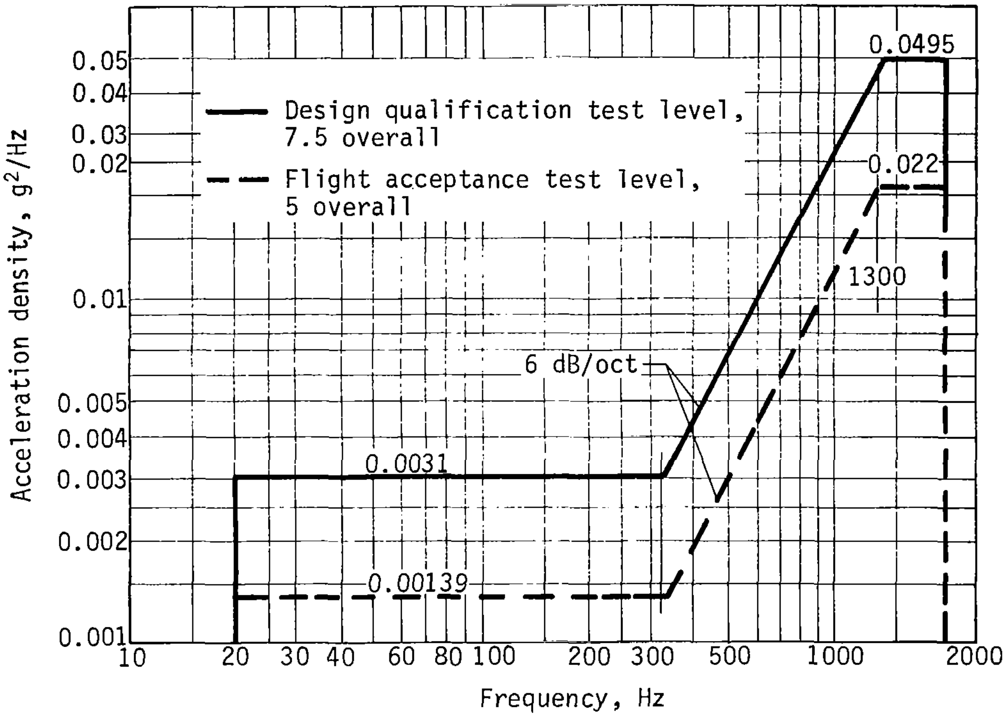

FIGURE 12.- RANDOM VIBRATION, ALL AXES

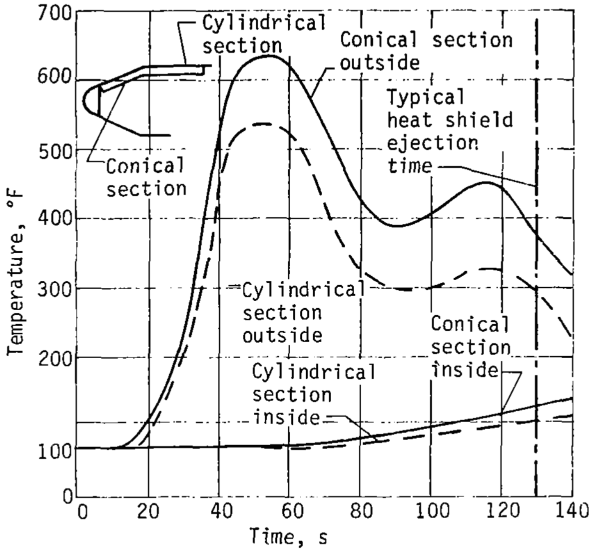

FIGURE 13.- SCOUT OUTSIDE AND INSIDE TEMPERATURES

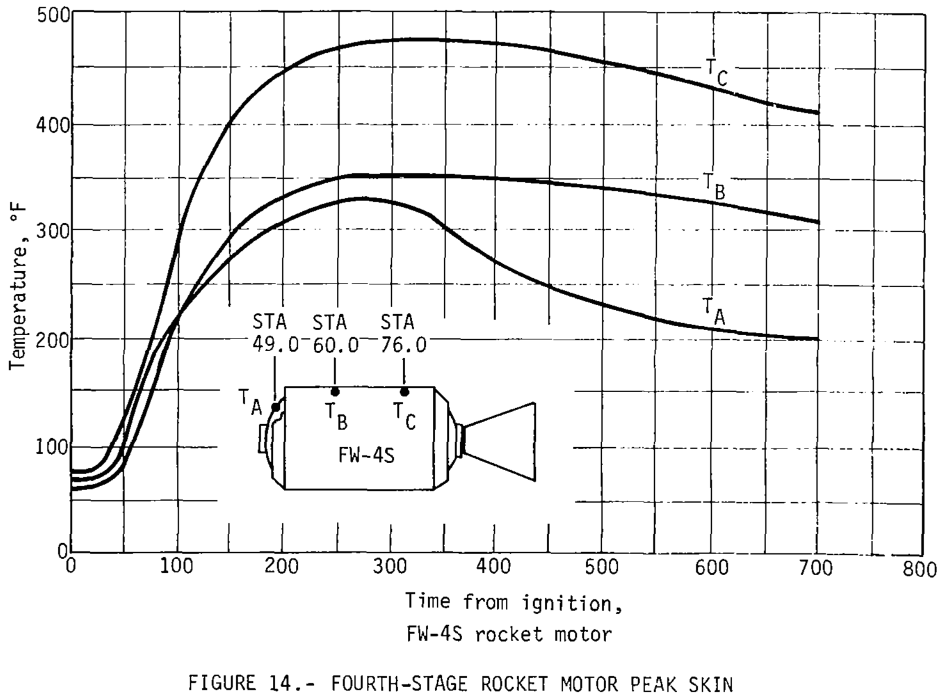

FIGURE 14.- FOURTH-STAGE ROCKET MOTOR PEAK SKIN TEMPERATURES VS TIME AFTER IGNITION

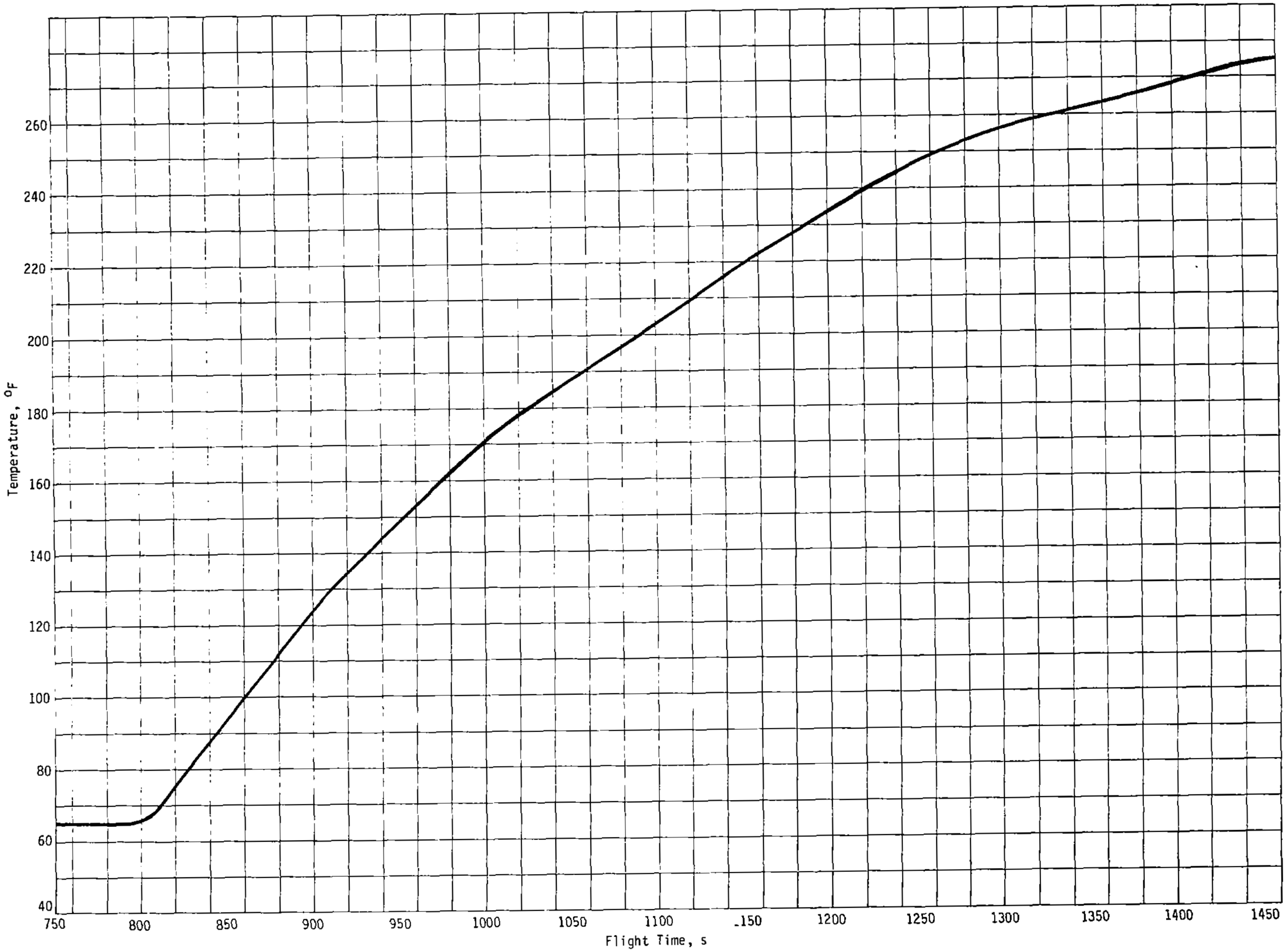

FIGURE 15.- SCOUT S-131 FW-4S MOTOR TEMPERATURE NO.2 VS FLIGHT TIME, E-SECTION

Wind Restrictions

Wind restrictions imposed on the Scout launch vehicle consist of surface winds during raising and launching the vehicle, winds at 9 000 to 12 000-foot altitudes based on control authority limitations, and winds from 27 000 to 45 000 feet based on maximum allowable bending moments. The maximum allowable levels for erection and launch are 43.5 and 35 knots respectively.

Flight Time

A nominal flight time of 760 seconds of boost and 45 minutes of coast was used in this study. Degraded performance during coast due to thermal conditions was considered and will ultimately be a function of payload requirements.

Applicable Documents

The following documents were used to establish a reference for budgetary pricing.

Specifications.-

Military:

MIL-P-116E(3) 18 August 1967	Preservation, Methods of
MIL-E-4158C(2) 9 July 1964	Electronic Equipment, Ground, General Requirements for
MIL-I-6181D 1 June 1962	Interference Control Requirements
MIL-P-7936A Chg 1 7 March 1966	Parts and Equipment, Aeronautical, Preparation for Delivery for
MIL-D-70327(2) 27 March 1962	Drawings, Engineering, and Associated Lists

Standards:

MIL-STD-129D 28 December 1964	Marking for Shipment and Storage
MIL-STD-130B C/N 1 7 February 1964	Identification Marking of U.S. Military Property
MIL-STD-143A 14 May 1963	Specification and Standards, Order of Procedure for Selection of
MS33586A 16 December 1958	Metals, Definition of Dissimilar

Publications:

NASA:

NPC 200-4 August 1964	Hand-Soldering of Electrical Connections, Quality Requirements for

GUIDANCE HARDWARE SURVEY AND SELECTION

This section summarizes the results of the inertial hardware survey and provides the rationale for selecting a reference configuration. Three categories of inertial hardware were considered and include the following:

1) Inertial measurement units (IMUs) were surveyed for use in a closed-loop guidance configuration;

2) Attitude reference units (ARU) were surveyed for use in an open-loop guidance scheme similar in concept to the present Scout guidance system with the exception that this hardware would be located in the fourth stage of Scout, along with a reaction control system as opposed to spin stabilization;

3) Developmental systems, i.e., next-generation guidance hardware is summarized for information only. It should also be noted that for completeness, the candidate Viking inertial hardware is included.

IMUs, as discussed in this report, are differentiated from ARUs by the fact that they are capable of providing velocity data as well as attitude data, whereas ARUs provide attitude data only. Also, when discussing the generic type of IMUs, platform will be used throughout to denote gimbaled systems in contrast to strapdown systems.

Approach

This effort was initiated by first preparing an IMU questionnaire with approximately 150 data requirements. This was then transmitted to the inertial hardware manufacturers for them to summarize, in a consistent format, the characteristics of their Scout-applicable candidate IMUs. The next step was to contact these manufacturers and discuss the applicability and projected modifications of their hardware for the Scout booster. As a result of this study and previous studies, a library containing data on 135 inertial systems has been established at the Martin Marietta Corporation. This is part of a guidance system, airborne computer, and inertial components data bank containing detailed data concerning all current and next-generation guidance hardware technology. The evaluation and final selection was based on the lowest estimated cost, minimum modifications and risk, minimum weight and power, and performance.

In performing this state-of-the-art survey of guidance system hardware, a number of items were considered. The following are common to all subsystems:

1) Cost;
2) Weight;
3) Power;
4) Size;
5) Cooling requirements;
6) Technical risk;
7) Reliability;
8) Growth potential;
9) Limitations;
10) Flexibility;
11) Development status;
12) Interface requirements:
13) Manufacturer's previous performance;
14) Required ground support equipment;
15) Storage requirements;
16) Shelf life;
17) Qualification history;
18) Checkout.

The criteria peculiar to inertial measuring units are:

1) Accuracy;
2) Calibration;
3) Initial alignment

All of these items are significant in choosing an IMU and were used in the tradeoff and cost analyses. Furthermore, test data from production programs and test reports from organizations such as Holloman AFB, JPL, NASA, etc, were factored into the evaluation to assess the actual IMU performance capability. Both IMU and inertial component data were reviewed.

Ground rules.- The ground rules and guidelines used in the selection of candidate guidance hardware for the Scout launch vehicle are as follows:

1) 1971 state-of-the-art hardware;
2) Established production base preferred;
3) No inertial component (gyro and accelerometer) development;
4) Minimum platform and computer modifications;
5) Flight operating time - 760 seconds during boost and 45-minute coast phase (maximum);

6) Weight goal for complete guidance system - 50 pounds;

7) Volume goal - must fit within 18-inch-diameter cylinder, 9 to 12 inches long;

8) Calibration cycle - 90 days or longer preferred;

9) Location - in nonspinning fourth stage;

10) Linear acceleration capability - 30 g along vehicle thrust axis;

11) Aximuth alignment - <60 arc-seconds;

12) Vertical alignment - self-leveling;

13) Accuracy at burnout (IMU errors),

    a) Velocity - 12 fps, 1σ all axes,

    b) Position - 10,000 ft, 1σ all axes,

    c) Attitude - <0.5°, 1σ all axes;

14) Storage Life - five years minimum;

15) Reliability - 1500 hr MTBF

Strapdown Versus Gimbaled

A major consideration when attempting to select an inertial system is strapdown versus gimbaled and the candidate IMUs include gimbaled, strapdown, and floated sphere-type systems. Each type of system has certain advantages and disadvantages; however, it appears that the more significant inertial sensor limitations apply to strapdown systems. The floated sphere system is operationally a gimbaled system. A short discussion of the advantages, disadvantages, and problem areas associated with the two types of systems follows.

Strapdown Advantages.- The important advantages of a strapdown system are:

1) A strapdown IMU generally provides the potential for the lowest overall weight, size, and higher reliability;

2) A strapdown IMU is more flexible in packaging;

3) A strapdown IMU may eliminate the requirement for a separate control system rate gyro package.

Strapdown Disadvantages.- The negative aspects of a strapdown system are generally considered to be:

1) Increased computation requirements;

2) Gyro scale factor errors become important due to the angular rate environment;

3) Angular vibration effects on the sensor loop dynamics;

4) Coordinate transformation computational errors;

5) Prelaunch calibration and alignment;

6) Inertial sensor inflight performance.

Computer requirements and errors.- The computational errors in 1) and 4) present no basic limitations since the present state of the art for digital computers permits sufficient computation complexity, repetition rates, and word length to maintain computation errors below any required level.

Gyro scale factor.- This critical problem is due to the fact that strapdown gyros must measure the total angular environment, whereas platform gyros are used as null sensors.

Calibration.- Prelaunch calibration is not practical with a strapdown system because the sensors cannot be calibrated via gimbal rotation as with a platform. Therefore, strapdown gyros must demonstrate better long-term stability than the equivalent platform gyros.

Alignment.- Preflight alignment of a strapdown system is technically more difficult. The gyros must computationally remove the effects of vehicle sway (angular rotation) in wind gusts and dynamically determine the time-varying orientation of the accelerometer triad with respect to vertical. Gyrocompass azimuth alignment is likewise difficult and high accuracy is difficult because on-pad calibration of the gyros is not feasible.

Examples of strapdown hardware difficulties.- The basic hardware problems associated with a strapdown system arise from the fact that the gyro portion of a strapdown system is an angular rate sensing device and, as such, is subjected to the actual missile body rates. These rates, or noises, may be caused by wind gusts, autopilot corrections, anisoelastic torques due to vibrations, step input commands, etc, and consequently may have extremely high instantaneous values. This high instantaneous rate environment dictates wide dynamic ranges in the gyro torque to balance loops to prevent saturation on the peak value and eventual loss of rate information.

Since the time integral of missile angular rate is required to yield accelerometer orientation, integrators are provided to determine the missile, and hence, accelerometer orientation. The resolution of angular orientation is essentially the same as for a gimbaled platform, even though this resolution must be obtained in a high-rate (noise) environment.

A high gyro torquer rate capability is an absolute requirement of a strapdown system. To achieve this rate capability, strong magnetic fields or low-H (angular momentum) wheels or a combination of both are required. Low-H wheels are generally associated with relatively high values of restriant, restraint instabilities, and g-sensitive coefficients and these characteristics are independent of the type of gyro incorporated in the system. Another type of hardware problem occurs when single-degree-of-freedom floated ball bearing gyros that have low-H wheels are used. This type of problem appears as noise generated inside the closed loop, and are modulations of the output axis caused by rotor imbalance (at fundamental wheel speed frequency), ballbearing retainer modulations (approximately 11/16 of the fundamental), and beat frequencies between the retainers (usually a fraction of a cycle per second). These gyro characteristics are also found in a gimbaled platform, though to a lesser extent.

Any noise, whether applied to the closed loop as a forcing function or generated internally within the loop (as is the case of output axis modulations), subtracts from the dynamic range of a torque-to-balance loop.

Gimbaled platform advantages.- The advantages of the gimbaled system are:

1) The gimbal system isolates the inertial sensors from vehicle rates (benign environment);

2) Less system computation is required;

3) On-pad calibration of gyro and accelerometer coefficients is possible to eliminate day-to-day and on-off instabilities;

4) The function of platform gimbals is to isolate the inertial sensors from vehicle body rates -- in fact, the sensors are afforded a near-ideal environment of being nonrotating in inertial space.

Gimbaled platfo m disadvantages.- The gimbaled system disadvantages include:

1) Greater complexity requires gimbals, servoloops, angle transducers, and a fourth redundant gimbal for all attitude systems;

2) Requires higher weight, larger size, more power;

3) Results in lower reliability because of increased parts count.

Gimbaled platform hardware difficulties.- The gimbaled platforms have error sources not found in strapdown systems. One type of error is caused by the gimbal servoloops. Position and following constants allow considerable platform hangoff during high acceleration because of gimbal imbalance and vibration (rectification torques).

Another error source is platform heading sensitivity (apparent bias and scale factor shifts as a function of platform azimuth to case angle). Several mechanisms can cause this sensitivity:

1) Temperature gradients;

2) Magnetic sensitivity of the inertial sensors and their proximity to wound components;

3) Rectification of synchronous vibrations applied to the platform through the gimbal torquers. This refers to vibrations of the same frequency as the gyro wheel speed. Differences in loop gains and gimbal transmissibilities at the gyro wheel speed cause this sensitivity, e.g., g^2 effect. Although these errors exist in a gimbaled platform, they can be reduced to an acceptable level.

The two-degree-of-freedom, dry, flex pivot gyro also has undesirable characteristics. By the nature of construction, the pickoffs are modulated by wheel rotation, torque-magnet anomalies, and the motor's rotating magnetic vector. This vector is usually phase sensitive with respect to the torquer magnet and thereby causes wheel on-off bias shifts. Adequate shielding, balancing, etc, are required. These undesirable modulations also cause an appreciable reduction in dynamic range. In some cases it is necessary to incorporate exotic filtering to reduce these modulations to an acceptable level.

In essence, there are obvious advantages for both IMU approaches; however, both gimbaled and strapdown systems appear to be adaptable to the Scout booster. A discussion of each of the candidate IMUs follows.

Inertial Measurement Units

Many types of inertial measurement units (IMUs) are in various stages of development. The Martin Marietta Corporation has conducted a continuous effort to evaluate these IMUs for the full range of applications -- ICBM, short-range ballistic missile, tactical aircraft, navigation, ballistic reentry, land navigation, planetary reentry, and interplanetary navigation. Therefore the IMUs evaluated include gimbaled, strapdown, stellar inertial, radio inertial, and floated sphere.

The inertial measurement units listed in table 2 were eliminated for reasons of mission applicability, weight, power, cost, performance, development status, obsolescence, or because they are no longer in production. These systems have all been evaluated at Martin Marietta for such programs as Titan, Pershing, SRAM, Phalanx, Viking/Voyager, Off-Road Mobile, MOL, LPTV, ATP, and in various MMC R&D technology studies such as TOS-843, *Advanced G&C Hardware*. Many of them have also been "flown" in Martin Marietta's trajectory error analysis programs for various vehicles and trajectories.

The IMUs listed in table 3 are the candidates selected for further consideration. It should be noted that several of these IMUs weigh more than the established goals and also several of them are currently under development; however, the discussion that follows will provide the rationale for having included them in the table of candidates.

KT-70 MSL.- The KT-70 missile system is a candidate because of its production base, projected low cost, and low weight. The KT-70 consists of three major subassemblies: the inertial platform, the guidance and control electronics, and a guidance computer. The four-gimbal platform is mounted in a vibration isolator containing two 2-degree-of-freedom gyros, a two-axis accelerometer, a single-axis accelerometer, intergimbal angle transducers, a resolver chain, and accelerometer and redundant gyro input axis capture loop electronics. The guidance and control electronics contains the platform electronics, the missile autopilot, and an ac voltage supply section. The guidance computer is the Magic 301 whole-number digital computer with a memory capacity of 1792 8-bit words, which can be expanded to 2048 words. This computer would not be used in the Scout configuration due to its limited memory and speed.

It is significant to note that the KT-70 family of platforms are used in the P3C, A7, and the F-105 aircraft. It is also part of the Collins commercial navigation system for the L-1011. The system under consideration for Scout is the KT-70 missile system with the modifications discussed in the section entitled *Guidance Hardware/Scout Vehicle Interfacing*. Another significant aspect of this system is its environmental capability, which is critical for the Scout application. It has been tested to levels in excess of 25 g's (linear acceleration).

TABLE 2.- INERTIAL MEASUREMENT UNIT SUMMARY

Gimbaled		Strapdown	
IMU	Design application	IMU	Design application
N10	Minuteman I	LM/ASA	Lunar module
N16	F111	SIGN I (H-394)	Reentry vehicle
N16M	SINS	SIGN II (H-404)	PRIME vehicle
N17	Minuteman II	SIGN III (H-429)	Missile and spacecraft
N17Z	Minuteman III	ESG IMU (H-413)	Spacecraft
N40B	Conceptual	LASER IMU	Tactical missile
ST-120	Pershing	H-408	Tactical missile
ST-124	Saturn	NASA-ERC (H-434)	VSTOL
ST-124M	Saturn	H-419	NASA-MSC lab unit
ST-323-M1	Improved Pershing	NUWS (H-439)	Torpedo
LN-12	F-4	DARS	Spacecraft
LN-14	F-111	IRAD	Spacecraft
LN-15	OV-1D, P-3A	IRA	Spacecraft
LN-15S	B-52 G/H	Lunar Orbiter IRU	Lunar Orbiter
LTN-51	Commercial aircraft	TG-166	Spacecraft
LCGS	Tactical missiles	TG-266	Spacecraft
MKI	Polaris	SIRU	Space Shuttle
MKII	Polaris A-2 and A-3	MICRON	Aircraft navigation
Gemini	Gemini	GG2200	Spacecraft
Dyna-Soar	Dyna-Soar/X-20		
Centaur	Centaur vehicle	Stellar inertial	
ESG INS	Aircraft navigation		
HI-G MINS	Reentry vehicles		
LCI	Aircraft navigation	STINGS	MMRBM
P-3C INS	P-3C aircraft	UNISTAR	ICBM
SUBROC	SUBROC	NAS-14	Aircraft navigation
SGN-10	Commercial aircraft	LN-16A	Aircraft navigation
Titan II	Titan II	Radio inertial	
Titan III	Titan III		
Carousel IV	Aircraft navigation	RIFC	ICBM
Carousel VA	Aircraft navigation	SRGS	ICBM
AN/ASN-82	Aircraft navigation	Radio - TARS	Titan III
SIGS	Tactical missile		
SABRE	Ballistic missiles		
TINI-1	Aircraft navigation		
C5-A(IDNE)	C5A aircraft		
NAS-15	Aircraft navigation		
AN/USD-5	Army drone		

TABLE 3.- CANDIDATE INERTIAL MEASUREMENT UNITS FOR SCOUT

Tradeoff parameter	Candidate IMU systems						
	KT-70	DIGS	H-478	LN-30	TDS-2	Carousel	H-448
Type system	4-gimbal	Strapdown	Strapdown	4-gimbal	Strapdown	4-gimbal	Strapdown
Design application	Short-range missile	Delta launch vehicle	Tactical missiles	Aircraft navigation	--	Titan IIIC	Agena launch vehicle
Status	Production	Production	Prototype	Preproduction	Developmental	Production	Production
Risk	Low	Low	High	Medium	High	Low	Low
Cost, recurring	Low	Medium	Low*	Low	Medium*	High	High
Weight (IMU)	15.1 lb	20.0 lb	5.0 lb	11.5 lb	6.5 lb	57.0 lb	38.0 lb†
Performance:							
Velocity	16.4 fps	7.26 fps	33.2 fps	14.4 fps	13.5 fps	Not flown on TEAP, high performance	Not flown on TEAP, high performance
Position	4 511 ft	2 258 ft	10 240 ft	5 806 ft	6 017 ft		
Attitude	0.079°	0.045°	0.167°	0.012°	0.031°		
Maximum design acceleration	Roll 10 g; Pitch 20 g; Yaw 20 g	16g	40 g	12 g	10 g	12 g	15 g

* Development required.

† Includes power supply.

DIGS.- The Delta inertial guidance system (DIGS) is a candidate because of its development status and planned use in the Delta launch vehicle. DIGS is a high-performance system very similar to the strapdown LM/ASA system. It incorporates three RI 1139E single-degree-of-freedom rate integrating gyros and three C702401030 single-axis pendulous accelerometers. The DIGS IMU weight was originally quoted at 48.16 pounds and consumes 65 watts of power. This weight has since been reduced to 20 pounds for the Scout application by removing the Delta-peculiar cradle and isolators as well as the phase-change heat sink. This wax heat exchanger has since been removed for the Delta application. The DIGS is also space qualified. Twenty-seven LM/ASA systems were delivered in 1969, one DIGS system was recently delivered, and 15 systems are scheduled for delivery by March 1972. Of greater significance is the fact that the United Aircraft strapdown system was chosen for the Viking lander application. The Viking IRU is summarized in table 4.

For the Scout applications, several modifications to the DIGS unit are required. This includes repackaging, elimination of the Delta shock mount and cradle assembly, and cooling during extended orbital operations.

Error analysis results were better for the "modified" DIGS than for any other system (see TEAP summary sheet in section entitled *Closed-Loop Error Analysis*.) However, some degradation may be expected due to hardmounting of the sensors (g^2 effects). The gyro test data from Hamilton Standard in-house testing, and D. T. Brown laboratories testing is a good indication of environmental capability and performance. Therefore, the DIGS system is a primary candidate and should receive further consideration for the Scout application.

TABLE 4.- VIKING LANDER CANDIDATE SYSTEMS

	ATTITUDE REFERENCE UNIT (ARU)				VELOCITY REFERENCE UNIT (VRU)			INERTIAL REFERENCE UNIT (IRU)			R/ARU†	R/IRU§
Parameter	Teledyne	Singer General-Precision	U.A.C. Hamilton Standard	Honeywell	Singer General-Precision	Honeywell	Bell Aerospace	Singer-General-Precision	U.A.C. Hamilton Standard	Honeywell	Teledyne	U.A.C. Hamilton Standard
Size (cu ft)	0.22	0.151	0.28	0.282	0.11	0.072	0.15	0.212	0.28	0.353	0.42	0.362
Weight (lb)	14.94	<15.0	16.44	16.92	11.6	4.97	5.0	22.0	18.9	20.26	24.48	24.58
Power (W)	50.06	18 at 125°F 33 at 0°F	58 operating	100 warm-up 60 operating	8.5 at 125°F 10 at 0°F	10 nom	6.5 nom	26 at 125°F 43 at 0°F	69 max	135 warm-up 70 nom	65 nom	92 max
Reliability	15.31 10^6 hr	5.45 10^6 hr		6.78 10^6 hr	3.40 10^6 hr	5.49 10^6 hr		7.47 10^6 hr		10.75 10^6 hr	2.79 10^6 hr	
Accelerometer type models	NA*	NA	NA	NA	SAP F-F 2401	SAP F-F GG177-P3	SAP F-F Bell ModIX	SAP F-F 2401	Bell Model IX SAP F-F	SAP F-F GG177P3	NA	Bell Model IX
Gyro type models	2DF Dry SDG-2	SDF-F Mod Alpha III	SDF-F RI1139-S	SDF-F GG334A-10	NA	NA	NA	SDF-F Mod Alpha III	SDF-F RI1139-S	SDF-F GG334A10	2DF Dry SDG-2	SDF-F RI1139-S

*NA = Not applicable. §Selected for Viking Lander, Redundant/IRU †Redundant/ARU

H-478.- The H-478 strapdown inertial sensor assembly is a candidate because it is a very lightweight system. Although it is currently in the prototype stage and undergoing van tests, contracts are being negotiated with Honeywell for a torpedo application and for the simplified helmet sight air-to-air guidance (SHAG) application. For the Scout application, it was suggested that this system be integrated with the HDC-250S digital computer containing a plated wire memory. This system is therefore a prime candidate in terms of cost, weight, and environmental capability. However it represents a higher risk due to its current prototype status.

The proposed Scout improved guidance package from Honeywell is designated the H-487 system. It retains the same basic leveling accelerometers and loops as the H-478 system.

Stability numbers (30-day and run-to-run) for bias and mass unbalance are not comparable to the other leading candidates. The performance from TEAP indicated typically 33 fps and 2 miles, only one-fourth as good as the leading strapdown system. For reasonable performance, prelaunch calibration and transfer to missile without power shutdown should be considered.

The GG-326 single-axis accelerometer is not backed by performance history, being just out of the development stage. The GG-177 accelerometer has been recommended for the thrust axis for the Scout application. Since this unit is larger and heavier than the GG-326, some upward adjustment of the size and weight estimates would be required.

The H-487 IMU is a development system. Because little is known about the accelerometers or gyros, it is therefore considered a relatively high-risk system. Conversely, its projected weight, power, and cost characteristics are attractive for the Scout application.

LN-30.- The gimbaled LN-30 system is a high-performance low-weight and highly maintainable aircraft navigator. It includes the P-1000 cantilevered four-gimbal platform. The cantilevered mechanization reduces the number of sliprings normally required and provides for ease of maintenance. It is currently at Holloman AFB undergoing tests and will ultimately be flight-tested in the F-4 and the C-131 aircraft. A production order has been placed for 28 systems for a tactical aircraft program. An LN-30 system has also been flying at Holloman AFB as part of the doppler inertial loran (DIL) system. The environmental effects for a launch vehicle application require consideration in light of the LN-30's intended aircraft environment. Also a tactical aircraft application generally employs high-performance gyros and accelerometers optimized for a low-acceleration range, with emphasis on long-term bias stability, which is not consistent with boost vehicle requirements. Conversely, the accelerometer has recently been tested in a high-g environment and has exibited remarkable stability.

The G-1200 third-generation gyro is a two-degree-of-freedom, dry, gimbaled flexure gyro. The A-1000 accelerometer contributed the largest error in the TEAP flight. This propagated error was primarily caused by accelerometer scale factor.

The electronic circuits, i.e., gimbal loops, capture loops, and gyro pulse torquing, all employ good standard techniques. Gain and compensation numbers are not available for analysis of platform hangoff.

The LN-30 is basically designed as a 2 n. mi./hr navigator and is presently being flown as part of a DIL system at Holloman AFB. Since it is not in production at the present time, and the historical data available on the G-1200 inertial sensors are not sufficient, it is considered a medium-risk system.

TDS-2.- The TDS-2 is currently under development at Teledyne. It incorporates two 2-degree-of-freedom SDG-2 strapdown gyros and three FP-1 force rebalance accelerometers. The projected unit cost is moderate and predicted performance is high. At the same time it is considered to be a high-risk system because of the state of development of the 2-degree-of-freedom gyro.

TEAP results for the TDS-2 look very good. This is due to the use of "design goal" values rather than test result numbers. It is felt at this time that the development costs and the concurrent risks would not be acceptable for the Scout program.

LCP-III.- The LCP-III system (although not included in table 3) was considered because of its low weight and low cost. This system was developed by the Raytheon Company for potential tactical missile applications. An earlier version, the LCP-III, completed Holloman tests in December 1970. It is a three-gimbal low-performance system employing the SIG-30 2-degree-of-freedom gyros and the United Control 4167 accelerometers. It is currently undergoing a cost and size reduction with an 18-pound weight goal. In evaluating this system it was eliminated as a prime candidate because of projected performance.

H-448.- The H-448 strapdown guidance system was developed for the Agena vehicle. It provides guidance, navigation, steering, attitude control, telemetry, and issuance of discretes during ascent and in orbit. It is a modification of the H-429 system that completed extensive laboratory and flight tests at Holloman AFB. The H-448 system recently flew very successfully with the Agena vehicle. Although this system is fully developed and in production, the unit costs are quite high.

Carousel VB.- The Carousel VB was included primarily for comparison since it is in production for a launch vehicle application (Titan IIIC). It is characterized by high performance and high reliability as demonstrated by the commercial Carousel VA version. On the other hand, since the IMU weighs 58 pounds, when integrated with a computer, the CVA would be well in excess of the Scout weight goals.

Attitude Reference Units (ARU)

This subsection summarizes the candidate attitude reference units (ARUs) for the Scout launch vehicle (table 5). The term ARU is used interchangeably with TARS (three-axis reference system) throughout this report. ARUs were investigated for use in a nonspinning fourth-stage configuration with an attitude control system.

TABLE 5.- CANDIDATE ATTITUDE REFERENCE SYSTEMS

	HSSC ARU	ODMAR	H-478 ARU
Manufacturer	Hamilton Standard	General Electric	Honeywell
Type System	Strapdown	Gimbaled	Strapdown
Weight	16.44 lb	24.2 lb	4 lb
Power	58 W	55 W	25 W
Acceleration capability	15 g	75 g	40 g
Gyro	RI1139	GG49D23	GG1009
Technical risk	Low	Low	Medium
Status	Developmental	Production	Conceptual (mod to H-478)

The ARU would be used on Scout in a similar "open-loop" manner as is presently used for the first three stages of flight. This mechanization was described in the section entitled *Introduction*.

The ARUs considered include strapdown pulse rebalance gyros, strapdown wide angle gyros, and gimbaled gyros.

HSSC-ARU.- The HSSC attitude reference system was configured to provide vehicle attitude information during boost. It is the same basic inertial package proposed for the Viking ARU with three RI1139 gyros.

In a previous HSSC analysis used to formulate the detailed error budgets, all inertial sensor performance coefficients, with the exception of pitch and yaw gyro bias, were based on 120-day 3σ stability values. The pitch and yaw gyros would require prelaunch calibration and therefore are assumed to have 2- to 3-day 3σ stability coefficients. The gyro dynamic errors induced by the Scout random vibration environment are not expected to be major error sources since the dynamic error coefficients have been experimentally proven in a series of shake tests simulating a similar environment at all frequencies from 0 to 2 kHz. There was an exception at the characteristic gyro wheel bearing frequency, which produced a negligible resonance spike. The HSSC ARU was the best performing system in the open-loop error analysis.

ODMAR.- The General Electric ODMAR system was originally designed for reentry vehicle attitude reference applications and is currently being supplied to Philco-Ford for the Army's FAIR program. The ODMAR system is a three-gimbal attitude reference unit. Four systems have been built and two have flown in the FAIR program. It is a Scout candidate because of its linear acceleration capability (75 g) and light weight. It contains three Honeywell GG49D23 floated rate-integrating gyroscopes. The three gyros are mounted to the stable member by a single alignment frame, so the gyro triad can be prealigned and tested as a subassembly.

An important feature of this platform is the matched set of vibration isolators that support the gimbal system within the case. They have a frequency of 70 cps and provide attenuation and/or isolation at all frequencies above 98 cps. This can provide low-drift inertial stability in the face of severe random and sinusoidal vibration inputs.

H-478 ARU.- The Honeywell ARU is a modification of the prototype H-478 system. It incorporates the GG1009 gyros and electronics in a miniature strapdown configuration. Potentially it is a low cost system but would require an extensive development and qualification program.

There are a number of other potential ARUs such as the GG2200, Teledyne Viking ARU, the Honeywell ARU, and the Singer-GPI Viking ARU. The latter three are summarized in table 4. The Viking systems shown in table 4 are peculiar to the Viking program and therefore do not carry the conventional platform notation such as DIGS, LN-30, etc.

Advanced Technology Systems

This category includes next-generation systems as well as advanced technology systems. These systems are in various stages of development; however, the emphasis in all cases is on weight and cost. They are generally characterized by low-to-moderate performance and will probably not be sufficiently developed nor will an inertial components history be established for the Scout time frame. However, to enhance the usefulness of this report, these systems are summarized in Table 6. It should be noted that the H-478 system is included since in terms of weight, cost, and development status, it also falls in the next-generation IMU category.

TABLE 6.- MINIATURE AND ADVANCED TECHNOLOGY INERTIAL SYSTEMS

System	Manufacturer	Type	System Weight, lb*	Comments
NIP-140	Nortronics	Floated sphere	6.5	Two systems at Holloman
H-478	Honeywell	Strapdown	5.0	Prototype stage
P-4	Litton	Gimbaled	4.5	Prototype stage
Micron	Autonetics	Strapdown electrostatic	3.0†	Prototype stage
MIT S/D	MIT	Strapdown	12.1	Conceptual
INU 73	Singer-GPI	Gimbaled	15.0	Developmental
Sperry laser	Sperry	Strapdown laser	35.0	Prototype (3-axis)
Autonetics laser	Autonetics	Strapdown laser	10.0	Developmental (3-axis)
Honeywell laser	Honeywell	Strapdown laser	28.0	Prototype (3-axis)
HSSC laser	HSSC	Strapdown laser	--	Developmental

*Does not include computer

†Includes inertial sensors, computer, electronics, power supply, and batteries.

Closed-Loop Versus Open-Loop Guidance System Selection

One of the areas investigated in the study was the comparison of performance between the various overall approaches. Specifically, the mechanizations considered include the present open-loop Scout system on the third stage (with a spin-stabilized fourth stage), an improved open-loop system on the fourth stage, and a closed-loop fourth-stage guidance. The section on the *Open-Loop Error Analysis* developed errors due to nonguidance and guidance perturbations from which covariance matrices were generated. A similar output was obtained for the closed-loop guidance and can be found in the *Closed-Loop Error Analysis* section. The results were presented in Figure 1 in isoprobability contour form. The isoprobability contouring technique discussed in Appendix D describes how the system parameters are generated from the system covariances and the way in which the contours are arrived at. Figure 1 is a composite of a number of contours that Martin Marietta has generated and a NASA contour extracted from the Scout *Users' Manual* for comparison. This figure graphically demonstrates the difference in orbital error expectation for different guidance equipment for a near-circular earth orbital mission. An interesting performance factor to be drawn from this graph is the virtually identical results for the original Scout equipment mounted in an open-loop configuration on the fourth stage (which of course implies an RCS system) and that of a more accurate TARS package (i.e., the DIGS ARU). This occurs since the errors due to attitude reference system hardware are very small in comparison to the other errors.

Another meaningful observation is in the difference between the third-stage open-loop guidance and the fourth-stage open-loop guidance. This occurs due to the elimination of a major source of error, that of the tipoff disturbances for the spinning fourth stage.

The results of the closed-loop IMU system are significantly better as was expected due to the elimination of the nonguidance errors, which are the most significant. The elimination of the nonguidance errors is based on the assumption that they are less than 10% of the guidance hardware errors. This is true for a properly designed closed-loop system.

Qualitatively there is no question of the increased performance to be gained using the closed-loop guidance approach. Virtually all nonguidance error parameters are eliminated except for the uncertainty in the FW-4S engine burn characteristics. The greatly improved accuracy of the Scout orbit plus the increased flexibility of the vehicle makes the closed-loop guidance the recommended approach since it is most consistent with the desires of NASA for the future of the Scout launch vehicle.

IMU Selection

The IMU selection was made on the basis of the preliminary goals set forth earlier in this report. Although all candidates in table 7 are adaptable to the Scout application, with the emphasis on cost, risk, and weight, the KT-70 system is most adaptable to the Scout vehicle and is therefore the preferred system for Scout. This has been a first round evaluation and should not preclude further evaluation of the alternative systems as the requirements become firm. A Phase I type activity as described in the *Guidance Integration Program Summary* section includes the generation of a detailed RFP and the enumerated Phase I tasks will therefore form the basis for the final IMU selection. However, in order to investigate the feasibility of improved guidance hardware for Scout, it was necessary to perform a preliminary comparison and selection.

Primary candidate.- The gimbaled KT-70 missile system was selected as the preferred IMU. This section provides the selecton rationale and a more detailed description of the existing system.

The KT-70 missile system was selected as the reference inertial system for the following reasons:

1) Low cost;

2) Weight--IMU, power supply, G&C electronics, 3 rate gyros (<30 lb combined);*

*Does not include computer.

TABLE 7.- IMU SELECTION MATRIX

TRADEOFF PARAMETER	RANK (R)	CANDIDATE IMU SYSTEMS													
		KT-70		DIGS		H-478		LN 30		TDS-2		CAROUSEL		H-448	
		Grade*	XR	Grade	XR	Grade	XR	Grade	XR	Grade	XR	Grade	XR	Grade	XR
Risk, development	8	3	24	3	24	1	8	3	24	1	8	3	24	3	24
Cost, recurring	7	3	21	2	14	3	21	3	21	2	14	2	14	1	7
Weight	6	2	12	2	12	3	18	2	12	3	18	1	6	1	6
Accuracy	5	2	10	3	15	1	5	2	10	2	10	3	15	3	15
Power	4	2	8	2	8	3	12	2	8	2	8	1	4	1	4
Environmental Capability	3	3	9	2	6	3	9	2	6	2	6	2	6	2	6
Qualification Status	2	3	6	3	6	1	2	2	4	1	2	3	6	3	6
Available GSE	1	2	2	3	3	1	1	2	2	1	1	3	3	3	3
TOTAL			92		88		78		87		67		78		71

*Grade 3 Excellent

2 Acceptable

1 Does Not Meet Goals

3) Power--<120 watts combined system;*

4) Size--600 in.^{3} combined system volume;*

5) Production status--More than 60 units delivered; anticipated high quantity production for foreseeable future; therefore, it is a low risk system;

6) Inertial components--Proven with extensive test data available;

7) Environmental capability--Tested to 25 g linear acceleration along two axes, 12.5 g on third axis (freeflight mode);

8) Angular rate capability--400 deg/s roll axis, 240 deg/s pitch axis, 450 deg/s azimuth axis.

One of the key factors considered in the selection of the KT-70 system is that it has a solid production base. The KT-70 series systems are currently being shipped for a wide range of applications including tactical missiles (SRAM), fighter aircraft (A-7 and F-105), patrol aircraft (P-3C), and for commercial applications in the L-1011 and DC-10 as part of the Collins Radio INS-60 system. These systems have the following military designations: AN/ASN-90 for A-7D and E, AN/ASN-84 for P-3C, and the AN/ASN-100 for the F-105. All systems incorporate the two-degree-of-freedom, dry, flexure-joint-suspended, free-rotor gyroscope. The KT-70 production prediction is as shown in figure 16.

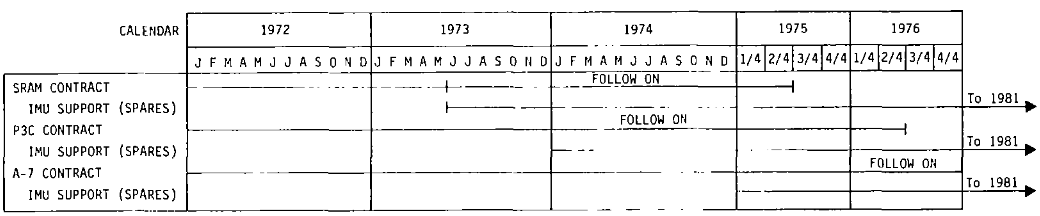

FIGURE 16.- KT-70 PROJECTED PRODUCTION

*Does not include computer.

The KT-70 missile system production will ultimately exceed 2000 systems; approximately 1500 units were delivered for aircraft programs.

It should also be noted that the next generation SKN2400 miniature platform is being developed to be interchangeable with the current KT-70 systems. In the future, this could result in even more significant weight reductions.

The KT-70 missile guidance system was designed to provide the following functions:

1) Erection and alignment:
2) Attitude reference;
3) Inertial sensing;
4) Navigation;
5) Trajectory shaping;
6) Missile steering;
7) Discrete generation.

The current application is a tactical missile program with emphasis on reliability and a high environmental capability.

System configuration.- The system consists of an inertial platform, guidance and control electronics, a guidance computer, power conditioner, and three flight control rate gyros.

The inertial platform has four gimbals, azimuth, inner roll, pitch and outer roll, from inner to outer, respectively. The four gimbals are mounted on vibration isolators, all of which are housed within an outer case. The platform cluster houses the two two-degree-of-freedom GYROFLEX* gyroscopes and a two-axis and a single-axis accelerometer. In addition, the platform contains intergimbal angle resolver readouts for azimuth, pitch, and roll as well as the gimbal torquers, heaters, and coordinate resolver.

The guidance and control electronics package includes the gimbal drive and isolation electronics, the digital accelerometer loops (DAL) and the autopilot electronic functions. In addition, system switching and reference supply voltage generation form a part of the electronics box. A second function of this package is to house all the autopilot drive electronics.

The power conditioner accepts an input of 28 Vdc and provides output voltages to both the electronics and computer subsystems. The voltages are nominally ±15 Vdc, ±16 Vdc and +5 Vdc.

The digital computer is a whole number machine with a memory capacity of 2048, 8-bit words. It controls the erection and alignment of the system as well as computing present position, desired trajectory, and missile steering signals. Furthermore, it provides the required system switching discretes and the autopilot gain computation and network selection logic.

*Trademark, Singer Company

The three rate gyros provide damping for the missile steering signals. The individually packaged rate gyros are spring-restrained single-degree-of-freedom rate gyros. The performance characteristics follow.

Nonlinearity	0.1 V rms/deg/sec ±6.5% including repeatability and day-to-day stability
Threshold	<0.02 deg/sec
Resolution	<0.01 deg/sec
Hysteresis	<0.3 deg/sec
Acceleration sensitive drift rate	<0.03 deg/sec/g
Rate sensitivity	<4% of full scale
Angular acceleration sensitivity about OA	0.05 deg/sec/rad/sec^2 (max)
Full scale rate	±100 deg/sec
Alignment	<0.1 deg IA to mounting plane

Table 8 summarizes the physical characteristics of the respective subassemblies.

TABLE 8.- KT-70 MISSILE SYSTEM CHARACTERISTICS

CHARACTERISTICS	INERTIAL PLATFORM	COMPUTER	PLATFORM AND AUTOPILOT ELECTRONICS	RATE GYROS	POWER CONDITIONER
Size, in.	7 dia x 7.6 long	10.4 x 3 x 5.4 high	10.6 x 4.6 x 5.2 high	Pitch & Yaw: 4 x 2 x 1 3/4 Roll: 4.2 x 1 x 2.3	9 x 4 x 4 in.
Weight, lb	15.1	5.2	7.7	1.8	5.5
Volume, in.^{3}	345	130	200	33	75
Construction	Aluminum castings hermetically sealed	Aluminum casting, box replaceable cards, integrated circuits	Aluminum casting, box replaceable cards, integrated circuits	Three individual rate gyro packages	Aluminum casting
Power, w	9.7	40.0	25.6	6.8	75.6

Functional description.- The platform-mounted accelerometers are maintained in the computational reference frame by the torqued gyros through the platform isolation loops. The accelerometer outputs are double-integrated in the missile computer prior to launch. After being resolved through the appropriate platform intergimbal angles, these signals are used to develop missile fin steering commands. The missile computer provides the necessary autopilot network and gain changing control to stabilize the missile in flight and generate various safety and action discretes. Prior to launch, the system is aligned to the reference frame by the carrier computer operating through the missile computer.

Operation.- The operational requirements of the missile guidance subsystem are satisfied by four modes of operation. The purpose and content of each of the required operational modes is detailed as follows:

1) Alignment mode.- The system is powered, temperature-stabilized, and aligned. Alignment consists of sequentially performing coarse and fine modes of operation with the aid of the carrier computer;

2) Load mode.- The missile system accepts from the aircraft navigation system all data required for freeflight navigation, direction cosine computation, steering, and discrete generation;

3) Verify mode.- The missile system provides verification of all data transferred during the load mode;

4) Flight compute mode.- This mode commences on separation of the missile from the carrier. It consists of

   a) Velocity computation, position computation, and gyro torquing to maintain the inertial platform in the tangent plane coordinate system;

   b) Trajectory shaping using a preloaded series of constants;

   c) Generation of steering signals to control fin position based on inertially derived direction cosines;

   d) Generation of discretes to control all flight compute mode events.

Two gyros are mounted on the azimuth cluster. Each gyro has two orthogonal axes sensitive to angular motion. Since only three sensitive axes are required to stabilize the gyro cluster, one axis of one gyro is redundant and is captured in a rate mode instead of being used for stabilization. One gyro is used to provide stabilization about the north and east axes and the other is used to provide stabilization about azimuth, with the redundant axis rate captured. The gyro redundant axis and accelerometer capturing electronics are contained within the inertial platform. The outputs of the three stabilization axes are preamplified in the inertial platform and transmitted to the platform and autopilot electronics where the isolation loop electronics is located. The isolation loop postamplifier outputs provide dc power to the gimbal torquers to cancel out disturbing torques about the inertial platform gimbal axes.

An orthogonal triad of accelerometers, mounted on the stabilized cluster, provides dc voltages representing sensed acceleration along three axes. Prior to launch, torquing signals to the gyro axes are provided from the gyro pulse torque electronics on command from the guidance computer. These torquing signals maintain the accelerometer triad aligned to a prelaunch coordinate frame.

Initial velocity and position information, trajectory-shaping information, and discrete data are transferred from the aircraft navigation system to the missile guidance computer and, in turn, are verified by the missile computer.

Following the missile launch, the inertial platform is maintained in a reference tangent plane coordinate system, as indicated in figure 17 with fixed gyro torquing rates, based on initial launch latitude and computed gyro biases.

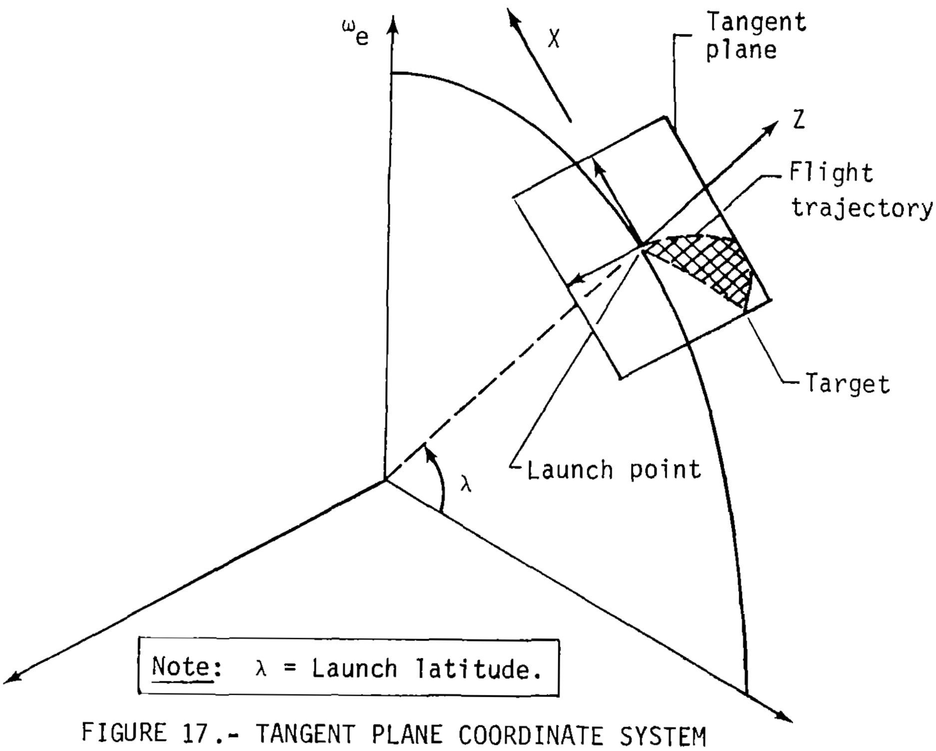

FIGURE 17.- TANGENT PLANE COORDINATE SYSTEM

In this coordinate frame, the inertial platform measures missile acceleration along three axes and transmits this information to the guidance computer through the capacitive reset integrators. During missile flight, the missile guidance subsystem operates independently of any external signals.

The missile guidance subsystem is capable of generating autopilot command signals to steer the missile along a number of different trajectories such as low-altitude skip, low-level flight or semiballistic, depending on the preselected type of trajectory inserted in the guidance computer prior to launch.

The guidance subsystem generates the autopilot command signals in roll, pitch, and yaw to steer the missile to the intended target by utilizing the computer distances-to-go-to-target in the following manner. The guidance computer determines the direction cosines of the line-of-sight (LOS) to the target in inertial platform coordinates. The direction cosines are the distance-to-go divided by the range to the target. These signals are transformed to missile body coordinates by resolving through the inertial platform angle transducers into roll, pitch, and yaw, demodulated, and then sent to the computer for routing to the autopilot.

The steering commands from the guidance subsystem are the errors between LOS from the missile to the target and the missile centerline (roll axis) for the pitch and yaw channels. For the roll channel, the steering input is the error between the reference fin and the vertical plane.

A signal flow diagram of the IMU resolver chain is shown below.

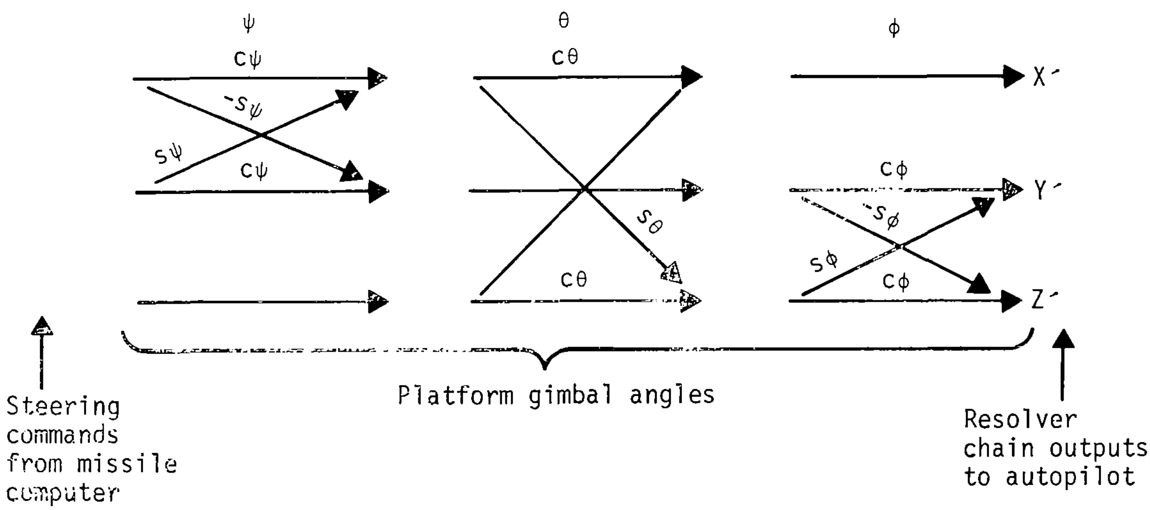

The yaw, pitch and roll steering commands are generated in the following manner.

Yaw steering command.- Assume roll (ϕ) and Pitch (θ) = 0

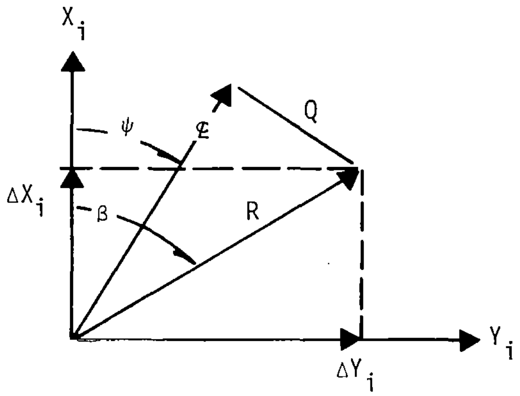

$$\cos \beta = \frac{\Delta X}{R}$$

$$\sin \quad = \frac{\Delta Y}{R}$$

R = Vector to target

℄ = Vector along missile centerline

Q = Vector normal to ℄

ψ = Aximuth angle

β = Target angle

X, Y = position in inertial (platform) coordinates

It is required to generate a yaw steering signal that will drive vector Q to zero, i.e., vectors R and Q are coincident when steering signal is zero.

$$\sin (\beta-\psi) = \frac{Q}{R}$$

$$Q = R \sin (\beta-\psi) = 0$$

Q will be zero when $\sin (\beta-\psi) = 0$

Since pitch (θ) and **Roll** (ϕ) = 0

$$X^{1} = \frac{\Delta X}{R} \cos \psi + \frac{\Delta Y}{R} \sin \psi$$

$$Y^{1} = \frac{\Delta X}{R} \sin \psi + \frac{\Delta Y}{R} \cos \psi$$

$$Z^{1} \quad \frac{\Delta Z}{R}$$

The required yaw steering signal has the form of sin $(\beta-\psi)$

$$Y^1 = \frac{\Delta Y}{R} \cos \psi - \frac{\Delta X}{R} \sin \psi$$

Substituting in terms of β

$$Y^1 = \sin \beta \cos \psi - \cos \beta \sin \psi$$

$$= \sin (\beta-\psi) = \text{yaw steering signal}$$

Pitch steering command.- Assume yaw (ψ) and roll $(\phi) = 0$

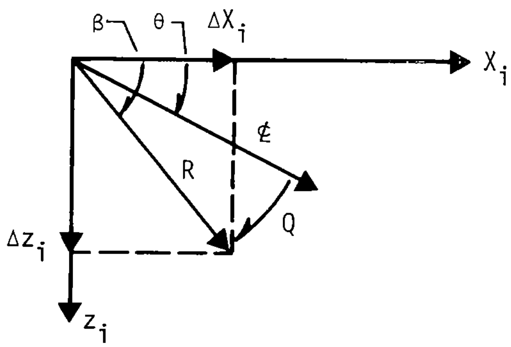

$$\cos \beta = \frac{\Delta X}{R}$$

$$\sin \beta = \frac{\Delta Z}{R}$$

It is required to generate a pitch steering signal that will drive vector Q to zero.

$$Q = R \sin (\beta-\theta) - 0$$

Q will be zero when $\sin (\beta-\theta) = 0$

Since yaw (ψ) and roll $(\phi) = 0$, from the signal flow diagram:

$$X^1 = \frac{\Delta X}{R} \cos \theta + \frac{\Delta Z}{R} \sin \theta$$

$$Y^1 = Y$$

$$Z^1 = \frac{\Delta X}{R} \sin \theta - \frac{\Delta Z}{R} \cos \theta$$

The required pitch steering signal has the form of sin $(\beta-\theta)$

$$Z^1 = \frac{\Delta X}{R} \sin \theta - \frac{\Delta Z}{R} \cos \theta$$

Substituting in terms of β

$$Z^1 = \cos\beta \sin\theta - \sin\beta \cos\theta$$

$$= \sin(\beta-\theta) = \text{pitch steering signal}$$

Roll steering command.- Since roll is the outermost gimbal, the dc potentiometer generates the roll steering signal directly. No coordinate transformation is required.

For all three body axes, the guidance subsystem outputs provide missile attitude feedback for the autopilot, and the lead required for stabilization in pitch and yaw is provided by body-mounted rate gyros. For all axes, continuously varying autopilot gain is necessary to meet the stability and performance requirements. The gain profile is loaded into the guidance computer at the same time as the trajectory-shaping constants.

The guidance computer generates discrete commands as a function of time, range to go, altitude and/or attitude. These commands initiate and control other missile subsystem functions. Typically, they control the following:

1) Flight control subsystem enable;

2) Flight control subsystem gain settings;

3) Flight control subsystem compensation control;

4) Propulsion subsystem arming;

5) Propulsion subsystem ignition;

6) Terminal guidance sensor enable;

7) Airburst fuzing.

Modifications Required

To adapt the KT-70 missile system to the Scout launch vehicle, several modifications are required. They include:

1) Addition of porro prism to fixed gimbal and viewing port to case;

2) Rescaling accelerometer loops;

3) Selecting a digital computer with increased capability;

4) Modifying control electronics to interface with Scout control and ignition system.

These modifications are discussed in detail in the section entitled *Guidance Hardware/Scout Vehicle Interfacing.*

KT-70 Performance

In this study each vendor was contacted relative to previously quoted performance numbers. In many instances specification performance numbers with broad tolerances have been established by the manufacturers for noncritical parameters simply to increase production yield. Frequently the hardware performs much better than the numbers imply. On the other hand, the intense competition within the inertial equipment field has caused some manufacturers to become overly optimistic (in our opinion) and judgments had to be made on what can be economically achieved.

The initial descriptive data received from Kearfott in response to the data format was informative but flagged some shortcomings. (The data reflected the Boeing requirements and system mechanization rather than the equipment's performance.) It was recognized that in some instances, acceptance test tolerance bands were given and these bands did not represent the performance capability of the equipment. Furthermore, an application task was necessary to permit a valid evaluation for Scout (e.g., spin axis mass unbalance was quoted as 2 deg/hr/g). On investigation, this was determined to be the trim level required in the missile. Consultation with the responsible gyro engineer revealed that the low stability from a large-volume production was approximately 0.08 deg/hr/g. After a third iteration, a new set of numbers was derived that is consistent with a reasonably high yield of gyros.

The error budget shown in table 9 illustrates the iterations required before arriving at an agreement on the KT-70 missile system/Scout launch vehicle specification limits. The last column contains the values used in the Martin Marietta error analysis program.

Alternative candidate No. 1.- The strapdown Delta inertial guidance system (DIGS) was selected as a prime candidate for the following reasons:

1) Production status - In production for Delta launch vehicle, modified redundant version selected for Viking lander;

2) Inertial components - Proven with extensive historical test data available;

3) Performance - Excellent, based on production unit test data and error analysis results.

This system is capable of meeting the Scout requirements and can be integrated into the vehicle with minimum modifications since it has already been married to a digital computer for a boost vehicle application.

TABLE 9.- KT-70 MISSILE SYSTEM ERROR BUDGET

Parameter	Missile application specification (max values)	Platform data (5 sample platforms)	Actual inertial component data	Achievable inertial component data	MMC supplied Scout budget	Singer-GPI provided Scout acceptable spec limits
Gyro restraint X&Y	5.0	0.191	0.5	0.1	0.05	0.2
(°/hr) Z	5.0	0.135	0.5	0.1	0.05	0.2
Gyro mass spin axis imbalance X&Y	1.5	0.0794	0.08	0.08	0.08	0.1
(°/hr/g) Z	3.5	0.111	0.08	0.08	0.08	0.1
Gyro input axis imbalance X&Y	0.6	0.041	0.035	0.035	0.01	0.05
(°/hr/g) Z	0.6	0.0536	0.035	0.035	0.01	0.05
Quadrature g X&Y	1.2	0.0281	--	0.05	--	0.07
(°/hr/g) Z	1.2	0.0691	--	0.05	--	0.07
Anisoelasticity X&Y	0.2	--	0.03	0.03	0.02	0.03
(°/hr/g) Z	0.2	--	0.03	0.03	0.02	0.03
Gyro torquer scale factor X&Y	4.5	0.222	0.2	0.2	0.1	0.25
(%) Z	4.5	0.682	0.2	0.2	0.1	0.70
2-axis accelerometer bias (μg)	100.0 (1σ)	52.8	50.0	50.0	50.0	50.0
SF (μg/g)	600.0	122.6	67.0	50.0	50.0	100.0
K2 ($\mu g/g^2$)	7.5	--	10.0	10.0	7.5	10.0
K3 ($\mu g/g^3$)	5.0	--	1.0	1.0	5.0	1.0
Cross bias (μg/g)	27.0	--	7.5	7.5	7.5	7.5
Crosscoupling sensitivity (μg/g)	250.0	--	--	250.0	--	250.0
1-axis accelerometer bias (μg)	300.0 (1σ)	106.7	70.0	70.0	70.0	100.0
SF (PPM)	500.0	255.1	60.0	70.0	70.0	100.0
K2 ($\mu g/g^2$)	20.0	--	10.0	10.0	7.5	10.0
K3 ($\mu g/g^3$)	5.0	--	1.5	1.5	10.0	1.5
Cross bias (μg/g)	15.0	--	15.0	15.0	7.5	15.0
Accelerometer alignment/orthogonality						
X-Y	206.0	34.2	--	40.0	40.0 (20/axis)	20.0
X-Z (arc-s)	103.0	17.3	--	40.0	40.0 (20/axis)	20.0
Y-Z	103.0	41.8	--	40.0	40.0 (20/axis)	20.0
Platform alignment						
Verticality X	--	No data	--	--	12.0	22.0
(arc-s) Y	--	available	--	--	12.0	22.0
Azimuth	--	--	--	--	--	47.0

The DIGS consists of a strapdown inertial measurement unit (IMU) and a guidance computer (GC). A functional flow block diagram of this system is shown in figure 18. It is used to sense angular and linear motions of the Delta vehicle during flight. The gyro and accelerometer data is processed in the guidance computer and guides the vehicle along a predetermined path by issuing analog and discrete commands to perform various steering and staging functions in order to achieve accurate injection into a specified orbital trajectory.

Within the IMU, the three rate integrating gyros and the three accelerometers each form an orthogonal triad. The digital pulse outputs of the three gyros, after compensation for deterministic errors, are employed in the numerical integration of the angular equations of motion, thus providing vehicle attitude relative to the inertial computational frame in terms of nine direction cosines. The digital output of the gyros (in the vehicle frame) are also available after launch for both the attitude error computations and control signal shaping functions. The accelerometer outputs, also after compensation, are resolved into the computational frame for further processing.

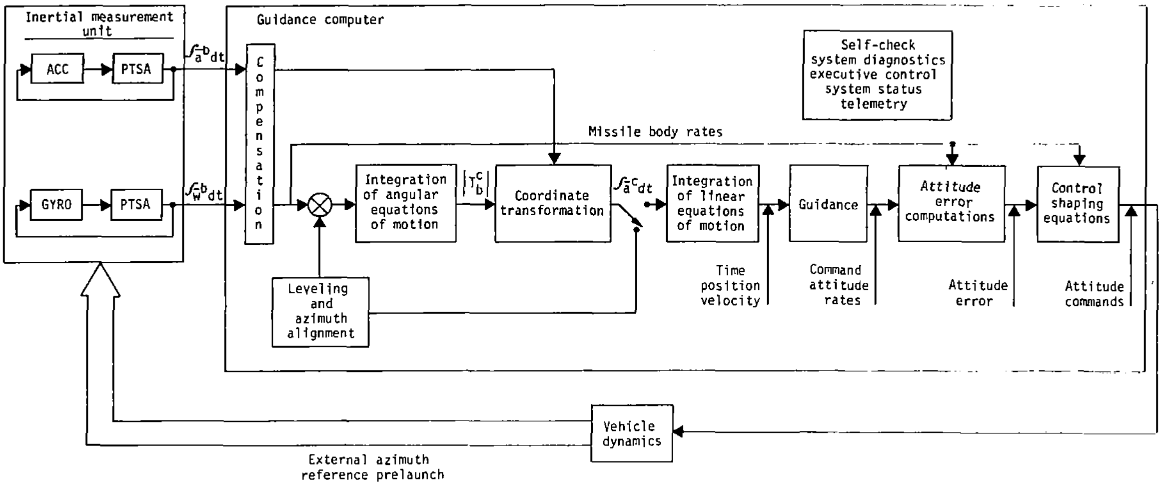

FIGURE 18.- DIGS FUNCTIONAL BLOCK DIAGRAM

Prior to launch, the accelerometers level the computational frame with respect to the local geodetic frame. After launch, the accelerometer outputs are used, along with a mathematical model of the Earth's gravitational potential through integration, to determine the missile's velocity and position. DIGS participates in the prelaunch checkout operations through self-test, and by exercising the vehicle subsystems.

After launch, during the closed loop guidance phases of flight and based upon indicated velocity and position obtained from the position tracking equations (navigation), the guidance computations determine the desired attitude expressed in terms of desired or commanded vehicle attitude rates. The guidance computations either estimate velocity and position at the end of each closed loop phase of guidance and compare this to desired but computed terminal conditions to determine present attitude commands (explicit guidance), or compare present velocity to desired velocity to determine attitude commands (implicit guidance). The computer is capable of solving either guidance scheme. In addition, the guidance computations perform the functions of timing and staging, as well as issuing preprogrammed command attitude rates during the open loop and coast guidance phases. The attitude error of the vehicle is computed from the integral of the difference between the command attitude rates and the vehicle body rates, as determined from the guidance computations and the strapdown gyros, respectively.

The basic inputs to the alignment scheme, as shown in figure 19, are the compensated sensor outputs (in terms of increments of angle and velocity in the body frame), and an optically derived azimuth measurement. Initial conditions for the attitude matrix computation are available as flight constants to an accuracy better than one degree.

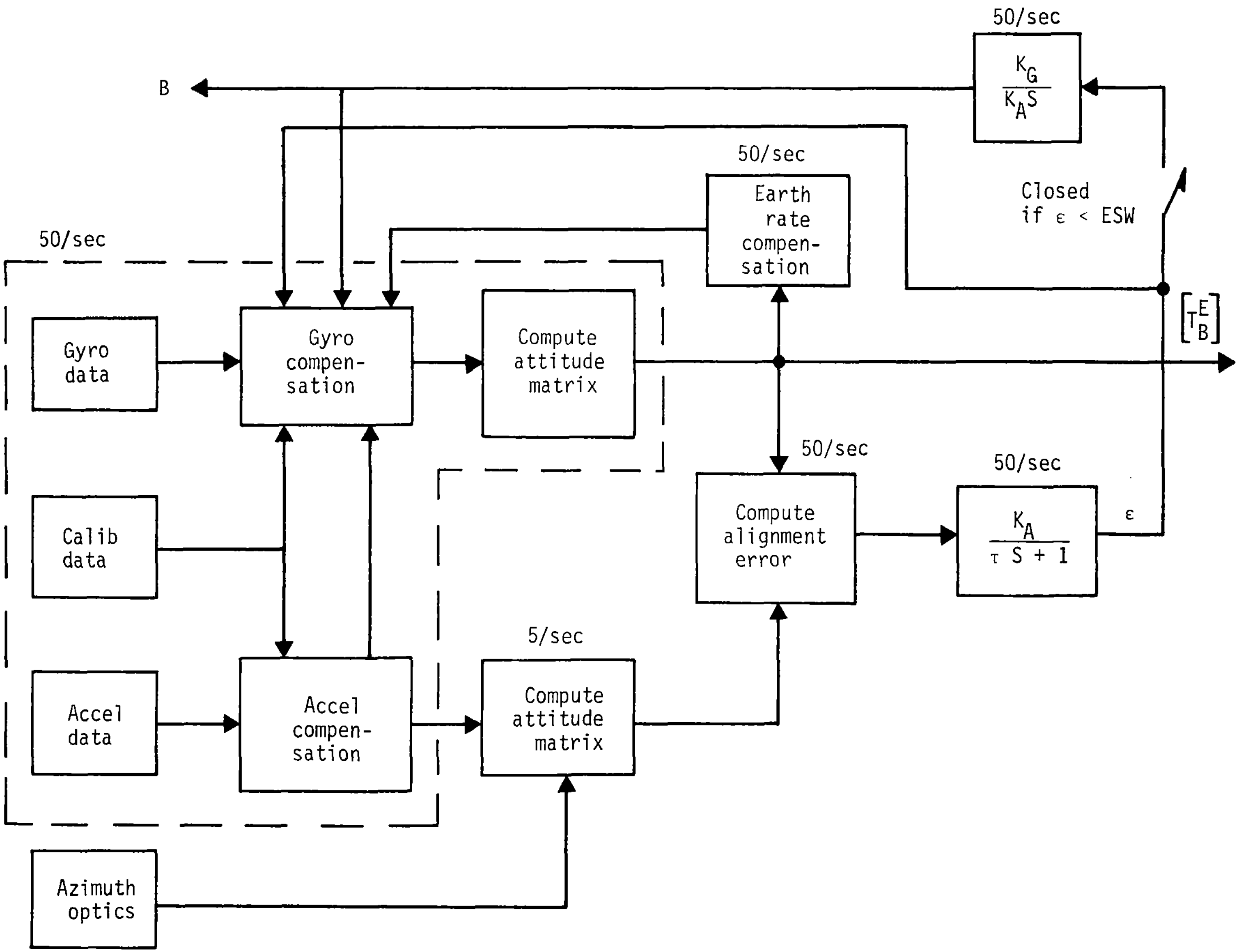

FIGURE 19.- STRAPDOWN PREFLIGHT COMPUTATIONS - ALIGNMENT AND GYRO BIAS CALIBRATION

Upon initiation of the alignment mode, the computation of two body-to-earth fixed geocentric attitude matrices will commence. One (the gyro matrix) is derived from the compensated gyro data, which has been further compensated for earth rate. It tracks instantaneous motion at a fine granularity of 3.6 arc-seconds at 50 times per second, but is corrupted by the gyro drifts.

The elements of the other (accelerometer leveling) matrix are computed, based on defined geometric relations between body, local level, and earth-fixed geocentric coordinates in conjunction with an optically derived azimuth and compensated accelerometer data. This matrix is computed at a rate of once every T_A seconds, so as to establish an accurate value of the vehicle tilt angles with respect to local level, in lieu of accelerometer pulse moding and in the presence of vehicle sway motion.

The selection of T_A will be based primarily on the expected vehicle sway amplitude and frequency and the accelerometer pulse moding. Note that the accelerometer leveling matrix elements are updated only once every T_A seconds.

Comparison of the two attitude matrices provides indicated alignment errors, defined in terms of small angular displacements about the body axes. The alignment errors are further filtered, so as to allow only the mean offset angles and gyro drift angles to pass through as a feedback correction. After first entering into alignment, the filtered alignment errors are multiplied by a constant feedback alignment gain, K_A, to yield the alignment corrections. The gain is predetermined, based on estimates of the measured noise and sensor quantization statistics, and considerations of the expected vehicle sway characteristics, and the desired instantaneous alignment accuracy. The alignment error corrections are fed back and applied to the compensated gyro outputs in the body frame. Whenever the sum square of the X, Y, and Z alignment error corrections is less than a preselected value, ESW, the filtered alignment error signals are additionally multiplied by a different gain, K_G (bias feedback gain), summed and fed back as gyro drift correction signals in the body frame. The bias feedback gain is predetermined, based on bias update settling times and anticipated worst case steady-state errors.

The IMU is a self-contained assembly that senses incremental angular displacements about the vehicle axes and velocity increments along the vehicle's orthogonal axes. These data are fed to the computer in the form of discrete pulse trains which indicate changes of angle and/or velocity.

The design configuration of the DIGS IMU is basically that of the LM/ASA with modifications. These principally consist of incorporating a new housing and repackaged LM/ASA electronics.

The IMU contains three HSSC RI-1139 gyros, three Kearfott 2401 accelerometers, six pulse torquing servo amplifiers, frequency countdown unit, warmup and fine temperature control amplifiers, interface electronics, power supply, and housing subassembly. The inertial instruments are mounted in an aluminum housing which provides a stable, rigid orientation of the inertial instrument triads, as well as a mounting base and thermal path for the IMU electronics.

The TDY-300 guidance computer (GC) is the advanced Centaur computer that was developed for NASA/Lewis by the Teledyne Systems Company. The GC is a general purpose, stored program machine designed specifically for space and boost vehicle environments. The design is based upon a single package housing with three major subassemblies mounted for proportionate thermal power distribution and interconnect harness simplicity. A functional modularity concept is used for subassembly design. These subassemblies consist of memory assembly, power supply assembly, and logic section assembly. The unit interconnect harness includes all subassembly interface connections and external system interface connectors. The DIGS system characteristics are as shown in table 10.

TABLE 10.- DIGS GUIDANCE SYSTEM CHARACTERISTICS

PARAMETER	STRAPDOWN INERTIAL UNIT (SDIMU)	GUIDANCE COMPUTER	SYSTEM TOTAL
Weight (lb)	32.1	41	73.1
Power (watts) (average)	61.9 (8 W for heaters)	131 (assumes 11 W for discretes)	192.9
Volume (cu ft)	0.46	0.66	1.29
Flight MTBF (hr)			4581
Flight operational time			Continuous, 90 min
Mission performance (3σ 90 day stability)			
All axes less than	----	----	Velocity 20 ft/sec Attitude 0.5 deg Position 1 n. mi.

The electrical interface, as shown in figure 20, between the system and the vehicle consists of three analog steering signals (±10 V dc), six discrete signals to pulse attitude gas jets, and 35 discrete commands to specific vehicle elements such as relays and solenoid valves. All discretes are at a 28 V level and are capable of driving the required load. In addition, analog and digital data are output to the telemetry system. The system also accepts discrete commands from the vehicle.

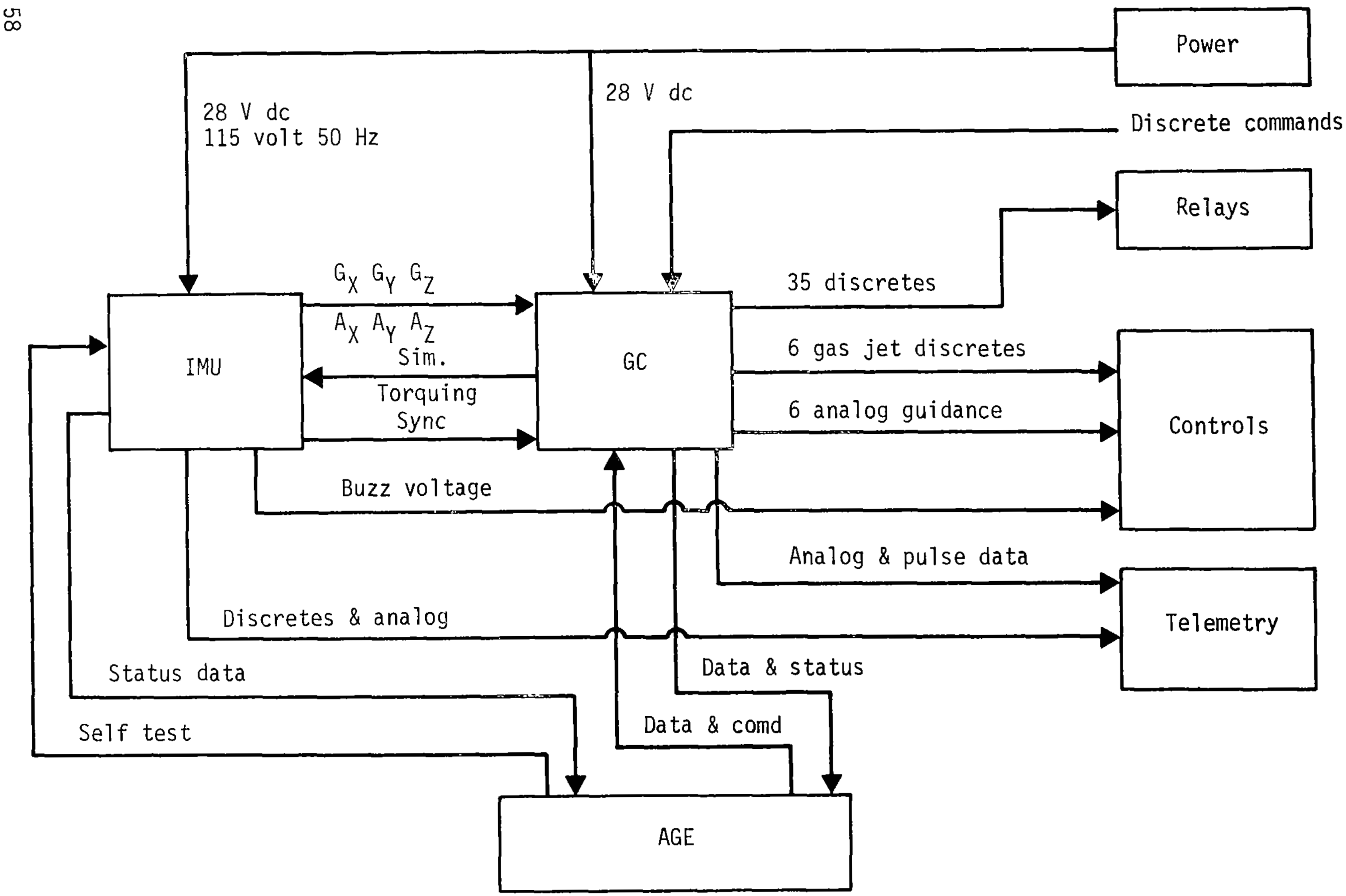

FIGURE 20.- DIGS/AGE/VEHICLE INTERFACES

The launch checkout equipment (LCE) which constitutes the AGE, consists of a digital computer, teleprinter, a high speed tape reader, a data acquisition system, power supply and control systems, a signal conditioning unit, an I/O extender for the computer, cooling fans, a console, data monitoring devices, interface simulators and software. A block diagram of the LCE is shown in figure 21.

The LCE features software control of all required functions and provides for test expansion capabilities with minimum hardware changes. The functions of the LCE are to perform hangar integration tests on the DIGS and the vehicle to insure proper hookup and continuity of electrical connections by performing GC discrete output tests, engine slew tests and flight simulation; perform fault isolation automatically using the diagnostic software routines, produce hard copy outputs of the DIGS voltage and frequency signals monitored for the launch status criteria; generate a go/no-go signal based on this criteria by monitoring the downlink discrete and analog signals via the read scanner and integrating digital voltmeter and decoding the GC status words derived during the self check testing; load the GC flight software automatically from paper tape via the umbilical and verify the proper loading; compute and perform the load/verif, of flight parameter (azimuth) updates; and, interface the DIGS with the operator over the 1000-foot umbilical. The voltage and frequency signals used in the go/no-go status determination are the three gyro spin motor rotation detection (SMRD) frequencies, the IMU block temperature, IMU dc voltage, IMU ac voltage, GC logic voltage, GC memory voltage, and the result of the software GC check.

Alternative candidate No. 2.- The LN-30 inertial navigation system is a prime candidate for Scout for the following reasons:

1) Projected production status; 24 preproduction sets have been built;

2) Performance;

3) Low weight and power.

The LN-30 inertial navigation unit (INU) is a self-contained inertial navigator with built-in gyrocompass-align capability. The INU consists of a platform, converter card, digital computer and power supply.

The LN-30 inertial navigation unit features (1) completely modularized configuration, (2) cantilevered platform construction for accessibility to stable element, (3) nonfloated instruments, (4) extensive use of LSI and MSI circuitry, and (5) high reliability with a predicted MTBF = 3000 hours (P-1000 only).

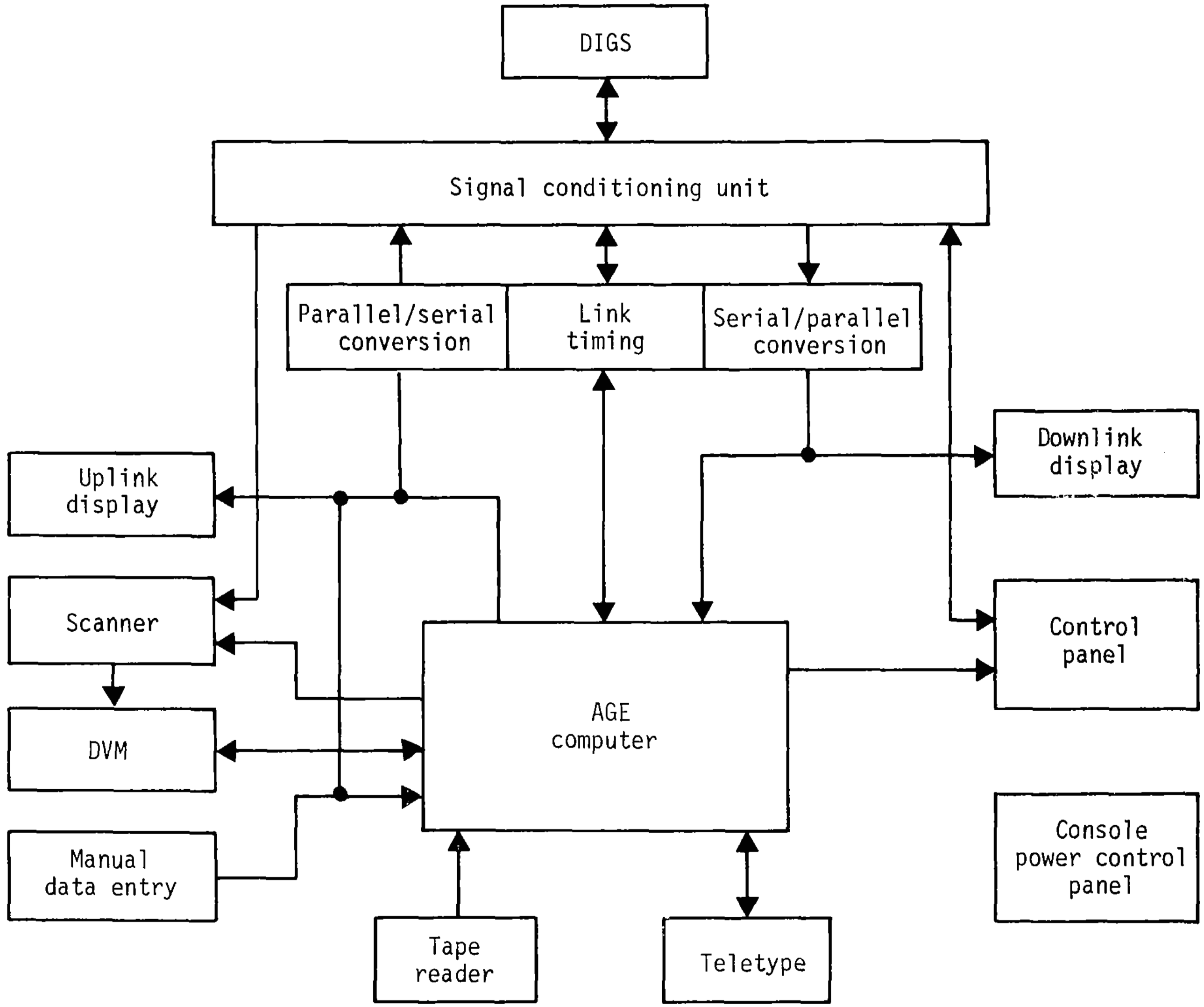

FIGURE 21.- LCE BLOCK DIAGRAM

The LN-30 has several modes of operation. These are:

1) Align (normal gyrocompass and heading memory);

2) Navigate;

3) GP;

4) Backup;

5) Ground test;

6) Gyro bias 1 and 2.

When the INU is operated in the normal gyrocompass align mode, the platform automatically levels to the local vertical and the computer determines the heading with respect to north. In this mode the platform is initially caged in azimuth to the heading of the platform's case (generally mounted along the aircraft's centerline). The computer determines the platform heading using a wide-angle gyrocompass mechanization. An estimate of true heading (a mag heading and mag var) must be inserted into the computer to reduce the alignment time required. The align period is normally about 10 minutes, and completion is sensed by a built-in circuit which outputs a ready-to-navigate signal.

The navigate mode uses a wander-azimuth mechanization, that provides latitude and longitude outputs without requiring special polar-navigational procedures. The computer may be updated at any time in this mode with position, velocity, and direction-cosine updates, and with tilt (torquing) corrections, permitting tie-in to a central computer with an optimal filter.

In the GP mode, the platform can be operated directly from a central computer, with the INU's own computer continuing to operate but not providing torquing inputs to the gyros. In case of central computer failure the INU computer can be switched back into control, thereby providing an effective redundancy feature.

The backup mode is used in case of an in-flight condition that causes the INU to be disabled. The platform is pendulously erected and can be slaved in azimuth to an external reference. The circuitry for torquing must be provided externally.

The ground test mode is used for preflight self-test. In this mode the platform is first aligned and then "fast-Schuler" tested. The Earth's radius term in the computer is shortened and velocity stimulii are inserted, causing rapid Schuler-type oscillations with a period of approximately 10 minutes. The zero-crossing time of the velocity data is monitored and proper operation is indicated if the time is within a specified interval. This check verifies platform and computer operation, as well as power supply and circuit performance. Total test time is approximately 10 minutes.

The gyro bias modes are used for periodic rebiasing of the gyros, which is normally performed at 500-operating-hour intervals. The INU is first operated in the gyro bias-1 mode and the Y- and Z-gyro biases determined. If the operator decides to correct the stored bias data, the new values are inserted (using the control panel data entry controls) and are nonvolatily stored in the bias memory. The gyro bias-2 mode is used for X-gyro biasing.

The LN-30 physical characteristics are shown in table 11.

TABLE 11.- LN-30 PHYSICAL CHARACTERISTICS

	INU	CIU	RACK
Navigation accuracy, n. mi./hr	1.5 CEP (unaided)		
Dimensions, in.	14.9 x 8.8 x 13.6	5.75 x 7.5 x 6.0	
Volume, cu in.	1783	258	
Weight, lb	39.5	7.1	2.1
Power, warmup	500 watts* -400 Hz, 3ϕ		
run	310 watts -400 Hz, 3ϕ	40 watts† 400 Hz, 3ϕ	
Cooling air	1.5 lb/min at 100F	none	
Predicted system MTBF, hr	1568		

*Including heaters for both platform and battery.
†Plus 15-watt edge lighting power.

The INU consists of the basic inertial sensors and the LC-4516 digital computer. It measures attitude and is stabilized in inertial space by two G-1200 Vibragimbal gyroscopes. The stabilized platform provides an earth-bound reference for the two accelerometers. The accelerometers are maintained locally level and their relationship (wander angle) to north is solved by the computer.

The P-1000 platform incorporates a high level of maintainability inherent in a cantilevered design. The stable element, consisting of the gyros and accelerometers, is removable without gimbal disassembly.

The platform gimbal order is conventional with the innermost gimbal being azimuth surrounded by the inner-roll, pitch, and outer-roll gimbals. The appearance of the platform, however, is not conventional, because of the application of cantilevered gimbals. The cantilevered outer roll gimbal acts as a mounting surface for the platform servo electronics, permitting the use of a large circuit board rather than a set of small cards. By mounting the electronics on the outer roll gimbal the necessity for routing servo signals back and forth through the outer roll slipring is eliminated. Included on the servo electronics cards are all the necessary power amplifiers for operation of the four platform gimbals.

The platform subunit is cooled by internally circulating dry nitrogen over the platform and electronics with a small blower. The heat is transferred by convection to the nitrogen that flows through the heat exchanger. The heat is then transferred by convections to the exchanger where it is transmitted to the aircraft cooling air. This cooling system maintains the platform ambient temperature at 148F (64C) maximum and maintains the gyros at a temperature that does not exceed 178F (81C).

The LC-4516 is a general-purpose, 16-bit parallel, fractional arithmetic computer. The LC-4516 provides functional and packaging modularity through use of a data bus structure, TTL bipolar MSI circuitry and simple, fine-line, etched circuit board component packaging. The CPU us mechanized on four 2-sided printed circuit boards. This CPU offers 43 basic instructions and a throughput of 172,000 operations per second on a typical mix.

Although the LN-30 was designed and developed for aircraft navigation, it can be modified for use in a boost vehicle application. This implies a complete qualification program for the boost environment. To further demonstrate the capability of the LN-30 system in a high g environment, Litton ran centrifuge tests on the A-1000 accelerometer.

A total of seven A-1000 analog restored accelerometers were centrifuged at two levels of maximum acceleration to determine experimentally, the second order nonlinearity of the instrument. The average second order coefficient of the seven instruments tested is 45.9 ug/g^2 with a minimum absolute value of 9.8 ug/g^2 and a maximum absolute value of 113 ug/g^2.

The first four samples were centrifuged at a maximum acceleration of 7 g while the last three were centrifuged up to 26 g. Data taken on the last three samples were reduced for a 7-g level and a 20-g level to verify that the coefficients are valid over the entire range and are true second order coefficients. Table 12 shows the results of this data reduction and verifies the validity of extrapolation of the first four sample coefficients to higher g levels.

TABLE 12.- CORRELATION BETWEEN LOW AND HIGH ACCELERATION

SAMPLE NO.	SERIAL NO.	2nd ORDER NONLINEARITY COEFFICIENT, ug/g^2		
		LOW g	HI g	% CHANGE
5	72-EX2	+71	+74	+4.2
6	96-L33	+60	+78	+30
7	102-L70	+78	+57	-27

In summary, in order to meet the high linear acceleration requirement for Scout, the following modifications to the inertial components and gimbal set were suggested by Litton.

G-1200 gyro

1) Bearings currently preloaded for 20 g; can be increased without design change;

2) Balance of gyro and loops capable of sustained 30-g environment;

3) Gyro successfully tested to 30 g, 11 msec shock.

A-1000 accelerometer

1) Replace analog restoring loop with pulse rebalance circuits;

2) Test and calibrate residual g, g^2 and bias;

3) Put g, g^2 and bias terms in computer;

4) Acceleromter successfully tested to 50 g, 11 msec shock.

P-1000 gimbal set

1) Redundant inner gimbal in existing design will be locked in place;

2) Bearing preload on outer gimbal can be increased without redesign;

3) Basic gimbal structure capable of sustained 30 g field.

Two methods of aligning the LN-30 for a boost vehicle application were investigated. The gyrocompass alignment technique would employ a Kalman (7 state) alignment mechanization. An azimuth alignment accuracy of better than 60 arc-sec (1σ) is predicted. Optical alignment is also practical with the LN-30 system since it is possible to mount a porro prism on the inertial components cluster and a window to the platform case.

The proposed Sc.)ut LN-30 inerial navigation system characteristics are as follows:

Navigation accuracy	1.5 n. mi./hr CEP
Dimensions	14.3 x 10.6 x 13.6 in.
Volume	2062 in.^{3}
Weight	43.5 lb
Computer memory capacity	4K x 16 bit words
Power consumption warmup	500 watts
run	310 watts
Cooling air	1.5 lb/min 100°F
Heat sink (flights exceeding 800 sec)	100°F with 310 watt input
Calculated MTBF prediction	1568 hr
Computer memory capacity	4K x 16 bit words

COMPUTER SIZING, SURVEY & SELECTION

This section provides the data and rationale for establishing requirements on the computer. The results of a market survey for airborne computers is given and a selection of the best candidates is presented using the noted requirements in this section.

Computer Selection Process

The major obstacle in computer selection is obtaining sufficient computational requirement definition so that bounding conditions can be placed on memory size, computational speed, and word length. Additional difficulty lies in that a given computational problem, memory size, speed, and word length can be traded against each other. Also, computer architecture will allow a given problem to dictate bounding conditions for one computer different from that for another. An ideal computer selection process follows.

1) Define the bounding computational problem.

2) Translate this to minimum requirements for a baseline computer.

3) Translate all candidate computers to this baseline computer such that architectural differences can be translated to time and size margins.

4) Eliminate those that will not meet the minimum requirements of the baseline.

5) Select the final computer on the basis of how it meets the critical criteria of cost, weight, power, sizing margin, timing margin, and risk.

This report attempts to illustrate how this process will work for selection of the final Scout computer. However, sufficient data is not now available to select the final candidate. The data is incomplete in two general areas:

1) Complete definition of the computational problem;

2) Accurate data from the manufacturers.

More work is required to define the guidance logic bounds and mission flexibility bounds that directly affect computer requirements. The usual approach for launch vehicle computer procurement is to buy considerably more computer than can be justified, or to select a simple, restricted mission definition and worry the problem later. Applications with serious weight and/or power restrictions simply cannot afford this luxury and effort should be expended to determine the optimum trades. Also, the proper data for final selection probably cannot be made without formal RFP activity with the manufacturers. It should be made clear that enough data is available to reduce the number of candidates and to illustrate the selection process.

Any airborne computer procurement should contain a planned amount of timing and sizing margin for the following reasons:

1) Errors and oversights in defining the computational problem;

2) System problems that occur late in the development cycle that must be solved with software because of the cost and schedule impact to modify the hardware;

3) Additional flexibility refinements become desirable later on and are justified on the basis of reducing foreseeable recurring costs.

The exact amount of margin needed at the time of procuring hardware is a matter of judgment based on the degree of confidence and knowledge of the above items as well as the restrictions on power and weight. It is recommended that a minimum of 25% planned margin for timing and sizing be established at the time of computer procurement.

Basic Assumptions

A few basic definitions and assumptions have been made so that the computer selection process can be carried far enough to give a number of leading candidates.

Since the guidance equations and logic are presently undefined, a technique adopted to establish an upper bound on computational problems follows.

1) Eliminate the lunar mission as a consideration on the basis that additional requirements reflect primarily on memory space and additional memory can be procured at the time other required hardware is procured (command data uplink, etc).

2) Select applicable portions from the guidance equations of Titan IIIC providing an explicit guidance scheme that can be considered as representing the upper bound of flexibility for Scout.

3) Use modified Titan guidance logic plus other Titan sizing data as baseline for interfacing with a gimbal IMU.

4) Use modified Titan guidance logic plus available Delta launch vehicle sizing data as baseline for interfacing with a strapdown IMU.

A certain amount of additional confidence exists in this method. The estimates are based on scaling down existing computer programs rather than building up from scratch with the risk of overlooking significant problem areas. During the scaling down process, only items definitely unnecessary are eliminated, thus leaving uncertain or overlooked areas within the estimates.

In summary, the guidance portion of the computational problem can be considered to be a worst case example for the mission capability to be used on Scout.

Additional guidance logic investigation will certainly optimize and further reduce the magnitude of the computational problem because the given definition is sufficient for achieving a synchronous equatorial orbit. The time for this type mission requires six hours, which makes the power requirements on the computer very critical. The present battery technology provides 30 watt-hours/lb which will translate to an increase of 15 pound for a 100-watt system when mission requirements increase from one hour to six hours. The power requirements are derived assuming a one-hour mission even though the guidance logic is fundamentally capable of handling more than this. The criteria for establishing the weight requirements has been simply to pick a weight limit that allows a reasonable number of candidates to be selected. The selected limit is based on the actual weight plus the battery weight required to operate for one hour.

A modification to the ideal selection process has been made at this time to allow for incomplete and somewhat unreliable data from the manufacturers. This modification ignores the differences of translating the candidate computers to the two baseline computers although the techniques involved will be discussed.

Computer Requirements

General.

Interfaces.- The computer requires, as a minimum, the following interfaces:

Digital (GSE, telemetry)

Accelerometer (x, y, z inertial velocities)

Attitude data (gimbal angles or direction cosines)

Analog

1) Autopilot variable gain

2) Yaw, pitch, roll displacement commands

Discretes

Telemetry Requirements.- The constraints imposed on a general-purpose computer by the telemetry requirement can be costly in both memory requirement and timing. There are techniques to effectively manage memory, but timing is a more serious problem unless a direct memory access channel (DMA) is available for use. The assumption for this exercise is that a normal digital data channel will be used instead of a DMA although firm requirements in terms of telemetry data cannot be stated at this point.

The traditional list below will be assumed in order to work the timing and sizing aspects necessary for computer selection.

1) Gyro compensation, x, y, z;

2) Accelerometer compensation x, y, z;

3) Minor cycle counter;

4) Computation status;

5) Discretes;

6) Velocity-to-be-gained;

7) Stage conditions;

8) Direction cosines;

9) Inertial velocity, Vx, Vy, Vz;

10) Steering commands - yaw, pitch, roll

11) Attitude errors;

12) Radius vector x, y, z components;

13) Yaw, pitch, roll angle rates.

Mode Switching Requirements.- Mode switching and discrete generation requirements are directly related to a sequence of events in obtaining mission objectives. The task of mode control and issuing discretes is dedicated to the executive system. This allows for an efficient manner of executing programs dependent on the sequence of events. Following is a list of output discretes that are under software control:

1) Liftoff;

2) Stage II ignition;

3) Activate Stage II control system;

4) Separate first stage;

5) Remove first-stage controls;

6) Switch in body-bending filter;

7) Separate payload heat shield;

8) Activate Stage III control system;

9) Stage III ignition;

10) Stage III separation;

11) Activate fourth-stage control system;

12) Stage IV ignition

13) Fourth-stage separation;

14) Payload function;

15) Payload separation.

The procedure used in sizing the Scout mission guidance computer is to form subprogram modules from the computer processing functions. Each module is analyzed for storage requirements and execution times. Table 14 shows a preliminary module list and the memory requirements within the computational cycles.

Timing and Discrete Generation Requirements.- The Scout guidance computer will employ a real-time interrupt to develop the timing interval. This time interval is the basis for establishing the computer program minor cycle or the smallest time step for data sampling and associated computational solutions. The executive routine will respond to the real-time interrupt (RTI) and control the execution of both minor cycle and major cycle routines. The executive will also develop from the RTI all counters or timers used for mission control.

It is the function of the executive to manage the discretes that provide for ultimate vehicle control from computer memory load to payload separation. The baseline discretes list assumed for Scout follows.

1) x, y, z torquer polarity commands;

2) Body bending filter switch;

3) Autopilot control 1, 2 (gain select);

4) Autopilot control enable;

5) Align discretes 1, 2, 3, 4, 5;

6) Second-, third-, fourth-stage RCS valve commands;

7) Second-, third-, fourth-stage activate control system;

8) Second-, third-, fourth-stage motor ignition commands;

9) Third-stage thrust reduction command;

10) Fourth-stage separation;

11) Fourth-stage OCS activate commands;

12) Payload separation command;

13) Payload functions;

14) Fourth-stage thrust reduction;

15) GSE functions.

Within the discussion on timing, it is pertinent to point out the basic difference in requirements placed upon computers used for controlling a gimbaled IMU system versus a strapdown IMU system. The gimbaled IMU contains the body attitude with respect to inertial space in a direct readout of the gimbal angle resolvers.

In the case of the strapdown IMU, there is no gimbal in which attitude is automatically stored. The computer must, therefore, derive attitude by reading the gyro inputs at a high frequency and update body attitude with respect to inertial space by solving a set of differential equations. These equations can vary greatly in their degree of complexity. The equations will be of higher order and, therefore, more complex and difficult to implement in a digital computer as system requirements for accuracy are increased. Whatever the degree of complexity, it is important to note that these equations must be solved on the minor cycle. When this set of differential equations is solved every 20 to 40 milliseconds, it is easily seen that the minor cycle computational load gets extremely heavy. Therefore, speed requirements on a digital computer to handle the computational problem for a strapdown IMU are significantly greater than speed requirements for the gimbaled IMU problem. To a lesser degree, but still significant, increased memory space requirements are placed on a computer to handle the strapdown IMU problem. The reason, of course, has just been described; the calculations of body attitude with respect to inertial space are an additional load upon the computer when using a strapdown IMU.

GSE.- Digital computer requirements in interfacing with the GSE are at a minimum -- IMU alignment support and memory load/verify capability.

The Scout digital computer will provide assistance for IMU alignment to establish the initial inertial reference. For the purpose of determining requirements upon the digital computer, limited activity is assumed.

For most efficient utilization of memory, the computer and GSE will exercise a digital interface for loading and verifying the computer memory at the launch site. This will allow the capability of using the computer in prelaunch testing and later loading the flight program over it. This means that liberal prelaunch calibration and testing can be done at no expense of memory to contain it.

General Computer Characteristics.

The general characteristics required in the Scout digital computer are rather traditional for most airborne applications. They are:

1) Binary;

2) 2's complement arithmetic;

3) Fixed point arithmetic;

4) Fractional data word;

5) Two accumulators (upper, lower);

6) Expandable memory.

Variables Affecting Computer Characteristics.

There are three areas that affect basic computer characteristics in speed requirements or memory size. These are index registers, memory addressing techniques, and instruction set. Proper selection in each area can minimize both speed and memory requirements.

Index registers.- The use of index registers allow for the optimization of computer memory versus execution time, handling tabulated data, etc. It has been determined empirically that there is a relationship between availability and use of index registers and memory and/or speed requirements. These relationships are included.

1) Memory.- In performing the guidance and control class problem, one or two index registers reduce the amount of memory required by 5%. Three index registers reduce the memory required by 10% when comparing the job as being done with no index registers.

2) Time.- The computer time required to perform a G&C-type task without index registers can be reduced somewhat if index registers are employed. One or two index registers allow the required time to be reduced by 6%; three index registers allow required time to be reduced by 13%. These figures must be altered downward if the computer requires extra memory cycles for indexed operations. To revise these figures on that basis requires knowledge of how many index operations per second there will be for the total problem.

Addressing capabilities.- The addressing technique employed in a computer also has an impact upon the memory required to perform a given task. A segmented memory, i.e., one which cannot be totally addressed within the range of the instruction's operand, requires extra manipulation to access data, subroutines, etc. This, in turn, is a requirement for additional instructions and indirect address tables. The following tabulation shows how memory required to do a task increases as the operand field is reduced:

Operand Size	Memory Increase Required
>9	0%
9	5% increase in instructions
8	10% increase in instructions
7	25% increase in instructions
6	50% increase in instructions

Instruction set.- The availability of more powerful instruction set obviously has advantages. It can reduce the amount of memory required for a task as well as the time required for the execution of the task. Included here are formulas that assist in the comparison and evaluation of instruction sets.

1) Memory size. - If by using the basic 26 instructions, the basic memory requirement, M_1, can be determined by instruction count, it is then possible to compute the impact of an improved instruction set on the problem.

$$M_2 = \frac{\log_e 26}{\log_e N} M_1$$

M_1 = total memory requirement using basic 26 instructions of Table 13.

M_2 = computed memory requirement for improved instruction set.

N = number of instructions in improved set.

TABLE 13.- RECOMMENDED INSTRUCTION REPERTOIRE

*1. ADD	*15. STORE B
*2. SUBTRACT	*16. TRANSFER and SAVE
*3. MULTIPLY	*17. TRANSFER indirect
*4. DIVIDE	*18. TRANSFER and INCREMENT index
5. ROTATE (right, left, single, double)	*19. TRANSFER
*6. SHIFT (right, left, single, double)	*20. TRANSFER on a negative
*7. Logical AND	*21. TRANSFER on a zero
*8. Logical OR	22. NEGATE A
9. Exclusive OR	*23. Input/Output (A/D, D/A discretes, incremental interrupt control internal)
*10. LOAD index	24. NORMALIZE
*11. LOAD A	25. ADD DOUBLE[†]
*12. LOAD B	26. SUBTRACT DOUBLE[†]
*13. STORE index	
*14. STORE A	

*Minimum instruction set for gimbaled system.

[†]Needed for computing attitude reference on strapdown IMU problem (minor cycle).

Gimbaled system has only 24 double precision adds in major cycle--hardware double precision instructions not necessary.

2) Timing.- If a problem has been sized and timing margins, T_1, calculated, using basic 26 instructions, it is then possible to predict the timing margin, T_2, in seconds/second if the improved instruction set were used.

$$T_2 = \frac{\log_e 26}{\log_e N} T_1$$

T_1 = timing margin associated with basic instruction set

T_2 = predicted timing margin for improved instruction set

N = number of instructions in improved set.

Memory Size

General.- One of the major considerations for determining memory size is to select an executive routine design that allows for significant changes in the mission requirements without causing changes to the programming. This implies that all changes be made by parameter modification. The technique has been demonstrated in the digital flight controls programming for Titan IIIC, but it has been costly in terms of memory usage. A concerted effort has been made to do the Scout guidance with 4K of memory words, and the sizing data precludes using anything but minimum executive design. Therefore, future changes will certainly cause recurring software expense. A discussion of a Centralized Executive System has been included in Appendix F of this report. The estimate for this type executive is 1200 words, and this should be considered only if the memory size is more than 4K. It should be pointed out here that larger memory size margins also contribute to reduced costs for software change activity.

Gimbal system baseline.- The modified Titan IIIC guidance logic to be used as the Scout baseline is described by the following general functions:

1) Major Cycles:

a) Initialization;

b) Accelerometer compensation for scale factor, bias, misalignment;

c) Navigation;

d) Thrust acceleration calculations;

e) Booster steering calculations;

f) Time-to-go calculations;

g) Explicit steering calculations;

h) Coast steering calculations (reduced to ¼);

i) Variable AIM;

j) IMU gimbal angle commands calculation;

k) Major cycle output commands calculation;

ℓ) Stage I guidance initialization;

m) Stage II guidance initialization;

n) Stage III guidance initialization (reduced to ½);

o) Stage II/III separation sequence discretes;

p) Time dependent discretes (reduced to ½);

q) Payload eject discretes (reduced to 1/3);

r) Initial Stage 0 roll maneuver;

s) Stage 0 burnout detection and Stage I ignition;

t) Stage 0/I separation sequence;

u) Stage III Ignition initialization;

v) Toasting and Telemetry orientation logic;

w) Vernier computations (increased to 2);

x) Initialize reference pitch axis;

y) Liftoff detection.

The Titan functions that were eliminated are:

a) Error command rates computation;

b) Stage II shutdown enable test;

c) Backup Stage III shutdown command;

d) Stage I/II separation detection;

e) Backup and primary Stage II shutdown sequence;

f) Stage III reorientation tests;

g) All logic to interface with digital flight controls.

2) Minor Cycles:

   a) Telemetry was reduced because of the reduced Scout requirements.

   b) Executive routine was reduced to eliminate requirements associated with flight controls.

The actual Titan sizing numbers are shown in table 14. The modified Titan sizing numbers are shown as the Scout requirements for a gimbal system.

The self-check requirements are shown as optional since this routine is not a requirement for flight. It provides the ability to isolate most computer malfunctions during software checkout, prelaunch, and flight phases, but the only value in flight is to have postflight knowledge of a computer malfunction via telemetry.

Strapdown system baseline.- The Delta sizing numbers were taken directly from available timing data. The major cycle data for the Scout strapdown baseline was taken to be the same as the gimbal baseline by ignoring differences in the architecture of the two machines. The minor cycle TM routine was reduced in the Scout baseline because of reduced telemetry requirements.

Margins.- The memory size margins for the two systems (ignoring architecture) are:

System	4K Margin
Gimbal	291 = 7.1%
Strapdown	-831 = -21%

The conclusion is that the strapdown system must be worked in more than 4K memory and the guidance logic must be worked harder to gain the desired 25% margin if the gimbal system is to fit.

Computer Speed

1) Gimbal system - The estimates for computer speed are based on redoing the Titan system to reflect an attitude sample rate of 50 sps. This was done to cover the unknown stability margins on Scout for a 25 sps system. This increased sample frequency amounts to an increased time usage of 3% for a total of 20% (80% margin). The desired Scout margin is 25%, meaning that the time usage can increase to 75%. Therefore, the instruction execution times can safely be increased by a factor of three for the gimbal system.

2) Strapdown system - The available timing data on Delta indicated a 34% time margin. Discussions with people close to the Delta programming indicates that the system has considerably less margin at the present time. It is a reasonable assumption that the 25% margin could be achieved by reworking equations and sample frequencies to reflect Scout accuracy requirements.

TABLE 14.- COMPUTER SIZING AND TIMING ESTIMATES

	GIMBAL SYSTEM					STRAPDOWN SYSTEM				
	TITAN IIIC		SCOUT			DELTA		SCOUT		
	Inst	Data	Inst	Data	Total	Inst	Data	Inst	Data	Total
Major cycle										
Navigation	442	127	442	127		889	411	442	127	
Guidance	2480	480	1836	350				1836	350	
Executive	267	44	240	36		345	57	240	36	
Orthonormalization (strapdown only)	--	--	--			94	13	94	13	
Minor cycle										
Telemetry	245	27	200	20		230	23	200	20	
Executive	339	21	160	10		345	57	345	57	
Attitude control	109	13	109	13		372	21	372	21	
Inertial reference (strapdown only)	--	--	--	--		156	121	156	121	
Math subroutines	131	10	131	10		200	47	200	47	
Ground										
Alignment	105	16	105	16		210	40	210	40	
Check out & calibrate	1548	258	--	--		--	--	--	--	
TOTAL			3223	582	3805	2841	790	4095	832	4927
Self check (optional)	195	41	195	41		230	115	195	41	

	GIMBAL SYSTEM		STRAPDOWN SYSTEM	
	TITAN IIIC	SCOUT	DELTA	SCOUT
	25 sps	50 sps	50 sps	50 sps
Add time	8 μsec	24 μsec	6 μsec	6 μsec
Multiply time	92 μsec	250 μsec	22 μsec	22 μsec
Divide time	138 μsec	300 μsec	40 μsec	40 μsec
Margin	80%	25%	less than 34%	25%

Market Survey

The final task prior to selecting candidates for the Scout guidance computer is that of examining the existing market. A field of approximately 100 computers was examined. From this field, those machines that were deemed possible candidates have been catalogued into a matrix with pertinent characteristics listed for each candidate. In compiling the data, an effort has been made to include all machines exhibiting characteristics that could qualify them for the Scout problem. This matrix, included as table 15, lists the 35 computers that are considered possible machines for use on Scout.

Leading Candidate Selection

The leading candidates were selected from a list of 35 computers. Table 16 lists seven leading candidates for the gimbaled system application. Table 17 lists seven leading candidates for the strapdown system application. It should be noted that all strapdown candidates can also qualify for the gimbaled system application.

A number of computers are in production status and these can be adapted to Scout with special considerations for power, input/output, qualification environments, and exact memory size. Final computer selection from this list should be made from a competitive RFP activity.

Computer Word Length

In all but a few places, the 24-bit single precision data word meets accuracy and range requirements for both the gimbaled IMU and the strapdown IMU problem.

The choice of a computer word length of 16 bits will require an increase of 200 to 300 data words to handle the gimbaled IMU problem. This is due to a large number of parameters and variables that would require more than 16 bits for accuracy and range. A reduced instruction word would shorten the operand field and thereby cause the instruction count to be increased. (See paragraphs on *Timing*. An increase of 200+ words would jeopardize the possibility of using a 4K memory for the gimbaled IMU approach as the memory size is already at 3800 words. The double precision arithmetic capability becomes a firm requirement when the word length is reduced to 16 bits.

In the case of the strapdown approach, timing margins become a serious problem. This case already has a large computational load and any increase would force the use of a faster machine than the one specified in the paragraph on *Computer Speed*. This computational load increase is due to the increase in the number of required instructions as described by paragraphs on *Timing* since the 16-bit computer, with index registers, will traditionally employ an 8-bit operand.

Computer Requirements Summary

	GIMBAL SYSTEM	STRAPDOWN SYSTEM
Instruction execution		
Add	24 μsec	6 μsec
Multiply	250 μsec	22 μsec
Divide	300 μsec	40 μsec
Word length	24 bits or 16 bits with an increase of 200 to 300 words and double precision	24 bits
Memory size	3805 words	4927 words
Instructions	20 minimum	26 minimum
Weight	28 pounds (includes 0.033 lb/watt power conversion)	28 pounds (includes 0.033 lb/watt power conversion)

TABLE 15.- MATRIX OF CANDIDATE COMPUTERS

Computer and manufacturer	AC Electronics						AMBAC Industries	
	Magic 301	Magic 311	Magic 321	Magic 331	Magic 341	Magic 351	1801	1808
Description	Serial, fixed point	Serial, fixed point	Serial, fixed point	Parallel, fixed point	Parallel, fixed point	Parallel, fixed point	Serial, fixed point	Parallel, fixed point
Application	SRAM	707, 747			Shuttle	Carousel IV		
Integrated with IMU	KT-70	Carousel IV				Carousel IV		
Date of working hardware	1967	1967	1966	1967	Development	1970	1966	1969
Number of units built	200	670					400	
Number of instructions	11	28	22	23	16	61	18	56
Word length, bits								
Data	16	24 + 2 parity	31 + parity	31 + parity	16	19	18	18
Instruction	8	12 + parity	15 + parity	15 + parity	16	19	18	18
Instructions times, µs								
Add	24	19	15	4.5	5 3	6	18 (12)[b*]	6.6
Multiply	96	104	121	34.5	20 18	24	342 (200)[b]	26.4
Divide	280	332	323	94.5	20 18	30	342	26.4
Addressing								
Direct	To 2K	Yes	To 512	To 512	To 2K To 2K	Yes		To 4K
Relative	Transfer	Yes				Yes		No
Indirect	No	Yes			No No	Yes		Yes, multiple
Indexed	No	No		Yes	Yes Yes	Yes		Yes
Index registers, notes				3	1 1	*8 incl* IR, PC		*3 (15 bit)*
Memory								
Type	DRO core	DRO core	DRO core	DRO core	DRO core MOS	DRO core	DRO core	DRO core
Word size, bits	8	13	32	16	16 16	19	18	18
Min size, words		6K	4K	4K	2K 2K	4K	4K	4K
Max size, words	2K		32K	32K	65K 65K	32K	32K	32K
Cycle time, µs	4	2.6		3	2.5 1.7	3	3.3	3.3
Input/output								
Number of channels	3	1	1	1	1		2	Parallel, serial
Numver of interrupts	1	1	3	1	Multiple nested	8	1	1, priority
A/D, D/A	Yes	Yes			Yes		Yes[c]	
Physical characteristics								
Weight, lb	5	22	23	23	10	22	5.75	9
Size, cu ft	0.08	0.44	0.44	0.35	0.35	0.44	0.07	0.2
Size, in.xin.xin.	4.9x3.2x8.8				4x7x15	4.875x?x7.625		7.5x5x5.875
Power, W	45	110	120	115	50	120	30	85
Hardware	TTL IC	TTL IC	IC	IC	IC	TTL MSI	TTL IC	TTL IC
Cooling	Cold plate	Forced air			Air, cold plate	Air		
Weight, size, power includes	2Kx8, CPU, I/O	PS, 9 I/O Modules	8Kx32, CPU		4K, CPU, PS, I/O card	16K, CPU, PS I/O card		CPU
Qualification	MIL-E-5400 Class 2	MIL-E-5400 Class 2			MIL-E-5400 Class 2	MIL-E-5400 Class 2	MIL-E-5400	MIL-E-5400
*Comments (see last page of table)					a	Double precision instruction	c	Direct memory access
Options						24 bits + parallel	Fast clock	

TABLE 15.- MATRIX OF CANDIDATE COMPUTERS - Continued

Computer and manufacturer	Autonetics				Bendix		Bunker-Ramo	Control Data
	D200-1	D200-10	D200-15	Micron	BDX 820	BDX-900 (910)	BR-1018	469
Description	Parallel, fixed point	Parallel, fixed point	Parallel, fixed point		Parallel, fixed point	Parallel, fixed point	Parallel, fixed point	Parallel, fixed point
Application					Pershing	Lockheed 53A		
Integrated with IMU				SD/ESG	Yes	Strapdown MK30 torpedo	NIP-140	
Date of working hardware	1969	Development	Development				Development	Development
Number of units built							43	
Number of instructions	35	35	66	24	108	70	66	42
Word length, bits								
Data	24				16	16	18	16
Instruction							18	16, 32
Instruction times, μs								
Add	8	2	2	2	2	6 (2)	5	2.4
Multiply	108	11	11	8	9.5	63 (21)	33	10.4
Divide	112	19	19	28	9.5	86 (29)	43	30.4
Addressing								
Direct	To 32K	To 32K			To 512	To 512	To 8K	To 400
Relative					No	No	No	No
Indirect					Yes	Yes, multi-level	Yes, to 131K	Yes
Indexed	Yes				Yes	Yes	No	Yes
Index registers, notes	3					10 GP Accumulators		16
Memory								
Type	MOS	MOS	MOS	MOS	Core NDRO ROM	Core NDRO	NDRO plated wire	Plated wire
Word size, bits	24	16	16	24	16 16 16	16 16	18	16
Min size, words	4K	4K	4K		4K 2K 64	4K 256	4K	512
Max size, words	32K	32K	32K		16K	32K	131K (12K mainframe)	65K
Cycle time, μs	4	1		1	2 1 1	3 3 (1)	1	1.6 read, 2.4 write
Input/output								
Number of channels						I/O bus, DMA	3	2
Number of interrupts	4	64			Expand to 32	Expand to 256	9[e*]	3
A/D, D/A						Yes		Yes
Physical characteristics								
Weight, lb	6	4	0.5	0.56	12	2.5	4.5	2.5
Size, cu ft	0.074	0.05	0.0046	0.026	0.166	0.064	0.04	47 cu in.
Size, in.xin.xin.			2x2x2		7.5x9.1x7.5	6.6x6.75x2.5	2.5x5.5x7.75	
Power, W	10	15	10		40	15	40	15
Hardware	MOS	MOS			TTL	MOS, TTL	MOS LSI	PMOS LSI
Cooling								Conduction, radiation
Weight, size, power includes	4K, CPU, PS		CPU, PS, cooling		CPU, memory	Processor, 2K NDRO	4K, CPU	8K, CPU
Qualification						MIL-E-5400 Class 2	MIL-E-5400 Class 2	MIL-E-5400 Class 2
*Comments (see last page of table)		d	Dimensions vary with memory size		Microprogrammed	Micro-programmed Data in parentheses apply to BDX 910		f
Options		24 and 32 bit word available						

TABLE 15.- MATRIX OF CANDIDATE COMPUTERS - Continued

Computer and manufacturer	General Electric	Honeywell					IBM		Kearfott
	CP24A	HDC-201	HDC-250	HDC-301	HDC-401	HDC-501	4π/SP1	4π/SP101	SKC-2000
Description	Parallel, fixed point	Parallel, fixed point	Parallel, fixed point	Parallel, fixed point	Parallel, fixed point	Parallel, fixed point	Parallel, fixed point	Parallel, fixed point	Parallel, fixed. point
Application	Proposed for Viking	DC9, F4			ATS	Agena	Proposed for Preshing	Proposed for Viking	Aircraft
Integrated with IMU			H478						
Date of working hardware	Development	1969	Brassboard 1970		Develop-ment	1966	Development		Development
Number of units built		100				17			5-10 within 6 months
Number of instructions	53	33	15			53	41		113
Word length, bits									
Data	24 + parity	12	24	16 & 32	16	20	16		32
Instruction	24		16	16	16	20	16		16 & 32
Instruction Times, μs									
Add	3.75	9	2.9	5	10	4	2.7, 4.7 DP	5	2.62
Multiply	30.5	100	12.5	21	90	24	5.7		5.32
Divide	44.75		37.6 (software)	65	160	24	8.0		8.12
Addressing									
Direct	To 16K		To 2K	To 2K	16K		To 512		To 131K
Relative	No		No		Yes		Yes		Yes
Indirect	Yes		No		Yes		Yes		Yes
Indexed	Yes		Yes	Yes			Yes		Yes
Index registers, notes	6 of 8 hardware registers		1	1			1 (base register) Tally		88
Memory									
Type	Plated wire	IC ROM IC ROM LSI	ROM RAM Plated wire	MOS Plated wire	NDRO plated wire	DRO core	DRO core	Core	DRO core
Word size, bits	25	12 12 12	24 24 24	16 16	16	20	16		16/32
Min size, words	8K	1K 256 32	256 64 2K	16 4K	2K	2K	4K		4K
Max size, words	32K	4K	2K total (expand by bank)	16K		16K	16K		131K
Cycle time, μs	0.5 read, 1.0 write	0.9 0.9 0.9	0.9 0.75 1	0.9	0.65	2	1.33		1.9
Input/output									
Number of channels	Serial, parallel		Special for missile G&C	1	1	5	Parallel, DMA, buffered I/O	Parallel only	64
Number of interrupts	120, priority			1	4	1	1 hard or soft priority		16
A/D, D/A			Yes				Yes		Yes
Physical characteristics									
Weight, lb	20	5.5	1.6	3.3	13	28	18.1, 21.7(16K)		19.7
Size, cu ft	0.55	0.217			0.17	0.49	0.35		0.32
Size, in.xin.xin.	9.5x10.5 x9.55		7.25x3.5x2	7.56x4.85 x6.5		92	4.1x10.1x3.6		7.5x4.88 x15.33
Power, W	36 (100% duty)	25			11.5		72 (100% duty)	30	245
Hardware	PMOS LSI, TTL	TTL	LP TTL	Low V_T PMOS; LSIC		DTL IC	TTL, MSI	LP TTL	
Cooling							Air, cold plate		Air, cold plate
Weight, size, power includes		4K, CPU	CPU, 1 I/O, memory, motherboard	g			CPU, 4K, PS	CPU, 16K, PS	8K, 3 card I/O
Qualification	30 g shock, 19.5 g ac-celeration, 7.5 g vibration			MIL-E-5400 Class 2			MIL-E-5400 Class 2		MIL-E-5400 Class 2
Comments	5 W, 5% duty cycle, micro-programmed, DMA	Same I/O structure as DDP-516	Alternative package, cylinder 13 in. dia x 2.5 in.	g	h	Double preci-sion add	Environmental test 1971 30 g ac-celeration no problem	LP version of SPI tailored for Viking	No space qualifi-cation planned
Options	Programmed counter, watchdog timer	18-bit word			Core memory, read only memory				LSI scratch pad pro-vides 0.75 μs add, 4.0 μs multi-ply

TABLE 15.- MATRIX OF CANDIDATE COMPUTERS - Continued

Computer and manufacturer	Lear Siegler		Litton Industries		Northrop	Raytheon	Teledyne		Westinghouse	
	LS-50	LS-51, LS-52	SPIRIT 1	LC-XX	NDC-1071	RAC-251	Series 20000	TDY-300	OBP	MILLI
Description	Parallel, fixed point	*Parallel, fixed point*	Parallel, fixed point		Parallel, fixed point	Parallel, fixed point	Parallel, fixed point	Parallel, fixed point	Parallel, fixed point	Parallel, fixed point
Application	Instrumentation 747, TAT	A4H aircraft	DC 10			Air Force	Airborne	Centaur, Delta	Orbiting Astro observatory	
Integrated with IMU		Kearfott								
Date of working hardware	1969		1971	Development		1970	1967	1970	1968	Development
Number of unit built	200	40	20					4	2	8
Number of instructions	32	44; expand to 64	40		31	123	29	42	55	16
Word length, bits										
Data	16 & 32	16 24 32	24		16	32	20	24	18	16
Instruction	16	16 16 16	16 to 24			16 & 32		24	18	16
Instruction times, µs										
Add	34	6 6.4 6.8	4	3.5	3	2.8	8	6	6.25	3 to 6
Multiply	184	13 17 21	16	20	20	14	32	22.5	45	17
Divide	184	29	16.5		50	26.4	41	40	90	17
Addressing		16K								
Direct	To 16K	No	To 1K			To 65K		To 131K	To 64K	To 256
Relative									No	256, 8-bit block reg
Indirect	Yes	Yes, multilevel	Yes			Yes			Yes	No
Indexed	Yes	Yes	Software			Yes	Yes	Yes	Yes	Yes
Index register, notes	Any of 64 file registers	Any of 32 file register				3 3 of the 4 accumulators serve as index registers	3	3	1	1
Memory										
Type	MOS DRO MOS ROM core	MOS ROM DRO core MOS	DRO core	DRO core	DRO core	DRO core	DRO core	DRO core	DRO core	ROM RAM Core
Word size, bits	16 16 16	16/24/32 16/24/32 16/24/32	24		16	32	20	24	18	16 16 16
Min size, words	2K 1K 64	1K 1K 8	2K		4K	4K	1K	4K	4K	4K 1K 4K
Max size, words	16K 8K	8K MOD 32	65K		16K	64K	8K	65K	64K	64K
Cycle time, µs	2 2 0.05	2 2 0.05	2	1	1	1.8	4	3	2	1 1 1
Input/output										
Number of channels		16 SER, 32 discrete I/O	Parallel, DMA		1	1	4	5	1	Many cards available
Number of interrupts		Multilevel, soft mask	8			3 priority; 8 hardware or 256 software			16	
A/D, D/A		Yes	Yes			Yes		Yes	No	Yes
Physical characteristics										
Weight, lb	11	10	15	18	16	40	12	25	20	5
Size, cu ft			0.39	0.27	0.27	0.23	0.18	0.27	0.3	
Size, in.xin.xin.		7.6x3.6x12.5	4-7/8 x7-5/8 x14							18 dia x 1
Power, W	50	50	118	150	150	165	70	110	35	4 to 12
Hardware		TTL	TTL IC	MOS LSI	IC	Bipolar LSI	IC	Hybrid LSI	LP DTL IC	TTL MSI
Cooling		Air	Air			Wax plate			Air, cold plate	Cold plate, 150°F 20 min
Weight, size, power inclues		4Kx32 MOS ROM	8K core, CPU, I/O	8K, CPU	4K, CPU	4K, CPU, PS, I/O, Wax plate			4K, CPU	4K ROM, 1K RAM, CPU
Qualification	*MIL-E-5400* Class 2	*MIL-E-5400* Class 2	MIL-E-5400 Class 2	*MIL-E-*5400 Class 2		*MIL-E-5400* Class 2			*NASA*[h]	To third stage Scout requirements
Comments (see last page of table)	Reg to reg times: 21 µs add, 116 µs multiply and divide	LS-52 is larger version of LS-51	Double precision add, subtract	Hardware by end 1971	Microprogrammed	Microprogrammed[i]	One of a series	j	Double precision	Microprogrammed, 20, 24 bits possible[i]
Options			1 µs & 0.5 µs memory, parity		Floating point hardware	Plated wire memory, direct memory access				

TABLE 15.- MATRIX OF CANDIDATE COMPUTERS - Concluded

COMMENTS:

[a] Microprogrammed instructions availabe. Standard I/O signal conditioning modules available. Can be space-qualified 10 months after receipt of order.

[b] Instruction times in parentheses achieved with optional fast clock.

[c] A/D and D/A cards available, but not qualified to same level as computer.

[d] Four instruction codes available for special functions.

[e] Interrupt priority software controlled. Direct memory access provided. Computer subassemblies tested to 100 g.

[f] Delivery of first unit scheduled for June 1971. Double precision add time, 3.6 μs. Must remove all C-MOS and plastic for space qualification: 12 to 15 months required. I/O structure similar to Honeywell DDP-516.

[g] Weight, size for 5.2K MOS memory. For 4K plated wire = 7.56 x 3.25 x 12.56, 4 lb. Has double precision instructions, add time 10 μs.

[h] Real-time simulator available on DDP-516. Memory power at 5 μs cycle time = 30 W.

[i] Register-to-register add - 1.8 μs, multiply - 13.3 μs, divide - 25.9 μs. Raytheon expecting space qualification contract soon. If received, no one-time development charge will be necessary

[j] Weight given for radiation cooling. Lighter models possibly available.

[k] Qualification specifications:

1) NASA SO-S345-1;
2) Memory (core) EMI TA902020269 (Electronic Memories Inc.);
3) OBP functional test procedure;
4) Sinusoidal vibration - 4 octaves/minute all axes,
   5 to 20 Hz, ½ in. double amplitude,
   20 to 100 Hz, 10 g,
   110 to 2000 Hz, 5g;
5) Random shock - 2 minutes/axis,
   0 to 15 Hz, 0.01 g^2/Hz,
   15 to 70 Hz, 0.31 Hz g^2/Hz linearly increasing,
   70 to 100 Hz, flat,
   100 to 400 Hz, 0.02 g^2/Hz linearly decreasing,
   400 to 2000 Hz, flat;
6) Shock-axis,
   X
      2 shocks 30 g, 6 ms,
      2 shock 30 g, 12 ms,
   Y, Z
      2 shocks 15 g, 6 ms,
      2 shocks 15 g, 12 ms;

[ℓ] Some versions of Milli delivered. Low-power version in production.

TABLE 16.- LEADING CANDIDATE COMPUTERS FOR GIMBALED IMU APPLICATION

NAME	APPLICATION	PRODUCTION STATUS (units)	WORD LENGTH	SPEED			WEIGHT	POWER	TOTAL WEIGHT*
				ADD	MULTIPLY	DIVIDE			
Delco, Magic 311	707, 747	670	24	19	104	332	22	110	25.7
Arma, 1801	--	400	18	12	200	342	5.75	30	6.75
Lear-Siegler, LS-50	747, TAT	200	16/32	34	184	184	11	50	12.7
Bunker-Ramo, BR1018	--	43	18	5	33	43	4.5	40	5.8
Honeywell, HDC-401	ATS	--	16	10	90	160	13	11.5	13.38
Honeywell, HDC-402	Viking	--	24	10	97	142	21	30	22
Bendix, 820	Pershing	--	16	2	9.5	9.5	12	40	13.3
Bendix, 900	Lockheed 53A MK30 Torpedo	--	16	6	63	86	2.5	15	3.0

*Total weight includes computer weight plus battery weight to support a one-hour mission.

TABLE 17.- LEADING CANDIDATE COMPUTERS FOR STRAPDOWN APPLICATION

COMPUTER	APPLICATION	PRODUCTION STATUS (units)	WORD LENGTH	SPEED			WEIGHT	POWER	TOTAL WEIGHT*
				ADD	MULTIPLY	DIVIDE			
Teledyne, TDY-300	Delta Centaur	4	24	6	22.5	40	25	110	28.7
Litton, Spirit I	DC10	20	24	4	16	16.5	15	113	19
Lear Siegler, LS-51	A4H	--	24	6.4	17		10	50	11.5
Kearfott, SKC-2000	Aircraft	5-10	32	2.6	5.3	8.1	19.7	245	27.7
Delco, Magic 351	Carousel IV	--	24 (available)	6	24	30	22	120	26
Autonetics, D200-10	Development	--	24 (available)	2	11	19	4	15	4.5
GE, CP24A	Development	--	24	3.75	30.5	44.7	20	36	22

*Total weight includes computer weight plus battery weight to support a one-hour mission.

INSTRUMENTATION SYSTEM

This section summarizes the preliminary characteristics of a new instrumentation system for Scout. On the present Scout, vehicle operations are monitored by an 18-channel IRIG PAM/FM/FM system. This system cannot transfer the 40 analog, 38 bilevel, and 10 digital signals (summarized in table 18) necessary to instrument the improved guidance system. The PCM/FM system described here is more appropriate.

The telemetry system will consist of an airborne system that is compatible with the ground stations available at the launch sites. It will be in accordance with the requirements of the *IRIG Telemetry Standards 106-69*. Its purpose is to transmit data concerning the performance of the vehicle's systems and subsystems to the ground for monitoring and analysis.

Airborne system.- The airborne system consists of a multiplexer-converter, a transmitter, and an antenna system. The multiplexer-converter's function is to perform a time division multiplex of the analog, bilevel, and digital signals; to convert the analog signals and the bilevel signals to digital words; and to assemble these words into a pulse code modulation (PCM) serial data stream. The transmitter is a 5-watt S-band FM transmitter that produces an FM signal in response to the filtered PCM input signal. The antenna system provides the proper pattern for transmission of the data to the ground.

Data for transmission.- Table 18 is a preliminary list of data to be telemetered. The analog and bilevel data are sampled at a rate commensurate with the bandwidth of the signals, and the digital signals will be transferred into the system at an adequate rate for monitoring the IMU and computer performance.

Data conditioning.- The multiplexer-converter is the data conditioning equipment. It includes the circuitry for sampling the analog and bilevel signals, for analog-to-digital conversion, for formating, for interleaving the converted signals, and for filtering the PCM output.

The format generator determines the sampling rates of the various signals. It can be synchronized to the computer clock and the computer minor and major cycles. This provides efficient transmission to the ground of the computer's information inputs, its command outputs, and other pertinent data regarding the computer's performance.

The signal multiplexing portion of the multiplexer-converter should be low-powered and specifically designed for the requirements. The reason for a custom design is to conserve weight and power.

The analog-to-digital (A/D) converter converts the sampled analog signals to a representative digital code. The A/D converter will be low power consuming about 100 milliwatts.

TABLE 18.- TELEMETRY SIGNAL LISTING (PRELIMINARY)

Item	Quantity	Type	Description
1	2	Analog	C/D receiver signal strength
2	3	Analog	H_2O_2 pressure
3	3	Analog	N_2 pressure
4	2	Bilevel	C/D receiver channel 4
5	1	Bilevel	Heat shield eject
6	1	Analog	Base A hydraulic pressure
7	1	Analog	FW-4S nozzle shield temperature
8	1	Analog	Castor nozzle pressure
9	1	Analog	Base A ambient temperature
10	1	Analog	Upper B ambient temperature
11	1	Analog	Lower D-section ambient temperature
12	1	Analog	Guidance, 400 Hz ac power
13	4	Analog	Fin position
14	4	Analog	Roll motors
15	2	Analog	Yaw motors
16	3	Analog	Pitch motors
17	4	Analog	Headcap pressure
18	2	Analog	Ignition current
19	1	Analog	IMU temperature monitor
20	1	Analog	IMU TCA output
21	4	Analog	IMU power supply voltages
22	1	Bilevel	SMRD discrete
23	1	Bilevel	IMU overtemperature
24	2	Digital	Inertial data
25	1	Bilevel	Computer clock
26	1	Digital	Computer serial output
27	3	Digital	Steering angles
28	3	Digital	Steering rates
29	1	Digital	Computer event word
30	8	Bilevel	Valve commands
31	3	Bilevel	Staging arm control
32	6	Bilevel	Motor ignition
33	1	Bilevel	Filter switching
34	1	Bilevel	Third-stage thrust reduction
35	2	Bilevel	Fourth-stage separation
36	2	Bilevel	Fourth-stage velocity vernier
37	2	Bilevel	Payload separation
38	6	Bilevel	Payload functions
39	1	Bilevel	Fourth-stage thrust reduction
40	3	Analog	Accelerometer outputs

Note: Total analog = 40,
total bilevel = 38,
total digital = 10.

The formatter's function is to control the output data sequence. It controls which, and at what rate, the analog and bilevel data are sampled, and when the digital data are accepted. The formater will be capable of being synchronized to the computer's clock and major and minor cycles.

The function of the filter for the PCM output is to reduce the bandwidth to the greatest extent possible and to provide a signal that is balanced around zero volts. The filter will be designed so that if the PCM bit stream consists of alternate ONEs and ZEROs, the output of the filter will be a sine wave. Thus, the highest frequency content will be one-half the bit rate. The balance is necessary for equal frequency excursions on either side of the center frequency of the transmitter.

The estimated size of the data conditioner is 8x4x4 inches and it will consume approximately 1 watt. The approximate weight will be 10 pounds.

Transmitter.- The transmitter will be an S-band FM transmitter with a minimum RF output of 5 watts. Several of these are available off-the-shelf from various manufacturers. An example is the Tele-Dynamics Type 1080A. It is small and has been designed for space and missile environments. It is 1 25/32 inches high, 3 9/32 inches wide, and 3 27/32 inches deep. It weighs approximately 20 ounces and will operate over the temperature range of -40 to +85°C. Maximum power consumption is 2 amps at 28 ± 4 volts.

Antenna.- The antenna system will be designed to produce the desired pattern and to be capable of being installed in the space available.

Ground system.- The ground system for telemetry will be the existing ground stations. Since the airborne system will be designed to meet the requirements of IRIG 106-69, there should be no difficulty in obtaining both real-time monitoring of various telemetered parameters and recording of the total telemetered data for later data reduction.

REACTION CONTROL SYSTEM SIZING

Background

The present Scout vehicle employs spin stabilization for attitude control of the fourth stage during the final burn and coast phase of the mission. This study of a proposed attitude reference unit or inertial measurement unit guidance package mounted on the fourth stage would preclude the spinning mode, necessitating a reaction control system for attitude stabilization. The system is designed to override the maximum torque disturbances anticipated. It must have this heavy-duty capability as well as a low-level efficient method of control used during the coast phase to simply effect attitude control. Another function is the adaptation of this system to correct the payload velocity after fourth-stage burn. The approach is discussed in more detail in the following section.

Sizing Considerations

Generally speaking, a reaction control system (RCS) is sized based on two criteria (sizing is the function used to identify such system requirements as weights, thrust levels, volume, and fuel). The criteria are:

1) The disturbing torques that the RCS jets must be capable of handling, thus sizing the jet thruster levels; and the hardware weights;

2) The deadband, or allowable angular excursions the vehicle will be rotated, will define the number of times the jets must be exercised. This will, in turn, size the amount of fuel needed to accomplish the task.

The remaining weights are functions of the bottle size, fuel lines, associated valves, regulators, etc.

Disturbance Torques

The major disturbing torques are:

1) Separation torques;

2) Ignition impulse torques;

3) Motor characteristics-generated torques,

   a) Thrust misalignment,

   b) Thrust offset;

4) Center-of-gravity offset torques;

5) Those needed to maintain a coast/limit cycle;

6) Those needed to effect a coast maneuver.

Separation torques.- Separation torques are caused by imperfections in the mechanisms used to jettison the third stage. The angular impulse imparted to the fourth stage can be expressed via a tipoff angle, originally obtained from the spin-stabilized system and defined as follows:

$$\text{Tipoff angle (rad)} = \frac{\text{angular impulse (ft-lb s)}}{\text{spin rate (rad/s) roll inertia (slug ft}^2\text{)}}$$

where the spin rate was the rotation of the fourth stage (150 rpm) and the roll inertia was 12 ft-lb s^2. Tipoff angles of 2.25° have been measured for separation, which yields an angular impulse equal to 7 ft-lb s.

Ignition impulse torques.- Another prethrust torque disturbance is caused by ignition impulse, the lateral thrust developed as the motor is igniting. It also is defined in terms of tipoff error and is about 3.5°, which reflects into an 11 ft-lb s angular impulse. The high-level reaction controls have a 65 ft-lb torque capability that will handle these prethrust impulses if they are on for a period of 0.2 second or more:

$$\frac{11 \text{ ft-lb s}}{0.2 \text{ s}} = 55 \text{ ft-lb.}$$

If they occurred in a shorter time, the torque would be greater than could be bucked out but the maximum excursion would be small (i.e., for 0.1 second, torque = 110 ft-lb, assuming no cancellation). Then

$$\alpha_{\text{fourth stage}} = \frac{110 \text{ ft-lb}}{68 \text{ ft-lb s}^2} = 1.62 \text{ rad/s}^2$$

$$\theta_{\text{fourth stage}} = \frac{1}{2} \alpha t^2 = 0.81 \ (0.01) = 0.0081 \text{ rad}$$

$$\theta = 0.0081 \text{ rad} \ \frac{57.3°}{\text{rad}} = 0.465°.$$

Therefore, the torques due to these angular impulses are small and are not the determining factor in sizing the vehicle torque disturbances.

Attitude hold torque requirements.- The torques needed to effect an attitude maneuver or a nominal deadband within which the vehicle would limit-cycle during the coast phases of flight are negligible as are the fuel requirements for these functions. The analysis supporting this follows.

The impulse needed to rotate an inertia of 44 ft-lb s (approximate fourth stage burnout inertia) 90° in 60 seconds would be

$$T\Delta t = I\Delta W = (44 \text{ ft-lb s}^2) \ \frac{(1.5°/\text{s})}{57.3°/\text{rad}} = 1.15 \text{ ft-lb s}.$$

Assuming a pulsing time of 1 second, 1.15 ft-lb of torque is needed plus another pulse of the same magnitude to cancel the rotation at the proper time.

The angular impulse required to maintain a ±1° deadband during coast using a limit cycle rate of 0.125°/s is

$$T\Delta t = I\Delta W = (44 \text{ ft-lb s}^2) \ \frac{(0.125°/\text{s})}{57.3°/\text{rad}} = 0.096 \text{ ft-lb s}.$$

Assuming a 5-pound jet at a moment arm of 0.75 foot (this will be shown to be part of the reference design), then

$$0.096 \text{ ft-lb s} = (5 \text{ lb}) \ (0.75) \text{ ft } \Delta t$$

and

$$\Delta t \approx 0.025 \text{ s}.$$

This corresponds to approximately the minimum pulsing time available and represents an impulse of (5 lb) (0.025 seconds) = 0.125 pound seconds that is needed twice every 16 seconds of coast. This implies an hourly impulse of

$$\frac{0.25 \text{ lb s}}{16 \text{ s}} \times 3600 \text{ s/hr} = 51 \text{ lb s/hr},$$

which is no more than a fraction of a pound of fuel and certainly does not imply a large torque capability.

This is presented to show that the major disturbances that will size the RCS thrusters are the motor characteristics and vehicle cg offset. Figure 22 describes these torques.

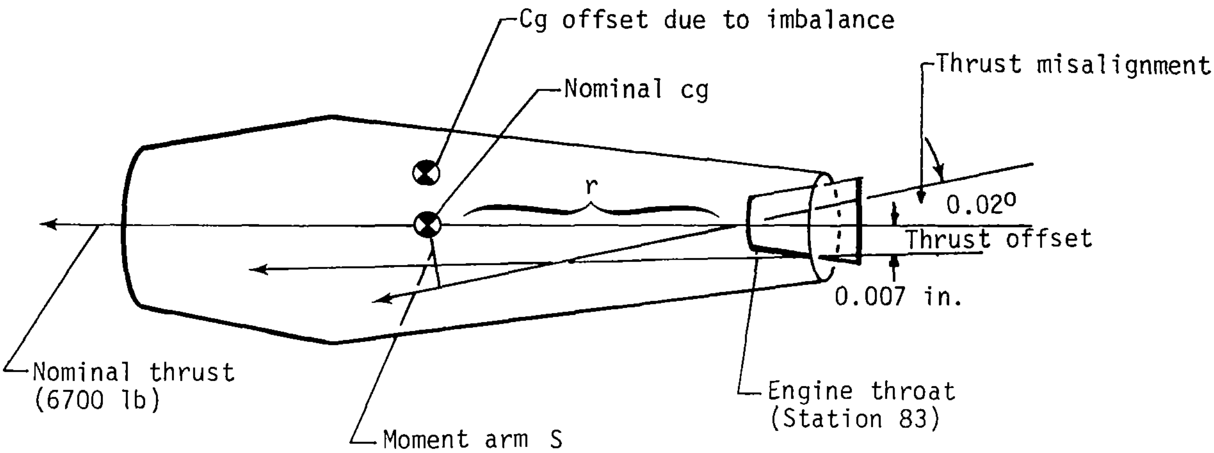

FIGURE 22.- TORQUE DISTURBANCES DUE TO FOURTH-STAGE MOTOR BURN

Motor-generated torques.- Values for errors induced by motor characteristics were obtained from United Technology Center (manufacturer of the FW-4S). The following numbers were quoted: 0.02° (3σ) of thrust misalignment and 0.007 inches of thrust offset (3σ). The cg offset torque is primarily a function of how well the cg can be maintained along the thrust axis during burn. The value of 0.1 inch was selected in light of previous experience.

The values used for 4th stage motor thrust misalignments and offsets agreed with those Convair used in their RCS design for OW-1 which featured a non-spinning FW-4S.

Torque due to misalignment of the thrust vector is equal to thrust (lb) multiplied by S, the moment arm due to the misalignment angle (0.02°):

$$S = r\theta$$

where r is the distance between the engine throat and the cg.

Using the largest value of r when the cg is forward,

$$r = 33 \text{ in.},$$

$$S = \frac{33 \text{ in.}}{12 \text{ in./ft}} \; \frac{0.02°}{57.3°/\text{rad}} = 0.00096 \text{ ft},$$

and

$$\text{torque} = 6700 \text{ (lb) } (0.00096) \text{ ft} = 6.4 \text{ ft-lb},$$

where 6700 lb represents an average thrust.

Cg offset torques.- The torque due to a thrust offset of 0.007 inch is:

$$6700 \text{ lb } \frac{0.007 \text{ in.}}{12 \text{ in./ft}} = 3.9 \text{ ft-lb.}$$

The torque due to a cg offset of 0.1 inch is:

$$6700\ (0.1/12) = 56 \text{ ft-lb.}$$

Disturbance torque summary.- The rss of these 3σ torques, with an added 10% safety factor, yields approximately 62 ft-lb of torque. It is not expected that this disturbance will be felt for any appreciable length of time since it represents an rss of three 3σ errors. Nevertheless it must be designed for since a torque of this level that was not taken out in 1 second would rotate the vehicle approximately 50° in this time. The maximum torque disturbance of 56 ft-lb is greater than the 500 in.-lb number quoted by Convair as the maximum they observed in their utilization of the FW-4S as a nonspinning fourth stage.

RCS Jet Selection

The RCS jet locations have been designated at approximately Station 97 (fig. 23), which yields a moment arm of 37 inches (97 - 60 in.) at Stage IV ignition and 46 inches (97 - 51 in.) at burnout. These values of cg location (60 and 51 in.) were arrived at via a weight calculation of the fourth stage, including a new RCS and guidance system.

It is therefore possible to use a blowdown system that reduces the thrust force of four pitch and yaw jets from 21 to 16 pounds over the 31 seconds of burn. This would yield a somewhat constant torque capability of about 65 ft-lb during the burn. Because some disturbances may be smaller, this value of torque is too large to be utilized for each disturbance. Therefore, a second set of pitch and yaw jets, henceforth referred to as the low-level jets, are added to provide a tighter limit cycle more efficiently. These jets can also be used in the orbital correction system described in the next section. The low-level thrusters can be added to this and preliminarily have been sized at 5 pounds of thrust mounted along the thrust axis. Figure 23 [illegible] a plan[illegible] view of the high- and low-level pitch and yaw thrust location [illegible] orientation.

The four high-level jets (J1, J2, J3, J4) are placed as far from the cg as possible to take advantage of the large moment arm. The design alternative would have led to mount the low-level jets in the same orientation as that of the high-level jets, which would allow a smaller [illegible] jet to be utilized to get the same torque capability. In other words, a [illegible] jet with a 4-foot moment arm yields about the same torque as a 5-pound jet [illegible] 75-foot moment arm. This was discarded for three reasons: (1) the [illegible] jets mounted along the roll axis would aid greatly in the orbital correction system option described in the next section and design commonality is felt to be desired if the cost in other areas is of low impact; (2) the 5-pound jets are no more costly in terms of weight and size than a smaller 1 to 2-pound jet; and (3) there is some ease in mounting gained by not constraining all the pitch and yaw jets to be firing along the same direction.

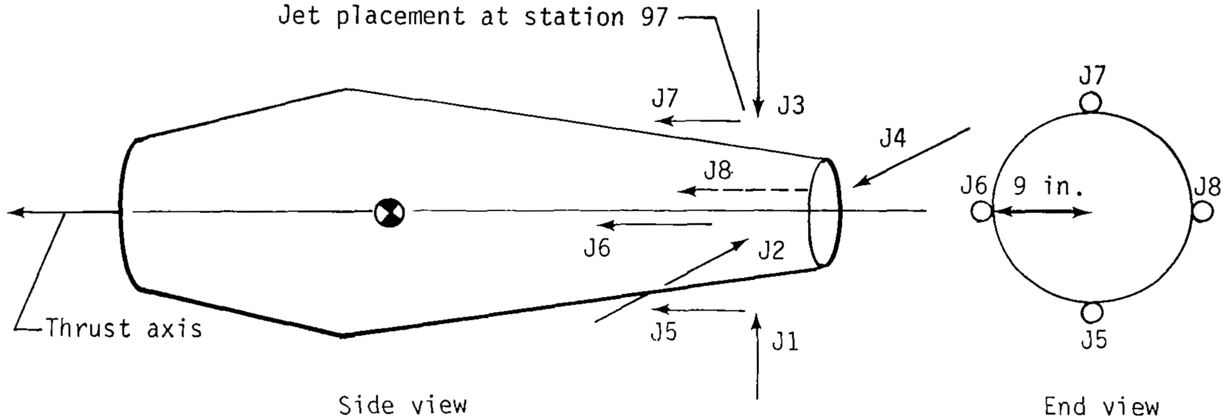

FIGURE 23.- HIGH-LEVEL AND LOW-LEVEL PITCH AND YAW LOCATION AND ORIENTATION

Fuel Considerations

This approach appears to be more costly in fuel since if the torque disturbances are much lower than expected they can be handled for the most part by the low-level thrusters. This would imply a five times more inefficient fuel usage since to obtain the same torque the 5-pound jet would be on all the time versus the 1-pound jet causing the impulse to be five times greater.

The logic behind this choice is as follows. The large amount of fuel sized for this mission, which is quite meaningful both in terms of its own weight and that of the tanks necessary to contain it, is determined by the high-level jets being exercised for a substantial time (high-duty cycle). As an example, suppose one high-level jet is on all the time. (It is remotely possible that two jets will be on in the case where the torque disturbance is distributed between two axes, but in this case they would be necessarily turned off and on since together they would overwhelm even the highest expected disturbance.) Then 21 pounds x 31 seconds is 651 pounds-seconds. At an I_{sp} of 140 seconds, about 4.7 pounds of fuel would be needed. If, on the other hand, only the low-level jets were needed, a 5-pound jet would be on all the time utilizing 1/4 of this total, or 1 pound. Had the 1-pound jet been employed, the fuel usage would have been 0.2 pound. In other words, while it appears 0.8 pounds of fuel might be saved, the design must consider that the low-level jets will be used very little in the worst case and therefore much more fuel will be loaded aboard than the difference between that consumed by the 5-pound jet as opposed to the 1-pound jet. Two pairs of 1-pound roll jets will be used to control the fourth stage in the roll axis.

As an example of the fuel necessary to take the vehicle through a 180° maneuver either for ΔV correction or for mission purposes, consider the rate necessary to rotate 180° in 140 seconds.

$$\Delta W = \frac{180°}{140 \text{ sec}} = 1.25°/\text{sec}$$

The angular impulse $T\Delta t = I\Delta W$. From this

$$\Delta t = \frac{I\Delta W}{T} = \frac{(44)\,\frac{(1.25)}{57.3}}{(5)\ (0.75)} = 0.25 \text{ sec}$$

Thus, a 5-pound jet pulsed for 0.25 second will rotate the vehicle 180° in 140 seconds at which time another 0.25 second pulse is needed to stop the rotation. The total impulse thus expended to rotate 180° and back is 4 (5 lb) (0.25 sec) = 5 lb/sec. This impulse at an ISP of 140 seconds will consume 0.028 pound of fuel and shows that isolated maneuvers use insignificant amounts of fuel.

A discussion of the ΔV increment caused by the 5-pound jets during coast control is presented in the succeeding chapter.

System Considerations

One major tradeoff will be the use of a regulator as opposed to a blowdown system approach. A first cut at a typical blowdown system approach is shown in figure 24. The parts for the system are listed in table 19.

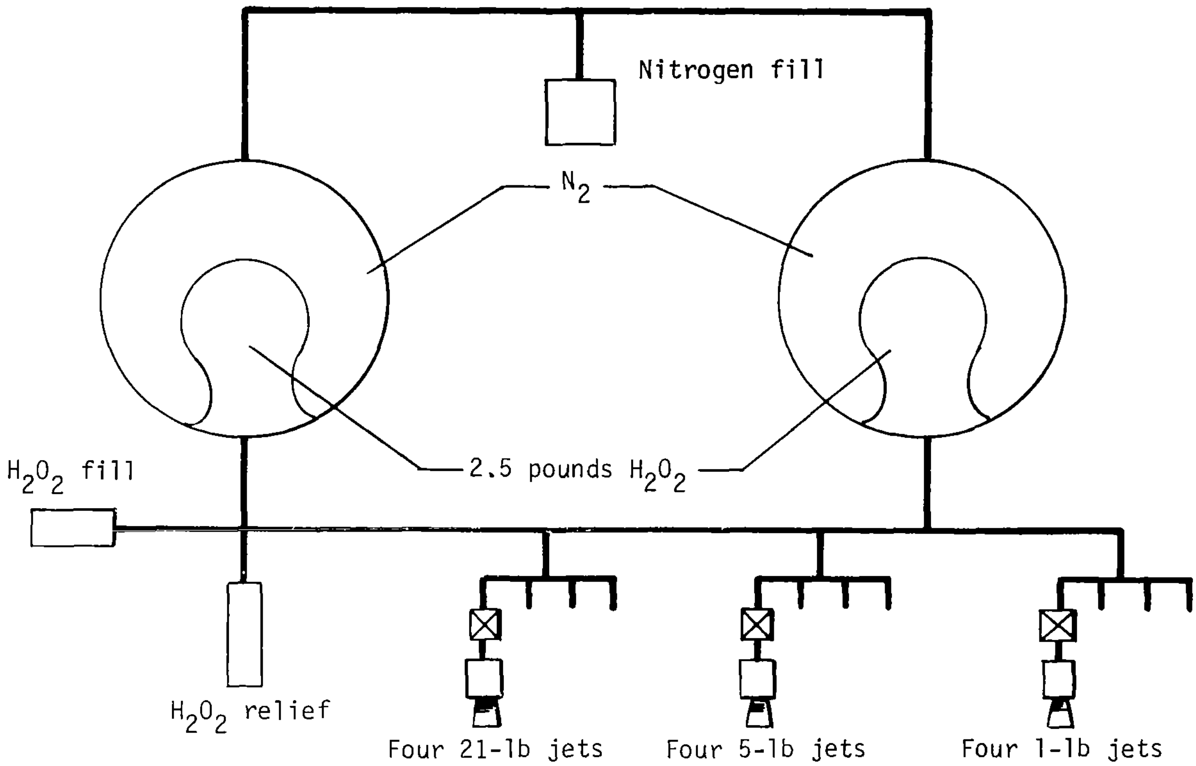

FIGURE 24.- TYPICAL BLOWDOWN REACTION CONTROL SYSTEM

TABLE 19.- PEROXIDE RCS WEIGHT SUMMARY (WALTER KIDDE CORP)

	Weight by unit (lb)	Total weight (lb)	Price ($)
Four 21-lb nominal motors (Burner II), P/N 875456	1.55	6.20	16 800*
Four 5-lb motors (2-lb nominal), P/N 875032	0.75	3.00	12 000*
Four 1-lb motors (2-lb nominal), P/N 875032	0.75	3.00	12 000*
One N_2 fill, P/N 893463	0.35	0.35	450
One H_2O_2 fill, P/N 893464	0.35	0.35	450
One H_2O_2 relief (P/N 874536)	0.29	0.20	1 100
Lines, fittings, miscellaneous		0.72	Assume supplied by NASA or integrator
Two H_2O_2 tanks, P/N 894193	3.8	7.60	6 800
H_2O_2 weight		5.00	
Approximate N_2 weight		0.45	
	Total	26.99	49 600.00

*This does not include design modifications of $1500 that would be necessary for drawing and specifications changes. This would not include development specification testing of the new component, and qualification would be by similarity to previous testing.

Table 19 costs do not include system analysis or development. Another factor was the design constraint of choosing flight-qualified parts. It was felt that a new design, specifically tailored to our needs, could optimize the weights from the present design of 27 pounds to approximately 20 pounds or a little less. This of course represents increased costs for new development and qualification. A ROM figure was unofficially quoted as an extra $50 000 to perform this function. This being a nonrecurring item, with the system recurring costs staying approximately the same.

Another approach considered was the use of a regulated system that could obviate the use of one of the fuel tanks. This would reduce the total weight by 3.8 pounds but would add one N_2 tank weighing 1.0 pound and costing about $625 and a regulator weighing 1.2 pounds and costing $2000. This approach saves 1.6 pounds but may make the system more difficult to balance because of asymmetry of the fuel tanks.

Although peroxide at this time represents the baseline approach (primarily due to commonality of fuel on other stages and the supporting equipment needed), a similar effort was made to size the same system featuring the use of other fuels. A nitrogen and hydrazine system is described in tables 20 and 21. The fuel for the systems differs as does the tankage to contain it because of the different specific impulses. Therefore hydrazine with an I_{sp} of 200 seconds requires 70% of the H_2O_2 system's fuel or about 3.5 pounds, while the nitrogen system, whose I_{sp} is 65 seconds, requires 10 pounds of fuel.

It is felt that the use of H_2O_2 is preferable from the commonality standpoint, and it represents a substantial cost saving item. Tables 20 and 21 show that there is no clear weight advantage in the hydrazine and nitrogen RCS systems, which supports the peroxide choice.

TABLE 20.- HYDRAZINE REACTION CONTROL SYSTEM WEIGHT SUMMARY (ROCKET RESEARCH)

	Weight, lb
Four 25-lb jets nominal (Titan IIIC Transtage)	11.1
Four 5-lb jets (REM-MONO, MR50)	4.8
Four 1-lb jets (MR6A)	2.0
Propellant (N_2H_4)	3.5
Propellant tank (9.5-in. diameter)	2.8
Fill and drain valve	0.6
Expulsion valve	0.5
Fuel lines	1.0
Total	26.3

TABLE 21.- NITROGEN REACTION CONTROL SYSTEM SIZING (STEHRER MANUFACTURING COMPANY)

	Weight, lb
Two "doubles" (one, 5-lb jet, one 25-lb jet)	5.50
Two "quadruples" (one 25-lb jet, one 5-lb jet, two 1-lb jets)	8.00
Pressure vessel	13.80
Pressure regulator	2.85
Nitrogen fuel	10.00
Total	40.15

Weight Tradeoffs

A significant factor to be discussed is the total weight of the RCS system, which at 27 pounds represents weight that, if reduced, would increase payload capability. The following paragraphs discuss a number of ways the system weight can be reduced and some of the ramifications that these weight-saving features generate.

The fuel calculation of 5 pounds was based on an estimate of one high-level jet being exercised continuously for the 31-second burn. This implies a rather conservative estimate of needed torque control. Based on mission analysis, the type of control logic employed and some probabilistic analysis as to how often these large disturbances occur will, to a much more accurate degree, provide a high probability of mission success and yet not oversize the system. This could eliminate on the order of 1 to 3 pounds of fuel.

The manufacturer of the reference system feels that if the constraint of using only flight-qualified equipment were lifted and a new design peculiar to the Scout application was initiated, approximately 3 pounds of weight could be saved in the tank and jet design. This will cost in the neighborhood of $50 000, depending on the requirements for qualification.

Since each of the two tanks used in the weight breakdown of table 19 weighs 3.8 pounds and has a 9-pound fuel capability, it would be possible to use one tank only for the 5 pounds of fuel and eliminate the other tank. However, two problems are associated with this approach. As more fuel is added to a tank and consumed during fourth-stage burn, the blowdown ratio is substantially increased. This would mean that the initial thrust of 21 pounds would decay to something probably less than half of this when most of the fuel was used up. This of course is an undesirable situation from the standpoint of a low torque capability toward the end of the burn. Also the use of one tank may cause an excessive balancing problem that will affect the cg offset and yield higher disturbance torques. A good insight into the practicality of this approach would be gained via the mission analysis where the probabalistic quantities resulting from cg offsets and subsequent fuel could be used in evaluating this approach.

Two pairs of roll jets are required so the roll torques can be applied in couple fashion since one roll jet would also cause a pitch or yaw torque. The elimination of one pair of these jets would save 1.5 pounds but add a small amount of fuel with which to buck out the unwanted pitch or yaw torque.

Summary

Based on these weight saving considerations and recognizing the corresponding implications, the weight of the peroxide system can be modified as shown in table 22.

TABLE 22.- MODIFIED WEIGHT PROFILE FOR THE PEROXIDE SYSTEM

	Weight (lb)
Four 21-lb nominal high-level jets	4.70
Four 5-lb jets (2-lb nominal)	3.00
Four 1-lb jets (2-lb nominal)	3.00
One N_2 fill	0.35
One H_2O_2 fill	0.35
One H_2O_2 relief	0.20
Lines, fittings, miscellaneous	0.72
One H_2O_2 tank	3.80
H_2O_2 weight	3.50
N_2 weight	0.45
Total	20.07

Table 22 demonstrates a 20-pound RCS system that can be realistically designed although the ramifications involved will have to be analyzed based on mission philosophy.

Figure 25 illustrates a reference RCS system.

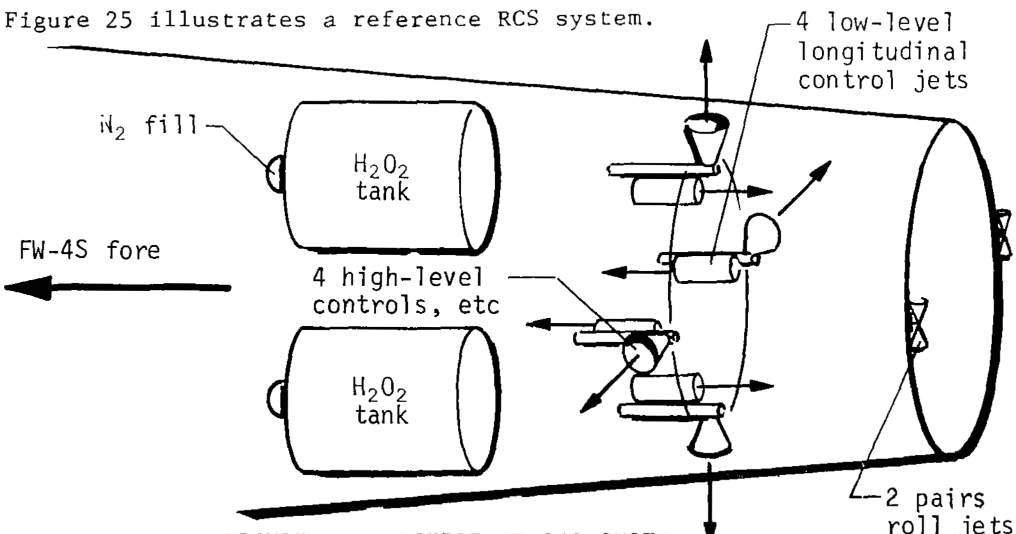

FIGURE 25 .- REFERENCE RCS SYSTEM

ORBITAL CORRECTION SYSTEM

Background

In the past NASA has had to accept open-loop Scout vehicle performance errors because of the lack of closed-loop guidance and also because the fourth stage has no means of thrust termination. With the addition of navigation equations it will now be possible to calculate the orbital errors and compute the ΔV required to place the payload in the proper orbit. This can be done despite the fact that the fourth stage will burn to depletion.

The fourth stage could be modified to shutdown on command and some methods that could be used to terminate fourth stage burn are venting ports and water quenching. It is felt, however, that the velocity errors can be compensated for by the selected RCS system. The gross sizing analysis presented in this section will only serve as an example of the thrusting philosophy and as an upper bound on sizing.

The basic approach of the ΔV correction involves using the RCS jets, which are normally used to take out disturbance torques, as the thrusters to add or subtract velocity.

After the fourth stage engine has burned out, the error in velocity (both magnitude and direction) can be computed from the accelerometer outputs. The low-level jets can be used to rotate the vehicle to the desired orientation at which time all of these low-level jets can be fired simultaneously to effect a thrust in the proper direction to yield the nominal vehicle velocity vector. At this point the vehicle can be rotated to its desired coast attitude and proceed in the desired orbit. Figure 26 depicts a typical jet placement scheme as sized for torque cancellation only. $(A, B, C, D)_1$ represent the high-level jets while $(A, B, C, D)_2$ depict the low-level jets. In this configuration it is of course not possible to apply a force along the X axis and perform a ΔV. For example, if the vehicle were rotated 90 degrees and jet A_1 fired, a large undesired torque would be applied about the Z axis.

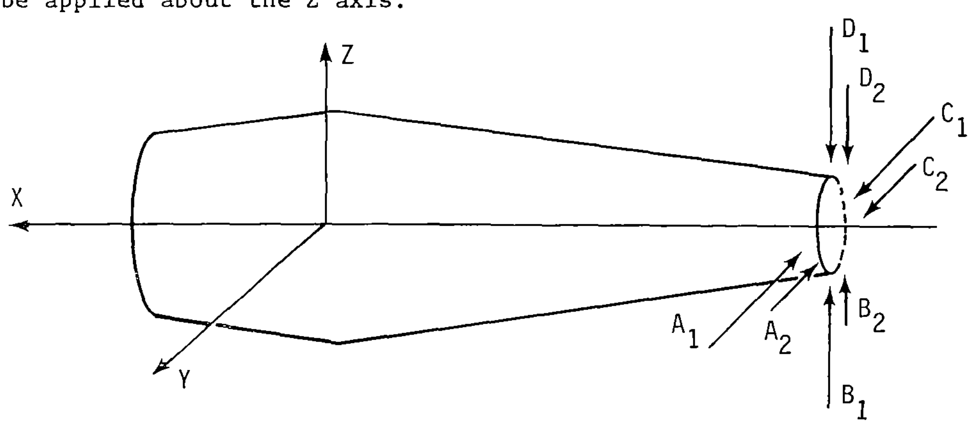

FIGURE 26.- STANDARD JET CONFIGURATION

Some other approaches to be considered are:

1) Canting the high-level jets at some angle to obtain both longitudinal thrust as well as torque cancellation;

2) Replaceing the $(A, B, C, D)_2$ low-level jets with longitudinally mounted thrusters;

3) Physically swiveling some or all of the jets.

Although the swiveled jet approach has been investigated and is certainly feasible, due to complexity, reliability problems, and cost in comparison to the other schemes mentioned, this approach was dropped.

Figure 27 demonstrates the canted approach.

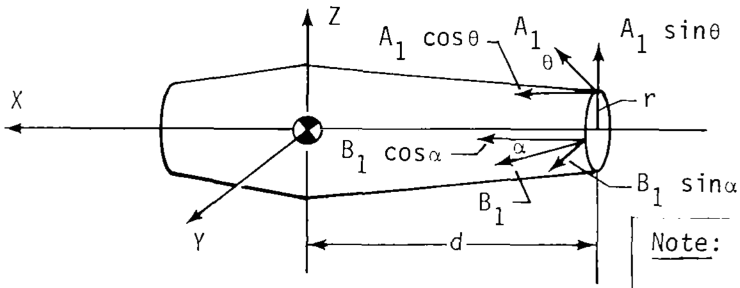

Note: Canted jets C_1 and D_1 are symmetrically located to A_1 and B_1.

FIGURE 27.- CANTED APPROACH

High-level jets such as A_1 and B_1 (for example) are canted by angles θ and α from the longitudinal axes of the vehicle while still being attached at the same point. It can be seen that both components of each jet provide rotational control. The total torque about the vehicle due to the high-level jets is

$$A_1 \cos \theta r\ (\hat{Y}) + A_1 \sin \theta d\ (\hat{Y}) + B_1 \cos \alpha r\ (-\hat{Z}) + B_1 \sin \alpha d\ (-\hat{Z})$$

$$+ C_1 \cos \theta r\ (-\hat{Y}) + C_1 \sin \theta d\ (-\hat{Y}) + D_1 \cos \alpha r\ (+\hat{Z}) + D_1 \sin \alpha d\ (+\hat{Z}) \quad .$$

A problem with this scheme is the fact that four large forces are canceling each other out during ΔV correction ($B_1 \sin \alpha$, $D_1 \sin \alpha$, $A_1 \sin \theta$, $C_1 \sin \theta$). Any differences in the forces between jets will result in undesired torques and will also be inefficient in terms of fuel usage. This leads naturally into analysis of the longitudinally mounted jets.

Using closed-loop guidance, the error in velocity to be corrected should theoretically be that of the guidance hardware only. In the case of Scout, however, the fact that the fourth stage engine cannot be shut down on command will be the primary contributor to the velocity error. Based on the perturbation analysis performed for the 1/6 mission, the three σ error for the fourth stage engine cut-off uncertainty was 160 fps. Using this velocity error as that to be compensated for and the fourth stage burnout weight of 322 pounds (211 lb + added guidance system weight minus some weight saving in the removal of the spin table), the impulse needed would be (approximately),

$$F\Delta t = M\Delta V = \frac{322 \text{ lb}}{32.2 \text{ ft/s}^2} (160 \text{ fps}) = 1600 \text{ lb-s}$$

At an I_{sp} of 160 for steady-state operation of the H_2O_2 motors, this correction would require 10.0 pounds of fuel. This, coupled with the 5 pounds needed for the RCS would total 15.0 pounds, which is almost the maximum fuel capacity for two 9-pound tanks. Therefore while it is possible to accommodate this, it is impractical from the blowdown ratio considerations. It must be remembered that 15.0 pounds represents two 3-σ high cases and is felt to be overly pessimistic. Once again a true evaluation of what is needed should be probabilistic in nature, implying that less total fuel would be carried. As an example, for a 1 σ case that would occur 67% of the time, only 3.3 pounds of fuel is needed instead of the 10.0 pounds originally calculated. This variation in itself will be more than enough to cause a system design change so that system definition is still very much a function of mission philosophy and constraints.

This discussion describes the technique used to size the fuel for a specific ΔV correction (53 fps, 1 σ). How much one wants to design for becomes a question of mission accuracy guaranteed in terms of some probability versus excessive weight. It is felt that the 5 pounds of H_2O_2 weight for motor torque cancellation will likely not be completely used (probably about half based upon Convair's usage) and can be utilized for orbital correction. A two-σ design will add 3.3 pounds to the total weight and ensure a substantially greater correction probability. One can decide to play greater capability against higher weight. As the fuel weight increases, the presently proposed tanks which are felt to be a realistic design optimizing weight and OCS (orbital correction system) capability, may have to be replaced. Larger tanks which will decrease the thrust reduction due to blow down will be necessary to maintain a high torque capability that protects against large mission attitude errors during fourth stage boost.

Figure 28 pictorially described the longitudinally mounted jet system.

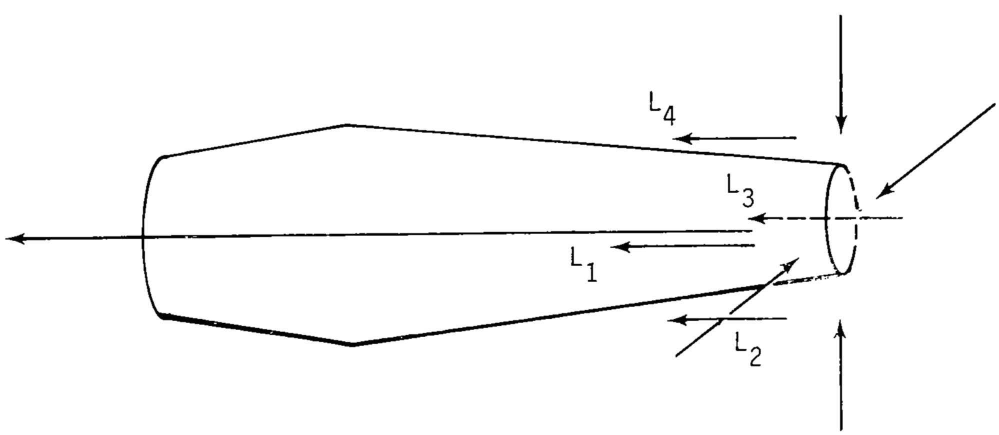

FIGURE 28.- LONGITUDINALLY MOUNTED SYSTEM

L_1, L_2, L_3, L_4 are the longitudinal jets and will have to be increased from 2 pounds of thrust to about 5 pounds to replace the low-level torque control of approximately 4 ft-lb. This is due to the moment arm going from a few feet to 0.75 feet. These four 5-pound thrusters will form the force used to perform the ΔV. Twenty pounds of force will take 80 seconds to yield the correct impulse (1600 lb-s).

The 5-pound thrusters used for coast control do cause a ΔV increment which is significant.

Assuming one uses the proposed ±1° deadband and a minimum on-time pulsing capability of the thrusters of 0.025 seconds. Then from

$$T\Delta t = I\Delta W,$$

$$\Delta W = \frac{T\Delta t}{I},$$

$$\frac{5\ (\text{lb})\ (0.75\ \text{ft})\ (0.025\ \text{sec})}{44\ \text{ft lb-sec}^2} = 2.12 \times 10^{-3}\ \frac{\text{rad}}{\text{sec}},$$

$$2.12 \times 10^{-3}\ \frac{\text{rad}}{\text{sec}} \times 57.3°/\text{rad} = 0.125\ \frac{\text{deg}}{\text{sec}} = \Delta W.$$

Therefore the limit cycle angular rate is 1/8 deg/sec and will take 16 seconds to rotate 2° (+1° to -1°). At this time a double pulse is needed to stop the original and start it back the other way. This requires a 0.050 sec Δt.

So that in the pitch plane 5 pounds (0.050 sec) is the linear impulse imparted to the vehicle every 16 seconds or 0.25 lb-sec every 16 seconds, which turns out to be 38 lb-sec every 45 minutes (coast time).

$$38\ \text{lb-sec will add a}\ \Delta V\ \text{of}\ \frac{F\Delta t}{m} = \frac{38\ \text{lb-sec}}{10\ \text{lb}\ \frac{\text{sec}^2}{\text{ft}}} = 3.8\ \text{F/sec}$$

A similar control system in the yaw plane will add another 3.8 ft/sec totaling 7.6 ft/sec. This must be studied to determine if it can be tolerated. One solution to this would be to mount the jets as shown in figure 29.

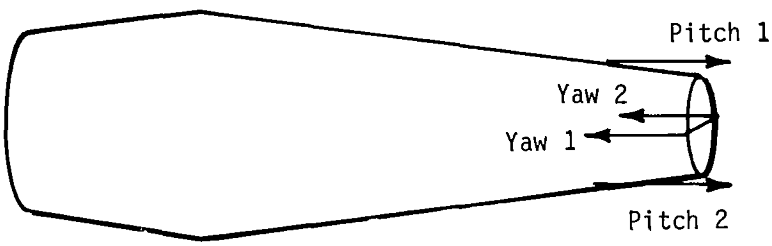

FIGURE 29 DIRECTION REVERSAL OF ONE PAIR OF LONGITUDINAL JETS

In this case, due to pitch and yaw coast control the ΔV would be cancelled. Of course only two jets could be used to provide ΔV correction which would double the impulse time. These two ramifications must be traded off to see their relative effect.

If a torque is developed due to differences in jet force, one or more of the jets (L_1, L_2, L_3, L_4) can be turned off for a short time to establish the proper attitude. This approach has been implemented on Titan and represents a simple, efficient scheme.

The capability to correct errors in velocity in any direction can be provided by rotating the entire fourth stage to the proper attitude.

The schematic of the RCS system is the same as the system described in the previous section with the addition of 3.3 pounds of H_2O_2 for a 1 σ orbital correction and the addition of 1 pound for nitrogen tankage.

The total tank volume (both tanks) is 384 in.^{3} and the pressure assumed at liftoff will be 580 psi.

The major problem associated with the blowdown approach is the amount of fuel needed for the fourth stage control during boost. If this is excessive the high-level thrusters will exhibit a low thrust toward the end of the burn. This will decrease control authority so that the attitude error of the vehicle will grow and cause large orbital inaccuracies. The blowdown effect upon the orbital correction system will mean a greater time to correct for ΔV uncertainty as well as increased maneuver and limit cycle times.

If the blowdown causes the longitudinal jet thrust to be reduced to 4 pounds (It will drop further during orbital correction.), and two jets instead of four are used to eliminate ΔV error due to coast thrusts, then the time to correct a 1 σ ΔV may increase from 40 seconds to 120 seconds or more.

Summary

A complete RCS system with an orbital correction capability weighs 20 pounds as shown in table 22 in the previous section plus 4.3 pounds for OCS fuel (1 σ) and nitrogen for a grand total of 24.3 pounds.

CLOSED-LOOP ERROR ANALYSIS

Performance analysis data are a very important part of the evaluation and comparison of guidance hardware. The Martin Marietta trajectory error analysis program (TEAP) is the tool used to compare the performance of the various candidate guidance systems. The TEAP allows computation of the errors in position, velocity, attitude, attitude rate, and other pertinent orbital parameters as a function of guidance hardware only. Since the closed-loop guidance will compensate for the state deviations of other perturbations, such as winds, I_{sp} variations, thrust errors, etc, and steer the vehicle to its desired state, the TEAP results will represent to a great degree the total system error. (Computational errors normally contribute only a few percent of the hardware errors.)

A reference trajectory is used as the flight profile to define nominal position, velocity, acceleration, orientation, and mass. Each candidate guidance system, representing only hardware errors, is another program input itemizing sources of error, (gyro drift rates, gyro misalignments, accelerometer bias, accelerometer scale factor errors, and misalignments). The TEAP program uses these hardware errors in conjunction with a nominal trajectory to generate vehicle errors such as position, velocity, attitude etc.

The basic TEAP computation sums the following hardware errors: those due to the imperfect accelerometers, those due to the misorientation of a perfect accelerometer because of platform drift (gyro imperfections), and those due to gravity computational errors. Another error computed by TEAP is attitude deviations due to drift phenomena. These error terms can be extended to provide deviations in orbital parameters, such as radius of perigee, apogee, flightpath angle, period, etc. The detailed computational algorithms and complete program inputs for TEAP are described in Appendix A.

Earth Orbital Trajectories - Six candidate systems were evaluated via the TEAP program using two basic reference trajectories supplied by NASA. One, the 176C mission, is a 585 to 635 nautical mile (near-circular) polar orbit launched from Vandenberg. The second flight profile is the 169C, an elliptical near-polar orbit (102 deg inclination). This trajectory information was supplied with data presented in a coordinate frame that differed somewhat from the TEAP frame. The TEAP program was modified to accept the trajectory information directly, avoiding transcription errors.

Lunar Mission Trajectories - As part of the lunar portion of the study, in which the errors and corresponding fuel requirements to perform the necessary correction for a lunar mission from injection to the moon are analyzed, a covariance matrix representing the errors associated with a lunar injection trajectory was generated via TEAP. This output was used as input conditions for the STEAP program described in Appendix C. The lunar injection trajectory was provided by NASA and represented an optimum flight profile targeted to the proper injection state. These data were generated by the TOLIP program at NASA. TEAP was modified to accommodate the TOLIP output as described in the following paragraphs.

The TEAP program requires position, velocity, and sensed acceleration on vectors in an inertial Greenwich meridian (S)/North Pole right-handed coordinate frame. Roll, pitch, and yaw unit vectors in the above frame are also required for strapdown error analysis and for presentation of attitude errors output in a body-axis frame.

The TOLIP outputs had to be converted to the above requirements. Geocentric latitude, longitude, and radius were used to generate the Cartesian coordinate inertial position vector (after converting through to inertial longitude using time and the earth's angular rotation rate). Inertial velocity, inertial flight-path angle, and azimuth of the inertial velocity vector were used to generate the three Cartesian coordinates of the inertial velocity vector.

Platform gimbal angles were used as Euler angles to solve for the transformation matrix from initial body to instantaneous body attitudes at a later time. The roll, pitch, and yaw unit vectors thus formed were used in the formation of the sensed acceleration vector. Thrust and drag were used with weight to scale the roll unit vector, while lift and weight scaled the yaw unit vector. Simple addition of the above vectors formed the sensed acceleration vector. Notice that there can be no sensed acceleration along the pitch axis in this formulation. The TOLIP/TEAP adaptation was thus completed.

Error Analysis Results

Table 23 lists the six candidate systems analyzed and their respective hardware inaccuracies in terms of a 1 σ error budget. These were the error budgets used for input on the TEAP computer simulation.

Table 24 lists the 1 σ TEAP results with regard to each system's performance for each reference trajectory. These results, as previously mentioned, represent very closely the total vehicle performance state for closed-loop guidance. Table 25 demonstrates the overall performance superiority of the DIGS system, which is predominantly a function of its low accelerometer scale factor error and tight alignment accuracy.

Three of the other candidates, KT-70, TDS-2, and LN-30, are very competitive from the performance standpoint, with the LN-30 demonstrating extremely low attitude results because of its high-performing gyros. Overall however, the gyro has a lesser effect on trajectory errors than the accelerometers, as one might imagine for a short-duration flight featuring an energetic light vehicle. The Honeywell H-478 system resulted in larger errors than the three previously mentioned IMUs due to the large accelerometer scale factor in the off-thrust axes and the relatively high drift rate due to mass unbalance. The Raytheon LCP system is clearly outdistanced, as can be seen by looking at the error budget numbers.

TABLE 23.- ERROR BUDGET FOR SIX CANDIDATE SYSTEMS

INPUT ERROR SOURCES†	UNITS	DIGS	KT-70 MISSILE	H-478	LCP	TDS-2	LN-30
Verticality alignment	arc-s	11.0	22.0	30.0	40.0	45.0	20.0
Azimuth alignment	arc-s	20.0	47.0	40.0	40.0	60.0	60.0
Non-g sensitive (fixed gyro drifts)	deg/hr	0.033	0.2	0.1, 0.25	1.0	0.01	0.003
Gyro spin axis unbalance	deg/hr/g	0.133	0.1	0.5	3.0	0.003	0.03
Gyro input axis unbalance	deg/hr/g	0.133	0.05	0.4	3.0	0.0	00.03
Gyro compliance	deg/hr/g^2	0.02	0.03	0.3	0.3	0.02	0.01
Accelerometer bias	μg	41.8	50.0	500.0	500.0	20.0	10.0
Vertical accelerometer bias	μg	41.8	70.0	50.0	500.0	20.0	10.0
Accelerometer scale factor	μg/g	66.0	100.0	620.0, 200.0	500.0	150.0	250.0
Accelerometer nonlinearity	μg/g^2	1.67	10.0	0.0	1000.0	20.0	35.0
Accelerometer misalignment to platform	arc-s	10.0	20.0	20.0	205.0	20.0	20.0
Gyro torquer scale factor error	$x10^{-6}$	50.0	NA	500.0	NA	3.0	NA
Gyro input axis misalignment input, spin axis plane	arc-s	10.0	NA	40.0	NA	20.0	NA
Gyro input axis misalignment input, output axis plane	arc-s	10.0	NA	40.0	NA	20.0	NA

*The six systems were:

1) Hamilton Standard DIGS;
2) Singer-General Precision, Inc. KT-70 missile system;
3) Honeywell H-478;
4) Raytheon LCP;
5) Teledyne TDS-2;
6) Litton LN-30.

All systems were flown for both the 169 trajectory (elliptical) and the 176 (circular) trajectory.

†See Appendix A for a detailed description of each of the error sources.

The individual error sources generate different state errors at injection because some errors are acceleration-sensitive, some attitude- or time-dependent, or some are combination of all three. Thus, the primary error sources for each system will predominate with its particular radial, tangential, and normal position and velocity errors, and will present different orbital elements. The primary error sources for each system are listed.

DIGS - Accelerometer bias and scale factor, platform alignment, and gyro spin axis mass unbalance.

KT-70 - Platform alignment and all gyro error sources.

H-478 - Accelerometer bias and scale factor, gyro torquer scale factor and spin axis mass unbalance.

LCP - Primary-Gyro input axis mass unbalance and accelerometer nonlinearity; however, all error sources gave errors substantially above the other systems except the platform alignment.

TDS-2 - Platform alignment, accelerometer scale factor, nonlinearity and alignment, and gyro alignment.

LN-30 - Platform alignment and accelerometer scale factor, nonlinearity and alignment.

When comparing guidance hardware performance, the figure-of-merit can affect the system that appears best. This means that the comparison should be on a basis of the actual mission requirements. For comparing systems, perhaps radius of apogee and perigee are of prime importance. The KT-70 IMU shows radius of perigee results comparible or better, and radius of apogee results much better, than the TDS-2 and LN-30 IMUs, while a RSS of velocity at injection comparison would show the KT-70 to have the worst performance of the three IMUs.

If the position and velocity components are investigated, along with orbital element perturbation knowledge, it is apparent that the radius of apogee is primarily affected by the tangential velocity error (when injecting at perigee), and the perigee is affected by the injection in-plane position errors (with some additional influence from the radial velocity error).

For some orbits the figures-of-merit may have to be analyzed with Monte Carlo results because of nonlinear characteristics. Radius of apogee and perigee, true anomaly, etc are some parameters that are degenerate with orbits where the eccentricity is equal to zero. The linear solution may not apply for some parameters, and then only Monte Carlo results would provide a valid figure-of-merit. The radius of apogee and perigee isoprobability contours were generated with a Monte Carlo approach (figure 1) and are more meaningful than the linear results presented in table 24.

The individual results from the computer runs are presented in tables 25 thru 27. They are specifically the individual 176 trajectory errors for the KT-70, DIGS, and H-478 systems at fourth stage burnout in terms of radial, tangential, and normal velocity and position errors as a function of each error source. (see Appendix A for a complete description of the individual error source definitions.) Table 28 briefly defines the TEAP computer printout symbology for these runs.

TABLE 24.- 1σ TEAP RESULTS FOR THE SIX CANDIDATE SYSTEMS FOR THE 176 TRAJECTORY

ERRORS*	DIGS	KT-70	H-478	LCP	TDS-2	LN-30
FOR THE 176 TRAJECTORY						
Radial Position**	1 234.0	1 966.0	5 539.0	61 897.0	3 404.0	3 516.0
Tangential Position**	1 139.0	2 228.0	6 244.0	69 304.0	3 187.0	3 279.0
Normal Position**	1 510.0	3 395.0	5 934.0	60 386.0	3 803.0	3 256.0
RSS of Position	2 259.0	4 511.0	10 241.0	110 818.0	6 018.0	5 807.0
Radial Velocity	3.71	10.68	21.91	210.67	8.34	8.22
Tangential Velocity	2.01	4.25	10.04	238.07	7.03	9.23
Normal Velocity	5.92	11.70	23.04	185.50	7.97	7.46
RSS of Velocity	7.27	16.40	33.34	368.06	13.51	14.44
Radius of perigee (ft)	4 498.0	11 223.0	22 339.0	276 876.0	11 067.0	12 314.0
Radius of apogee (ft)	8 672.0	19 341.0	43 065.0	889 825.0	29 633.0	34 182.0
Orbit eccentricity	0.000187	0.00054	0.0012	0.016	0.00052	0.00058
Orbit inclination (deg)	0.0145	0.0289	0.056	0.46	0.0209	0.019
Period (s)	2.018	3.288	6.47	206.0	7.201	8.37
Flightpath angle (deg)	0.0077	0.0225	0.039	0.51	0.017	0.021
Attitude rate (deg/s)	0.0000162	0.0000968	0.000091	0.00048	0.00008	0.0000011
Attitude (deg)	0.0454	0.079	0.167	1.065	0.031	0.012
FOR THE 169 TRAJECTORY						
Radial Position	743.0	1 238.0	3 839.0	NOT RUN	1 895.0	1 621.0
Tangential Position	666.0	1 179.0	3 190.0		1 837.0	2 101.0
Normal Position	1 067.0	2 118.0	3 755.0		2 427.0	2 165.0
RSS of Position	1 461.0	2 722.0	6 246.0		3 586.0	3 425.0
Radial Velocity	3.52	8.63	21.47		7.92	5.85
Tangential Velocity	2.12	4.01	8.96		6.58	9.16
Normal Velocity	5.82	10.77	20.84		9.10	8.57
RSS of Velocity	7.13	14.37	31.23		13.74	13.84
Radius of perigee (ft)	701.2	1 140.0	3 576.0		1 799.0	1 552.0
Radius of apogee (ft)	12 269.0	21 002.0	40 715.0		38 808.0	43 610.0
Orbit eccentricity	0.00018	0.000326	0.00065		0.00058	0.000813
Orbit inclination (deg)	0.0125	0.023	0.044		0.02	0.018
Period (s)	2.569	4.31	8.194		8.12	11.15
Flightpath angle (deg)	0.00657	0.0165	0.038		0.0147	0.0144
Attitude rate (deg/s)	0.000017	0.0000968	0.000087		0.000096	0.00000165
Attitude (deg)	0.0357	0.059	0.138		0.028	0.022

*These are rss values of individual 1σ errors.

**This is an instantaneous inertial coordinate system with radial along the radius, normally perpendicular to the orbital plane; the tangential direction forms a right-hand-system.

TABLE 25.- DIGS SYSTEM

INDIVIDUAL 176 TRAJECTORY ERRORS AT FOURTH-STAGE BURNOUT

NAME	TD	RD	ND	T	R	N	NAME
PHIX0	-1.19472960E-02	-2.99619714E-02	3.95162311E-01	-1.65804901E+01	-2.05052074E+01	4.87171460E+02	PHIX0
PHIY0	7.36733549E-02	1.02128987E-01	-2.19751125E+00	3.38225817E+01	3.70323238E+01	-9.20107479E+02	PHIY0
PHIZ0	-8.86557510E-01	1.36997256E+00	4.78220659E-03	-6.65652301E+02	3.80635617E+02	-1.29418198E+01	PHIZ0
RU	-4.72661911E-02	-1.55054179E-02	1.24016322E+00	-3.67563505E+00	-6.55212332E+00	1.96067374E+02	RU
RV	2.75281580E-02	4.28625594E-02	-7.75221987E-01	1.82227719E+00	2.47833586E+00	-5.58074061E+01	RV
RW	-2.67989506E-01	1.59146607E+00	1.82934876E-02	-1.78592206E+02	1.38940281E+02	-4.17585551E+00	RW
PSU	6.22523625E-03	4.51913613E-03	-1.45665104E-01	3.52310632E+00	2.54891025E+00	-7.59660210E+01	PSU
PSV	1.67854390E-01	2.21134405E-01	-4.77264249E+00	1.72749003E+01	2.42581327E+01	-5.52343691E+02	PSV
PSW	4.72575820E-03	-3.58102285E-02	-5.43982009E-05	3.06509956E+00	-2.40078958E+00	7.38945593E-02	PSW
PIU	-1.22903669E-03	-2.36736919E-04	3.26159346E-02	-1.52984253E-01	-1.14305696E-01	3.46522453E+00	PIU
PIV	-1.68965670E-04	-8.23452369E-04	5.13360198E-03	-2.66718806E-02	-4.16289215E-02	8.63049071E-01	PIV
PIW	1.00904983E-01	-2.15522827E-01	-8.07206192E-04	7.23847523E+01	-5.09251336E+01	1.39304610E+00	PIW
C1U	3.94380323E-05	5.05025580E-06	-1.05499153E-03	3.40008452E-03	2.53767309E-03	-7.74526791E-02	C1U
C1V	-9.00157473E-05	-1.35149168E-03	3.13564894E-03	-1.38365335E-02	-2.70828397E-02	4.55051039E-01	C1V
C1W	-1.11825701E-04	1.12521735E-03	4.97616772E-07	-6.99279065E-02	5.33423459E-02	-1.69947002E-03	C1W
C2U	0.	0.	0.	0.	0.	0.	C2U
C2V	0.	0.	0.	0.	0.	0.	C2V
C2W	0.	0.	0.	0.	0.	0.	C2W
C3U	0.	0.	0.	0.	0.	0.	C3U
C3V	0.	0.	0.	0.	0.	0.	C3V
C3W	0.	0.	0.	0.	0.	0.	C3W
C4U	0.	0.	0.	0.	0.	0.	C4U
C4V	0.	0.	0.	0.	0.	0.	C4V
C4W	0.	0.	0.	0.	0.	0.	C4W
C5U	0.	0.	0.	0.	0.	0.	C5U
C5V	0.	0.	0.	0.	0.	0.	C5V
C5W	0.	0.	0.	0.	0.	0.	C5W
DBU	-5.00658326E-01	8.95714540E-01	-1.46986406E-02	-2.66767132E+02	2.62156592E+02	-8.27758931E+00	DBU
DBV	-6.33252634E-01	-7.05556299E-01	-5.38070314E-02	-2.17215658E+02	-3.06218552E+02	-1.98484451E+01	DBV
DBW	5.22397133E-02	2.21997339E-02	-9.27194837E-01	1.93423280E+01	1.00146677E+01	-3.69686337E+02	DBW
CU	2.15121419E-02	-2.78734620E-02	7.14739931E-04	1.75934439E+01	-7.39463303E+00	6.37643305E-01	CU
CV	-1.08178529E+00	-1.82293993E+00	-9.72667135E-02	-3.18327541E+02	-9.63792291E+02	-4.27981922E+01	CV
CW	-9.74421340E-04	-6.79571551E-05	1.54762296E-02	-4.91707723E-02	-3.44344013E-02	1.03799473E+00	CW
DCU	-7.34949562E-05	1.75623523E-04	-2.90163415E-06	-6.72148054E-02	1.95339656E-02	-2.68578324E-03	DCU
DCV	-4.20287753E-01	-3.00586543E-01	-2.90921023E-02	-6.82549078E+01	-1.57254455E+02	-7.64909766E+00	DCV
DCW	6.89470763E-06	7.34613992E-08	-1.21839651E-04	7.40467316E-05	1.12719038E-05	-1.32607057E-03	DCW
PHIUV	-7.92731592E-01	1.27639680E+00	-2.15267364E-02	-6.01888508E+02	3.62715233E+02	-1.81868651E+01	PHIUV
PHIVW	-8.07640573E-04	1.14860808E-02	-1.81560939E-05	-6.47519712E-01	4.37757491E-01	-2.08145589E-02	PHIVW
PHIWU	1.09949875E-02	1.46169070E-03	6.61623143E-04	3.04069305E-01	7.90533467E-01	7.33373203E-02	PHIWU
PHIUW	-1.22056103E-02	-3.02833669E-02	-1.32857251E-03	-2.96359514E+00	-1.64169042E+01	-6.39550841E-01	PHIUW
PHIVU	-1.25863596E-03	-9.46468021E-04	2.57524240E-02	-6.34297003E-01	-5.45442910E-01	1.36208276E+01	PHIVU
PHIWV	-6.73545144E-02	-4.30933141E-02	1.37333662E+00	-3.00591005E+01	-2.39730110E+01	6.59835363E+02	PHIWV
NCNIMU	0.	0.	0.	0.	0.	0.	NCNIMU
DKU	4.53550257E-04	2.69018797E-04	-1.10527584E-02	2.10622844E-01	1.57485010E-01	-4.62403336E+00	DKU
DKV	-7.25807423E-04	-1.12336005E-03	2.11265985E-02	-1.16479754E-01	-1.69676105E-01	3.83364692E+00	DKV
DKW	6.62982453E-01	-1.70558713E+00	-1.00977272E-02	4.76415654E+02	-3.24863943E+02	1.28968718E+01	DKW
THUIO	-1.04222019E-03	-2.93415181E-04	2.45735227E-02	-3.61167575E-01	-2.00456760E-01	6.76367432E+00	THUIO
THVIO	2.41506999E-04	4.13654787E-04	-7.12599698E-03	5.13329777E-02	7.41550998E-02	-1.67478803E+00	THVIO
THWIO	-1.00582650E-02	3.55992535E-02	2.97327903E-04	-7.21896427E+00	4.58663294E+00	-2.27903131E-01	THWIO
THUIS	4.90441990E-02	2.70127407E-02	-1.16651691E+00	2.29092719E+01	1.59173436E+01	-4.82318149E+02	THUIS
THVIS	3.36896988E-02	4.31222842E-02	-9.81067265E-01	5.70808405E+00	8.28532637E+00	-1.87428810E+02	THVIS
THWIS	-6.25039161E-03	1.53836049E-02	3.52580100E-05	-4.49019353E+00	3.10372639E+00	-1.14661757E-01	THWIS

ALGEBRAIC SUM OF TRAJECTORY ERRORS

-3.57912[illegible]E+03	7.19870256E-01	-9.04716384E+00	-1.71438450E+03	-6.27220586E+02	-1.37626617E+03

RSS VELOCITY = 8.83617575E+00
RSS POSITION = 2.28618206E+03

RSS OF TRAJECTORY ERRORS

2.01237965E+00	3.70909316E+00	5.91822328E+00	1.13923334E+03	1.23442106E+03	1.50979458E+03

RSS VELOCITY = 7.26803046E+00
RSS POSITION = 2.25856761E+03

ORBITAL UNCERTAINTIES (1.0 SIGMA)

DPP / DRA	DP / DVA	DA / DTA	DECC / DINC	DDFL / DPER	DGAM
4.49393279E+03	5.37184654E+03	5.12237178E+03	1.87631770E-04	1.65957675E+02	7.73766971E-03
3.67268694E+03	6.21966950E+00	2.98181759E+03	1.45747051E-02	2.01883551E+00	

TABLE 26.- KT-70 SYSTEM

INDIVIDUAL 176 TRAJECTORY ERRORS AT FOURTH-STAGE BURNOUT

NAME	TD	RD	ND	T	R	N	NAME
PHIXO	-2.38945920E-02	-5.99239428E-02	7.90324622E-01	-3.31609802E+01	-4.10104148E+01	9.74342920E+02	PHIXO
PHIYO	1.84894143E-01	2.40003121E-01	-5.16415144E+00	7.94830669E+01	8.70259609E+01	-2.16225258E+03	PHIYO
PHIZO	-1.77311502E+00	2.73994513E+00	9.56441318E-03	-1.33130460E+03	7.61271234E+02	-2.58836396E+01	PHIZO
RU	7.47372212E-02	3.93850220E-02	-1.93623297E+00	-2.37672962E+01	-3.01483886E+01	7.04070816E+02	RU
RV	3.10811753E-01	3.22182858E-01	-8.59244374E+00	3.66640606E+01	3.95549897E+01	-9.93450685E+02	RV
RW	-1.60970002E+00	9.46761134E+00	2.46161335E-01	-1.06981495E+03	8.31551123E+02	-1.38531258E+01	RW
PSU	1.19771364E-02	-1.92311740E-02	-2.20054273E-01	-2.48432161E+01	-3.15904249E+01	7.37145148E+02	PSU
PSV	1.24881961E-01	1.53485090E-01	-3.46885991E+00	4.46346036E+01	4.84319789E+01	-1.20829719E+03	PSV
PSW	-2.75464603E-03	8.12856900E-03	1.42689128E-04	-1.89030745E+00	1.46313606E+00	-2.48207418E-02	PSW
PIU	7.24343033E-06	-1.89197063E-05	-1.06301631E-04	-2.09521493E-02	-2.66823996E-02	6.21988564E-01	PIU
PIV	8.08209436E-02	9.14681624E-02	-2.23691336E+00	1.93153550E+01	2.08502530E+01	-5.21183955E+02	PIV
PIW	-9.55643006E-01	1.99951182E+00	2.13484714E-02	-6.76920329E+02	4.97392079E+02	-9.74703425E+00	PIW
C1U	6.50407557E-05	-2.11470163E-05	-1.49256732E-03	-6.45222423E-02	-8.31755954E-02	1.92352705E+00	C1U
C1V	1.26242072E-01	1.55034264E-01	-3.49807251E+00	4.59718407E+01	4.95859062E+01	-1.23890349E+03	C1V
C1W	-3.61173566E-03	1.05154948E-02	1.81093495E-04	-2.45391769E+00	1.97795515E+00	-2.97796113E-02	C1W
C2U	0.	0.	0.	0.	0.	0.	C2U
C2V	0.	0.	0.	0.	0.	0.	C2V
C2W	0.	0.	0.	0.	0.	0.	C2W
C3U	0.	0.	0.	0.	0.	0.	C3U
C3V	0.	0.	0.	0.	0.	0.	C3V
C3W	0.	0.	0.	0.	0.	0.	C3W
C4U	0.	0.	0.	0.	0.	0.	C4U
C4V	0.	0.	0.	0.	0.	0.	C4V
C4W	0.	0.	0.	0.	0.	0.	C4W
C5U	0.	0.	0.	0.	0.	0.	C5U
C5V	0.	0.	0.	0.	0.	0.	C5V
C5W	0.	0.	0.	0.	0.	0.	C5W
DBU	-1.01313495E+00	-5.23915736E-01	-5.14230692E-02	-4.05123536E+02	-1.84651516E+02	-2.04702551E+01	DBU
DBV	6.54388613E-01	-1.93068213E+00	-2.91681138E-02	2.55998446E+02	-6.71639683E+02	-1.15373271E+01	DBV
DBW	3.88001711E-02	4.74206680E-02	-1.10644949E+00	1.55709392E+01	1.66596469E+01	-4.41113061E+02	DBW
CU	-2.00404992E+00	-1.10140948E+00	-1.02372765E-01	-8.42556281E+02	-3.98637938E+02	-4.27764856E+01	CU
CV	4.10640114E-01	-1.67784354E+00	-1.65678760E-02	3.90834928E+02	-1.05972252E+03	-1.71881982E+01	CV
CW	9.51317784E-05	1.44521138E-04	-2.79463483E-03	6.23402366E-02	7.00528100E-02	-1.78089289E+00	CW
DCU	-2.26669352E+00	-1.09782140E+00	-1.14693389E-01	-5.00271937E+02	-2.35483251E+02	-2.53800962E+01	DCU
DCV	3.34555117E-01	-1.07306595E+00	-1.45244761E-02	1.55979423E+02	-4.21411362E+02	-6.88154250E+00	DCV
DCW	1.71373693E-07	2.74349014E-07	-5.07373745E-06	1.26874523E-04	1.43060040E-04	-3.62717769E-03	DCW
PHIUV	-3.19047297E-01	-2.65786606E-01	-1.69750244E-02	-4.05299175E+02	-1.92999672E+02	-2.05959671E+01	PHIUV
PHIVW	1.26613710E-03	7.84994710E-04	6.53160441E-05	8.15446370E-01	3.85360450E-01	4.13903811E-02	PHIVW
PHIWJ	6.58332375E-04	-2.24097341E-03	-2.82201352E-05	3.85213643E-01	-1.03813576E+00	-1.70462876E-02	PHIWJ
PHIUW	-4.86914075E-01	1.51121621E+00	2.13224849E-02	-1.99839281E+02	5.39032051E+02	8.83067637E+00	PHIUW
PHIVJ	3.80730423E-02	5.02794990E-02	-1.09882094E+00	1.50958445E+01	1.81308014E+01	-4.60095130E+02	PHIVU
PHIWV	-1.15195105E-02	-2.49971824E-02	3.59266685E-01	-1.54583865E+01	-1.76029619E+01	4.42900192E+02	PHIWV
NONIMU	0.	0.	0.	0.	0.	0.	NONIMU
DKU	0.	0.	0.	0.	0.	0.	DKU
DKV	0.	0.	0.	0.	0.	0.	DKV
DKW	0.	0.	0.	0.	0.	0.	DKW
THUIO	0.	0.	0.	0.	0.	0.	THUIO
THVIO	0.	0.	0.	0.	0.	0.	THVIO
THWIO	0.	0.	0.	0.	0.	0.	THWIO
THUIS	0.	0.	0.	0.	0.	0.	THUIS
THVIS	0.	0.	0.	0.	0.	0.	THVIS
THWIS	0.	0.	0.	0.	0.	0.	THWIS

ALGEBRAIC SUM OF TRAJECTORY ERRORS

-8.07716395E+00	9.00015885E+00	-2.62437730E+01	-4.46993197E+03	-3.72123451E+02	-4.35158927E+03

RSS VELOCITY = 2.89147485E+01
RSS POSITION = 6.24940772E+03

RSS OF TRAJECTORY ERRORS

4.24909412E+00	1.05822681E+01	1.17013648E+01	2.22754515E+03	1.96619981E+03	3.39477304E+03

RSS VELOCITY = 1.64038895E+01
RSS POSITION = 4.51136156E+03

ORBITAL UNCERTAINTIES (1.0 SIGMA)

DRP DRA	DP DVA	DA DTA	DECC DINC	DDEL DPER	DGAM
1.12239731E+04 1.93412632E+04	8.25055828E+03 1.55021937E+01	3.34355805E+03 3.60314809E+03	5.44587570E-04 2.89859540E-02	4.78920022E+02 3.28837378E+00	2.25506310E-02

TABLE 27.- H-478 SYSTEM

INDIVIDUAL 176 TRAJECTORY ERRORS AT FOURTH-STAGE BURNOUT

NAME	TD	RD	ND	T	R	N	NAME
PHIXO	-3.25835345E-02	-8.17144675E-02	1.07771539E+00	-4.52195184E+01	-5.59232930E+01	1.32864944E+03	PHIXO
PHIYO	1.57356718E-01	2.04257975E-01	-4.39502250E+00	6.76451633E+01	7.40646475E+01	-1.84021496E+03	PHIYO
PHIZO	-2.41788412E+00	3.73628881E+00	1.30423816E-02	-1.81541537E+03	1.03809714E+03	-3.52958721E+01	PHIZO
RU	-1.41798573E-01	-4.65162537E-02	3.72048965E+00	-2.60269051E+01	-1.96563865E+01	5.88203621E+02	RU
RV	2.06883396E-01	3.22126597E-01	-5.82605481E+00	1.36950280E+01	1.86255303E+01	-4.19411487E+02	RV
RW	-8.03968517E-01	4.74439820E+00	5.48804627E-02	-5.35776617E+02	4.16820843E+02	-1.25275665E+01	RW
PSU	2.24048668E-02	1.62644158E-02	-5.24250151E-01	1.26976914E+01	9.17355324E+00	-2.73402462E+02	PSU
PSV	6.04111412E-01	7.95864914E-01	-1.71767876E+01	6.21725372E+01	8.73052598E+01	-1.98789041E+03	PSV
PSW	1.70080505E-02	-1.28881367E-01	-1.95779664E-04	1.10313237E+01	-8.64046547E+00	2.65947250E-01	PSW
PIU	3.68726007E-03	7.10360752E-04	-9.78478036E-02	4.58952757E-01	3.42917085E-01	-1.03956735E+01	PIU
PIV	5.06897008E-04	2.47035711E-03	-1.54008059E-02	8.00156416E-02	1.24885764E-01	-2.58914721E+00	PIV
PIW	-3.02714949E-01	6.46568482E-01	2.42161858E-03	-2.17154257E+02	1.52775401E+02	-5.67913829E+00	PIW
C1U	-5.91570483E-04	-7.57538366E-05	1.58248729E-02	-5.10012674E-02	-3.80650961E-02	1.16179016E+00	C1U
C1V	1.35023621E-03	2.04223752E-02	-4.70347341E-02	2.07548092E-01	4.06242595E-01	-6.82576559E+00	C1V
C1W	1.67738551E-03	-1.68782602E-02	-7.46425159E-06	1.04891860E+00	-8.07642689E-01	2.54920503E-02	C1W
C2U	0.	0.	0.	0.	0.	0.	C2U
C2V	0.	0.	0.	0.	0.	0.	C2V
C2W	0.	0.	0.	0.	0.	0.	C2W
C3U	0.	0.	0.	0.	0.	0.	C3U
C3V	0.	0.	0.	0.	0.	0.	C3V
C3W	0.	0.	0.	0.	0.	0.	C3W
C4U	0.	0.	0.	0.	0.	0.	C4U
C4V	0.	0.	0.	0.	0.	0.	C4V
C4W	0.	0.	0.	0.	0.	0.	C4W
C5U	0.	0.	0.	0.	0.	0.	C5U
C5V	0.	0.	0.	0.	0.	0.	C5V
C5W	0.	0.	0.	0.	0.	0.	C5W
DBU	-5.97093337E+00	1.06322253E+01	-1.75294899E-01	-3.18144506E+03	3.12646009E+03	-9.87179169E+01	DBU
DBV	-8.14842089E-01	-8.42633808E-01	-6.41698670E-02	-2.59049785E+02	-3.65193976E+02	-2.36711085E+01	DBV
DBW	6.23006939E-01	2.64752382E-01	-1.10576569E+01	2.30675172E+02	1.19434185E+02	-4.40885187E+03	DBW
CU	2.00263182E-01	-2.59529226E-01	6.65420102E-03	1.63829404E+02	-6.88393921E+01	5.93601875E+00	CU
CV	-3.24860443E+00	-5.47429410E+00	-2.92092233E-01	-9.55938561E+02	-2.89427114E+03	-1.28523100E+02	CV
CW	-8.14025872E-03	-6.31796339E-04	1.44073008E-01	-4.57745928E-01	-3.20560492E-01	9.66301400E+00	CW
DCU	0.	0.	0.	0.	0.	0.	DCU
DCV	0.	0.	0.	0.	0.	0.	DCV
DCW	0.	0.	0.	0.	0.	0.	DCW
PHIUV	-1.58546318E+00	2.55279359E+00	-4.32534728E-02	-1.20377702E+03	7.25430466E+02	-3.63737301E+01	PHIUV
PHIVW	-1.61528115E-03	2.29721617E-02	-3.63121878E-05	-1.29503942E+00	8.75514981E-01	-4.16291178E-02	PHIVW
PHIWU	2.19899750E-02	2.92338140E-03	1.32324629E-03	6.08138610E-01	1.58117693E+00	7.77746417E-02	PHIWU
PHIUW	-2.44112206E-02	-6.05667335E-02	-2.65714503E-03	-5.92719028E+00	-3.28338084E+01	-1.27910168E+00	PHIUW
PHIVU	-2.51727192E-03	-1.89293604E-03	5.15048479E-02	-1.26859401E+00	-1.09088582E+00	2.72416552E+01	PHIVU
PHIWV	-1.35709029E-01	-8.61876281E-02	2.75777323E+00	-6.01182010E+01	-4.79460220E+01	1.31967073E+03	PHIWV
NONIMU	0.	0.	0.	0.	0.	0.	NONIMU
DKU	4.53550257E-03	2.69018797E-03	-1.10527584E-01	2.10622844E+00	1.57485010E+00	-4.62403386E+01	DKU
DKV	-7.25807423E-03	-1.12336005E-02	2.11265885E-01	-1.16479754E+00	-1.69676105E+00	3.83364682E+01	DKV
DKW	6.62982453E+00	-1.70558713E+01	-1.00973272E-01	4.76415654E+03	-3.24863943E+03	1.28968718E+02	DKW
THUIO	4.16888075E-03	1.17366072E-03	-9.82940907E-02	1.44467030E+00	8.01827038E-01	-2.70546973E+01	THUIO
THVIO	-9.66027996E-04	-1.65461915E-03	2.85035879E-02	-2.05331911E-01	-2.96620400E-01	6.69915211E+00	THVIO
THWIO	4.02330600E-02	-1.42397014E-01	-1.18931161E-03	2.88758571E+01	-1.83465318E+01	9.11612525E-01	THWIO
THUIS	-1.96176796E-01	-1.08050963E-01	4.66606764E+00	-9.16373874E+01	-6.36713942E+01	1.92927260E+03	THUIS
THVIS	-1.34758795E-01	-1.96489137E-01	3.92426906E+00	-2.28323362E+01	-3.31413055E+01	7.49715239E+02	THVIS
THWIS	2.50015672E-02	-6.15344194E-02	-1.41032040E-04	1.79607741E+01	-1.24149055E+01	4.58647027E-01	THWIS

ALGEBRAIC SUM OF TRAJECTORY ERRORS

-7.26692728E+00 -5.58130227E-01 -2.33530787E+01 -3.04606645E+03 -1.09987406E+03 -3.22972807E+03

RSS VELOCITY = 2.44639741E+01
RSS POSITION = 4.57377166E+03

RSS OF TRAJECTORY ERRORS

1.00440611E+01 2.19117198E+01 2.30405548E+01 6.24372908E+03 5.53937904E+03 5.93425261E+03

RSS VELOCITY = 3.33447716E+01
RSS POSITION = 1.02413001E+04

ORBITAL UNCERTAINTIES (1.0 SIGMA)

DRP DRA	DP DVA	DA DTA	DECC DINC	DDEL DPER	DGAM
2.23390476E+04 4.30658781E+04	1.62364118E+04 3.48587189E+01	1.64306516E+04 1.51039729E+04	1.22076196E-03 5.66190291E-02	8.40618927E+02 6.47566317E+00	3.96874575E-02

TABLE 28.- COMPUTER SYMBOL DEFINITIONS

SYMBOL	DEFINITION
PHIXO, PHIYO, and PHIZO	Initial platform alignment errors
RU, RV, RW	Gyro non-g-sensitive drift rate error
PSU, PSV, PSW	Gyro drift rate due to spin axis mass unbalance
PIU, PIV, PIW	Gyro drift rate due to input axis mass unbalance
C1U, C1V, C1W	Gyro drift rate due to compliance effects
C2U, C2V, C2W, C3U ... etc	Higher order compliance terms
DKU, DKV, DKW	Gyro torquer scale factor error
THUIO, THVIO, THWIO	Gyro input axis misalignment to desired gyro frame in one plane
THUIS, THVIS, THWIS	Gyro input axis misalignment to desired gyro frame in the other plane
DBU, DBV, DBW	Accelerometer bias error
CU, CV, CW	Accelerometer scale factor errors
DCU, DCV, DCW	Accelerometer nonlinearity errors
PHIUV, PHIVW, PHIWU	Accelerometer misalignments to platform (block)
PHIUW, PHIVU, PHIWV	Accelerometer misalignments to platform (block)
DRP:	Error in radius of perigee (ft)
DRA:	Error in radius of apogee (ft)
DECC:	Error in orbital eccentricity (dimensionless)
DINC:	Error in orbital inclination (deg)
DPER:	Error in orbital period (s)
DGAM:	Error in flightpath angle (deg)
T, R, N	Vehicle position in ft in the tangential, radial, and normal directions
TD, RD, ND	Vehicle velocity in fps in the tangential, radial, and normal directions

The KI-70 guidance hardware covariance was used to generate an isoprobability contour (figure 1) which shows the possible reduction of errors for radius of perigee and apogee. The covariance was transformed to a diagonal matrix (Eigenvector/value solution), a random number generator scaled the diagonal elements, the scaled diagonals are transformed into the original covariance state, and the nominal state was perturbed by the square-root of the variances of the new covariance matrix. This perturbed case was transformed into parameters of interest and these were then compared to the nominal parameters. After a sufficient number of parameter deltas have been generated, then the isoprobability contour can be drawn. See Appendix D *Isoprobability Contour Program* for further details.

OPEN-LOOP ERROR ANALYSIS

The purpose of this dispersion analysis is to compare and evaluate the accuracies of three potential open-loop three-axis reference systems (TARS) and the present Scout TARS. This will provide a comparison for evaluating the potential candidates with the present system to determine the feasibility of incorporating a new TARS on the Scout launch vehicle. Throughout this section, TARS and ARU are used interchangeably.

The present Scout vehicle has the IRP on Stage III with Stage IV spin stabilized. Part of the open-loop error analysis includes analyzing TARS on Stage IV, both with the present Scout IRP and the candidate attitude reference systems.

The nominal trajectory parameters for a launch from Vandenberg placing 211 pounds into a near-circular (630 x 585 n. mi.) earth orbit having an eccentricity of 0.005 and an inclination of 89.9° are shown in table 29. The trajectory data were obtained from Scout vehicle S-176C, N-14 payload mission and the flight test plan.

TABLE 29.- NOMINAL TRAJECTORY PARAMETERS AT FOURTH-STAGE BURNOUT

Parameter	Value
Time of ejection	760.36 s
Inertial velocity	24 046.0 fps
Inertial flightpath angle	0.01°
Altitude	3 555 980 ft
Apogee	629.7 n. mi.
Perigee	585.2 n. mi.
Inclination	89.94°
Eccentricity	0.005
Period	6 467.0 s

Error Sources

The total guidance system error analysis was determined from two basic error categories--guidance and nonguidance. The guidance system errors relate to the attitude sensing instruments and the nonguidance errors and all other performance uncertainties. The discussion of these errors will be divided into the two basic error categories.

Nonguidance error sources.- The significant error sources for the present Scout launch vehicle are presented in table 30. These error sources are due to physical differences between the desired (or predicted) vehicle environment and the actual flight conditions. Deviations among components, system response, and environment for any flight are to be expected, and provide the basis for identifying the error sources and their magnitudes. The error sources are used as perturbations to a nominal trajectory that is assumed representative of the vehicle environment of an actual flight.

For stage motor errors--the motor variances for any one stage--were assumed to be simulated by one trajectory. Thus, the temperature, burn time, thrust, loaded propellant, flow rate, I_{sp} etc, for each class of motors could be simulated by changing the burn time, thrust, propellant load, and weight change in one dispersed trajectory. Table 30 gives the combination of these parameters that were used for each stage variance.

The drag force and atmospheric density were simulated by the variances given in table 30; the tailwind and sidewind are defined in figure 30. These errors constitute the aerodynamic and atmospheric perturbations on the Scout vehicle.

TABLE 30.- NONGUIDANCE SYSTEM ERROR SOURCES

Error source	3σ magnitude
Motor performance	
Algol IIB	0.9409, time, t_{nom}; 1.0018, weight, $W_{c_{nom}}$; 1.076, thrust, T_{nom}
Castor II	0.9891 t_{nom}, 1.00162 $W_{c_{nom}}$, 1.0299 T_{nom}
X-259	0.8918 t_{nom}, 1.0018 $W_{c_{nom}}$, 1.1326 T_{nom}
FW-4S	0.8863 t_{nom}, 1.0015 $W_{c_{nom}}$, 1.1455 T_{nom}
First-stage thrust misalignment	
Pitch	0.25°
Yaw	0.25°
Axial force coefficient	10%
Atmosphere	
Density	5%
Tailwind	99% Vandenberg AFB average annual
Crosswind	99% Vandenberg AFB average annual
Control system deadband	
Second-stage boost - pitch	0.8°
Second-stage boost - roll	1.4°
Second-stage boost - yaw	0.8°
Third-stage boost - pitch	0.8°
Third-stage boost - roll	1.4°
Third-stage boost - yaw	0.8°
Fourth-stage tipoff (present Scout system only)	
Pitch attitude	3.54°
Yaw attitude	3.54°
Fourth-stage attitude control (candidate systems only)	
Pitch	0.5°
Yaw	0.5°

The control system deadband errors were simulated by assuming that the actual vehicle will have some perturbation that keeps the vehicle continuously on one side of the attitude deadband during any stage burn.

The Stage IV tipoff errors (present Scout only) can only be simulated properly by using a 6-degree-of-freedom trajectory program that includes the inertias, spinup, staging, and rotational disturbing forces and moments. However, this was not done because of uncertainties in determining the disturbing forces and moments and was simulated by a constant initial attitude error as in previous analyses.

For the advanced Scout considerations, the Stage IV control system deadband errors were simulated with the attitude errors given in table 30. The errors resulting from the control system deadband during Stage II and Stage III coast were assumed negligible and omitted.

The nonguidance errors were assumed to remain the same for comparison of the various candidate guidance systems except for Stage IV attitude errors. This was because the present Scout Stage IV is spin stabilized and the advanced Scout vehicle was assumed to have a reaction control system (RCS). Thus, the present Scout vehicle had Stage IV tipoff errors and the Advanced Scout had the TARS and its associated attitude errors. The Advanced Scout comparison used the present Scout IRP on Stage IV, along with three other candidate systems.

Guidance system error sources.-Table 31 presents the known error sources assigned to the guidance hardware systems given. It lists the present Scout IRP, Modified HSSC DIGS without accelerometers, General Electrics' ODMARS, and Honeywell ARU (1009 gyro) hardware system error budgets. The last three systems are considered as candidates for an updated Scout vehicle and were used in comparing the TARS. The present Scout data were obtained from NASA.

TABLE 31. - TARS 1σ ERROR BUDGET NUMBERS

Input error sources	Original Scout IRP	Modified DIGS-ARU	ODMARS	Honeywell ARU (1009 gyro)
Verticality alignment, arc-s	66.0	20.0	30.0	30.0
Azimuth alignment, arc-s	20.0	20.0	30.0	30.0
Non-g-sensitive (fixed gyro drifts),* deg/hr	0.175°/hr (0 < t < 73.85) 0.77°/hr (73.85 < t < 154.98) 0.276°/hr (154.98 < t < 738)	0.033	0.15	0.015, 0.05
Gyro spin axis unbalance, deg/hr/g	(1.17)	0.133	0.25	0.434
Gyro input axis unbalance, deg/hr/g		0.133	0.15	0.434
Gyro compliance, deg/hr/g^2	0.0067	0.02	0.02	0.02
Gyro torquer scale factor, x10^{-6}	850.0	50.0	600.0	400.0
Gyro input axis misalignment to spin axis, arc-s	30.0	10.0	30.0	20.0
Gyro output axis misalignment to spin axis, arc-s	30.0	10.0	30.0	20.0

*This non-g sensitive drift term is the 1 sigma rss of the 0.5°/hr (3 sigma) fixed drift term and that portion due to the 1.62°/hr/deg elastic restraint term (also 3 sigma). An attitude error of 0.1° was used through Stage 1 coast, 1.4° was used through Stage 3 coast, and 0.41° was used to coast cutoff.

Analysis Approach

The errors were generated by using two methods--nonguidance errors utilizing trajectory dispersions via UD213, and the TARS system errors obtained from the TEAP guidance error analysis program. Both methods generate a covariance matrix and the two covariance matrices were added at orbital injection. The combined covariance matrix is a total system error covariance and provides the basis for generating the isoprobability contours and for comparing the candidate guidance systems. A detailed explanation of the covariance matrix follows.

The covariance matrix of a random vector $\bar{x}$ having a mean value $\bar{\mu}_x$ is defined as

$$\Sigma_{\bar{x}} \triangleq E\left[\left(\bar{x} - \bar{\mu}_x\right)\left(\bar{x} - \bar{\mu}_x\right)^T\right]$$

where E is the expectation operator and T denotes transpose. If the vehicle state vector is represented by three components of position and velocity, $\Sigma_{\bar{x}}$ is a 6x6 matrix. Other variational parameters could be included such as burnout time or weight. Time can be excluded by choosing a fixed time to compute the covariance matrix that exceeds all possible burnout times.

The nominal, or reference trajectory, is defined as the trajectory obtained when all performance parameters are at their mean or nominal value. Since each error source is taken to have a zero mean, the average value of the state vector at a fixed time becomes equal to the nominal trajectory state vector.

The average value of the perturbed state is

$$\bar{\mu}_x = E[x] = \bar{x}_{nom}.$$

The state covariance matrix becomes

$$\begin{aligned}\Sigma_x &= E\left[\left(\bar{x} - \bar{\mu}_x\right)\left(x - \bar{\mu}_x\right)^T\right]\\ &= E\left[\left(\bar{x} - \bar{x}_{nom}\right)\left(\bar{x} - \bar{x}_{nom}\right)^T\right]\\ &= E\left[\Delta\bar{x}\ \Delta\bar{x}^T\right]\end{aligned}$$

where

$$\Delta\bar{x}_i = \bar{x}_i - \bar{x}_{nom}$$

for

n error sources $(i = 1,2\ldots n)$

and

$$\Delta\bar{x} = \begin{bmatrix} \Delta x_1 & \Delta x_2 & \cdots & \Delta x_n \\ \Delta y_1 & & & \vdots \\ \vdots & & & \vdots \\ \vdots & & & \vdots \\ \vdots & & & \vdots \\ \Delta z_1 & \cdots & \cdots & \Delta z_n \end{bmatrix}$$

A detailed description of the nonguidance and guidance covariance generation follows to better define the detailed approach for this analysis.

Nonguidance system dispersion approach.- The UD213 trajectory simulation program described in Appendix B was used to generate a nominal trajectory and the position and velocity state dispersion for each error source given in Table 30. This gave a 6x18 error matrix that, in turn, was used to generate the 6x6 nonguidance system covariance in the manner previously described.

The errors were considered independent with zero mean. Each 3σ value was simulated with an individual trajectory run using the UD213 program. To reduce computer run time, the effects were assumed linear, and only one-sided errors were considered.

The motor performance runs were simulated by adjusting the total burn time and vacuum thrust by the values shown. The stage propellant weights were increased by a weight consumed factor and the propellant flow rate curve multiplied by the same factor. This gave a shorter burn time, higher thrust and flow rates, higher initial propellant weight, and the same burnout vehicle weight as the nominal trajectory.

The second and third stage RCS errors were simulated by incrementing the nominal attitude by the amount shown during the specified trajectory segment. This is equivalent to a mean shift (from nominal) of the attitude history due to nonsymmetric disturbing torques.

The present Scout Stage IV thrust pointing error results from a combination of attitude error and tipoff disturbances. This results in a complicated coning and precessing motion because it is spin stabilized. A simulation that includes products of inertia and precisely defined separation disturbances is necessary to accurately generate the resulting trajectory dispersion. It is felt that the additional accuracy was not warranted since the primary purpose is not to precisely evaluate the current Scout accuracy but rather to evaluate candidate systems relative to Scout.

The candidate systems differ from present Scout in that a Stage IV RCS is used. The attitude errors are based on the same rationale as that for the Stage II and Stage III RCSs. A 99% average annual Vandenberg AFB wind profile (figure 30) was used for sidewind and tailwind disturbances.

The effects of atmospheric density variations were simulated by varying the atmospheric pressure since the dynamic pressure is calculated from

$$q = 0.7\ M^2\ p_a.$$

The aerodynamic drag variation was considered equivalent to a variation in the axial force coefficient since the angle of attack is very small.

The first-stage thrust misalignment error was provided by NASA. The thrust offset angle effect is much greater than the actual misalignment angle. This is due to the vehicle response from the internal/external aerodynamic control vanes' characteristics when given a control deflection command. The thrust misalignment effect can only be properly simulated with a 6-degree-of-freedom simulation program and the additional effort required to develop a deck for this program was not justified for this error source. Therefore previously generated NASA results were used.

<u>Guidance system dispersion analysis approach</u>.- The trajectory error analysis program (TEAP) was used to compute the 6x6 covariance matrix resulting from guidance hardware error sources, table 31. Neither the present Scout IMU or the candidates have accelerometers (to navigate) so the accelerometer errors and gravity feedback effects are zero. The errors in the vehicle state result from gyro reference attitude drifts and can be represented by

$$\Delta\bar{a}_v = -\Delta\overline{PG} \times \bar{a}_s$$

where $\Delta\overline{PG}$ is the vehicle attitude error due to the gyro drift and $\bar{a}_s$ is a time history of sensed acceleration generated from the nominal trajectory. [illegible] differential equation is integrated to obtain vehicle velocity and position errors. The state vector covariance matrix at Stage IV [illegible] is then formed. A general description of TEAP can be found in Appendix A.

<u>Isoprobability contouring</u>.- Isoprobability contouring is a means to present in a simple graphical manner the effects of state vector dispersions on selected orbital elements. The approach used to generate a contour is described in Appendix D.

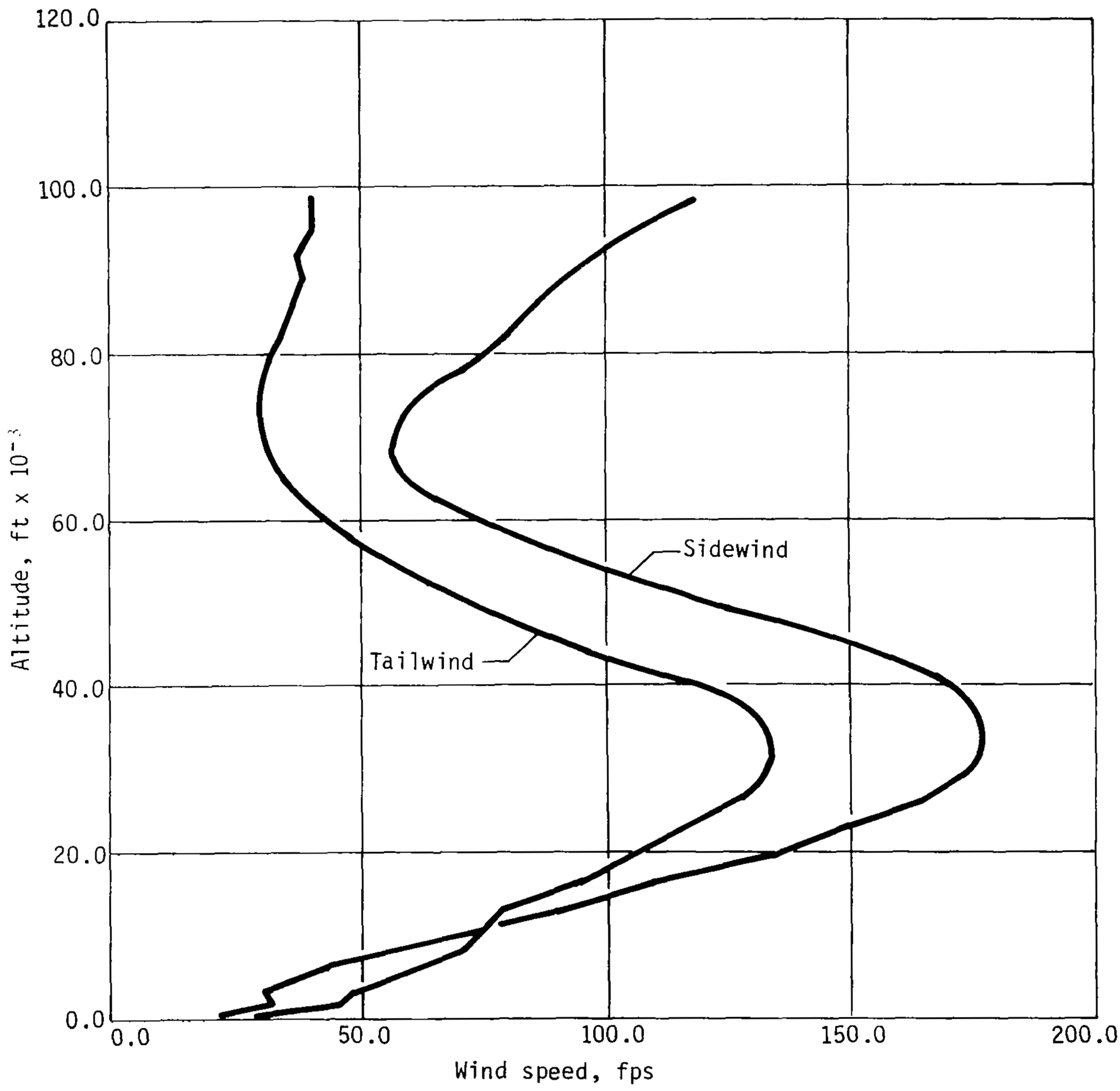

FIGURE 30.- VANDENBERG AFB WIND PROFILE, 99% AVERAGE ANNUAL

Results

Based on the nominal state given in table the 3σ results of the nonguidance dispersions are given in table 33, and are presented in the form in which they were used to generate the covariance for the basic scattergram input.

TABLE 32.- NOMINAL STATE AT ORBIT INJECTION

State error	Nominal value
X, ft	-11 734 339.0
Y, ft	-20 872 605.0
Z, ft	5 083 626.0
XD, fps	-2 427.9
YD, fps	-4 368.7
ZD, fps	-23 520.8
Radius, ft	24 478 635.0
Inertial velocity, fps	24 045.9

These dispersion results are given in an earth-centered inertial (ECI) coordinate system with X being along the Greenwich meridian at launch, Z along the North Pole, and Y forming a right-hand system. XD, YD, and ZD are the velocity components of the trajectory positions, X, Y, and Z, respectively.

The Stage IV tipoff errors were used with the present Scout configuration analysis and the deadband errors were used for the updated Scout vehicle.

The results of the TEAP guidance analysis of the TARS are presented in table 34. These results were based on the error sources in table 31 and the trajectory acceleration profile provided by NASA. These TEAP results are only presented with the rss of position, velocity, and attitude errors to give the relative merits of the listed systems, while the system covariances contain the complete error state.

The complete system covariance is generated by adding, element by element, the guidance and nonguidance covariances at the same time point. Only the complete system covariances for the DIGS and original Scout are given in table 35. This is because the DIGS TARS gave the least error and the original Scout the most. These system covariances point up the fact that the nonguidance errors comprise most of the errors and that the system performance cannot be significantly improved with a perfect TARS.

The 99.7% isoprobability contours given in figure 31 show the relative merits of the present Scout IRP on Stage III, present Scout IRP on Stage IV, and the DIGS ARU on Stage IV.

TABLE 33.- 3σ NONGUIDANCE ERRORS AT ORBIT INJECTION

Error source	State error							
	X, ft	Y, ft	Z, ft	XD, fps	YD, fps	ZD, fps	Radius rss, ft	Velocity rss, fps
Stage I motor	-50 000.0	-84 100.0	39 990.0	-84.2	-145.2	67.7	105 710.0	181.0
Stage II motor	-29 560.0	-48 243.0	-580.0	-51.5	-86.5	11.5	56 580.0	101.4
Stage III motor	-38 110.0	-62 510.0	3 740.0	-59.6	-101.6	31.0	73 310.0	121.8
Stage IV motor	-1 250.0	-1 110.0	-16 960.0	-20.3	-24.5	-156.5	17 050.0	159.7
Stage I thrust misalignment, pitch	-3 310.0	-5 880.0	1 432.0	2.6	9.9	83.1	6 900.0	83.7
Stage I thrust misalignment, yaw	-250.0	-445.0	180.0	214.7	106.0	-11.6	520.0	239.8
Aerodynamic drag	18 870.0	31 030.0	3 380.0	33.2	56.0	-11.4	36 480.0	66.2
Atmospheric density	19 190.0	31 580.0	-3 840.0	33.7	56.7	-12.0	37 150.0	67.1
Tailwind	-7 000.0	-8 810.0	-45 760.0	-6.2	-7.3	-50.8	47 120.0	51.7
Crosswind	-60 600.0	38 370.0	1 800.0	-65.7	43.8	1.3	71 750.0	79.1
Stage II deadband, pitch	-14 560.0	-28 240.0	78 690.0	-42.2	77.1	115.1	84 860.0	144.9
Stage II deadband, roll	28 130.0	-19 010.0	1 760.0	52.2	-40.7	3.1	33 990.0	66.2
Stage II deadband, yaw	-51 710.0	33 320.0	990.0	-45.0	32.7	-0.2	61 520.0	55.6
Stage III deadband, pitch	-17 240.0	-32 200.0	72 220.0	-40.5	-74.1	111.1	80 930.0	139.6
Stage III deadband, roll	4 040.0	-3 030.0	670.0	12.4	-12.5	1.5	5 100.0	17.6
Stage III deadband, yaw	60 740.0	38 750.0	1 780.0	-76.0	51.7	1.5	72 070.0	91.9
Stage IV tipoff, pitch	3 040.0	-4 990.0	1 540.0	-337.7	-555.3	171.0	6 040.0	672.0
Stage IV tipoff, yaw	-5 140.0	3 150.0	370.0	-571.6	350.8	40.5	6 040.0	672.0
Stage IV deadband, pitch	-430.0	-710.0	200.0	-48.0	-78.9	21.6	850.0	94.9
Stage IV deadband	-730.0	450.0	30.0	-80.6	-49.8	3.0	850.0	94.9
Rss of error sources, original Scout	130 390.0	147 330.0	124 270.0	722.1	712.5	310.8	232 710.0	1061.0
Rss of error sources, TARS on Stage IV	130 250.0	147 220.0	124 270.0	299.0	291.4	257.3	232 550.0	490.5

TABLE 34.- 1σ RSS GUIDANCE ERRORS DUE TO THREE-AXIS RATE PACKAGE

Errors	Original Scout	DIGS	ODMARS	Honeywell (1009 gyro)
Velocity, fps	56.93	7.057	25.03	22.38
Position, ft	12 240.0	2 225.0	7 780.0	6 146.0
Attitude, deg	0.26	0.04	0.08	0.11

TABLE 35.- VARIANCES AND CORRELATION COEFFICIENTS AT ORBIT INJECTION, TOTAL SYSTEM - DIGS AND ORIGINAL SCOUT

Format					
σX					
ρXY	σY				
ρXZ	ρYZ	Z			
ρXXD	ρYXD	ZXD	XD		
ρXYD	ρYYD	ZYD	$\rho XDYD$	YD	
ρXZD	ρYZD	ZZD	$\rho XDZD$	YDZD	ZD
Original Scout IRP on Stage III and nonguidance errors					
43872.121					
0.16126178	49313.353				
-0.27673527	-0.42457731	42567.716			
0.30168313	0.08388381	-0.12260028	244.25558		
0.090227870	0.30997242	-0.21322612	-0.03639737	239.76997	
-0.23376944	-0.35741575	0.67088782	-0.41268421	-0.45591054	105.46154
DIGS ARU and nonguidance errors					
43439.676					
0.17174206	49081.178				
-0.27988244	-0.42591211	41447.714			
0.59699551	0.22760702	-0.25988009	99.823810		
0.25085517	0.85049222	-0.47151945	-0.00383169	97.225394	
-0.26104452	-0.41165516	0.78550096	-0.17438961	-0.40285979	85.817112

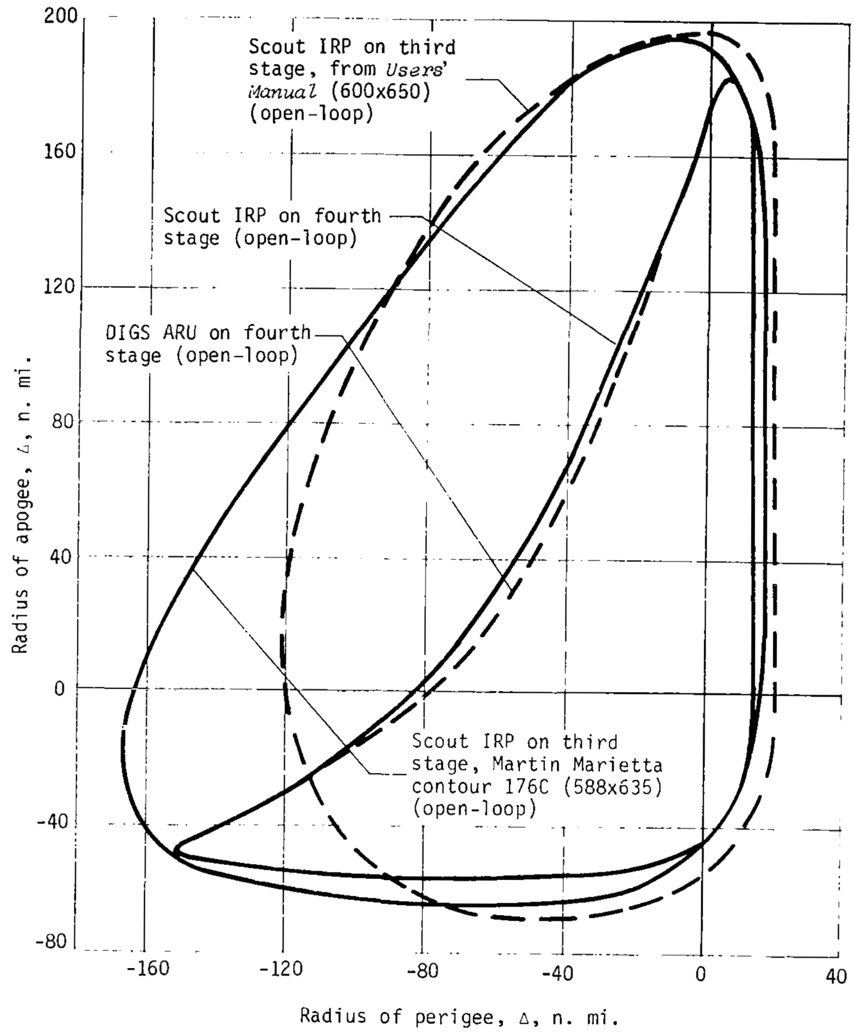

FIGURE 31.- ISOPROBABILITY CONTOURS

Conclusions

The nonguidance errors constitute the major portion (greater than 90%) of the present Scout vehicle system errors. Moving the present Scout IRP to Stage IV improves system accuracy (Note figure 31 where the radius of apogee and perigee is the factor of merit.) by about 30%. Comparing the best ARU system (DIGS) and the present Scout IRP on Stage IV, figure 31 indicates very little difference between their isoprobability contours. This means that the quality of the TARS does not appreciably change the total system errors and the nonguidance errors still predominate even with the TARS on Stage IV.

Significant benefit is obtained by moving the TARS to the fourth stage and the choice of equipment should largely be influenced by weight, size, power requirements, and cost.

Closed-loop systems must be considered before orders of magnitude accuracy improvements can be obtained.

LUNAR MISSION ANALYSIS

The objective of this task was to preliminarily investigate the feasibility of using the Scout vehicle for lunar missions. Five lunar trajectories were targeted. For each of these trajectories, lunar orbit insertion maneuvers were computed for orbits with eccentricities of 0.1, 0.4, and 0.7. From these trajectories one translunar trajectory with one lunar orbit insertion maneuver was selected for a more detailed error analysis to determine the amount of propellant required for a midcourse correction maneuver.

The results of these studies indicate that if a midcourse/orbit insertion engine having an I_{sp} of 200 seconds is used, the Scout vehicle can put a minimum of two-third of the payload weight after translunar injection into lunar orbit. The lunar orbit will have a periapsis height of about one lunar radius and an eccentricity range of 0.1 to 0.7 (for an eccentricity of 0.7, over 80% of the injection weight can be delivered into lunar orbit).

Translunar Trajectories

Since no definite lunar mission or mission type has been identified, it was decided to target several translunar trajectories chosen to span a modest range of trajectory parameters. Each of the targeted trajectories was a ballistic nominal trajectory from an injection state near the earth to specified closest approach conditions at the moon. The only constraints on the injection state were that it be approximately 285 kilometers above the earth and that the orbit plane established by the injection state be on an inclination approximately equal to the latitude of Wallops Island. This last constraint permits a 90° launch azimuth.

The target parameters at the lunar closest approach were:

1) Time at closest approach (t_{CA});

2) Radius at closest approach (r_{CA});

3) Inclination (relative to the lunar equator) of the osculating conic (i_{CA});

4) The semimajor axis of the osculating conic (a_{CA}).

Five ballistic nominal trajectories were targeted. The time at closest approach was 1/1/73, 0^h, 0^m, 0.0^s (Greenwich time) for all trajectories since the time of lunar encounter has a negligible effect on the delta V requirements for the mission. The remainder of the trajectory parameters are shown in table 36.

Table 36 shows that the injection conditions are relatively insensitive to the target conditions. It takes about the same energy to put a pound of payload in the vicinity of the moon regardless of the exact target conditions. As expected, a slight penalty is paid for the short flight time trajectories.

TABLE 36.- LUNAR TRAJECTORY PARAMETERS

	TRAJECTORY NO.				
	1	2	3	4	5
Flight Time (hr)	64.1	79.2	94.3	94.4	94.6
Injection Condition					
VI (km/s)	10.98	10.95	10.94	10.94	10.94
I (deg)	0.255	0.551	1.10	1.12	1.11
r (km)	6560	6560	6560	6560	6560
i (deg)	38.0	36.6	31.8	31.6	31.0
Closest Approach					
r_{CA}	3480	3490	3500	2620	2630
i_{CA}	4.8	6.5	6.9	6.8	44.9
a_{CA}	-2990	-4990	-6890	-6970	-7000

Lunar Orbit Insertion

If, on the other hand, one is interested in putting a payload in orbit around the moon, there are definite differences in the trajectories. To show this, the delta V required for coplanar lunar orbit insertion was computed. For each trajectory, three lunar orbit insertions with eccentricities of 0.1, 0.4, and 0.7 were computed. The maneuver was assumed to occur at closest approach and to involve no change in periapsis position or radius. The delta V required for each trajectory and each lunar orbit is shown in table 37.

TABLE 37.- DELTA V (m/s) REQUIRED FOR LUNAR ORBIT INSERTION

	TRAJECTORY NO.				
	1	2	3	4	5
Eccentricity					
0.1	890	720	670	770	730
0.4	730	570	510	580	540
0.7	590	420	370	400	370

It is evident from table 37 that substantially less orbit insertion delta V is required for the long flight time trajectories. Also as eccentricity decreases, the orbit insertion delta V increases as would be expected.

Error Analysis

Trajectory No. 3 was selected for more detailed analyses. It was chosen over the shorter flight time trajectories and the smaller r_{CA} trajectories because more payload could be delivered into lunar orbit. The purpose of the error analysis was to determine the amount of delta V required for midcourse maneuvers. In setting up the error analysis, a number of assumptions were made.

First of all, the translunar injection state covariance was found using a powered boost trajectory targeted to the trajectory No. 3 injection conditions and optimized for maximum payload. This was done at LRC. A guidance system error analysis was then performed using this trajectory. This was done at Martin Marietta using the TEAP program. The KT-70 guidance hardware characteristics program was used since it represents the reference guidance system. The state covariance matrix generated by TEAP was used as the initial state covariance for the translunar trajectory.

The deep-space network (DSN) was used as a model for the ground tracking network. The tracking stations were assumed to be located at Goldstone, Madrid, and Canberra. The equivalent station location errors were assumed to be 10 times those projected for the DSN during the 1975-1980 era (this being the most accurate and expensive tracking available). Only doppler measurements were assumed, with a range-rate white noise of 5 mm/s for a 1-minute count time. The current DSN value is 1 mm/s for a 1-minute count time.

In addition to the above measurement errors, the following dynamic errors were considered:

1) Lunar gravitational constant error = 0.06 km^3/s^2, 1σ;

2) Lunar orbit semimajor axis error = 1 km, 1σ;

3) Lunar orbit inclination error = 2.6×10^{-6} radians, 1σ;

4) Lunar orbit argument of periapsis error = 2.6×10^{-6} radians, 1σ.

Two terms are of interest in making an error analysis of a ballistic trajectory -- the knowledge covariance and the control covariance. These terms are defined as follows. Let the state along the nominal trajectory (the trajectory we would fly if the system were error-free) be designated by $\bar{X}$, a six-element vector having three position and three velocity components. Let the state along the actual flown trajectory be X. Finally, let $\hat{X}$ be the state that is calculated or estimated on the basis of initial conditions and measurements taken along the actual trajectory. Then the control covariance, Pc, is given by

$$Pc = E\ (X - \bar{X})\ (X - \bar{X})^T$$

where superscript T designates the matrix transpose. The control covariance provides us with the statistics of how far the actual trajectory will be from the nominal. The knowledge covariance, Pk, is given by

$$Pk = E\ (\hat{X} - X)\ (\hat{X} - X)^T \quad .$$

Thus the knowledge covariance tells us how well we know the actual location of the spacecraft.

The knowledge and control covariances are assumed to be equal at the beginning of a ballistic trajectory segment. As the spacecraft is tracked, the knowledge covariance decreases. When the knowledge covariance has decreased sufficiently, a midcourse correction can be calculated. This amounts to finding a new nominal trajectory that passes through the presently estimated position and meets the same conditions at the target body as the original nominal. The probable magnitude and direction of the midcourse correction depends on the control covariance before midcourse. If the midcourse maneuver were executed without error, the control covariance after midcourse would be equal to the knowledge covariance. In practice, the midcourse maneuver execution error must be added to the knowledge covariance to obtain the control covariance. Four parameters are used to model the midcourse maneuver:

1) Resolution error - The uncertainty in delta V resulting from uncertainty in thrust tailoff. A value of 0.0002 km/s, 1σ, was assumed;

2) Proportionality error - The uncertainty in delta V resulting from uncertainty in thrust level. A value of 0.01, 1σ, was assumed;

3) and 4) Error in thrust direction - An uncertainty of 1.5 deg in each of two orthogonal directions was assumed.

Once a midcourse maneuver has been analyzed, the control covariance can be propagated along the trajectory to determine whether the errors in the target parameters were the three components of the r_{CA} vector. If these errors are satisfactorily small, no further midcourse corrections are needed.

For preliminary analyses, the errors in position and/or velocity may be conveniently measured by the square root of the maximum eigenvalue of the covariance matrix. The covariance of a vector may be conceived of as defining an ellipsoid centered at the head of the vector. Each point on the ellipsoid has equal probability of occurrence. The square roots of the eigenvalues equal the lengths of the semiaxes of the 1σ ellipsoid. Thus the square root of the maximum eigenvalue is equal to the length of the semimajor axis of the 1σ error ellipsoid.

The first step in the error analysis is to establish the need for a midcourse correction. If no midcourse is performed the error in r_{CA} (square root of the maximum eigenvalue) was found to be 20 857 kilometers. Assuming that this is unacceptably large, the time of occurrence of the first midcourse must be established. This is usually chosen to be the time when the velocity knowledge error is one-half the execution error. Figure 32 is a plot of the velocity knowledge error and the midcourse execution error versus time for the first half-day of the trajectory. Based on these data, the first midcourse correction was set at 0.28 day after injection.

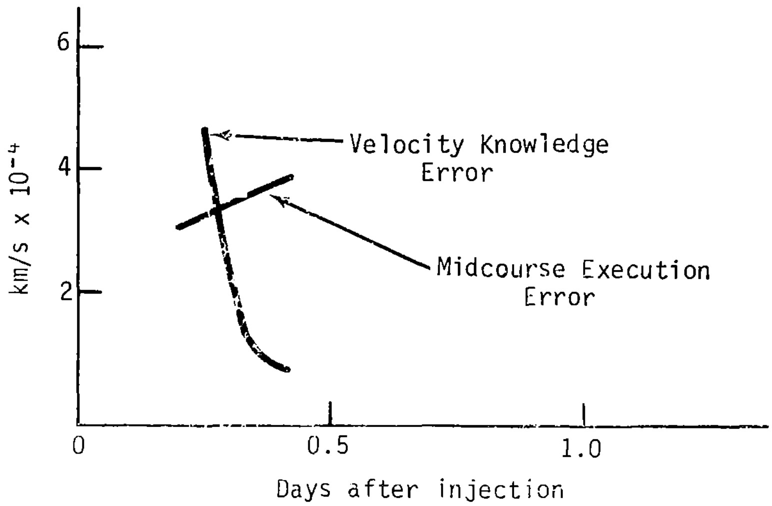

FIGURE 32.- ERROR VS TIME

The data for this maneuver are tabulated.

CONTROL ERROR	BEFORE MIDCOURSE	AFTER MIDCOURSE
Position (km)	259	4.6
Velocity (km/s)	1368×10^{-4}	3.5×10^{-4}
Error in r_{CA} (km)	2085	370

Note. 1. Execution error = 3.3×10^{-4} km/s and occurs at initiation of midcourse correction.

2. Expected value of Delta V = 12.7 m/s; 1σ value of expected delta V = 9.6; delta V required for 3σ mission = 41.5 m/s.

It was further assumed that a 370-kilometer error in r_{CA} was also unacceptable, thus requiring a second midcourse correction. This was set well inside the lunar sphere of influence at 3.4 days. The closest approach occurs at 3.93 days. The data for this maneuver are tabulated.

CONTROL ERROR	BEFORE SECOND MANEUVER	AFTER SECOND MANEUVER
Position (km)	132	1.4
Velocity (km/s)	7.4×10^{-4}	2.0×10^{-4}
Error in r_{CA} (km)	370	19.6

Note: 1. Execution error = 2.0×10^{-4} km/s and occurs at initiation of second maneuver.

2. Expected value of delta V = 3.7 m/s; 1σ value of expected delta V = 2.2 m/s; delta V required for a 3σ mission = 10.3 m/s. Thus the total midcourse delta V for this trajectory is 51.8 m/s, To this must be added the lunar orbit insertion delta V of 670 m/s, or a total of 722 m/s.

Note the statistics of the orbit insertion maneuver were not found. This would require an expensive and time-consuming Monte Carlo study.

If a midcourse/orbit insertion engine having an I_{sp} of 200 is used, the ratio of payload mass in lunar orbit, M_o, to mass injected into the translunar trajectory, M_I, is given approximately as

$$\frac{M_o}{M_I} = \text{Exp}\left\{-\frac{V}{g\, I_{sp}}\right\} = 0.69.*$$

The above analysis does not answer the question of the possibility of using the Scout for lunar missions. It can only serve as a benchmark and to point out some of the subsidiary questions that must be answered before feasibility can be established. First and foremost among such questions are:

1) If the ultimate objective of the mission is a lunar orbit, what are its parameters?

2) If orbit trim maneuvers are required to maintain an orbit, how accurately must the orbit be established and for how long?

3) What midcourse and orbit insertion engine will be used and what is the correct execution error model?

*0.69 is the mass ratio for a 0.1 eccentric orbit, 0.82 is the mass ratio for a 0.7 eccentric orbit.

RECOMMENDED GUIDANCE AND CONTROL SYSTEM

Qualitatively there is no question of the increased performance to be gained using the closed-loop guidance approach. Virtually all nonguidance error parameters are eliminated except for the uncertainty in the FW-4S engine burn characteristics. The greatly improved accuracy of the Scout orbit plus the increased flexibility of the vehicle makes the closed-loop guidance the recommended approach since it is most consistent with the desires of NASA for the future of the Scout launch vehicle.

As a result of this guidance hardware and control system sizing study, the following closed-loop mechanization is recommended for the Scout launch vehicle.

1) An inertial guidance system containing a platform, autopilot electronics, and digital computer should be added to the fourth stage of the Scout vehicle in place of the present third-stage open-loop system. The recommended system, based on the established criteria, is a modified KT-70 missile system as produced by Singer-General Precision Incorporated. Two of the more significant modifications include the additions of general-purpose computer with a memory capacity in excess of 4000 24-bit words and an optical azimuth alignment scheme. Alternative candidates to be considered in future studies include the Hamilton Standard DIGS system and the Litton LN-30 navigation system;

2) A hydrogen peroxide reaction control system weighing approximately 20 pounds should be added to the fourth stage and the present spin-stabilization hardware removed;

3) Due to the absence of a thrust termination capability in the fourth stage of Scout, it is recommended that a postboost velocity correction capability be provided by incorporating the appropriate control logic and extra fuel requirements into the reaction control system design. The sizing results of this study indicate that 4.3 pounds of extra fuel would provide for a velocity correction capability of 53 fps (1σ);

4) A pulse code modulation telemetry system with a 5-watt S-band FM transmitter is recommended in place of the current system. Total system weight will be in the vicinity of 12 pounds. This system was selected because the present system cannot transfer the required analog, bilevel, and digital signals necessary to instrument the improved guidance system.

The recommended guidance and control system characteristics are as shown in table 38.

TABLE 38.- RECOMMENDED GUIDANCE AND CONTROL SYSTEM

Subsystem	Characteristics	Weight, lb	Power, W
KT-70 missile platform	4-gimbal	15.1	9.7
	Two 2-axis Gyroflex gyros One single-axis C70-2401 accelerometer One 2-axis C70-2414 accelerometer		
G&C electronics	Platform electronics and autopilot electronics	7.0	25.6
DC power conditioner		5.5	75.6
Power transfer unit		1.0	--
Rate gyros	3 required for pich, roll, and yaw	1.5	6.8
Computer	General-purpose, memory > 4000 24-bit words	20.0	50.0
Subtotal		50.1	
Hydrogen peroxide reaction control system		20	
Orbital velocity correction system		4.3	
Batteries	28-V batteries	10.1	
Total		84.5	167.7

GUIDANCE SOFTWARE

Although the specific task of designing the guidance software is beyond the scope of this study, a generalized description of the necessary procedures for defining the guidelines for a complete guidance system appears to be quite appropriate.

The function of the guidance system is to control the vehicle state to satisfy the desired final conditions within prescribed bounds under normal dispersions in the vehicle performance characteristics. The attitude of the Scout vehicle and the fourth stage reaction control jets are used as the means of control to attain the required state. Intelligence derived from the guidance measurement unit applied to a mathematic algorithm yields the required attitudes to steer the vehicle to the desired targeted state. After the motors are depleted, the guidance system can use the control jets to correct for velocity dispersions.

The design of guidance software revolves about system interfaces, guidance algorithms to satisfy mission goals, and prelaunch procedures. All facets of the vehicle system, mission goals, launch site, and facilities must be known and available to assure that final guidance software design will function in the proper manner.

Requirements

The design procedure is to establish the requirements and existing systems and then apply this information to establish design criteria for interfacing with the control system, the operational sequencing, telemetry, prelaunch checkout, and mission accuracy. The addition of a closed-loop guidance system then imposes changes of the existing system that would be defined by the guidance contractor as a change or new requirement. The guidance logic is designed as a function of the criteria dictated by the design requirements, mission accuracy, costs, and subsequent recurring costs.

Software design criteria.- The guidance software design requirements are derived from specifications of the Scout vehicle, its missions, and associated data. This information is used as the basic guideline for the specific design and checkout criteria of the guidance software.

Mission specification.- Specifications of a mission are based on the results of a mission analysis. The analysis includes confirmation of the feasibility of the applicable vehicle to perform the mission. The specifications cover all general areas concerned with the mission:

1) Vehicle to be used;

2) Launch site;

3) Range safety considerations;

4) On-pad targeting requirements, if any;

5) Type of mission--orbit or reentry;

6) Final payload state;

7) Accuracy of required state;

8) Range of launch azimuth;

9) Payload orientation;

10) Inflight requirements.

The previous statements are generalities and other types of requirements that are more specific may be given.

The major requirements of the guidance equations are determined by the mission specifications. The types of missions considered are ground-launched only, in which the final injection may be earth orbit, reentry, translunar, or other earth escape orbits.

Although the guidance software equations should ideally apply to all the specified missions, this is generally not possible because of the different mission-peculiar situations. The penalty one pays to cover all missions is the need for an unnecessarily large computer unit that degrades vehicle performance predictions and increases hardware costs. The one exception is the class of missions that has the same schedule of events and the same type of constraints. For example, a guidance scheme that permits a payload to be launched into an earth orbit can be supplied with constants to be used for a reentry mission that has no range constraint.

The state-of-the-art guidance equations applicable to the Scout vehicle are generally in two classes--range-constrained reentry and orbital or suborbital nonrange-constrained schemes. The type of missions specified is one of the principal factors involved in the method of steering to be used. The accuracy requirements of the mission may be strict enough to render some methods unacceptable. If these requirements are too stringent, development time and costs will be increased.

Because of range safety constraints or mission requirements, a mission profile may require the flexibility of dogleg maneuvers. This would be included in the design of the software equations.

Missions that are target/time-dependent will require that guidance parameters be continually updated so the proper trajectory can be flown relative to the time of launch. These types of missions are rendevous with other solar bodies or orbiting satellites. Additional software will be necessary for this function. Simple and accurate procedures would place the software for guidance update in the airborne computer rather than requiring a ground computer and interfacing equipment for a complex updating program.

Vehicle characteristics.- All of the vehicle operating characteristics must be known to insure proper interfacing between the vehicle systems and the guidance system, including:

1) Vehicle configuration description;

2) Vehicle operating sequence of events;

3) Mass properties;

4) Structural constraints;

5) Heating constraints;

6) Propulsion system data;

7) Staging and ignition mechanisms;

8) Control system operation;

9) Performance capability;

10) Aerodynamic characteristics;

11) Pertinent vehicle performance dispersions.

The sequence of events and other essential information relating to each stage will become an integral part of the guidance logic flow. Any discrete event such as an inflight stage ignition that is to be controlled by the guidance system must be specified so the physical interface can be designed.

The guidance software to interface with the control system will be determined by the characteristics of each stage's control system. This will be done to assure that the proper vehicle attitude is achieved.

The vehicle characteristics will also be used in trajectory simulation programs to verify that constraints have not been violated and that the guidance philosophy to be applied satisfies the accuracy requirements and mission requirements under any applicable dispersed conditions.

Guidance hardware.- The guidance hardware interfacing data involve the inertial measurement unit, computer unit, timing synchronization, and platform alignment. The following functions must be considered for the respective subsystems:

1) Inertial measurement unit,

   a) Gimbal axes alignment,

   b) Gimbal angle measurement system,

   c) Accelerometer measurement system,

   d) Platform slew rates,

   e) Compensable error terms,

   f) Gimbal angle constraints;

2) Computer unit,

   a) Instruction repertoire,

   b) Instruction cycle time,

   c) Bits/words,

   d) Clock frequencies,

   e) Available memory,

   f) Digital-to-analog converters,

   g) Type of words (fixed, floating);

3) Platform alignment - The software requirements relative to the platform alignment are that the computation requirements be consistent with the method and hardware to be used. The alignment of the platform and platform measurement system provides the navigational means a guidance scheme programmed into the computer uses to calculate a required attitude that converges to the desired state.

The memory requirements of the computer are based on the total computation requirements of the software. The ideal situation is when the software can be fully identified and tradeoff studies conducted prior to specifying the computer memory core size. However, the usual case is that lead time and other factors require specifying core size long before the software is identified. In this instance, a good estimate would create no problem.

This information is most critical in establishing the proper usage of the guidance hardware.

Guidance Concepts

The improved inertial platform for Scout will provide attitude references relative to the launch site when the guidance system goes inertial, and integrating accelerometers to provide the effects of external forces acting on the vehicle mass in the form of three orthogonal components of velocity counts. The velocity terms are scaled, compensated for known errors, and transformed to a convenient coordinate system where a gravity model is added. These results are numerically integrated in the computer and yield position and velocity at the measured time. Navigation need not be this complete; it is solely a function of guidance equation requirements.

The guidance algorithm used during the ascent phase through the atmosphere may be different than that used for the upper stages. This strictly depends on the functional characteristics of the upper stage guidance philosophy.

The guidance algorithm is used to compute the desired attitude and is compared to the gimbal angle measurement in the appropriate coordinate frame. This signal is then used to drive the vehicle control system to obtain the required attitude.

Since the Scout vehicle final burn is to fuel depletion, any required velocity must be attained by the final stage attitude control jets. The guidance during the final stage will be designed to augment the burnout velocity by pulsing these control jets in the proper orientation.

Figure 33 illustrates the general inflight closed-loop guidance system.

Guidance equations and logic philosophy.- The structure of the guidance logic is designed to be synchronized with the vehicle operational sequence of events. This does not imply that the vehicle sequence is independent of the guidance logic, only that the guidance system will be cognizant of the sequence. The guidance logic is usually made up in terms of two primary time cycle frames--a major cycle in which the main frame navigation and guidance equations are computed, and a minor cycle in which attitude commands are issued at a high rate, instrumentation data are sampled, and normally thrust termination is executed.

Guidance steering algorithms are classified by two categories--explicit and implicit. The explicit form is basically a solution of the two-point boundary value problem, i.e., traversing a path from an initial state to a desired final state. The solution should not degrade performance to any extent. The solution in general is not in closed form, but rather approximating solutions. Since these approximations are valid only over short arcs, at the commencement of guidance steering large steering signals may result because of the initial state and then converge to the proper solution as the flight progresses. These types of equations are not truly explicit due to the approximations.

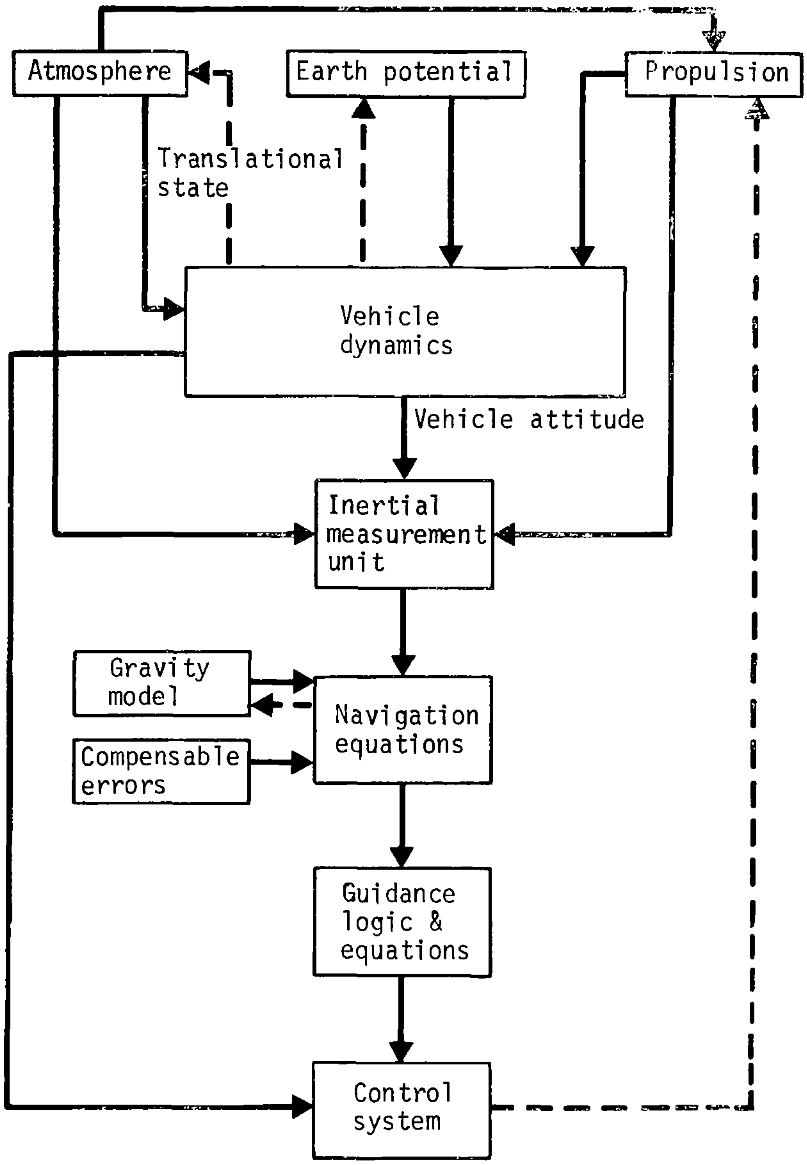

FIGURE 33.- CLOSED-LOOP GUIDANCE SYSTEM BLOCK DIAGRAM

The implicit form of guidance equations solves the two-point boundary value through indirect means. The method of using the applied equations depends on other functions that are precomputed.

There are two major considerations in determining the use of an explicit or implicit set of guidance equations. The first is that the implicit set generally is given by a smaller set of equations than the explicit set. This reduces the core requirements of the computer, the cycle time to compute the guidance function, and the cost because of less core requirement. It is also simpler to program. The second consideration is the targeting procedure (guidance constants generation) required of each guidance type. The implicit set generally requires much more effort to arrive at the necessary constants than the explicit set. This increases recurring costs and does not easily lend itself to flexible situations.

Proper selection of the guidance philosophy is thus a tradeoff between costs, flexibility, and complexity.

Guidance Equations

Linear sine.- The "linear sine" method described here satisfies radial position and velocity, nulling normal components of position and velocity while simultaneously satisfying total velocity.

The pitch plane steering is derived as discussed in the following paragraphs.

The two-body equation of motion in the radial direction in polar coordinates operating in a central force field:

$$\ddot{r} = A_{Tr} - \frac{\mu}{r^2} + \omega^2 r \tag{1}$$

where

A_{Tr} = radial thrust acceleration,

$-\frac{\mu}{r^2}$ = gravitational acceleration,

$\omega^2 r$ = centripetal acceleration.

An assumption is made with regard to the radial direction required:

$$\frac{A_{Tr}}{A_T} = A + Bt\left(\frac{\frac{\mu}{r^2} - \omega^2 r}{A_T}\right) \tag{2}$$

where t = time. Substituting (2) into (1) for A_{Tr},

$$\ddot{r} = (A + Bt)\ A_T \quad . \tag{3}$$

The determination of thrust acceleration proceeds in the following manner:

$$A_T = \frac{\text{Thrust}}{\text{Mass}} \quad . \tag{4}$$

Division by mass flow rate $\dot{M}$,

$$A_T = \frac{\frac{\text{Thrust}}{\dot{M}}}{\frac{\text{Mass}}{\dot{M}}} = \frac{V_e}{T_r} \tag{5}$$

where

$V_e = \frac{\text{Thrust}}{\dot{M}} = g_0\ I_{sp}$ = effective exhaust velocity,

$T_r = \frac{\text{Mass}}{\dot{M}}$ = time to mass depletion.

It is assumed that a constant thrust and flow rate propulsion system is being portrayed.

Functionally, T_r is derived from the ideal velocity equation

$$\Delta V_s = - V_e \int_{t_{N-1}}^{t_0} \frac{dM}{M} \quad . \tag{6}$$

After manipulating this equation,

$$T_r = \frac{\Delta t}{(\Delta V_s/V_e)\ [1 + \frac{1}{2}\ (\Delta V_s/V_e)]} \quad . \tag{7}$$

Operationally, T_r is obtained by (7) where Δt is the sample interval and ΔV_s is the sampled "sensed" velocity. V_e remains a constant, the nominal exhaust velocity. Though the I_{sp} can change, the sensed velocity changes proportionally, which gives T_r the proper value in calculation of the thrust acceleration.

T_r is also $T_{r0} - t$, where T_{r0} is the original value:

$$\ddot{r} = (A + Bt)\left(\frac{V_e}{T_{r0} - t}\right) \quad . \tag{8}$$

Manipulating (8),

$$\ddot{r} = -BV_e + (A + BT_{r0})\ (T_T) \quad . \tag{9}$$

The parameters A, B, V_e and T_{r0} are assumed constant:

$$\ddot{r} = A_r' + B_r\ A_T \quad . \tag{10}$$

Equation (10) is the steering law, A_r' and B_r are next found. Integrating (10) from t_N to cutoff (T_g):

$$\dot{r}_f = \dot{r} + \int_0^{T_g} A_r'\ dt + B_r \int_0^{T_g} A_T dt \tag{11}$$

$$r_f = r + V_r\ T_g + \int_0^{T_g} \left[\int_0^t A_r'\ ds\right] dt + B_r \int_0^{T_g} \left[\int_0^t A_T\ ds\right] dt \quad . \tag{12}$$

The integrals

$$\int_0^{T_g} A_T\ dt = V_g \tag{13}$$

$$\int_0^{T_g} \left[\int_0^t A_T\ ds\right] dt = V_g\ T_g - V_g\ T_r + V_e\ T_g \tag{14}$$

where

$$V_e = \int_0^{T_g} \frac{V_e}{T_r - t}\ dt = -V_e\ \ell n \left(1 - \frac{T_g}{T_r}\right) \quad .$$

Substituting (13) and (14) into (11) and (12) performing the integration, solving for A'_r and B_r, then substituting A'_r and B_r into (10) gives

$$\ddot{r} = A_r = \frac{1}{T_g} (\dot{r}_f - \dot{r} - V_g B_r) + B_r A_T \tag{15}$$

where

$$B_r = \frac{\left[r_f - r - \frac{T_g}{2} (\dot{r}_f + \dot{r}) \right]}{\left[- V_g \quad T_r - \frac{T_g}{2} + V_e T_g \right]} \quad . \tag{16}$$

It is now easily seen that this derivational procedure was to supply an approximating function to the equations of motion that could be solved. This solution cannot be carried out to cutoff since T_g goes to zero and is in the denominator, Thus, at some arbitrary time prior to $T_g \leq 0$ where B_r has converged to a suitable solution, A_r is then computed by extrapolation of B_r:

$$A_r = A_{r_{(N-1)}} + B_r \frac{(\Delta t) \; (A_T)}{(T_r + \Delta t)} \tag{17}$$

This means that in the last few seconds of the burn, guidance is open loop. Assuming that vehicle performance does not change in those few seconds, guidance will function properly.

The desired radial thrust acceleration is

$$A_{rd} = A_r - \frac{\mu}{r^2} - \frac{\dot{r}_t}{r} \tag{18}$$

where

$\dot{r}_t$ = tangential velocity.

Yaw steering is similar. An orbital plane is defined where normal components of the state are desired to be zero:

$$A_{nd} = A_N + B_n A_T \quad . \tag{19}$$

The estimate of T_g (time-to-go to cutoff).- One procedure is to use angular momentum required with respect to a desired value:

$$\Delta h = h_f - h \tag{20}$$

where

h_f = desired angular momentum magnitude at cutoff

h = present angular momentum magnitude.

The required angular momentum to be gained can also be expressed by

$$\Delta h = \int_0^{T_g} \dot{h} \, dt \quad . \tag{21}$$

The magnitude of $\dot{h}$ is given by the radius R times the tangential acceleration. The mechanization to the solution of (21) can be evaluated using Simpson's integration formula. Five equally spaced points of the integral $\dot{h}$ are set up.

Tangential acceleration at each point.- This is derived by

$$A_{TT}(t_j) = [A_T^2(t_j) - A_{TR}^2(t_j) - A_{TN}^2(t_j)]^{\frac{1}{2}} \quad . \tag{22}$$

The accelerations to be used in (22) are the solutions to the guidance problem given previously:

$$A_{TR} = A_R' + B_r A_T - \frac{\mu}{r^2} + \omega^2 R$$

$$A_{Tn} = A_n + B_n A_T$$

$$\omega^2 R = h^2/R^3 \quad .$$

These equations are applied at the equally spaced points with linear interpolation used to obtain gravity and centripetal accelerations to define $\dot{h}$ at each point. The solution to (21) is then

$$\Delta h' = [\dot{h}(t_1) + 4\dot{h}(t_2) + 2\dot{h}(t_3) + 4\dot{h}(t_4) + \dot{h}(t_5)] T_g'$$

where

T_g' is the initial estimate of T_g.

$\Delta h'$ is compared to the true angular momentum to provide an adjustment of the initial estimate of T_g:

$$T_g = T'_g + [(h_f - h) - \Delta h']/\dot{h}\ (t_5) \tag{23}$$

The time-to-go provides the means to simultaneously satisfy position, flightpath angle, and velocity. T_g provides the time frame within which the steering equations are to operate to satisfy position and flightpath angle. Since T_g is a function of angular momentum $\vec{r} \times \vec{V}$, it can be seen that simultaneous satisfaction of the desired state can be obtained.

Thus the steering is accomplished by (18) and (19), which define the desired attitude of the vehicle, and T_g will determine the satisfaction of velocity. These equations are designed to operate out of the atmosphere. These equations can be set up for rendezvous missions, injection into orbits with desired true anomoly, or other conditions when inflight targeting to update r_f, $\dot{r}_f$, and V_f is made part of the guidance equations. This scheme is set up to satisfy end conditions on a per-stage basis. Thus, multistage vehicles require a reference trajectory or procedures to define intermediate target points.

Q-matrix guidance.- The theory and concepts of the Q-matrix guidance were developed by the Instrumentation Laboratory of MIT. The Q-matrix guidance scheme as described is used to place a vehicle in a freefall-type of trajectory.

The required velocity of a vehicle at the start of free flight to satisfy a given range is defined to be the correlated velocity vector, $\vec{V}_c$:

$$\vec{V}_c = f\ (\vec{r}, \vec{r}_{TL}, t_{FT}, t_E) \tag{24}$$

$$\vec{r}_{TI} = f\ (\vec{r}_{TL}, t_{FT}) \qquad (25$$

where

$\vec{r}$ = vehicle position,

$\vec{r}_{TL}$ = target position at launch,

r_{TI} = target position at intercept time,

t_E = time since launch,

t_{FT} = total time of flight,

t_{FF} = free-flight time.

If the total time of flight is defined to be constant, then $\vec{r}_{TI}$ is constant and (24) reduces to

$$\vec{V}_c = f\ (\vec{r},\ t_E) = f\ (\vec{r},\ t_{FF}) \quad . \tag{26}$$

This function is expanded in terms of the partial derivatives of the variables

$$\frac{d\vec{V}_c}{dt_E} = \left(\frac{\partial V_c}{\partial \vec{r}}\right)\left(\frac{d\vec{r}}{dt_E}\right) + \frac{\partial \vec{V}_c}{\partial t_E} \quad . \tag{27}$$

In free flight, at some point A on the powered portion of the trajectory at time t_E:

$$\left(\frac{d\vec{V}_c}{dt_E}\right)_{FF} = \vec{g} \tag{28}$$

$$\left(\frac{d\vec{r}}{dt_E}\right)_{FF} = \vec{V}_c \quad . \tag{29}$$

Then

$$\left(\frac{d\vec{V}_c}{dt_E}\right)_{FF} = \vec{g} = \left[\left(\frac{\partial V_c}{\partial \vec{r}}\right)\vec{V}_c\right]_A + \left(\frac{\partial \vec{V}_c}{\partial t_E}\right)_A \quad . \tag{30}$$

Rearranging

$$\left(\frac{dV_c}{dt_E}\right)_A = \vec{g} - \left(\frac{\partial V_c}{\partial \vec{r}}\right)_A \vec{V}_c \tag{31}$$

At the same point A at time t_E, the departure from powered flight is the vehicle velocity $\vec{V}_M$:

$$\left(\frac{d\vec{V}_c}{dt_E}\right)_{PF} = \left(\frac{\partial \vec{V}_c}{\partial \vec{r}}\right)_A \left(\frac{d\vec{r}}{dt_E}\right)_{PF} + \left(\frac{\partial V_c}{\partial t_E}\right)_A \quad . \tag{32}$$

Substituting (31) into (32),

$$\left(\frac{d\vec{V}_c}{dt_E}\right)_{PF} = \left(\frac{\partial \vec{V}_c}{\partial \vec{r}}\right)_A \vec{V}_m + g - \left(\frac{\partial V_c}{\partial \vec{r}}\right) \vec{V}_c \quad . \tag{33}$$

Velocity-to-be-gained until thrust termination is

$$\vec{V}_g = \vec{V}_c - \vec{V}_M \quad . \tag{34}$$

Rearranging (33) and using (34),

$$\left(\frac{dV_c}{dt_E}\right)_{PF} = -\left(\frac{\partial \vec{V}_c}{\partial \vec{r}}\right)_A \vec{V}_g + \vec{g} \quad . \tag{35}$$

The differentiation of $\vec{V}_g$ yields

$$\dot{\vec{V}}_g = \dot{\vec{V}}_c - \dot{\vec{V}}_M + \dot{\vec{V}}_c - (a_T + g) \quad . \tag{36}$$

Substituting (36) into (35),

$$\dot{\vec{V}}_g = -\left(\frac{\partial \vec{V}_c}{\partial \vec{r}}\right)\left(\vec{V}_g\right) - \vec{a}_T \tag{37}$$

Equation (37) is the generalized Q-matrix guidance law, and expanded into matrix form is

$$\begin{bmatrix} \dot{V}_{GX} \\ \dot{V}_{GY} \\ \dot{V}_{GZ} \end{bmatrix} = - \begin{bmatrix} Q_{XX} & Q_{XY} & Q_{XZ} \\ Q_{YX} & Q_{YY} & Q_{YZ} \\ Q_{ZX} & Q_{ZY} & Q_{ZZ} \end{bmatrix} \begin{bmatrix} V_{GX} \\ V_{GY} \\ V_{GZ} \end{bmatrix} - \begin{bmatrix} a_{TX} \\ a_{TY} \\ a_{TZ} \end{bmatrix}$$

where

$$[Q_{ij}] = \begin{bmatrix} \frac{\partial V_{CX}}{\partial X} & \frac{\partial V_{CX}}{\partial Y} & \frac{\partial V_{CX}}{\partial Z} \\ \frac{\partial V_{CY}}{\partial X} & \frac{\partial V_{CY}}{\partial Y} & \frac{\partial V_{CY}}{\partial Z} \\ \frac{\partial V_{CZ}}{\partial X} & \frac{\partial V_{CZ}}{\partial Y} & \frac{\partial V_{CZ}}{\partial Z} \end{bmatrix} \quad .$$

Delta guidance equations.- These equations are based on approximations to the sensitivities of target miss with respect to the delta from nominal burnout state vectors.

Define x and z to be in the pitch plane. There is some point in the vehicle flight path whose coordinates are x, y, z, $\dot{y}$, t where an $\dot{x}$ and $\dot{z}$ exist that will satisfy the target miss requirement of zero. This is the required velocity and is defined to be for the nominal burnout point.

If the required velocity is compared to the measured velocity, a velocity increment that must be gained to obtain the required velocity is defined as

$$\Delta\dot{x}_g = \dot{x} - \dot{x}_{req}\ (x,\ y,\ z,\ \dot{y},\ t) \tag{44}$$

$$\Delta\dot{z}_g = \dot{z} - \dot{z}_{req}\ (x,\ y,\ z,\ \dot{y},\ t) \tag{45}$$

Perturbations on the trajectory require small corrections that define a new required velocity

$$\Delta\dot{x}_\varepsilon = \dot{x}_0 - \dot{x}_{req}\ (x,\ y,\ z,\ \dot{y},\ t) \tag{46}$$

$$\Delta\dot{z}_\varepsilon = \dot{z}_0 - \dot{z}_{req}\ (x,\ y,\ z,\ \dot{y},\ t) \tag{47}$$

where $\dot{x}_0$ and $\dot{z}_0$ are the nominal values of required velocity.

The required velocity is now

$$\Delta\dot{x}_g* = (\dot{x} - \dot{x}_0) + \Delta\dot{x}_\varepsilon \tag{48}$$

$$\Delta\dot{z}_g* = (\dot{z} - \dot{z}_0) + \Delta\dot{z}_\varepsilon \tag{49}$$

The delta errors can be approximated by a Taylor series expansion of the nominal cutoff state vector. Many terms are generated, but only a few have any significance:

$$\begin{aligned}\Delta\dot{x}_\varepsilon &= D_1\ \Delta x + D_2\ \Delta y + D_3\ \Delta z + D_4\ \Delta\dot{y} + D_5\ \Delta t + D_6\ (\Delta x)^2 + D_7\ (\Delta y)^2 \\ &+ D_8\ \Delta x\ \Delta y + D_9\ (\Delta\dot{y})^2 + D_{10}\ \Delta x\ \Delta\dot{y} + D_{11}\ \Delta y\ \Delta\dot{y}\quad ,\end{aligned} \tag{50}$$

and

$$\Delta\dot{z}_\varepsilon = C_1\ \Delta x + C_2\ \Delta y + C_3\ \Delta z + C_4\ \Delta\dot{y} + C_5\ \Delta t \tag{51}$$

These results are then the correlation of the required velocity in free flight to that in powered flight.

$\vec{V}_g$ is used to affect the direction of the thrust vector and can be done by cross-product steering:

$$\vec{\omega}_c = - K_w (\vec{V}_g \times \vec{V}_G)$$

where

$\vec{\omega}_c$ = a command turning rate in inertial space and $\vec{a}_T$,

K_w = a gain consistent with the vehicle stability requirements and trajectory shape.

$\vec{V}_g$ must be misaligned with $\vec{V}_g$ by at least 90° when steering commences or the method will not function properly.

The application of this method for orbital injection would require modification of the correlation functions, e.g., as redefining, by the proper mathematics, the Q-matrix to be functions of orbital parameters.

Trajectory fit method.- Various steering methods can be derived directly from the functions of a nominal trajectory. Some are applied only during the atmospheric phase of the boost trajectory--for example, to approximate a gravity turn.

A general velocity steering method can be defined by controlling the flight-path of the vehicle so

$$V_Z = f_1 (V_X, x, z, t) \tag{38}$$

The implementation of (38) is to define a function that describes the deviation of V_Z in terms of attitude and combining this with the nominal attitude for the total commanded attitude.

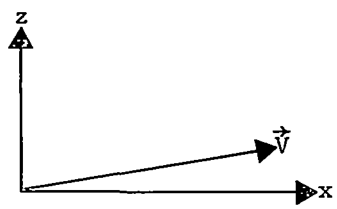

The coordinate system in which the function to be used is sketched.

The deviation from the nominal is derived by comparing the measured V_z to the nominal V_z. The nominal can be defined by fitting points along the nominal trajectory by the least-square fitting techniques. The exactness of fit using the least-squares fitting method will depend on the complexity of "shape" to determine the order of fit. The order of fit actually imposed depends on the required accuracies. The general function to describe the attitude deviations can be

$$\delta\theta_c = -K_c \left[V_{Z_{MEASURED}} - f_2 \left(V_x, x, z, t\right) \right] \quad . \tag{39}$$

The function f_2 is fitted to the nominal case and can be of the form

$$f_2 = K_{X1} + K_{X2} V_x + K_{X3} V_x^2 \tag{40}$$

where x, z, t are determined to have no significant effects. K_c is a gain and conversion factor that is determined on the basis of tradeoff between vehicle stability and effective steering. $\delta\theta_c$ is added to the nominal attitude command, which may be of the form given in (40).

A similar method called velocity-wire, which is functionally self-descriptive, that can satisfy velocity, altitude, and flightpath angle is now described.

Define $V_g = \vec{V}_{DESIRED} - \vec{V}_{MEASURED}$. Fit $\dot{R}$ (radial rate) to a polynomial that is a function of V_g to the required order. This defines a desired radial rate:

$$\dot{R}_c = A_1 + A_2 V_g + A_3 V_g^2 + \cdots + A_n V_g^{n-1} \quad . \tag{41}$$

Then define the error in $\dot{R}$ by

$$\dot{R}_\varepsilon = \dot{R}_c - \dot{R} \tag{42}$$

The commanded attitude is made a function of $\dot{R}_\varepsilon$ in the following manner:

$$\theta_c = \theta_{c_{IC}} + K_{TD} \dot{R}_\varepsilon + K_{ID} \int_{t_1}^{t} \dot{R}_\varepsilon \, dt - K_D \dot{R}_\varepsilon \Big|_{t-t_1} \quad . \tag{43}$$

It is seen that this function is to null the errors to zero, with memory built in to eliminate altitude errors. Thus, using V_g to attain velocity in conjunction with the attitude steering to satisfy flightpath angle and altitude, the simultaneous satisfaction of the desired state is attainable.

where

$$\Delta x = x - x_{nom},$$

$$\Delta y = y - y_{nom},$$

$$\Delta z = z - z_{nom},$$

$$\Delta t = t - t_{nom} \quad \text{(time)}.$$

Equations (50) and (51) are used in (48) and (49) to provide the attitude commands in terms of velocity-to-be-gained vectors such as shown in the Q-guidance or used in the form given in the velocity-wire method.

The coefficients are derived from an overdetermined set of data obtained by perturbing the nominal burnout by a series of vehicle and navigational dispersions, propagating the dispersed burnout state to the target and computing the miss sensitivities with respect to the perturbed state at burnout.

Summary.- There are other available guidance equations, some of which are included in Appendix E, that are not discussed herein. The intent is to show some of the rationale used in the rudimentary development of guidance equations. The functional form of the equations does not necessarily reflect the actual mechanization of the guidance logic and equations. For example, in (43), the integral is a numerical procedure. The actual implementation of the steering commands is not given since attitude reference systems vary and control system interfaces are different from vehicle-to-vehicle.

Targeting

Targeting is the procedure by which the necessary mission-dependent guidance constants are derived. Other constants such as the universal gravity constant are true constants that need not be generated on a mission-to-mission basis. The importance of targeting is not only reflected in the satisfaction of mission requirement, but also in the time and complexity of the required procedure. This reflects directly on the flexibility of the entire operation and varying degrees of recurring costs.

Generally, the simple guidance equations require much precomputation work, whereas the more complex explicit types require a minimum amount of effort. Therefore, the explicit equations can be targeted to a new mission much more rapidly, thereby enhancing flexibility and reducing recurring costs.

The explicit guidance equations called "linear target" used on the Centaur solve the guidance problem by solving the equations of motion to the specified end conditions, treating each staging point of the vehicle as a discontinuity, and setting up the sensitivities of the end boundary point with respect to the steering algorithm. This treatment of the problem only requires specification of the final state as the targeting procedures and is somewhat similar to trajectory shaping methods where sensitivities of final state with respect to control parameters are used.

The velocity-wire scheme requires the generation of a shaped trajectory, obtaining data by which to fit, manipulating the data into the required form, fitting the data, and establishing the proper gains.

The Q-matrix type of guidance requires the generation of many perturbed trajectories to establish the "best" sensitivity matrix ([Q]) for the given mission.

The targeting procedure ranges from simply stating desired end conditions, to complex procedures that require much time, effort, and computer runs. This is a direct result of the type of guidance method used.

Functional capabilities of guidance logic.- It must be proved that the guidance equations and constants satisfy mission requirements. There are two basic levels of approved acceptance of the guidance logic. Both are done by implementing tne guidance logic in a computer simulation such as a trajectory program to simulate flight.

The first is to implement the guidance logic in a trajectory program in the format of a large scientific computer. The guidance logic is exercised under various perturbed conditions to show that it will function properly.

The second level is the checks imposed on the guidance logic that is in tne format of the operational computer. This can be done by either loading the operational guidance logic into the operational computer or by using a computer program that simulates the operational computer. The guidance logic is then exercised to prove that it will function as designed.

The reason for performing the two very similar tasks is that use of the large scientific computer checkout procedure is much more cost-effective. It also provides comparative checks between two independent procedures.

Platform Alignment

The function of the inertial sensing instruments is to provide the means to navigate in a specified coordinate system such as an earth-centered, right-handed frame with coordinates in the equatorial plane and in a meridian plane. The measuring instruments are generally aligned in an earth-fixed geographic coordinate system related to the local vertical and the launch site azimuth.

The alignment process is to level the platform and to place the instruments along a line known with respect to north. This then satisfies the theoretical ideal relation between the measurement and navigational coordinates:

$$\begin{bmatrix} X_{NAV} \\ Y_{NAV} \\ Z_{NAV} \end{bmatrix} [A_{ij}] \; [B_{ij}] \begin{bmatrix} X_{MEAS} \\ Y_{MEAS} \\ Z_{MEAS} \end{bmatrix}$$

where

$[A_{ij}]$ = f (LATITUDE, LONGITUDE, AZIMUTH)

$[B_{ij}]$ = f (INSTRUMENT ORIENTATION RELATIVE TO PLATFORM AXES).

The leveling of a platform is accomplished by the application of various sensors and methods to the measurement of the local gravity vector. The gravity vector is generally deflected from the ideal model due to local anomalies. This error is known from geological surveys and is applied in the $[A_{ij}]$ matrix.

A method that is used to level platforms is to use the measuring accelerometer outputs to provide the signal in the leveling electronics. Assume that the orientation of two accelerometer input axes are to be in the desired level plane; then these two instruments would not sense any gravitational effects.

Since the measurement unit is fixed to earth, it is in a rotating frame. The inertial acceleration of the instruments is given by

$$\ddot{R}_{I/E} = \ddot{R}_E + 2\,\bar{\omega}_{EI} \times \dot{\vec{R}}_E + \omega_{EI} \times (\omega_{EI} \times \vec{R}_E)$$

where

I denotes inertial space,

E denotes W/R earth,

$\vec{\omega}_{EI}$ = earth rotation rate with respect to inertial space,

$\vec{R}_E$ = position vector.

Under terrestrial equalibrium, gravity is equal to centripetal acceleration plus anomalies:

$$\ddot{R}_{I/e} = \ddot{\bar{R}}_E + 2\,\bar{\omega}_{EI} \times \dot{\bar{R}}_E + \bar{g}$$

Since the level is defined to be normal to $\bar{g}$, components of $\bar{g}$ cannot be sensed. Therefore, if the platform is not level, the accelerometers will sense this, providing the basis to level the platform. The actual implementation of this method involves the use of filtering techniques for system noise and vehicle motion caused by wind gusts.

The azimuth alignment can be accomplished by the use of optical devices based on surveys. Gyrocompassing could also be used utilizing the gyroscopes and accelerometers.

The survey method for azimuth alignment is to use a precise known location to use as a reference. This reference in existing systems is communicated to the platform by optical devices. A porro prism mounted on the platform with its axes known in relation to the platform axes is used to effect a return image to a theodolite established at the surveyed location. This then sets up the null point in azimuth and further changes in azimuth are measured by the theodolite, which is an angle-measuring device.

Gyrocompassing can be used to effect azimuth reference. Since the site location is well known, the components of earth's rotation needed to torque the gyros to maintain an earth-fixed system until go-inertial is also well known. If the platform is not properly aligned to north, the gyros will sense the earth rotation that is not being compensated by the gyro torquing program. This causes the platform to tilt so the level accelerometer outputs could be used or gyro precission operated on to effect alignment.

These alignment procedures can be used to drive the platform hardware to its proper orientation and they can moniter the system to update $[A_{ij}]$, $[B_{ij}]$, and other data such as accelerometer bias.

Prelaunch Checkout

Operational correctness of the guidance system is assured by exercising the entire system before launch. Programs are set up to check out the computer and all interfaces. These programs range from verifying that the computer can add data from two locations in the computer, to moving the control vanes given any preconditioned situation.

Any indication of anomalies will be given by an incorrect comparative answer. The total system's and subsystems' operational characteristics are used to establish the checkout criteria.

Guidance Software Summary

The various aspects of the guidance system and the general procedures to design the guidance software were presented in terms of parts of the overall system. These parts are represented in figures 34 and 35 to show the relationship between design requirements and areas of design in an overall sense.

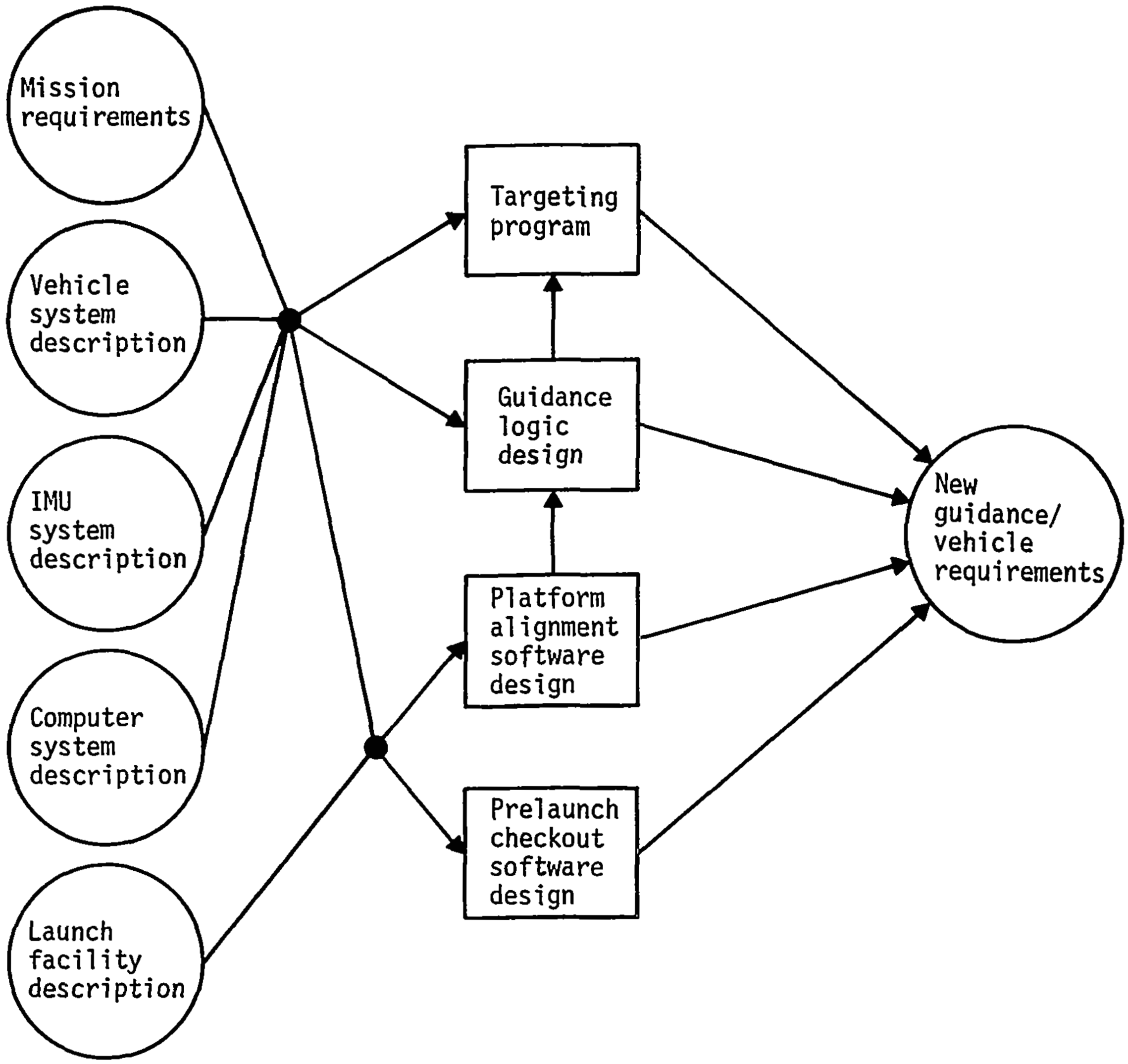

FIGURE 34.- INTERFACING OF DESIGN REQUIREMENTS

Each portion of the guidance software is designed using the information indicated in the diagram.

The guidance software is integrated into the system operation and is shown functionally.

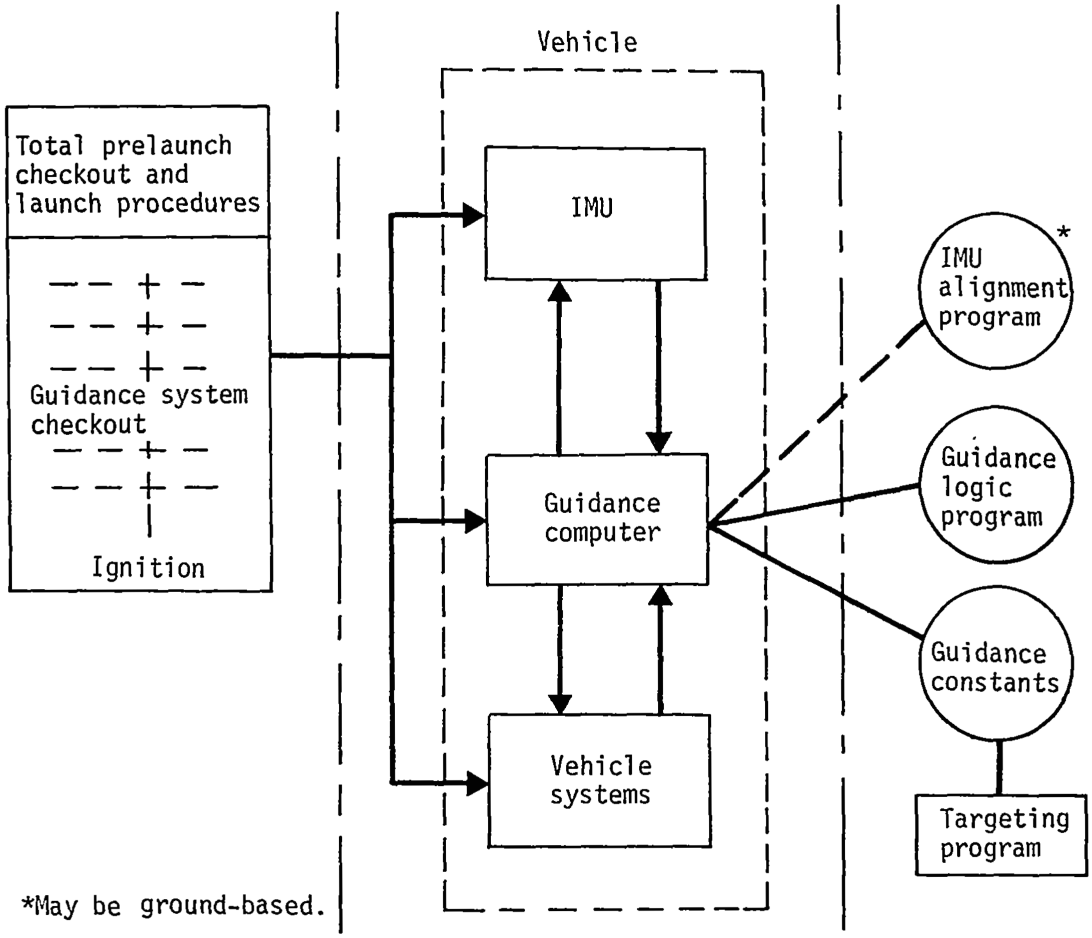

FIGURE 35.- GUIDANCE SOFTWARE ON-PAD OPERATION

The functional diagram is an oversimplification of the integration of the guidance system into the total system. Specific details, such as the sequence point within the operation at which the guidance computer programs may be loaded, will be a task to be done during the design phase.

The generalities of the necessary process to produce the guidance software have been provided to show what must be done and the various tradeoffs that must be considered, e.g., targeting procedures relative to guidance equation sets or use of better quality accelerometers to provide better initial alignment of the IMU. Stringent requirements and general flexibility increase costs.

Realistic estimates of requirements will provide for the most cost-effective guidance software and hardware system.

GUIDANCE HARDWARE/SCOUT VEHICLE INTERFACING

Requirements and goals for the Scout inertial guidance system should provide for improved performance coupled with minimum modifications and low development costs. Since weight, power, and environmental capability are also important criteria and influence the final hardware selection, the selected hardware can rarely be adapted to the intended vehicle application without some modifications. These modifications, along with a preliminary interfacing definition, are outlined in this section.

Scout/KT-70 Missile System Applications Study

To adapt the KT-70 missile system to the Scout launch vehicle, several modifications are required:

1) Change IMU gimbal orientation;

2) Add porro prism and viewing port to IMU;

3) Rescale accelerometer loops;

4) Select a digital computer with increased capability;

5) Add viewing port in Scout "E" section and optical window in heat-shield.

A discussion of each of these modifications follows.

Recommended gimbal orientation for Scout.- Only three gimbals are required to isolate a platform from angular motions of the vehicle in which it is located. Unless the angular deflections are less than 90°, a condition commonly termed gimbal lock may occur during certain angular deviations of the vehicle. Gimbal lock occurs when two gimbal axes of a three-axis system are colinear. In this case, angular motion can be transmitted to the platform. With a fourth gimbal, as in the KT-70 missile system, full angular freedom is permitted the platform because of the fourth or redundant gimbal axis. The KT-70 has a redundant roll axis whereby the inner gimbal freedom is reduced and the outer roll gimbal is servoed to the inner roll gimbal. As the system pitches through 90°, the inner roll axis becomes aligned with the yaw axis and the outer roll axis flips 180° with no gimbal lock. The torque required to rotate it becomes infinite. Therefore it is desirable to avoid this 90° pitch maneuver and the resultant gimbal flip.

For a missile application in which the vehicle is launched vertically, i.e., Scout, the azimuth axis should be normal to the orbital plane (pitch angle approximately zero). For the Scout vehicle, the KT-70 gimbal orientation will be pitch (cluster axis), yaw (middle axis), and roll (outer axis). The platform will be side-mounted to achieve this orientation. This will then transfer the 90° gimbal flip from pitch to yaw.

This particular system allows the better accelerometer to see the high-acceleration levels. The accelerometer, whose input axis lies parallel to the vehicle's yaw axis at launch, becomes the downrange accelerometer. The accelerometer-sensitive axis lying parallel to the vehicle roll axis at launch becomes the vertical accelerometer.

The orientation restricts the Scout missile because the platform must be oriented in the orbital plane, or approximately so, rather than in a north-east and vertical coordinate frame. The basic constraint is that the normal platform azimuth axis must take the pitch maneuver.

Azimuth alignment.- Direct optical transfer alignment to the azimuth axis will not be possible since there is insufficient room to mount a porro prism directly on the platform cluster. Since in the Kearfott-recommended orientation, the platform roll axis is vertical before launch, the inner roll axis becomes the axis that must be aligned optically. If the platform case is used as the azimuth reference, three additional error sources contaminate azimuth alignment accuracy. They are the outer roll axis pickoff device, inner roll pickoff device, and shock mount repeatability. Therefore the prism should be mounted in from the vibration isolators. A detailed approach to azimuth alignment follows.

In order to meet the desired performance requirements of the improved guidance system, ground initialization of the guidance platform to better than 50 arc-seconds is required. Initialization consists of leveling the platform and determining the azimuth orientation of the stabilized cluster in the earth coordinate frame. The numerical requirements for leveling are: 22 arc-seconds and an azimuth knowledge of 47 arc-seconds.

Discussion of alignment techniques will be limited herein to the recommended KT-70 platform. The assumption of a different platform or IMU would result in a somewhat different mechanization, particularly in the computer software for the strapdown configuration. However, the basic optical measurement techniques would probably not be greatly different.

Gyrocompassing.- With regard to azimuth determination, it may properly be asked if the technique of gyrocompassing can be used. The method is desirable in that alignment capability is internal to the launch vehicle, thereby eliminating the need for launch site optical instruments, bench marks, and surveying activity. Further, it can normally be accomplished automatically in a shorter period of time than by optical methods. However, in the case of the KT-70 missile platform, the gyro bias uncertainty is too great to permit use of this method. Azimuth error in the gyrocompassing mode for a level platform is given by an expression:

$$\Delta H = \frac{\omega_e}{\Omega \cos \lambda}$$

where

ΔH = azimuth error from a true east-west line

ω_e = drift uncertainty of the east-west gyro

Ω = earth rate

λ = local latitude.

For the KT-70 missile platform, the drift uncertainty of the gyro can probably not do better than 0.02°/hr. The gyrocompassing azimuth error will then be at least:

$$\Delta H = \frac{0.02}{(15)(0.8)}$$

$$= 0.00166 \text{ radians,}$$

or approximately 330 arc-seconds at typical launch latitudes (VAFB and Wallops Island). At San Marco, the error would be slightly less due to the greater horizontal earth rate at almost the equator. However, the error would still be in excess of that permitted to achieve the desired goals. It is, therefore, proposed that optical methods be used.

Optical Alignment.- To optically determine the orientation of the platform azimuth gimbal, the requirements follow:

1) An azimuth reference related to earth coordinates such as surveyed bench marks within view fo the launch complex;

2) A porro prism on the platform with a known angular relation to platform gimbal axes;

3) An angular measuring device between the platform porro and the azimuth gimbal such as an electrical resolver;

4) An autocollimating theodolite to transfer a line-of-sight from the bench marks to the platform porro.

A typical arrangement is shown in figure 36 using bench marks 1 and 2. However, due to certain conditions that necessarily exist, variations of the setup shown will be required. These conditions and instrumentation concepts are discussed in the following paragraphs.

In normal surveying practice, a direction can be determined by setting up over a bench mark and sighting on another bench mark target, the direction between the two having been previously established. However, variations in booster vertical, sway, and particularly the requirement to launch on more than a single azimuth, preclude setting up over a known bench mark. As an example, at Wallops Island where launch azimuth varies from 85° to 129°, in order to see into the alignment porro prism, the theodolite position may fall anywhere on an arc of equal extent (44°) about the launcher.

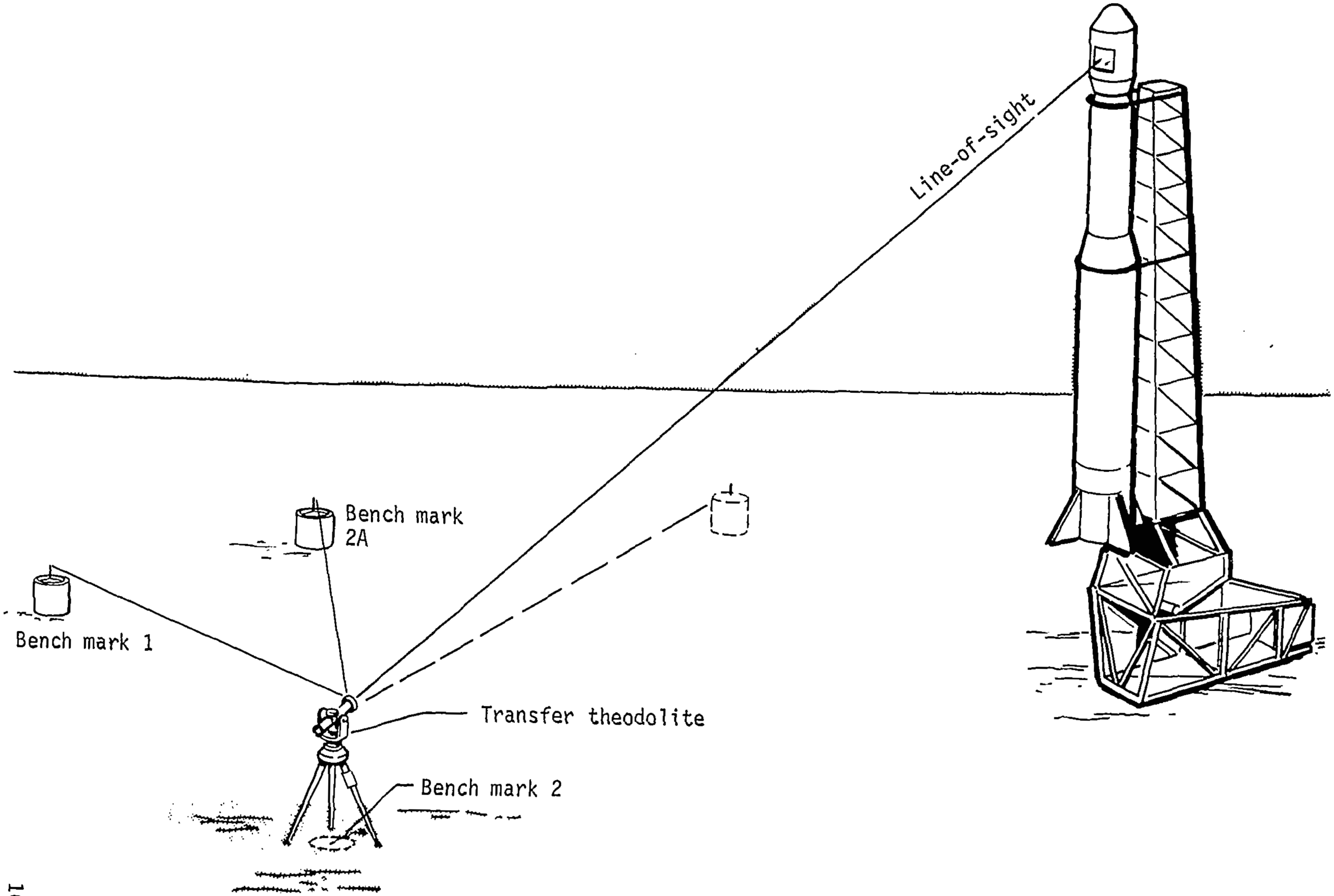

FIGURE 36.- SCOUT OPTICAL ALIGNMENT METHOD 1

Three methods of setting up an azimuth reference without restricting the location of the theodolite that may be employed are:

1) A third bench mark may be established as shown by dotted lines in figure 36, and bench mark #2 then located remotely to position 2A as shown in the same figure.

2) Instead of bench marks, a stable monolith with a precision indexing head containing a mirror or porro prism can be installed. Once surveyed to North at its zero position, it can then be accurately turned to allow autocollimation off the mirror by the theodolite at any arbitrary location of the theodolite. (See figure 37.)

3) A third method employs two theodolites with one located on a bench mark to establish the known line to a second bench mark. It can then be turned a known angle to co-align the transfer theodolite which is located so as to autocollimate off the IMU porro prism. This method is illustrated in figure 38.

Of the three methods described, method 2. requires the fewest number of surveyed bench marks and hence the fewest number of measurements taken for prelaunch alignment. It also lends itsself to being instrumented with electrical readout so that if desired, computation of alignment angles could be handled in AGE equipment, thereby reducing the possibility of human error in computation or data taking. This method may also be preferable at the San Marco sight where there may be insufficient space for the multiple bench mark methods, although method 3 could be used as shown in figure 38. Further studies are required and measurements need to be taken to see if the San Marco tower is sufficiently rigid over long periods to maintain a surveyed azimuth line to the accuracy required. If not, a procedure using method 2 might be worked out to permit reestablishing azimuth shortly before launch. The procedure would involve taking a sight on a fixed reference on shore prior to beginning the aligment procedure.

The preceding paragraphs have described methods by which a known azimuth may be determined with respect to a porro prism mounted on the platform. A method of aligning the cluster to the porro prism is described in the following paragraphs.

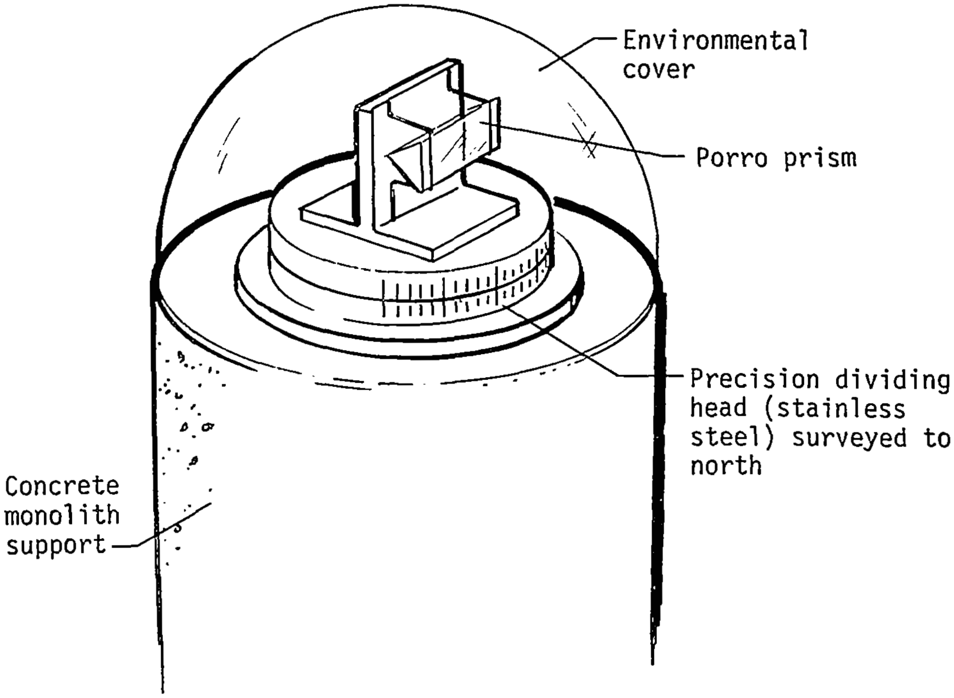

Note: May be used as alternative to Bench Mark 2 in Figure 38

FIGURE 37.- STABLE MONOLITH WITH PRECISION INDEXING HEAD

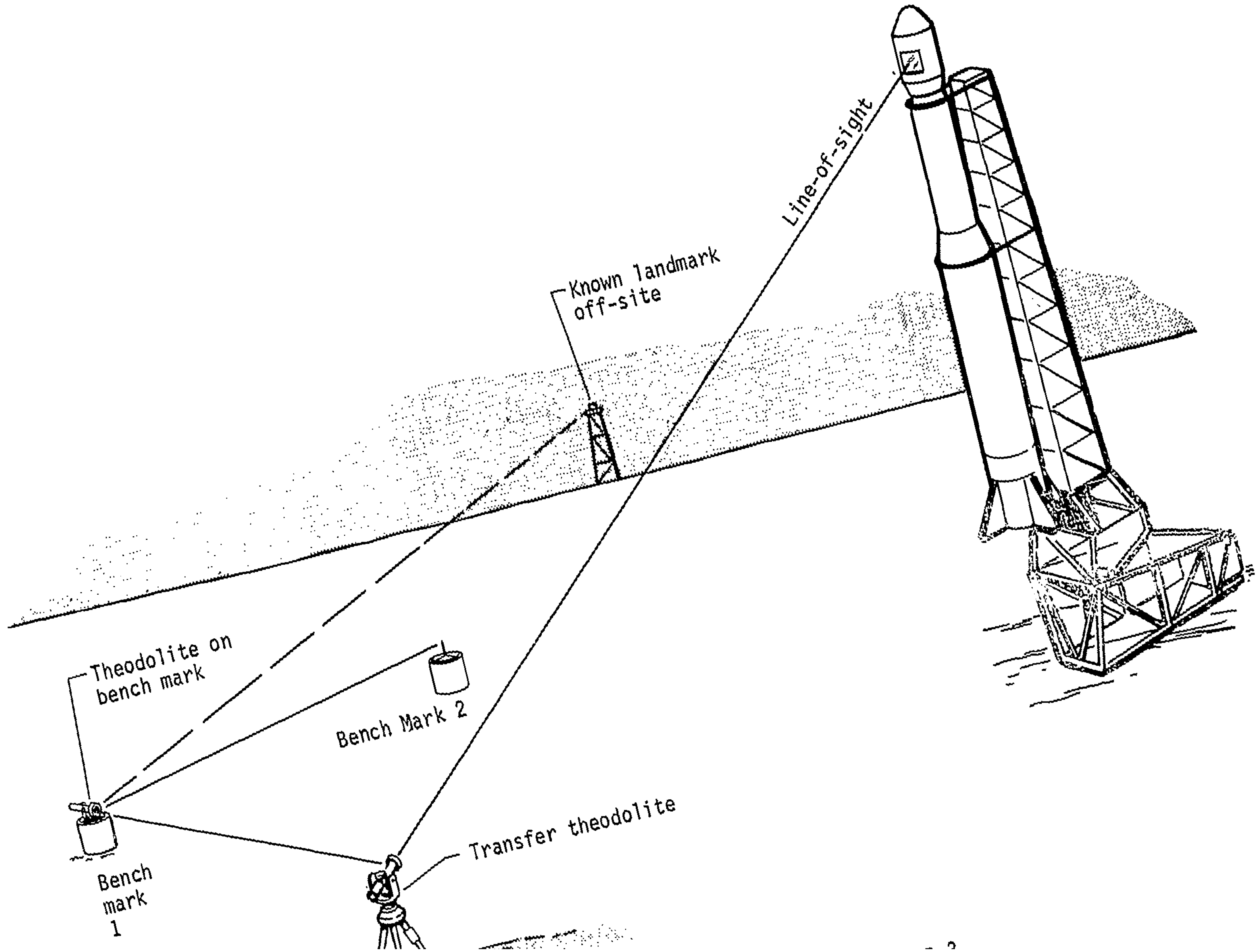
Line-of-sight
Known landmark
off-site
Theodolite on
bench mark
Bench Mark 2
Transfer theodolite
Bench
mark
1

The porro prism will be mounted on the inertial platform frame as shown in figure 39. Note that the prism is on the "inside" of the vibration isolators to avoid misalignment errors resulting from nonrepeatability of the elastomeric mount. The porro prism and gimbal cluster are shown schematically in figure 40. The gimbal resolver sine windings are "zeroed" during factory assembly so that the innermost gimbal axis is parallel to the prism roof azis when the resolvers are at null. See figure 40 for gimbal orientation at launch. The predominate nonsystematic error in azimuth will then be due to deviation from true horizontal of the porro roof axis when the vehicle is erected in the launch position. This error, using the small angle approximation, is expressed as

$$\Delta H = \psi \tan \theta$$

where

> H is the azimuth error,
>
> θ is the prism look down angle,
>
> ψ is the deviation from true horizontal (in radians) of the porro roof axis.

Assuming the transfer theodolite is approximately 70 feet away, θ would be nominally 45° as a worst case example. To limit the azimuth error to less than one arc-minute, it is immediately obvious that the tilt of the vehicle must be known to better than an arc-minute. This can be measured quite readily by caging the gimbals on their resovers and taking a reading on the cross range accelerometer. Then, if the entire cluster is rotated 180° by reversing polarity on the outer roll servo, a second tilt reading can be taken from the same accelerometer and the arithmetic average of the two is the angle ψ. The data can then be fed into the guidance computer and a launch azimuth correction can be computed. The computer can also be loaded with the measured azimuth so that at liftoff a small angle roll maneuver to the proper launch azimuth can be made.

Alignment sequence.- A typical alignment sequence might proceed as follows, assuming bench marks of the type described previously in method 2 are available, and that its "zero" has been checked against another bench mark. It is further assumed that the booster is in the launch "erect" position.

1) Set up the transfer theodolite and adjust laterally until a sharp autocollimated return image is observed. This may require several iterations, leveling the instrument after each shift.

2) Swing the leveled theodolite in azimuth and sight in on the bench mark mirror. Have an assistant move the mirror roughly in azimuth until the return image can be seen. Make the final autocollimating adjustment with the theodolite. Read and record the angle of the bench mark mirror. Set the theodolite azimuth scale to this same setting. The azimuth scale will now read true azimuth.

3) Re-sight on the porro prism and record the azimuth reading.

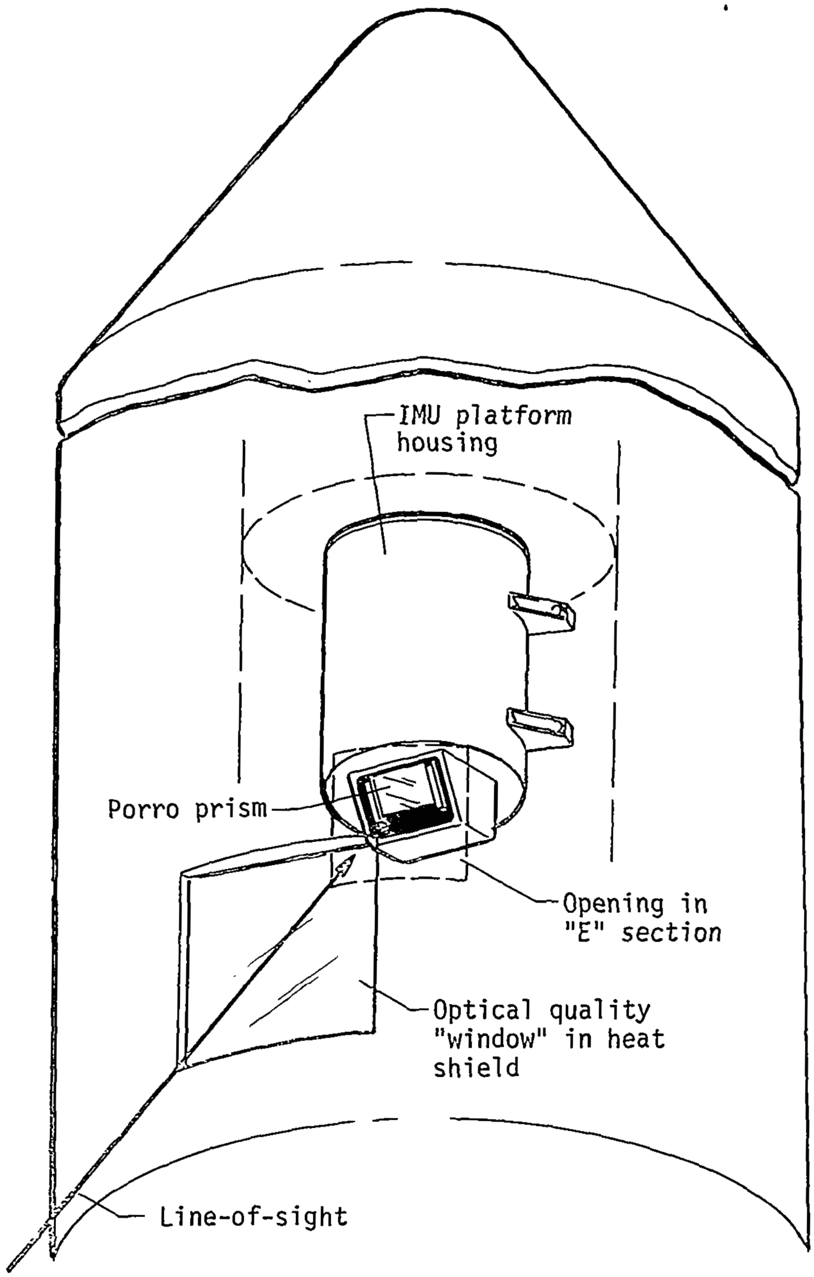

FIGURE 39.- IMU INSTALLATION IN VEHICLE

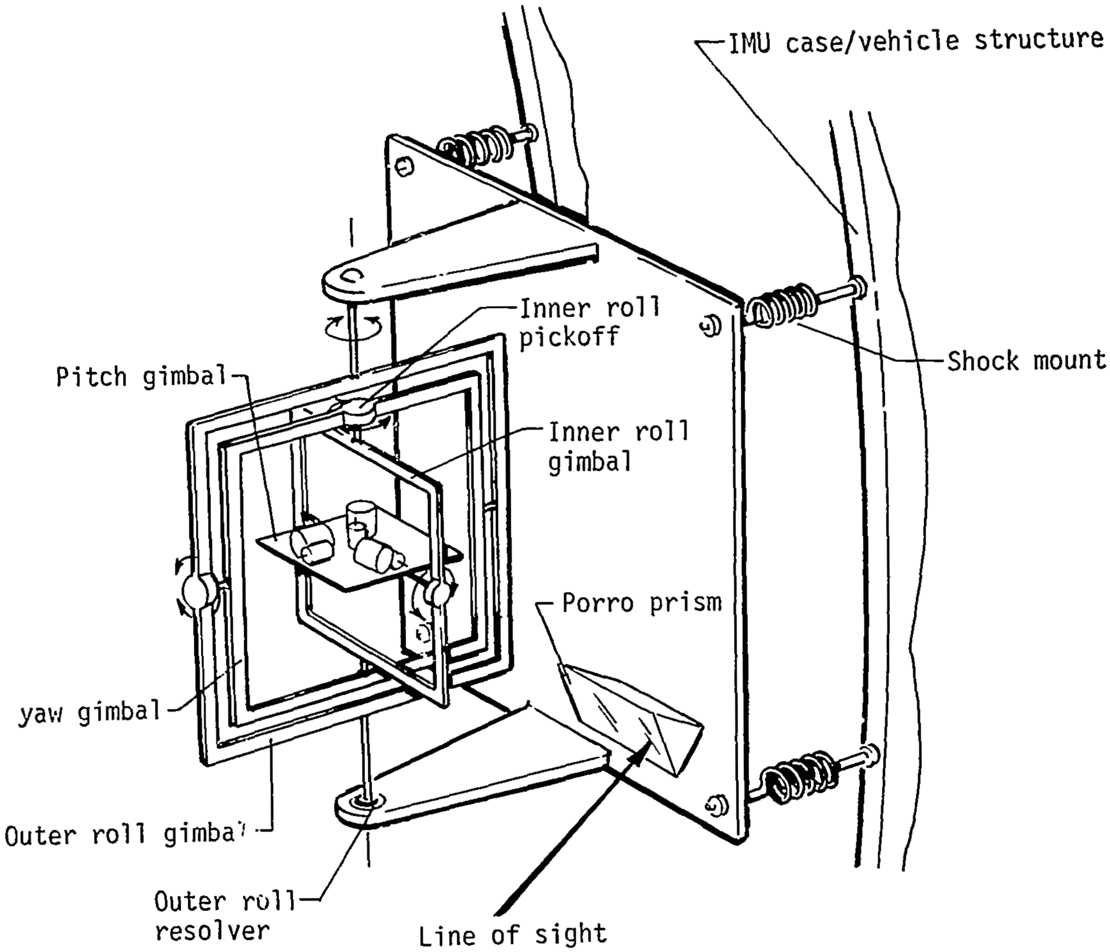

FIGURE 40.- SCHEMATIC REPRESENTATION GIMBAL SYSTEM

4) Initiate the platform start-up sequence and proceed to that point where all gimbals are caged, accelerometers "on", gyros "off". Measure and record the crossrange accelerometer output.

5) Proceed to the next step which reverses the outer roll gimbal (launch azimuth gimbal). Measure and record the crossrange accelerometer again

6) Proceed to the next step returning the outer roll gimbal to its proper orientation, and starting the gyro wheels.

7) Maintain the gimbals caged and load the computer with the true azimuth and tilt data.

8) Proceed to "fine level" mode.

9) Just prior to launch, uncage the roll gimbal, and allow the computers to torque the cluster (by means of the roll gyro) to the computed launch azimuth. (This angle should be small--one degree or less.)

10) The computer will make a self-check tolerance test on the precomputed roll synchro reading in azimuth, pitch, and yaw synchro outputs for a cluster verticality check.

Alignment error summary.- The dominant errors that contribute to inaccuracy in determining the launch azimuth and their estimated magnitudes are described below. They are categorized into two basic groups: (1) surveying and optical instrumentation errors and (2) calibration uncertainties and instabilities. Surveying and optical instrumentation errors are as follows:

1) Accuracy of surveying-in bench marks, set-up errors, and theodolite transfer errors in autocollimating off the porro prism typically can be held to 25 arc-seconds (3σ) or less.

2) Atmospheric shimmer is variable but has been observed to be as much as 15 arc-seconds (3σ).

3) Azimuth error resulting from porro tilt was previously defined as $\Delta H = \psi \tan \theta$, and a method of determining the azimuth correction was described. However, uncertainties in the measurements used to compute the correction result in a residual error. The contributions are approximately as follows:

   a) Accelerometer short-term instability and outer roll gimbal runout--10 arc-seconds (1σ),

   b) Porro mounting accuracy and long-term stability--20 arc-seconds (1σ),

   c) Short-term vehicle sway during alignment--15 arc-seconds (1σ).

   The root sum square of the above is 27 arc-seconds, which at a nominal "look-up" angle of 30° results in an azimuth error of 16 arc-seconds (1σ).

4) In addition to the purely geometric azimuth error $\Delta H = \psi \tan \theta$, there is an optical error associated with the porro prism. If the line-of-sight is not normal to the entrance face of the prism, then tilt of the prism roof axis (due to nonverticality of the booster) will cause an azimuth error:

$$\varepsilon = \tfrac{1}{2} \alpha \sin 2\psi$$

where

α is the departure from normal of the line-of-sight with respect to the porro face;

ψ is the porro roof axis tilt with respect to the horizontal as previously defined.

This term, if not accounted for, can cause substantial errors in the determination of azimuth. As an example, for vehicle tilt resulting in both α and ψ of 1°, ε will be approximately one arc-minute.

However, ε can readily be computed and the azimuth corrected. ψ is accurately measured in the alignment procedure as previously described, and α may be read off the pitch resolver to sufficient accuracy once the cluster is leveled. Assuming knowledge of α and ψ to 10 arc minutes and 20 arc-seconds respectively, ε can be computed to an accuracy of approximately 12 arc-seconds (3σ)

Calibration uncertainties and instabilities are as follows:

1) The accuracy of setting the platform cluster alignment to porro roof axis at resolver electrical null is budgeted to be 25 arc-seconds (1σ) including long-term electromechanical instabilities.

2) Computational and torquing errors during final alignment steps should not exceed 20 arc-seconds (3σ).

3) Resolver null repeatability on the inner and outer roll gimbals should not exceed 10 arc-seconds each (1σ).

Table 39 summarizes the 1σ errors just discussed. The rss assumes statistical independence.

TABLE 39.- ALIGNMENT ERRORS

Surve	ARC-SECONDS
Surveying errors	8
Atmospheric shimmer	5
ΔH	16
ε	4
Porro to cluster (long-term)	25
Computational	7
Resolver null (inner)	10
(outer)	10
rss (1σ)	35

For the assumed allowable azimuth error of 47 arc-seconds, the above provides a contingency margin of

$$\left[(47)^2 - (35)^2\right]^{1/2} = 31 \text{ arc-seconds.}$$

Rescale accelerometer loops.- Accelerometers are used to level two axes. Due to the relatively high accelerometer scale factors (80 pps/g), fine alignment around level becomes impractical even with third-order systems. The current application has a 20 g range at 0.4 ft/sec/pulse. Kearfott proposes to torque the platform off-level approximately 1° in each of the level axes, determine the tilt angle from the component of g into each axis, then open-loop-slew to level. To attain 20 arc-seconds on each axis, accelerometer scale factor, scale factor stability, gyro torquer scale factor stability, and bias stability will all have to be comparable to a 1 n. mi./hr navigator, in addition to requiring Kalman or another type of filtering inthe computer. It is suggested that a scale factor change be made in the accelerometer loop to facilitate conventional leveling. Another possible option would be to use analog capture and CAPRI electronics as found in the KT-70 aircraft navigators.

Acceleration effects.- Some degradation in performance could be expected at higher accelerations, (20 to 25 g), because of the gimbal servoloop performance (static stiffness) and gimbal axis imbalance (fig. 41). The performance degradation can be summarized as:

1) For azimuth loop, 310 oz, in./milliradian;

2) For roll loop, 930 oz in./milliradian;

3) For pitch loop, 1080 oz in./milliradian;

4) Torquers saturate at 20 oz in. in azimuth and 40 oz in. in pitch and roll.

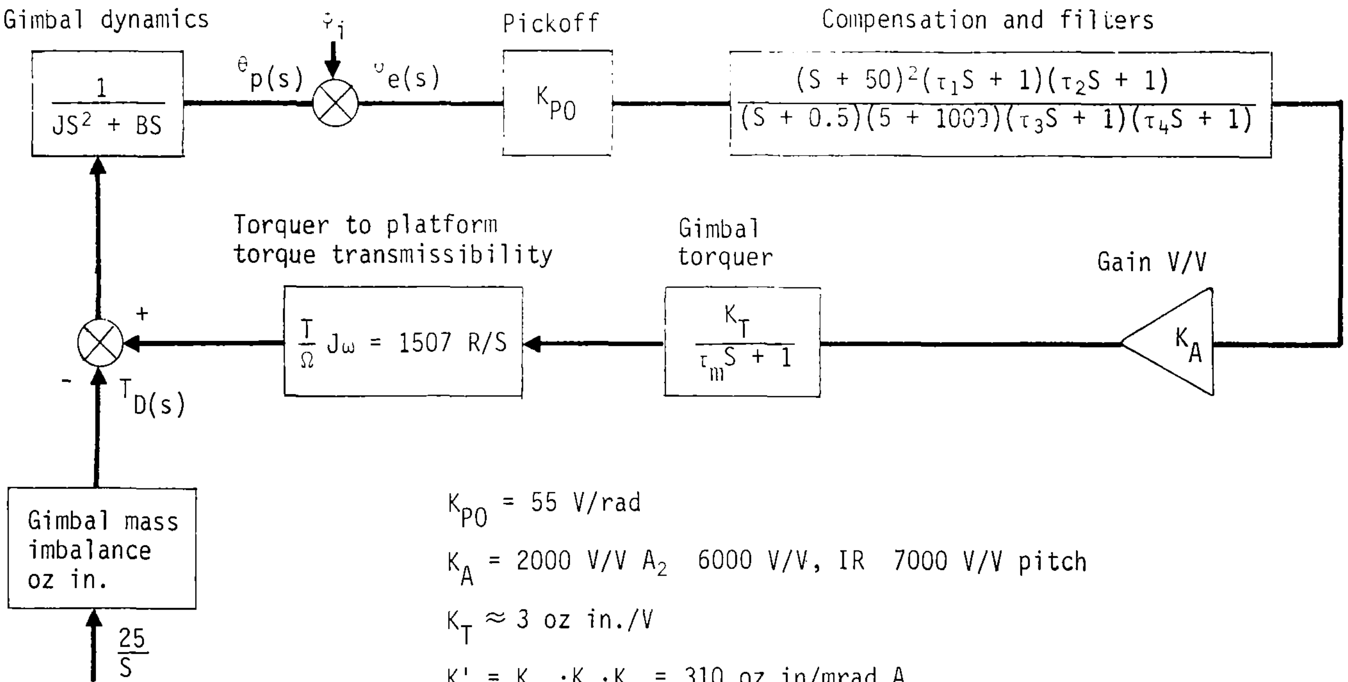

K_{PO} = 55 V/rad

K_A = 2000 V/V A_2 6000 V/V, IR 7000 V/V pitch

$K_T \approx$ 3 oz in./V

$K' = K_{PO} \cdot K_A \cdot K_T$ = 310 oz in/mrad A_Z

= 930 oz in./mrad IR

= 1080 oz in./mrad P.

$$\theta_e = \tau_D \cdot \frac{1}{K}$$

$$= 12.5 \frac{1}{310}$$

$$= \frac{1}{40} \text{ mrad} = 5.25\pi$$

FIGURE 41.- GIMBAL SERVOLOOP

The maximum gimbal imbalance for any axis cannot be greater than 1.6 oz in., which leaves no dynamic range in the loop. A more realistic gimbal imbalance limit would be 0.2 oz in. or 35 gm cm. This hangoff would amount to an additional 8.6 arc-second accelerometer misalignment during 25 g accelerations.

It has been observed in 2-axis, dry, flex joint gyros that wheel modulation noises increase with wheel hangoff. It is therefore anticipated that platform heading sensitivity will increase under high-g accelerations.

Guidance computer.- The computer sizing has shown that the Magic 301 computer will not be adequate for the Scout application. The Magic 301 computer now in production for the KT-70 missile system is a fixed-point, two's complement computer with a maximum memory capacity of 2048 8-bit words. For this reason a number of miniature airborne computers have been surveyed and were tabulated in the section entitled *Computer Sizing Survey and Selection*. This sizing study resulted in the recommendation of computer with a memory capacity in excess of 4000 24-bit words.

Interfacing

To establish a preliminary interfacing, it is necessary to investigate three areas: electrical, structural, and thermal interfaces. This section begins with a preliminary description of electrical interfaces followed by a physical layout of the recommended system.

Electrical interface.- The goals of minimum weight and minimum developmental costs are not necessarily compatible. In other words it may be more weight-effective to redesign the entire guidance and autopilot system with the computer being the central element interfacing with the rest of the vehicle subsystems. This is similar to the approach taken on the Titan IIIC digital autopilot design. On the other hand, one might consider using the computer as an arithmetic unit only and having a centralized control electronics unit for gain switching, interfacing, autopilot functions, etc.

Figure 42 illustrates the signal flow for the present Scout guidance and control system. Each block represents a component in the third stage with the exception of the Base A servos and second-stage control motors. The improved guidance and control system will be located in the fourth stage and must replace or interface with and/or, when applicable, provide the required functions currently provided by the following Stage III Scout components:

1) Guidance unit (IRP);
2) Amplifier demodulator - poppet valve (PVE);
3) Intervalometer;
4) Programmer;
5) Diode unit;
6) Filter, body-bend;
7) Inverter;
8) Roll/yaw compensation unit;
9) Rate gyro unit;
10) Power control relay box.

It must also interface with a telemetry system, the ignition system, and the first-, second-, third-, and new fourth-stage control systems.

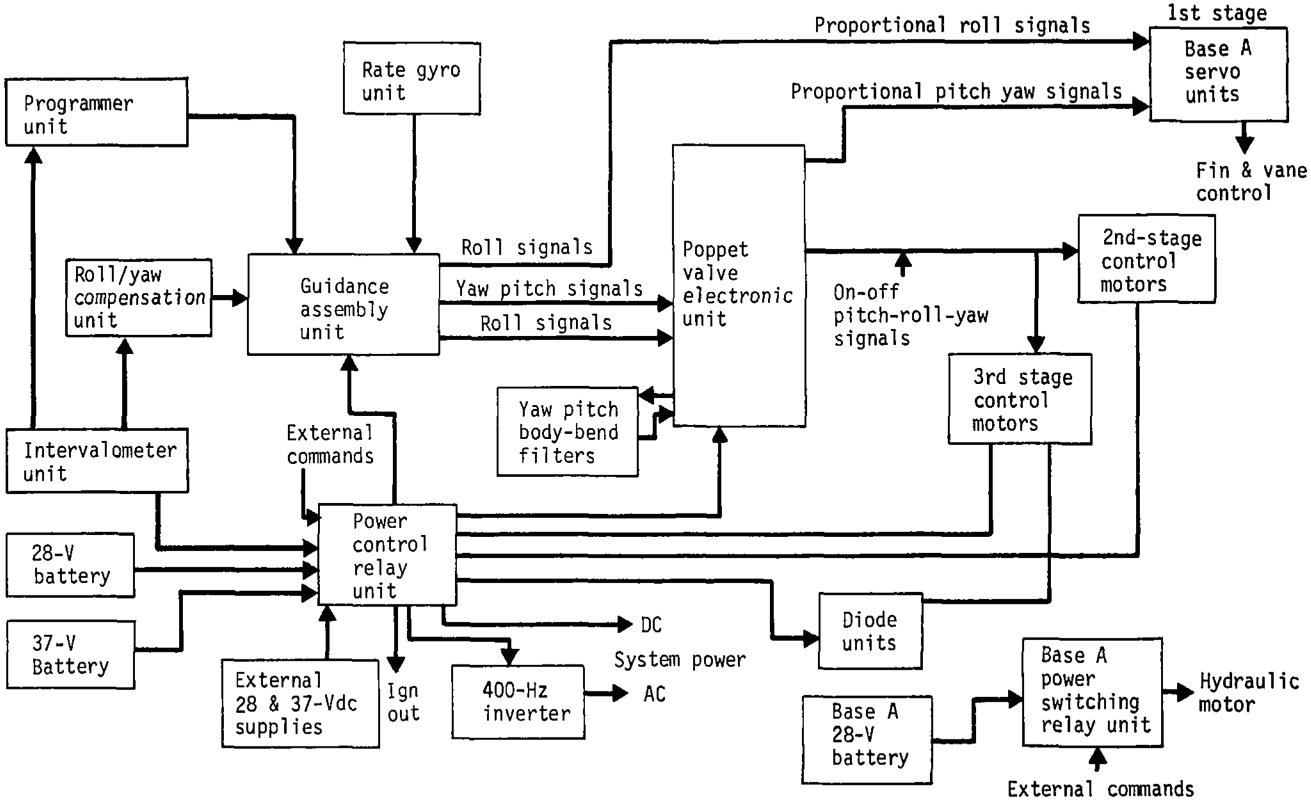

FIGURE 42.- SCOUT GUIDANCE AND CONTROL SYSTEM BLOCK DIAGRAM

Figure 43 illustrates the signal flow for the production KT-70 missile guidance systems. The reference guidance system integrated with Scout is illustrated in figure 44. The advantage of this approach is that it utilizes production hardware with minimum modifications. As can be seen, the central element is the control electronics that interfaces with the guidance sensors, computer, and vehicle subsystems. A major advantage of this approach is that by redesigning several cards in the KT-70 missile control electronics, it can be adapted to the Scout application. Although not shown in figure 44, a separate relay box may be required for high-current switching functions.

The electrical interface involves the raw power, autopilot, and ground support equipment. Additional cards will be required in the guidance and control electronics to provide the reference for the servoamplifier demodulators and the 400 Hz autopilot output signals. Modifications will be required to the digital accelerometer loops as required to meet the accelerometer scaling and saturation requirements. Also autopilot scaling changes and level detectors will be required.

The improved guidance and control system consists of the KT-70 missile platform, a digital computer, the control electronics unit, a dc power conditioner, a power transfer unit, three rate gyros, and the required 28-V batteries. These components will interface with one another in the manner shown and with the first-, second-, third-, and fourth-stage control system hardware, the telemetry system, and the ground support equipment.

The interfacing signals are summarized in tables 40 thru 46. This is a representative listing of the component and system interface signals. It is expected that this listing will evolve as the improved Scout configuration becomes more rigid.

Thermal interface.- It is assumed that ambient air of 100°F maximum is available on the launch pad prior to launch. It also appears that the hardware cooling scheme will allow the performance objectives to be met. According to Kearfott this is achievable, based on the temperature/time profiles given in the *Scout Launch Vehicle Characteristics and Constraints* section. However, a detailed thermal analysis will ultimately be required since the thermal interface is coupled with preflight cooling provisions and in-flight cooling required versus the active flight time.

Structural interface.- Figure 45 illustrates a layout of the KT-70 missile guidance hardware. It would be located in the cylindrical E-section of the fourth-stage. The 18-inch diameter is adequate; however, several additional inches in length would be required to accommodate the existing KT-70 hardware with minimum redesign. Optical flat is required in the heat shield for azimuth alignment.

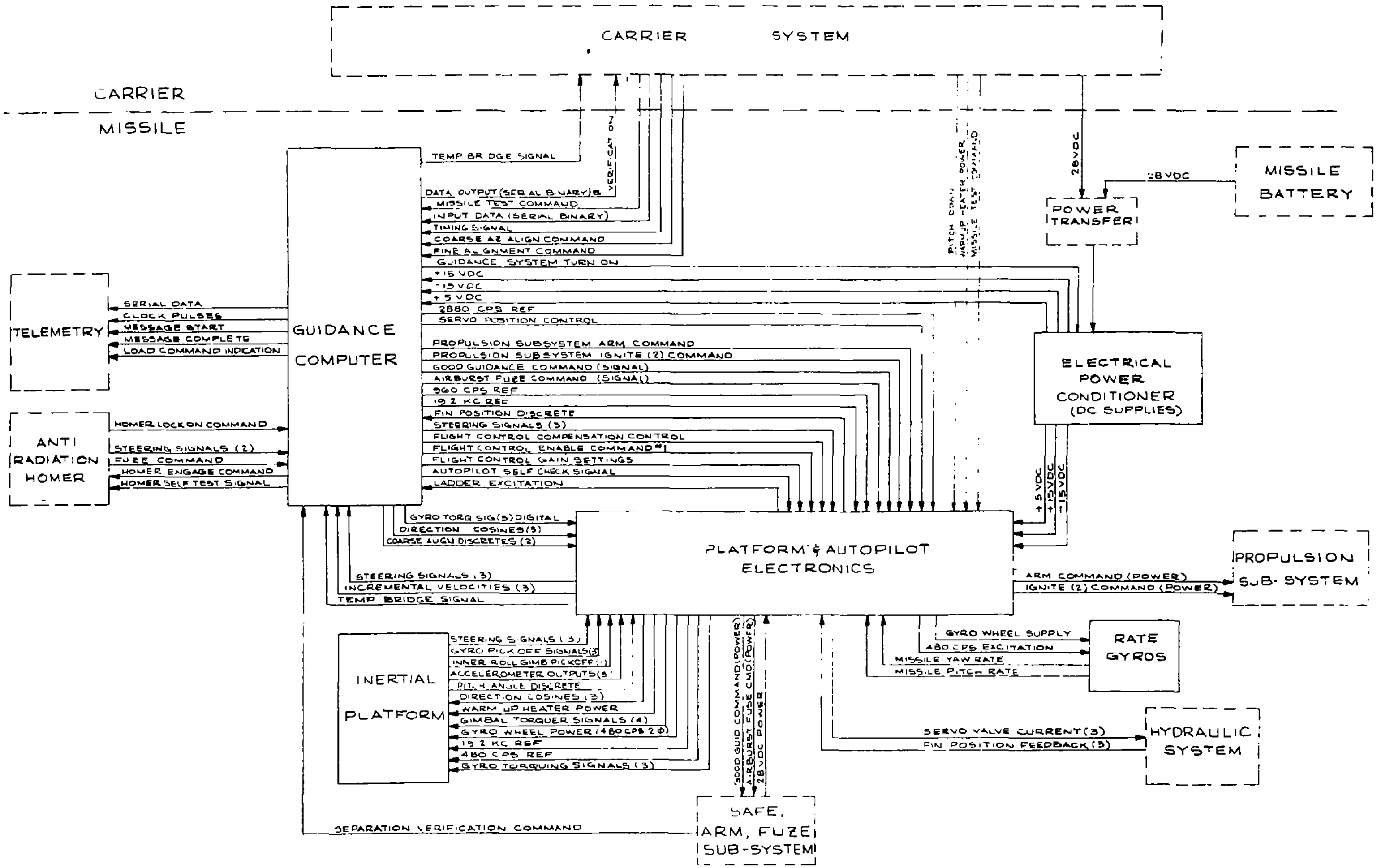

FIGURE 43.- SIGNAL FLOW DIAGRAM OF KT-70 MISSILE GUIDANCE SYSTEM

TABLE 40.- INTERFACING SIGNALS FROM MISSILE COMPUTER

Description	To	No. of wires	Signal characteristocs
Clock pulse train	Telemetry system	1	2-MHz pulse train, ±0.45 V min, 2.55 to 5.5 V max
Instruction counter (serial)	Telemetry system	1	
Memory register data (serial)	Telemetry system	1	Logic 0 = ±0.45 V
Data timing gate	Telemetry system	1	Logic 1 = 2.55 to 5.5 V
Instruction start marker	Telemetry system	1	
Timing	Telemetry system	1	120.19 Hz min ±0.45 V, 2.55 to 5.5 V max
Body-bending filter switching	Guidance and control electronics	1	Logic*
Payload separation	Relay unit	2	Logic*
Payload functions	Relay unit	6	Logic*
Spares	Relay unit	6	Logic*
RCS commands	Guidance and control electronics	10	TBD†
Motor squib ignition	Relay unit	3	Logic*
Activate second-, third-, fourth-stage RCS	Relay unit	3	Logic*
Third-stage thrust reduction	Relay unit	2	Logic*
Autopilog gain switching	Guidance and control electronics	10	Logic*
Direction cosines and common	Guidance and control electronics	4	2404 Hz, 8.11 V rms max
Gyro torque polarity commands	Guidance and control electronics	2	Logic* pulses, 120/s
Course align discretes	Guidance and control electronics	5	Logic*
Compensation control discretes	Guidance and control electronics	2	Logic*
2404 Hz reference	Guidance and control electronics	1	0 to 5 Vdc square wave, 2404 Hz
19.2 kHz reference	Guidance and control electronics	1	0 to 5 Vdc square wave, 19.2 kHz
480 Hz reference	Guidance and control electronics	2	0 to 5 V square wave, 480 Hz at $\angle 0°$ and $\angle 90°$
Fourth-stage separation command	Relay unit	2	Logic*
Activate fourth-stage OCS	Relay unit	2	Logic*

*For logic signals: Logic 0 = 0 Vdc; Logic 1 = 5 Vdc, except as otherwise noted.

†TBD = To be determined.

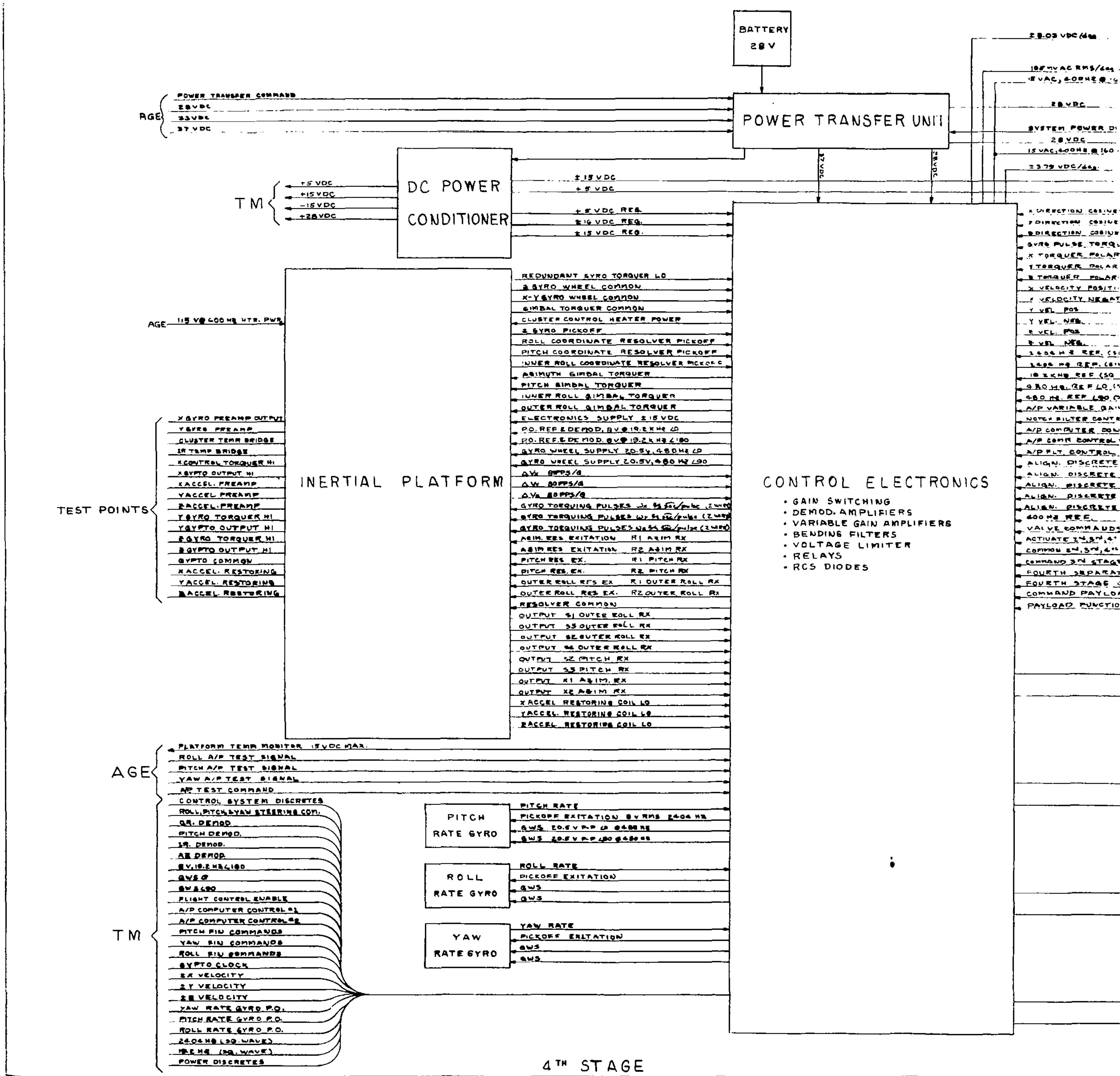

BATTERY 28 V
POWER TRANSFER UNIT
AGE
POWER TRANSFER COMMAND
28 VDC
33 VDC
37 VDC
DC POWER CONDITIONER
TM
+5 VDC
+15 VDC
-15 VDC
+28 VDC
±15 VDC
+5 VDC
+5 VDC REG.
±16 VDC REG.
±15 VDC REG.
INERTIAL PLATFORM
AGE
115 V @ 400 HZ HTR. PWR.
REDUNDANT GYRO TORQUER LO
Z GYRO WHEEL COMMON
X-Y GYRO WHEEL COMMON
GIMBAL TORQUER COMMON
CLUSTER CONTROL HEATER POWER
Z GYRO PICKOFF
ROLL COORDINATE RESOLVER PICKOFF
PITCH COORDINATE RESOLVER PICKOFF
INNER ROLL COORDINATE RESOLVER PICKOFF
AZIMUTH GIMBAL TORQUER
PITCH GIMBAL TORQUER
INNER ROLL GIMBAL TORQUER
OUTER ROLL GIMBAL TORQUER
ELECTRONICS SUPPLY ±15 VDC
RESOLVER COMMON
X ACCEL RESTORING COIL LO
Y ACCEL RESTORING COIL LO
Z ACCEL RESTORING COIL LO
TEST POINTS
X GYRO PREAMP OUTPUT
Y GYRO PREAMP
CLUSTER TEMP BRIDGE
IR TEMP BRIDGE
X ACCEL PREAMP
Y ACCEL PREAMP
Z ACCEL PREAMP
GYRO COMMON
X ACCEL RESTORING
Y ACCEL RESTORING
Z ACCEL RESTORING
AGE
PLATFORM TEMP MONITOR 15 VDC MAX.
ROLL A/P TEST SIGNAL
PITCH A/P TEST SIGNAL
YAW A/P TEST SIGNAL
A/P TEST COMMAND
TM
CONTROL SYSTEM DISCRETES
ROLL, PITCH & YAW STEERING COM.
PITCH DEMOD.
FLIGHT CONTROL ENABLE
A/P COMPUTER CONTROL #1
A/P COMPUTER CONTROL #2
PITCH FIN COMMANDS
YAW FIN COMMANDS
ROLL FIN COMMANDS
YAW RATE GYRO P.O.
PITCH RATE GYRO P.O.
ROLL RATE GYRO P.O.
POWER DISCRETES
PITCH RATE GYRO
PITCH RATE
ROLL RATE GYRO
ROLL RATE
PICKOFF EXITATION
YAW RATE GYRO
YAW RATE
CONTROL ELECTRONICS
• GAIN SWITCHING
• DEMOD. AMPLIFIERS
• VARIABLE GAIN AMPLIFIERS
• BENDING FILTERS
• VOLTAGE LIMITER
• RELAYS
• RCS DIODES
4TH STAGE

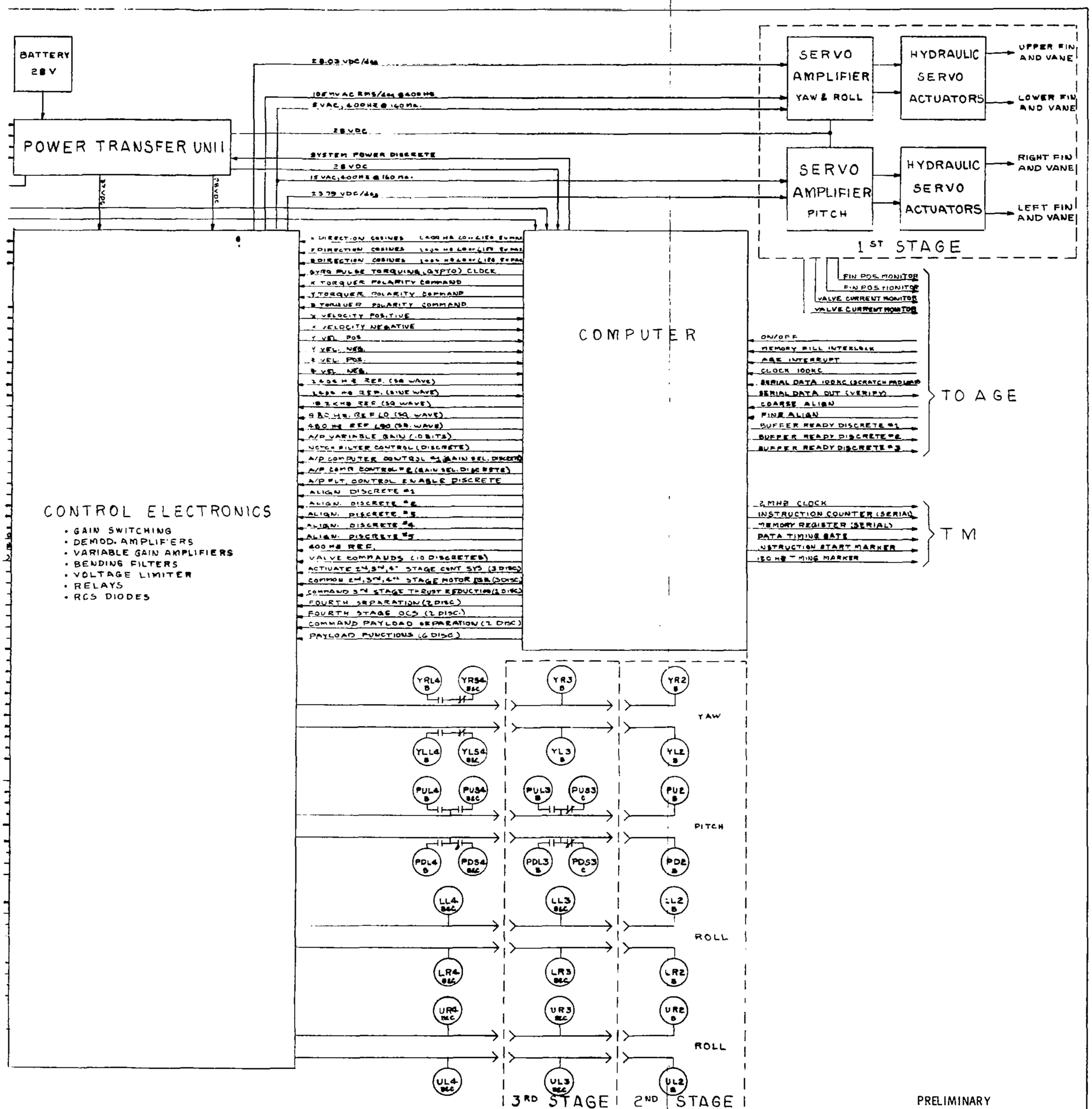

FIGURE 44. - SCOUT/KT-70 INTERFACING DIAGRAM

TABLE 41.- INTERFACING SIGNALS FROM GUIDANCE AND CONTROL ELECTRONICS

Description	To	No. of wires	Signal characteristics
Resolver excitations; pitch outer roll, azimuth, common	Platform	7	8 V rms (max), 2404 Hz
+15 Vdc	Platform	1	+15.1 Vdc ±1%
-15 Vdc	Platform	1	-15.1 Vdc ±1%
Inertial sensor pickoff excitations and common	Platform	3	19.2 kHz ±0.01%, 8 V rms at ∠0° and ∠180°
Gyro wheel supply and 2 commons	Platform	4	480-Hz square wave, 20.5 V peak-to-peak at ∠0° and ∠90°
Power and signal ground	Platform	1	0 Vdc
Gimbal torquers: azimuth, inner roll, outer roll, pitch, common	Platform	5	±12 Vdc max, ±0.595 max
Cluster heater, high	Platform	1	+15.1 Vdc referenced to -15.Vdc
Accelerometer restoring coils, low	Platform	3	±49.17 ma, dc, max
Gyro pulse torquing commands	Platform		Logic, square wave with 60-Hz max frequency
Thrust reduction, third stage	Relay unit	2	28 Vdc
Squib iginition, second stage	Relay unit	2	28 Vdc
Squib ignition, third stage	Relay unit	2	28 Vdc
Squib ignition, fourth stage	Relay unit	2	28 Vdc
Fourth-stage separation	Relay unit	2	28 Vdc
Rate gyro wheel supply and common	Rate gyros	9	480 Hz 20.5 V peak-to-peak at ∠0° and ∠90°
Rate gyro pickoff excitation	Rate gyros	6	8 V rms, 2404 Hz
First-stage steering commands			
Pitch displacement	Base A servoamplifier	2	±3.79 Vdc/deg
Yaw displacement	Base A servoamplifier	2	±8.03 Vdc/deg
Roll displacement	Base A servoamplifier	2	105 mV ac rms/deg at 400 Hz
Reference	Base A servoamplifiers	2	15 Vac at 160 ma rms 400 Hz
Second-, third-, and fourth-stage valve commands	Second-, third-, fourth-stage valves	10	TBD†
Missile steering commands	Telemetry system	3	Linear between ±4 Vdc, max
Activate second-, third-, and fourth-stage RCS	Relay unit	6	28 Vdc
Activate fourth-stage OCS	Relay unit	2	28 Vdc
Fourth-stage thrust reduction	Relay unit	2	28 Vdc
Missile velocities (linear, X, Y, Z) and common	Missile computer	7	Logic,* pulsed
2404-Hz supply	Missile computer	2	8 V rms, 2404 Hz

*For logic signals: Logic 0 = 0 Vdc; Logc 1 = 5 Vdc, except as otherwise noted.

†TBD = To be determined.

TABLE 42.- INTERFACE SIGNALS FROM INERTIAL PLATFORM

Description	To	No. of wires	Signal characteristics
Platform revolsers, trimmed and untrimmed	Guidance and control electronics	10	2404 Hz 8 V rms, max untrimmed 4 V rms, max trimmed
Inner roll pickoff	Guidance and control electronics	1	19.2 kHz, 7 V rms, max 120 mV normal
Azimuth gyro preamp	Guidance and control electronics	1	19.2 kHz, 10 V peak-to-peak max 120 mV rms, normal max
Pitch and roll gyro coordinate resolver outputs	Guidance and control electronics	2	
Roll steering command	Guidance and control electronics	1	+15.1 Vdc max
Redundant gyro torquer	Guidance and control	1	±45 ma, max

TABLE 43.- INTERFACE SIGNALS FROM DC POWER CONDITIONER

Description	To	No. of wires	Signal characteristics
+15 Vdc	Guidance and control electronics	4	+15.1 Vdc ±1%
-15 Vdc	Guidance control electronics	4	-15.1 Vdc ±1%
Platform electronics common	Guidance and control electronics	1	0 Vdc
Autopilot common	Guidance and control electronics	1	0 Vdc
+16 Vdc	Guidance and control electronics	1	+16 Vdc ±4%
-16 Vdc	Guidance and control electronics	1	-16 Vdc ±4%
+5 Vdc	Guidance and control electronics	1	5.2 Vdc ±1%
Accelerometer digitizer return	Guidance and control electronics	1	0 Vdc
Gimbal torquer return	Guidance and control electronics	1	0 Vdc
Rate gyro wheel return	Guidance and control electronics	1	0 Vdc
Gyro wheel return	Guidance and control electronics	1	0 Vdc
Power and signal common	Guidance and control electronics	1	0 Vdc
28 Vdc and return	Relay unit	2	28 Vdc battery
28 Vdc and return	Missile computer	2	28 Vdc battery
28 Vdc and return	Base A servoamplifiers	2	28 Vdc battery

TABLE 44.- INTERFACE SIGNALS FROM RATE GYROS

Description	To	No. of wires	Signal characteristics
Yaw rate gyro output	Guidance and control electronics	2	10 V rms, max, 2404 Hz
Pitch rate gyro output	Guidance and control electronics	2	10 V rms, max, 2404 Hz
Roll rate gyro output	Guidance and control electronics	2	10 V rms, max, 2404 Hz

TABLE 45.- INTERFACE SIGNALS FROM POWER TRANSER SWITCH

Description	To	No. of wires	Signal characteristics
28 Vdc	Power conditioner	4	28 Vdc battery
System ground	Power conditioner	1	0 Vdc

TABLE 46.- INTERFACE BETWEEN GUIDANCE SUBSYSTEM AND GSE

Description	To and from	No. of wires	Signal characteristics
Inner roll gimbal heaters	To platform	2	115 V rms, 400 Hz
Steering test: Pitch, roll, yaw	To guidance and control electronics	3	10 V (peak), 25 Hz
Missile test command discrete	To guidance and control electronics	1	Logic*
Platform temperature monitor	From guidance and control electronics	1	±15 Vdc
Clock	To missile computer	2	Logic* 1×10^5 bps, max
Serial data-in and complement	To missile computer	2	Logic* 1×10^5 bps, max
Serial data-out and complement	From missile computer		Logic* 1×10^5 bps, max
Discretes and complements	From missile computer		Logic*
Buffers ready		6	
Coarse align		2	
Fine align		2	

*For logic signals: Logic 0 = 0 Vdc; Logic 1 = 5 Vdc, except as otherwise noted.

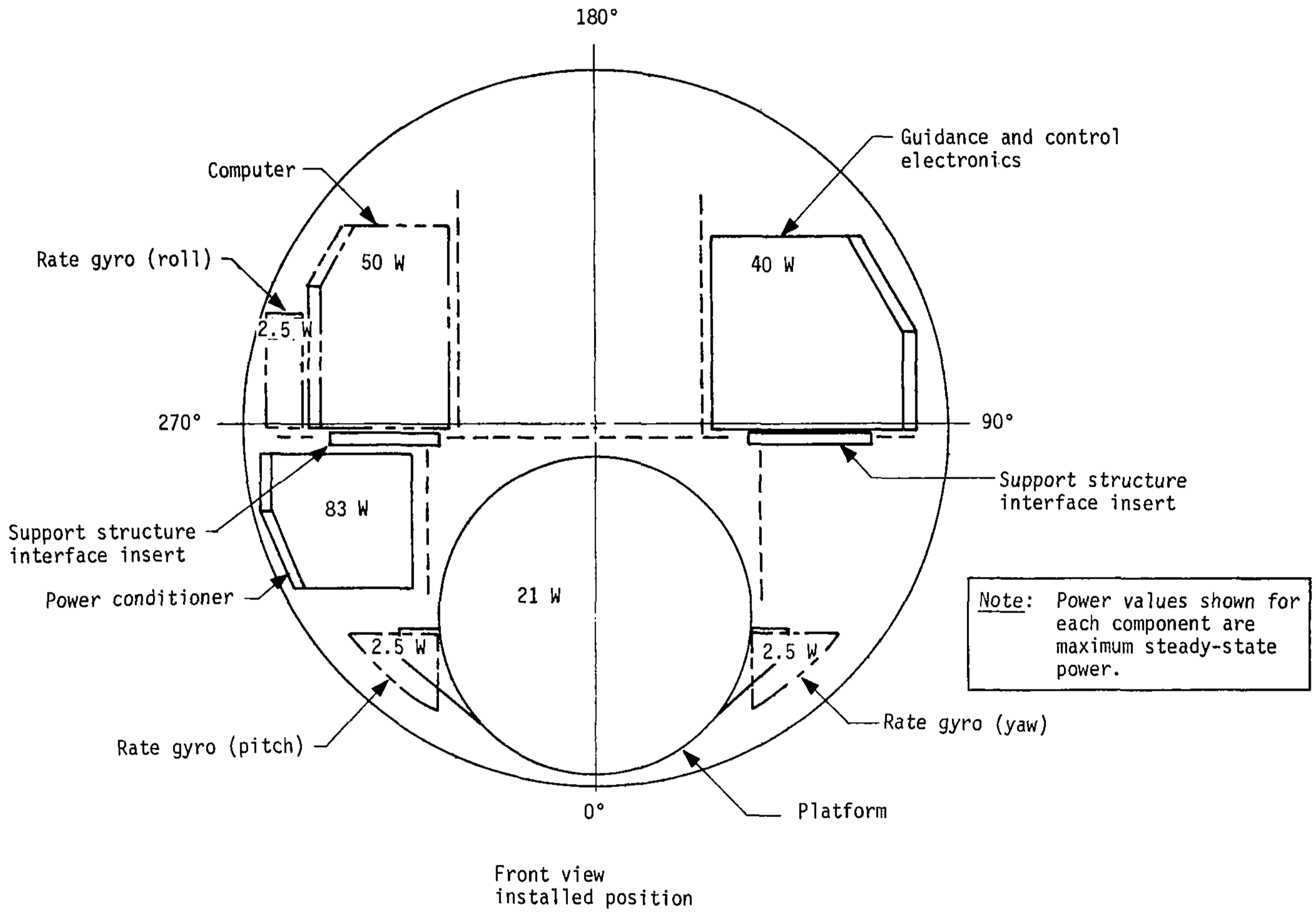

FIGURE 45.- TYPICAL KT-70 MISSILE SYSTEM LAYOUT

The physical characteristics and power utilization of the current production KT-70 missile system are as shown in Table 47. The interelationship of these components is shown in figure 43. The same basic components with the appropriate modifications discussed earlier in this section would be used for the Scout configuration with the exception of the Magic 301 computer.

TABLE 47.- PHYSICAL CHARACTERISTICS AND POWER UTILIZATION

PARAMETER	VOLUME (cu in.)	WEIGHT (lb)	POWER (watts)
Inertial platform	310	15.1	9.7
Guidance and control electronics	200	6.5	25.6
Power conditioner	75	5.5	75.6
Digital computer	123	5.2	40.4
Rate gyros		1.5	6.8
Total		33.8	158.1

The environmental capability of the KT-70 missile system is as shown in table 48. KT-70 missile system capabilities more closely approach the environmental requirements of Scout than any of the candidate IMUs that are in the production stage.

TABLE 48.- KT-70 ENVIRONMENTAL CAPABILITIES

ENVIRONMENT	MAXIMUM LEVELS/DURATION	
Shock	20 g	10 ms per axis
Vibration		
Sinusoidal	6.8 g	90 minutes per axis
Operating random	8.4 g rms	30 minutes per axis
Nonoperating random	3.3 g rms	480 minutes per axis
Captive Flight Acceleration.- system operating. All test items were exposed to linear acceleration levels in each of six axis as follows:		
(Fore and aft)	X - 2 g	
(Left and right)	Y - 12 g	
(Up and down)	Z - 12 g	
Free Flight Acceleration.- system operating. All test items were exposed to linear acceleration levels in each of 5 axes as follows:		
(Fore and aft)	X - 12.5 g	
(Left and right)	Y - 25 g	
(Down)	Z - 25 g	
Humidity	85°F, 95% RH	300 hours*
	75°F, 100 RH	60 hours*
Temperature/altitude	-85°F to +345°F 0.007 to 14.7 psia	98 hours
EMI	Radiated and conducted interference and susceptibility tests per MIL-I-6181D	
Note:		
*Total time for 15 cycles (of 24 hours each)		

Ground Support Equipment

The following pages present a description of the functional uses of the ground support equipment (GSE) modules relative to the system tests. The modules have been grouped, where possible, in accordance with the functions they perform.

In addition to the usefulness of the GSE modules in performing the various system integration and performance tests, they also facilitate fault isolation down to a black box level.

Figure 46 is a block diagram of the system test GSE modules. It is anticipated that the existing GSE described herein could be modified for the Scout program. This equipment is currently being used for KT-70 missile system testing.

Functional description of test modules

Timer module (A1).- This module contains a real-time clock and two elapsed timer counters. It provides a real-time reference for all timed testing.

Vidars, signal conditioner, EAIs, gyro control module (A14, A15, A16, A17, A18, and A31).- These modules lumped together provide the system test operator with a network for developing gyro torquing signals based on either the outputs of the level accelerometer and the azimuth resolver or the outputs of the roll, pitch, and yaw resolvers. These signals, as seen by the gyro torquers, may be either analog or digital. If it is desired to analog torque the gyros, the input resolver signals are amplified by the EAIs and then go directly to the gyro torquers. If digital torquing signals are desired, the input accelerometer or resolver signals are amplified by the EAIs, converted from analog to digital by the Vidars and the signal conditioner, and presented to the GYPTO modules. The gyro control module contains a patch panel which facilitates jacking either the roll, pitch, yaw resolver outputs or the level accelerometer outputs into the EAIs.

The analog torquing mode is used in all testing. The digital torquing mode is used in all tests, except the power and temperature test, which do not incorporate the missile computer.

Bias readout and insertion module, GYPTO control module, R&Y registers, regulated power supply (A4, A5, A8, A21, and A22).- The GYPTO control module plus the R&Y registers are used to simulate that portion of the missile computer that calculates and outputs the digital, gyro torquing pulses (i.e., $\pm\omega_x$, $\pm\omega_y$, $\pm\omega_z$). The logic circuitry on the above modules receives its B^+ inputs from the regulated power supply. The bias readout and insertion module provides the test operator with the capability of manually setting up and inserting gyro torquing pulses.

The above modules are used in all tests, except the power and temperature test, which do not incorporate the missile computer.

Power and temperature control module, 28 Vdc control console power supply, 28 Vdc prime power supply (A6, A9, B6).- The power and temperature control console provides switching for turning on or off the control console power and the system prime power. In addition, this module provides the on/standby control for the 400 Hertz platform heater power, and an adjustment for the heater voltage level. The 28 Vdc control console power supply is used to provide power to various control relays in the console, and simulates the 28 Vdc from the prime power source to the missile computer. The prime power supply provides the dc power conditioner with 28 Vdc, and simulated the missile battery.

These modules are used for all testing.

Analog signal module, computer reference frequency module, gimbal readout module, solid state power source (A2, A11, A13, A19).- The analog signal module provides the platform resolvers with the direction cosine inputs (i.e., $\Delta X/R$, $\Delta Y/R$, $\Delta Z/R$), and is a simulation of a portion of the missile computer I/O. Also, this module provides a simulation of the antiradiation homer inputs to the yaw and pitch steering channels. The computer reference frequency module simulates that portion of the missile computer I/O that provides the G&CE with 19.2 kHz, 2404 Hz, 480.8 Hz, and 120 Hz reference frequencies. The gimbal readout module provided a visual representation.of the cluster-to-case angular orientation. In addition, this module provides the test operator with the ability to change the position of the cluster relative to the case (i.e., by using the RDXs). The solid state power source amplifies the 2404 Hz sine wave, from the G&CE, allowing additional loads, presented to this power source by the test control console, to be driven.

The gimbal readout module and the solid state power source are used in all testing. The computer reference frequency supply and the analog signal module are used for all tests that do not incorporate the missile computer.

Computer discretes module, power discretes load module, auxiliary power supply (A12, B4, B5).- The computer discretes module simulates the discrete output section of the missile computer I/O. It provides the autopilot gain discretes, coarse align discretes, and power discretes. The power discretes load module simulates the missile propulsion, arm, and fuzing system loads for the power discrete outputs. The auxiliary power supply provides the 28 Vdc power to the missile battery number two.

The computer discretes module is used for all tests that do not incorporate the missile computer. The power discretes load module and auxiliary power supply are used for the IMU/AP power discretes test and the system free flight test.

Servo Valve Simulator Module (B3).- The servovalve simulator module simulates the missile servovalve system loads on the autopilot outputs, and provides the autopilot with simulated fin feedback signals. The module is used in all autopilot tests and in the systems free flight test.

Power conditioner interface box, platform interface box, and G&CE test point module (B2, B1, and A3).- The major function of these modules is to provide the capability to monitor the critical and pertinent system performance parameters at various points in the systems interface and inside the guidance and control electronics. The power conditioner interface box provides a switch to enable the test station to be used for testing of engineering model as well as DDT&E and production systems and switching to place the rate gyros in either a normal operating mode or a noise test mode. The platform interface box (PIB) contains a switch that places the system in either a captive flight or free flight mode of operation.

Also, the PIB houses switching to perform the following:

1) Place the platform resolvers in either the test or system mode of operation. In the test mode, each resolver (i.e., outer roll, pitch, and azimuth) receives a 2404 Hz excitation signal and provides electrical outputs relative to the pitch, azimuth, and outer roll angular gimbal orientations. These signals may be used as inputs for the gimbal slaving loops. In the system mode, the platform resolvers are connected in a resolver chain configuration and receive the direction cosines as inputs. The output of the chain is the yaw and pitch steering commands (Y_c, P_c) to the autopilot.

2) Place the platform accelerometers in either the test or system mode of operation. In the test mode, the accelerometer outputs are disconnected from the DAL circuitry and are available as inputs to the gimbal slaving loops. In the system mode, the accelerometer outputs are connected to the DAL circuitry in the G&CE.

The G&CE test point module houses switching which permits the gimbal torquing loops to be opened.

These modules are used for all tests.

Interface simulator module, load verify and display unit, tape reader, buffer box, GYPTO transfer matrix (C1, C2, C3, C4, C5).- The interface simulator simulates the interface between the carrier computer and the missile computer. The buffer box buffers the computer information exchange between the LVDU and the missile computer. The load verify and display unit (LVDU) controls the loading of the missile computer from a punched tape and the verification of the data entered. In addition to the load and verify functions, the LVDU provides the following switching and visual display capability:

1) Switching to permit stepping through the program step-by-step;

2) Display of any memory location and the ability to observe these locations while the computer is operating;

3) Keyboard data entry and location addressing.

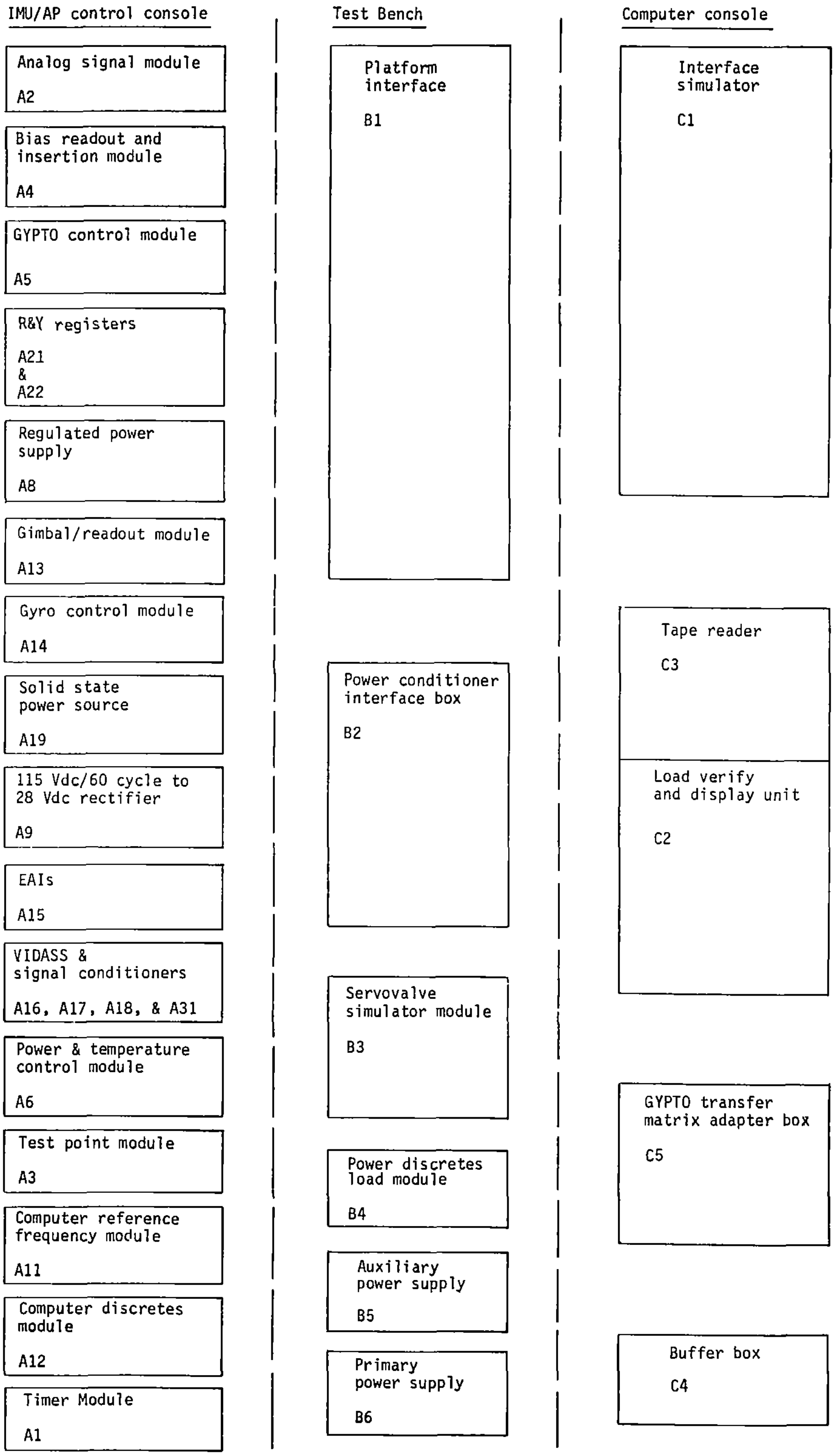

FIGURE 46.- SYSTEM BLOCK DIAGRAM

The tape reader is the device through which the missile computer is loaded. The GYPTO transfer matrix houses switching to facilitate using either the control console GYPTO control module (DDA) or the missile computer (computer) GYPTO to torque the gyros.

The above modules are used for all tests that incorporate the missile computer.

GUIDANCE INTEGRATION PROGRAM SUMMARY

This report outlines an overall plan for the development and integration of improved guidance for Scout. This summary was assembled to assist NASA in planning future improvements in the guidance and control system for the Scout launch vehicle. The baseline system assumes the Scout D vehicle configuration with a closed-loop guidance system located in the fourth stage. The basic guidance system consists of an inertial measurement unit (IMU), a general-purpose digital computer, and a guidance and control electronics unit. This estimate does not include vehicle structural modifications.

The plan is outlined in two phases to demonstrate an overview of the total program. The subsequent sections describe in greater depth the individual tasks to be performed, and a detailed program schedule is presented that outlines the time and cost phasing of the individual tasks.

The integration program described herein is based on previous experience such as the Titan III guidance integration and the Viking lander guidance development programs.

The guidance integration program includes a complete software validation program in a closed-loop mode utilizing as much of the flight hardware that can be implemented. Based on past experience, this scheme is most cost-effective in light of the confidence levels established. This would allow the very first vehicle to be flown with authentic payloads. This approach also serves another purpose. Should there be a fault within the software system, not only can it be flagged but also easily located, changed, and checked out. If a failure occurred in flight it might not be possible to isolate, which would necessitate some other corrective action and even delay subsequent flights. It is for these reasons that the software validation effort is cost effective.

Each of the tasks comprising Phase 1 and Phase 2 and hardware development are described in the following sections. The schedule shown in figure 47, which includes a schedule of the Phase 1 and Phase 2 tasks as well as a hardware development schedule, will obviously vary as a function of date of Phase 1 initiation.

Phase 1 Task Description

Mission analysis review.- Before the initiation of Phase 1, NASA will provide mission guidelines that identify desired accuracies and success probabilities. These characteristics will be used as preliminary limits to some of the individual designs that have been developed up to this point.

Vehicle constraints on inertial guidance system (IGS) and preliminary data book.- The preliminary data book comprises the results of the mission analysis data as to mass characteristics, trajectory information, aerodynamics, structural parameters, bending data, etc. The effect of design constraints on the vehicle can be generated at this time. Items such as quality of power needed, grounding point philosophy, instrumentation interface, and preliminary interfacing in general (of the vehicle only) would be included in the preliminary data book.

Preliminary guidance and controls logic selection.- Based on mission analysis results that describe the desired orbital parameters, their accuracy, probabilities of mission success etc, a number of candidate guidance and control logic schemes can be proposed. One of the major factors to be addressed in this selection is that the guidance software exhibit nonoptimal performance steering. This scheme has the capability of wasting energy in order to accommodate the lack of cutoff control to the solid rocket motors. Using the preliminary data book and a number of three-degree-of-freedom runs for check purposes, the finalized logic schemes will be chosen during Phase 1. The control logic approach will include the orbital correction capability that utilizes the ACS jets to make up velocity errors after fourth stage shutdown.

A more detailed discussion of guidance logic selection can be found in the section entitled *Guidance Software*.

Computer sizing and timing.- This effort will lag the logic selection task by a few months so the preliminary factors that bound a worst-case condition as to required computer operations will be defined. Items such as the number of adds, multiplies, divides, etc will form some of the timing cycles. Mission constraint items such as accuracy will affect sizing (e.g., double precision requirements, etc). The design goal will be to select a minimized set of required instructions. The following mission functions will be addressed in this tradeoff task:

1) Navigation;
2) Guidance;
3) Powered flight control;
4) Coast control;
5) Sequencing;
6) Malfunction checks;
7) Telemetry;
8) Ground checkout.

Generation of an inertial guidance system (IGS) RFP.- This task entails writing the detailed specifications describing the computer, IMU, and guidance and control electronics unit that form the IGS. These RFPs will define the environment to which these units will be subjected and the units' physical characteristics, power requirements, component quality, and performance. The response to these RFPs identifying the developmental qualifications and production programs with their associated costs will be used to select the flight hardware.

Ground equipment tradeoffs.- The ground operations equipment is used to minimize the checkout and calibration tasks that must be performed by operator and maintenance personnel. The degree to which these systems are implemented and the overall program philosophy will be developed and defined in this Phase 1 task. System integration, reliability, maintainability, and operational flexibility are the criteria to be addressed in the selection of the final systems. The cost effectivity of using standard off-the-shelf hardware as opposed to specially built units designed specifically for the Scout application will be another area to be studied in depth.

Alignment tradeoffs.- The accuracy of the alignment will be a direct function of the mission requirements and will be used to establish the philosophy of alignment. Methods such as gyrocompassing, optical schemes using portable autocollimation, or a closed-loop tracking theodolite will be studied for final selection.

The aforementioned tasks will all be initiated at the very beginning of Phase 1 and will be completed within the first six months as shown in figure 47 .

IGS selection.- Two months after the RFP responses are received, the final hardware equipment selections will be made.

IGS integration plan.- A detailed plan describing the schedule to be implemented during Phase 2 to perform the guidance integration will be initiated about halfway through the first phase. It will outline in depth the verification and validation tasks that serve as the finalized checks on the IGS system.

Engineering development test planning.- The output of this task will be detailed procedures describing the testing approach for the various subcomponents at the blackbox level. Each of the components will be tested for its electromagnetic compatibility (EMC), thermal, and other individual capabilities leading ultimately to the marriage of these components into the system configuration.

IGS/vehicle interface specifications.- A documented detailed interface specification will be developed to provide compatibility between the IGS and the vehicle components. The parametric interface specification is composed of:

1) The power and electrical requirement interface specification;

2) Physical interface--- configuration, weights, moments of inertia, location;

3) Electrical installation interface--- control drawings describing the wiring interface;

4) Test interface.

Error analysis.- A continuing effort will be expended during Phase 1 to iterate on the existing hardware sensitivities and the current system philosophies to provide high confidence that the system concepts being used are meeting the overall prescribed mission requirements.

Simulation programs such as TEAP, UD213, etc will be used as the pertinent analysis tools.

Phase 2 proposal.- The culmination of the Phase 1 task will be a Phase 2 proposal in which the Phase 1 effort will be documented. The more significant trade-offs earlier identified, such as in the alignment and ground equipment areas, will by this time be completed. A detailed Phase 2 schedule and cost program plan will be presented proposing the tasks to be performed in the final phase.

Phase 2 Task Description

Guidance and control equation development.- Once the logic schemes have been chosen, the equations necessary to compare measured velocity and position with the desired state will be developed, and from these the control corrections needed to achieve the final desired state will be computed. The control equations needed to stabilize the vehicle attitude will be developed in a similar fashion.

Ground checkout equation development.- This effort is needed to define the logic to perform the following functions: alignment, calibration, leveling, program loading, etc. This task will be performed concurrently with the ground checkout equipment design.

The aforementioned tasks will be undertaken at the inception of Phase 2. The following tasks will also be initiated at the start of the program so the individual hardware systems will be completed at the time of integration.

Finalized data book.- At this point in time the vehicle configuration and objectives will be described in more refined fashion and a finalized data book will be assembled. Since this was constantly iterated during Phase I, the changes will be minimum.

Software tool development.- This task identifies the programs requiring development or modification to serve as aids in developing the software:

1) Assembler - Converts the code to machine language;

2) Source code analyzer - Performs nonexecuting edit and prints out error flags prior to the code becoming machine language;

3) Interpretive computer simulator - Provides the method by which the airborne computer can be simulated on the CDC computer;

4) Flow charter - Generates flow charts when input with the coded airborne program. This is a verification tool in that only software is being checked;

5) Accuracy study processor - Performs computations in exactly the same manner as does the airborne computer and checks the outputs for accuracy;

6) Open-loop automatic analyzer - Performs branch point, dimension analysis, etc;

7) Miscellaneous - Error analysis, trajectory programs, etc;

8) Targeting programs utilizing the UD213 program.

These software development aids have evolved from other Martin Marietta programs and can likely be used as is or with minor modifications.

Error analysis.- This task represents a more in-depth investigation of software design than that described in Phase 1. A six-degree-of-freedom computer program will be used to simulate the logic equations and representative flight trajectories to demonstrate compliance with mission objectives and the accuracy that can be achieved.

The aforementioned tasks will be initiated at the start of Phase 2.

Targeting.- The purpose of targeting is to select the guidance polynomial coefficients driving the control system to steer the vehicle to a nominal state (implicit guidance) or to some new trajectory whose aim point represents the final desired state. Different mission parameters require new targeting. A range of mission parameters targeted are expected to bound all of those expected to be flown.

Stability analysis.- This task entails the study of the stability of the closed-loop IGS. Margins must be established to insure proper vehicle response to control commands and to assure that the total loop including guidance is stable.

Software specification generation.- This effort involves generating flow chart diagrams, logic sequencing, and the equations in specification form in which they will eventually be coded.

Coding.- Computer coding is the process of transforming the problem description given in terms of algebraic equations, instructions, or general flow diagrams into a binary code the computer can interpret and execute.

In effect coding converts the equations written in the specification into assembler language. (Although assembler language is a more difficult machine language to program and so is not normally used with the CDC, it is much more efficient and lends itself very well to airborne computer design.) Both the ground and flight equations must be coded.

Hybrid computer mode and guidance control logic (GCL) build.- An analytical model of the airframe can be simulated on the analog computer with associated transfer functions to simulate the autopilot control functions. Preliminary data book values can be used since the major problem is one of scaling, with potentiometers used to input the correct constants that are functions of weights, structural modes, etc. The inputs to the model will be computer outputs in the form of actuator control commands that reorient the vehicle. Comparing thrust values at a known attitude with some reference frame provides a measure of the vehicle linear motion in terms of vehicle position, velocity, and acceleration. Therefore a 6-dimensional state is output from the hybrid computer and input to the airborne computer to be compared with the desired state for the generation of a new control command.

The GCL build or modification (hardware marriage tests) effort requires government-furnished equipment such as actuators, fins, electronics, and other hardware, e.g., an airborne computer, so the interfaces between the IMU and computer and computer-to-vehicle can be determined.

Verification.- Verification of the coding to insure that the software matches the software specification is the last step before release of the operational software program packages. A complete and controlled verification of the operational software before release is mandatory to minimize change and schedule impact as a result of subsequent performance validations.

The principal verification tool will be an interpretive computer simulator (ICS). The ICS is a program written for a large "host" or general-purpose computer. The program is designed to allow the host computer to simulate the operation of another "target" computer. The ICS interprets each target computer instruction as it is encountered in the execution sequence and implements its function by host computer instructions. The structure of the ICS readily lends itself to the addition of diagnostic aids that may be coupled to the powerful input/output equipment associated with the host computer. The ICS will be used to verify the coding of each module by verifying the equation flow through each logic path on an instruction-by-instruction basis.

Validation.- A set of defect-free program/parameter tapes is required to ensure successful vehicle acceptance and prelaunch testing, and overall mission success. This, by definition, requires an error-free validation to insure that all software defects (programming or specification) are detected and removed before the appropriate punched tapes are used with the vehicle. The purpose of generating a set of validation procedures is to provide a systematic, controlled plan for obtaining an error-free validation, and to provide customer visibility of the validation itself. The validation procedures must provide definitions of specific validation tests and associated success criteria, and also software controls for all validation runs.

In addition, appropriate procedures for spot-checking the guidance equation software will be included. These tests will include such perturbation runs as thrust, specific impulse, and weight tolerance variations to check powered flight guidance equation performance, and some special tests to functionally check logic during coast phases of flight.

Test plans and procedures.- This task will generate documentation of the test plan and procedures needed to check out the IGS both at the integration location as well as at the launch site.

Hardware

In order to arrive at representative hardware cost estimates, a preliminary specification was generated and transmitted to the respective guidance hardware manufactures. They, in-turn, responded with ROM cost estimates along with a discussion on the exceptions taken to the preliminary specification.

Cost analysis played a vital role in the tradeoffs performed throughout this study. However, due to the highly proprietary nature of the cost data and at the request of the component manufacturers, it has been published in a separate document for limited distribution. These data can be acquired by contacting NASA or the author of this report.

It should be noted however that a representative schedule for hardware procurement is shown in figure 47 .

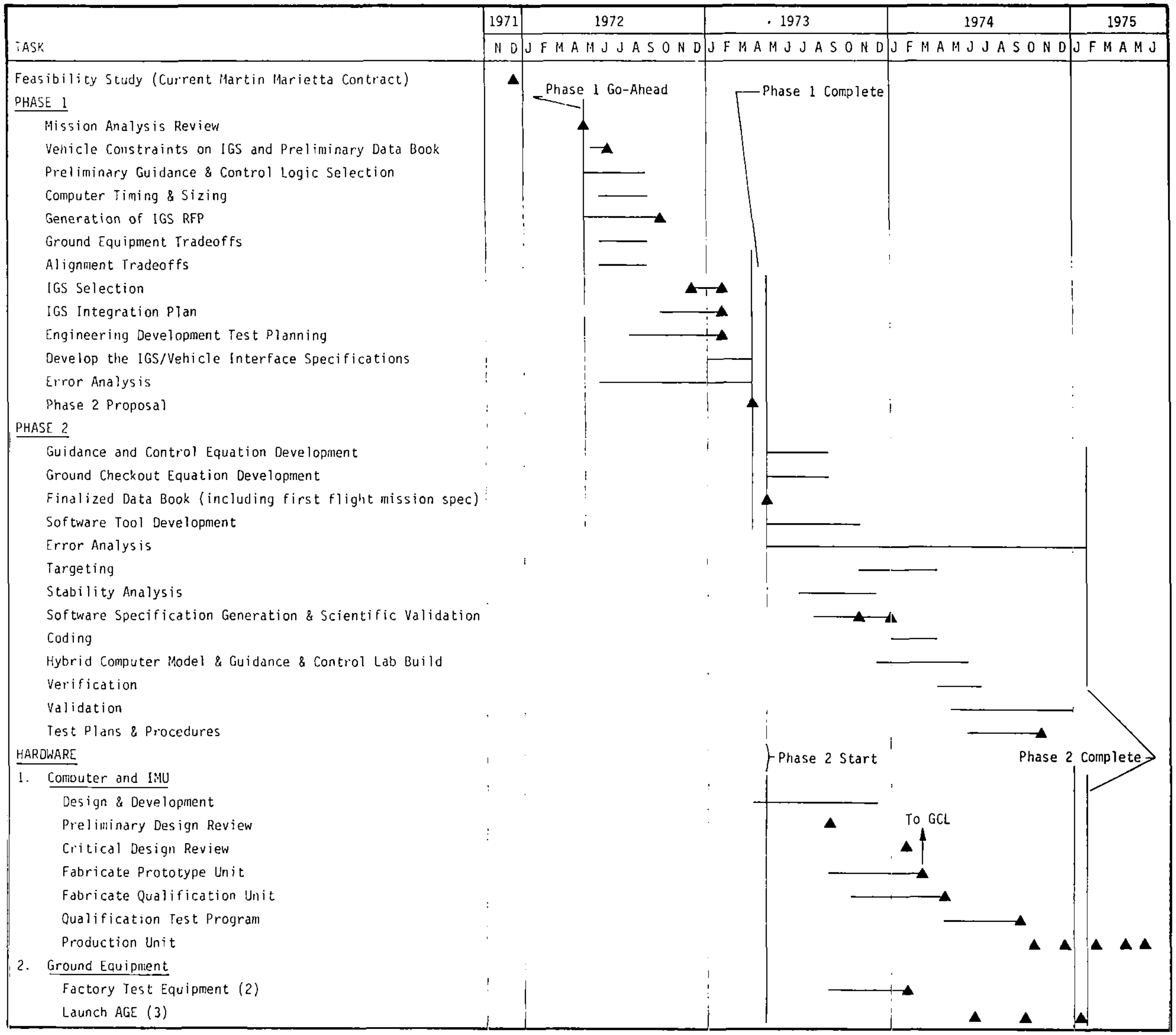

Figure 47 Guidance Integration Time Schedule

RECOMMENDATIONS

This study showed that an improved guidance and control system for Scout can be implemented with state-of-the-art hardware. This will result in increased accuracy, greater mission flexibility, and extended payload life. It is therefore recommended that the following tasks be initiated to minimize risk and to insure an optimized guidance and control system design:

1) Mission Analysis - Review future payload requirements in order to estimate accuracy and vehicle performance through 1980.

2) Continue definition of system modifications, vehicle interfacing, and environmental requirements. It is recommended that at least two inertial systems be included -- the KT-70 gimbaled platform and the DIGS strapdown system;

3) Initiate Phase 1 of the Guidance Integration Program as outlined in the preceding section. Phase 1 will result in a minimum cost low-risk approach to establishing a preliminary design of an improved guidance system for Scout. A significant task included in Phase 1 is the guidance logic study. This study would investigate method for providing low-cost functional guidance software that will meet the present and future Scout requirements. The resultant output would be a candidate set of guidance algorithms, a plan for implementation of guidance equations, and the schedule and costs for implementation.

BIBLIOGRAPHY

Alexander, J.: Procurement Specification for Twenty-Eight Channel Intervalometer. 304-613. LTV Aerospace, 1965.

Black, C. E.: *Flight Test Plan SLV-1A, Vehicle S-176C.* Report 3-34100/OR-85. LTV Aerospace Corporation, July 24, 1970.

Black, C. E.: *NASA Scout S-169C (GRS - A Mission) Preflight Planning Report.* Report 3-34100/9R-100. LTV Aerospace Corporation, 1969.

Brabeck, P. G. *et al.*: *Final Technical Report - Digital Autopilot Design and Computer Sizing Study.* NAS12-2048 ERC. Martin Marietta Corporation, Denver, Colorado, 1969.

Cohen, L. B.: *Errata, Error Analysis of the Scout Launch Vehicle.* NASA CR-66596, 1968.

Cohen, L. B.: *Scout Error Analysis Phase I Final Report.* NASA CR-66596, 1968.

Fremming, P. D.: *Roll and Yaw Compensation Feasibility Study.* NASA CR-1209, 1969.

Herring. G. P.: A Comprehensive Astrodynamic Exposition and Classification of Earth-Moon Transits. NASA TM X-53151, 1964.

Knauber, R. N.: *Scout Flight Restrictions.* Report 23,434. LTV Aerospace Corporation, 1970.

Knauber, R. N.: *Scout Preflight Mission Planning and Launching Constraints.* Report 23,434. LTV Aerospace Corporation, 1970.

Lee, Gentry *et al.*: *STEAP - Simulated Trajectory Error Analysis Program.* Vol I. NASA CR-66818. Martin Marietta Corporation, Denver, Colorado, 1966.

Nickens, C. D.: Procurement Specification for Solid State Interval Timer Assembly. 304-789. LTV Aerospace Corporation, 1968.

Pitman, G. R., Jr.: *Inertial Guidance.* John Wiley & Sons, Inc., 1962.

Roy, N. G.: *Analysis Procedures for Determining Scout Motor Performance.* Report 23,420. LTV Aerospace Corporation, 1970.

Scout Planning Guide. LTV Aerospace Corporation, 1968.

Scout Users' Manual. LTV Aerospace Corporation, 1970.

Vogt, Dr. D. *et al.*: *Simulated Trajectories Error Analysis Program.* Vol II. Martin Marietta Corporation, Denver, Colorado, 1970. (Prepared under Contract NAS5-11795.)

Weinberger, M. R.: *Flight Instrument and Telemetry Response and Its Inversion.* Rev. A. AVSD-0263-70 CR. Avco Corporation, Systems Division.

APPENDIX A

TRAJECTORY ERROR ANALYSIS PROGRAM (TEAP)

The basic function of the TEAP program is to generate errors in vehicle position and velocity as a function of the guidance system hardware error sources and the particular trajectory profile the vehicle is expected to fly.

The original TEAP program (which handled only a gimbaled version) was developed in 1963. It has been validated via checks against associate contractor's independent programs numerous times with virtually identical results. The modification to the program to handle strapdown IMUs was incorporated about two years ago. This modification was also validated against the output of an independent program by an associate contractor.

Vehicleborne accelerometers do not sense gravitational acceleration. Consequently, resultant spacecraft inertial accelerations must be derived in a computer using measured accelerations (thrust, aerodynamic) and a mathematical formulation for the acceleration of gravity:

$$\bar{a}_{veh} = \bar{a}_{sensed} + \bar{a}_{grav} \quad . \tag{A1}$$

Errors in vehicle acceleration come from these two fundamental sources and may be written as

$$\Delta\bar{a}_v = \Delta\bar{a}_s + \Delta\bar{a}_g \quad . \tag{A2}$$

Expanding this

$$\Delta\bar{a}_{in} = [c(t)]\ \Delta\bar{a}_{cc} - (\Delta\Phi_i \times \bar{a}_{si}) + \left[\frac{\partial\bar{a}_g}{\partial\bar{r}}\right] \Delta\bar{r} \tag{A3}$$

where

$\Delta\bar{a}_{in}$ = vehicle acceleration error in inertial space,

$$[C(t)]^* = \begin{bmatrix} X_{IO} & & U(t) \\ Y_{IO} & \leftarrow & V(t) \\ Z_{IO} & & W(t) \end{bmatrix}$$

is the transformation of the U, V, W (gyro and accelerometer frame) to the inertial launch reference coordinate system,

$\Delta\bar{a}_{cc}$ are the accelerometer errors,

$\Delta\Phi_I$ are the guidance package and gyro errors,

$\bar{a}_{SI}$ is the actual sensed inertial accelerations, and

$\left[\frac{\partial \bar{a}_g}{\partial \bar{r}}\right]$ is a 3x3 matrix of partial derivatives that yields gravitational acceleration errors caused by errors in position with respect to the attracting body. This is not a function of hardware errors, which are the terms that comprise $\Delta\Phi_I$ and $\bar{a}_{cc}$:

$$\Delta\bar{a}_{cc} = \begin{bmatrix} D_{BU} \\ D_{BV} \\ D_{BW} \end{bmatrix} + \begin{bmatrix} C_U & \phi_{VU} & \phi_{WU} \\ \phi_{UV} & C_V & \phi_{WV} \\ \phi_{UW} & \phi_{VW} & C_W \end{bmatrix} \begin{bmatrix} a_{SU} \\ a_{SV} \\ a_{SW} \end{bmatrix} + \begin{bmatrix} D_{CU} & 0 & 0 \\ 0 & D_{CV} & 0 \\ 0 & 0 & D_{CW} \end{bmatrix} \begin{bmatrix} a_{SU}^2 \\ a_{SV}^2 \\ a_{SW}^2 \end{bmatrix}$$

where D_{BU}, D_{BV}, and D_{BW} are the accelerometer bias errors in (g),

C_U, C_V, C_W are accelerometer scale factor errors in (g/g),

D_{CU}, D_{CV}, D_{CW} are accelerometer nonlinearity errors in (g/g^2),

a_{SU}, a_{SV}, and a_{SW} are actual sensed accelerations along the ideal U, V, W axes, and

ϕ_{UV}, ϕ_{UW}, ϕ_{VU}, ϕ_{VW}, ϕ_{WU}, and ϕ_{WV} are accelerometer misalignment angles representing mutual nonorthogonality in radians (Fig. 48).

---

*C(t) is a constant matrix for a gimbaled platform, but is time-dependent for a strapdown system.

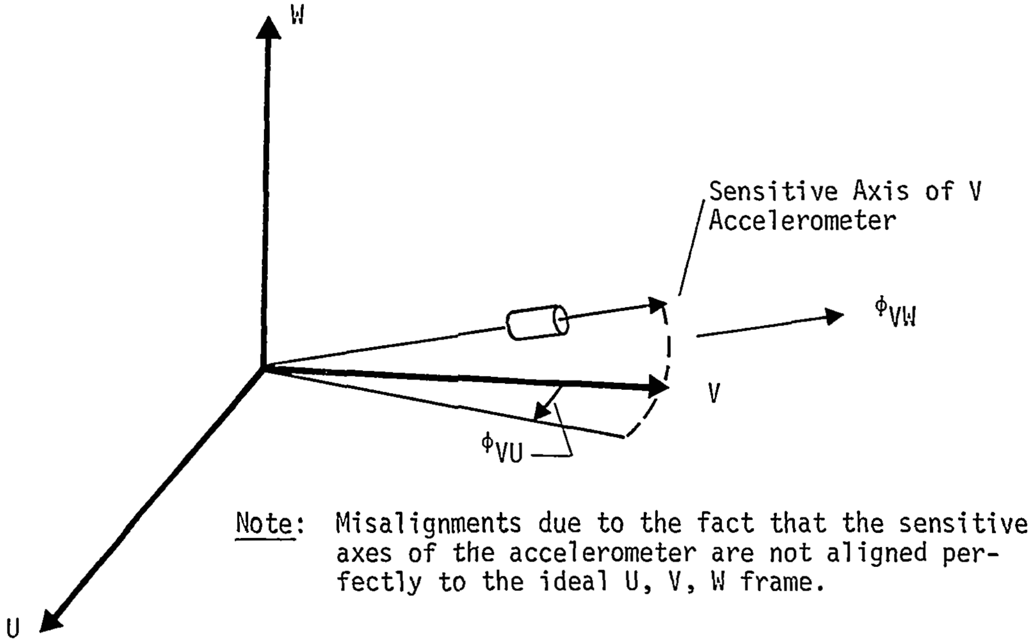

Figure 48.- Accelerometer Misalignments

Figure 48 describes the two misalignment angles associated with the V accelerometer. ϕ_{VU} is the angle in the VU plane that the sensitive V axis accelerometer is out of alignment with the desired V axis. ϕ_{VW} is that error in angle in the VW plane. It can be seen that six angles describe this error. Further defining components of Eq. (A3),

$$\Delta\Phi_I = \begin{bmatrix} \phi_{XO} \\ \phi_{YO} \\ \phi_{ZO} \end{bmatrix} + \int_{t_0}^{t} \left\{ [C(t)] \left[\begin{bmatrix} R_U \\ R_V \\ R_W \end{bmatrix} + \begin{bmatrix} P_{SU} & 0 & P_{IU} \\ P_{IV} & P_{SV} & 0 \\ 0 & P_{IW} & P_{SW} \end{bmatrix} \begin{bmatrix} a_{SU} \\ a_{SV} \\ a_{SW} \end{bmatrix} + \begin{bmatrix} C_{1U} & & \\ & C_{1V} & \\ & & C_{1W} \end{bmatrix} \begin{bmatrix} a_{SU} & a_{SW} \\ a_{SU} & a_{SV} \\ a_{SV} & a_{SW} \end{bmatrix} \right. \right.$$

$$\left. \left. + \, SDF \left[\begin{bmatrix} D_{KU} & 0 & 0 \\ 0 & D_{KV} & 0 \\ 0 & 0 & D_{KW} \end{bmatrix} + \begin{bmatrix} 0 & \theta_{VU} & \theta_{WU} \\ \theta_{UB} & 0 & \theta_{WV} \\ \theta_{UW} & \theta_{VW} & 0 \end{bmatrix} \right] \begin{bmatrix} \dot{\phi}_U \\ \dot{\phi}_V \\ \dot{\phi}_W \end{bmatrix} \right] \right\} dt$$

where ϕ_{XO}, ϕ_{YO}, and ϕ_{ZO} represent the alignment error of the guidance package to the ideal reference frame (XO, YO, ZO) in radians, and SDF is a strapdown flag.

R_U, R_V, and R_W are the non-g-sensitive gyro drift rate terms in radians/second,

P_{SU}, P_{SV}, and P_{SW} are the gyro drift rate terms due to mass imbalance along the spin axes of the U, V, W gyros, respectively, in radians/second/g,

P_{IU}, P_{IV}, and P_{IW} are the gyro drift rate terms due to mass imbalance along the input axes of the U, V, W gyros, respectively in radians/second/g,

C_{1U}, C_{1V}, C_{1W} are the drift rate errors due to major compliance (anisoelastic effect) in radians/second/g^2,

D_{KU}, D_{KW}, and D_{KV} are gyro torquer scale factor errors in percentage, and

θ_{UV}, θ_{UW}, θ_{VU}, θ_{VW}, θ_{WU}, and θ_{WV} are gyro misalignment angles representing mutual nonorthogonality. These misalignments occur because the sensitive axes of the gyro are not perfectly aligned with the ideal U, V, W frame.

Similarly, as in the accelerometer misalignments described in Figure A1, six angles will identify the two angular errors of each gyro input axis.

$\dot\phi_U$, $\dot\phi_V$, and $\dot\phi_W$ are the actual rotation rates about the U, V, and W axes.

As previously described, these error sources define $\Delta\bar{a}_{veh}$, which is integrated to yield velocity error and once again to yield position error.

The output of the program is formated to present individual components (X, Y, Z, inertial, or tangential, radial, and normal) of each error source's contribution to errors in position and velocity. These individual errors are root-sum-squared to obtain the totals. The totals are root-sum-squared for both position and velocity error to obtain one number for position and one for velocity. A similar output is presented for the attitude errors associated with each of the error sources (see table 49).

TABLE 49.- TEAP OUTPUT OF INDIVIDUAL ERRORS

$$\begin{array}{c} \\ \Phi_{X0} \\ D_{BU} \\ C_U \\ \cdot \\ \cdot \\ \cdot \\ \cdot \\ \eta \end{array} \begin{array}{c} \begin{array}{cccccc} \dot X & \dot Y & \dot Z & X & Y & Z \end{array} \\ \left[\begin{array}{cccccc} \; & \; & \; & \; & \; & \; \\ & & & & & \\ & & & & & \\ & & & & & \\ & & & & & \\ & & & & & \\ & & & & & \\ & & & & & \end{array} \right] \end{array}$$

rss from Φ_{X0} to η

$\dot X_{rss}$ $\dot Y_{rss}$ $\dot Z_{rss}$ X_{rss} Y_{rss} Z_{rss}

Attitude errors are presented as above except errors are mapped via a transformation to roll, pitch, and yaw (body axes)

By calculating sets of velocity and position errors for each input source error and dividing each element of the set by that input error, a matrix of partial derivatives may be formed

$$\frac{\partial \bar{X}}{\partial \bar{E}} = a(6 \times \eta)$$

that yields the errors in the state variables resulting from η input error sources The statistical transformation is then

$$\underset{(6 \times 6)}{\sum_{\bar{X}}} = \underset{(6 \times \eta)}{\left(\frac{\partial \bar{X}}{\partial \bar{E}}\right)} \underset{(\eta \times \eta)}{\sum_{\bar{E}}} \underset{(\eta \times 6)}{\left(\frac{\partial \bar{X}}{\partial \bar{E}}\right)^{T}} \qquad \text{where } T \equiv \text{transpose}$$

where $\sum_{\bar{X}}$ = a(6 x 6) covariance matrix of state variables (X, Y, Z, $\dot{X}$, $\dot{Y}$, $\dot{Z}$) and and $\sum_{\bar{E}}$ = a($n \times \eta$) covariance matrix of input errors (including off-diagonal correlation terms, if available) that yield errors in the state variables resulting from input error sources.

At the end of each powered flight segment, the integrated velocity and position errors become injection errors for the subsequent coast period. These velocity and position errors are propagated to later orbital times by taking space derivatives through the Keplerian equations of ballistic flight. The STEAP program, which maps trajectory errors in deep space, uses these covariance matrices as part of its input (table 50).

TABLE 50.- COVARIANCE MATRIX GENERATION

$$\underset{\text{Covariance matrix}}{\begin{array}{c|c} & \dot{X} \cdot \cdot \cdot \cdot \cdot \cdot \\ \hline \dot{X} \\ \vdots & \begin{bmatrix} \\ \quad 6 \times 6 \quad \\ \\ \end{bmatrix} \end{array}} \quad \underset{B}{\begin{bmatrix} \\ 6 \times \eta \\ \text{(Individual} \\ \text{trajectories)} \\ \\ \end{bmatrix}} \quad \underset{\text{Error coefficients}}{\begin{bmatrix} \sigma^{1}_{E1} & & & \\ & \sigma^{2}_{E2} & & \\ & & \ddots & \\ & & & \sigma^{2}_{\eta} \end{bmatrix}} \quad \underset{B^{-1}}{\begin{bmatrix} \\ \qquad \qquad \\ \\ \end{bmatrix}}$$

Other outputs generated by the TEAP program are

(1) The final trajectory state representing such orbital parameters as radius of perigee, radius of apogee, vehicle velocity magnitude, semimajor axis, semilatus rectum, eccentricity, inclination, period, and flightpath angle;

2) The individual errors in each of the above-stated orbital parameters as a function of each of the guidance hardware error sources;

3) The algebraic sum of these errors;

4) The rss of these errors.

APPENDIX B

UD-213 TRAJECTORY PROGRAM

Introduction

The UD-213 is a point mass, three-degree-of-freedom trajectory simulation program. Its generalized nature allows a large variety of launch and reentry vehicles to be simulated in single or multistage modes under various control laws. As many as 20 phases may be used to describe the trajectory. Each phase consists of a burn and coast period.

The program incorporates a single attracting body and general atmosphere model that can be described by input. As a result, any attracting body may be used merely by making the appropriate input.

The equations of motion are solved in a pad-centered inertial rectangular coordinate system. The gravity forces are calculated in an earth-centered inertial system that is parallel to the pad-centered system. Auxiliary calculations allow for the computation of position and velocity in other coordinate systems as well as the computation of other useful variables. Three computational options may be used -- point mass, three-axis, or moment balance.

The program has a simultaneous iteration/optimization scheme that allows as many as six dependent variables to be satisfied using as many as 12 independent variables. The generalized nature of the iteration scheme allows the user the option of selecting the dependent and independent variables from an extensive list of available variables.

The program flow chart is presented in figure 49.

Coordinate Systems

The program utilized several coordinate systems to provide auxiliary information and such reference systems for calculating optional data as tracker look angles, sun-shadows capability, and various guidance controls. With the aid of Figure 50, the coordinate systems are described in the following paragraphs.

X_P, Y_P, Z_P (plumb line) coordinate system.- A rectangular inertial coordinate system X_P, Y_P, Z_P is established with its origin specified by the initial geodetic latitude, ϕ_{GO}, east longitude λ_O, and height above the reference ellipsoid h_O. The Y_P axis is perpendicular to the local horizontal plane at launch, the X_P axis

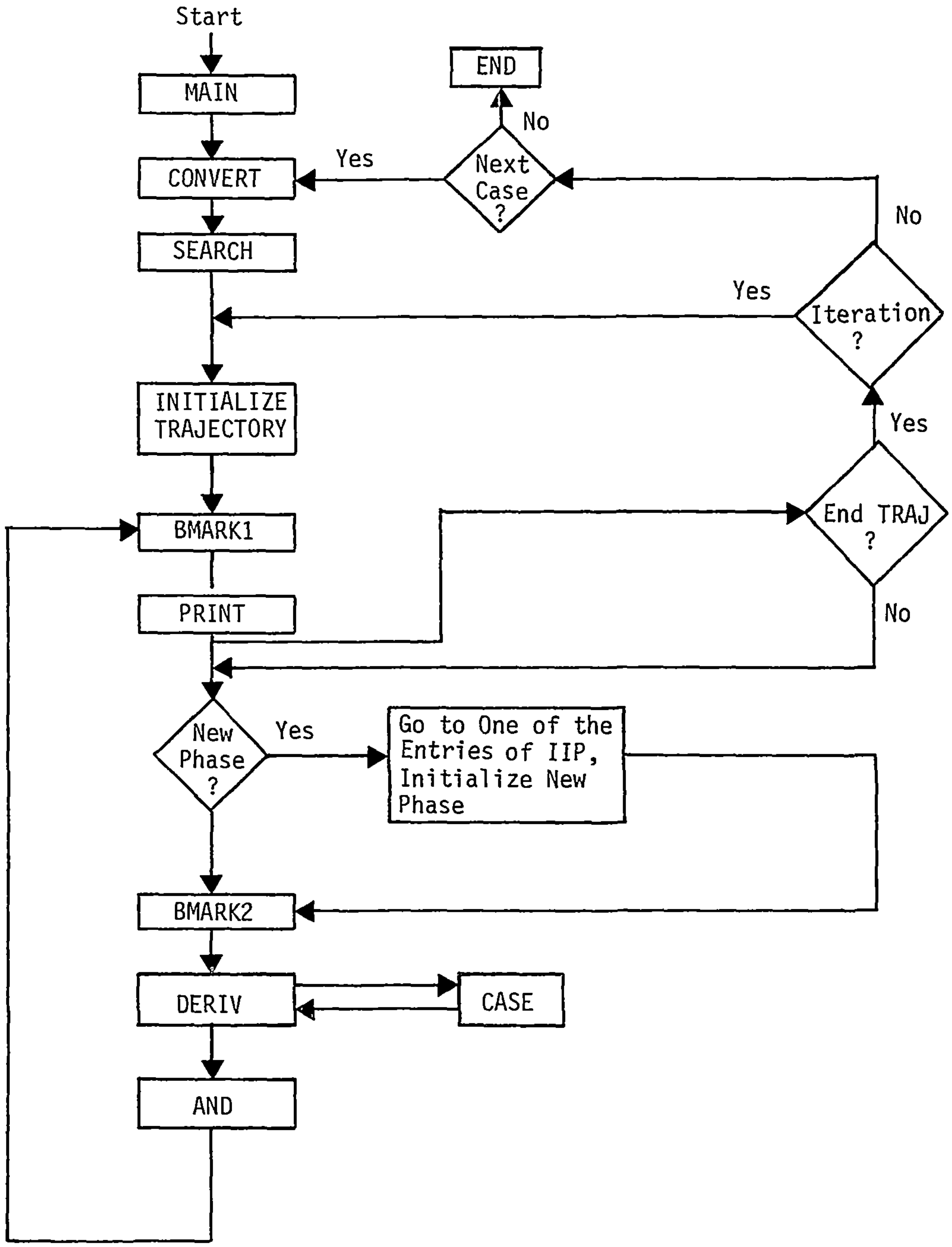

FIGURE 49.- PROGRAM FLOW CHART

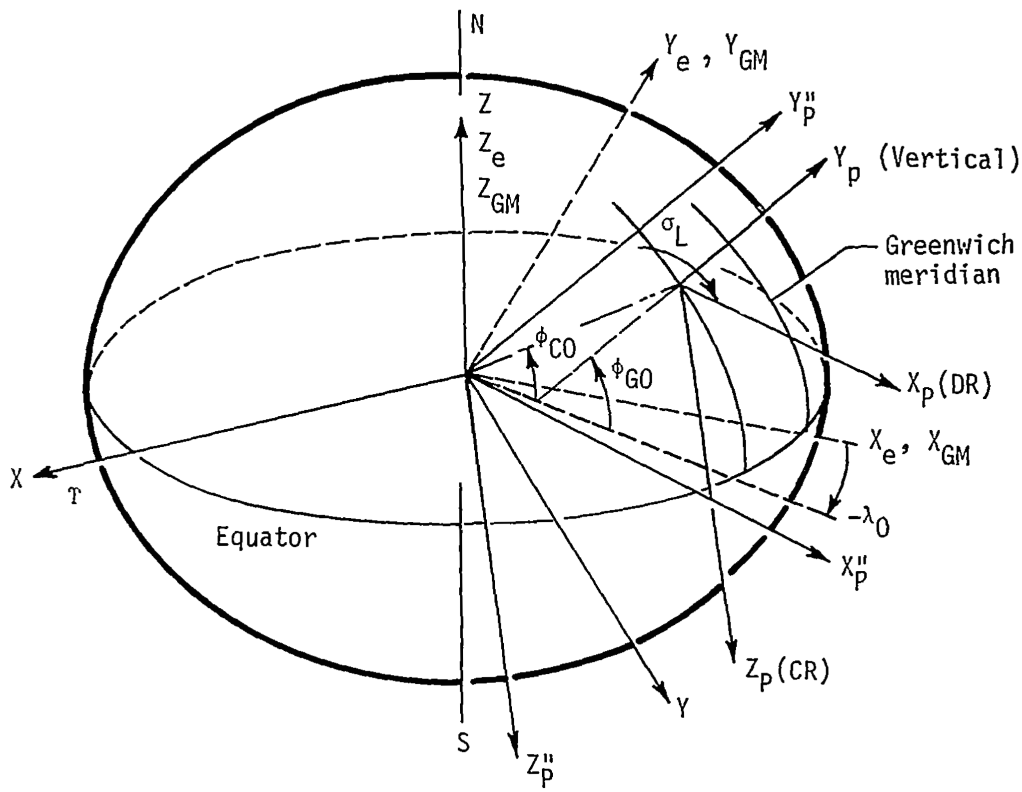

Legend:

XYZ	Space-fixed inertial coordinate system
X_p Y_p Z_p	Launch-centered geodetic inertial coordinate system
X_p'' Y_p'' Z_p''	Earth-centered inertial coordinate system parallel to X_p Y_p Z_p
X_e Y_e Z_e	Earth-centered rotating coordinate system with the X_e axis passing through the Greenwich meridian
X_{GM}, Y_{GM}, Z_{GM}	Earth-centered inertial coordinate system with the X_{GM} axis passing through the Greenwich meridian at launch
σ_L	Flight azimuth measured from true north (deg)
ϕ_{GO}	Geodetic latitude (deg)
ϕ_{CO}	Geocentric latitude (deg)
λ_0	Longitude measured east from the Greenwich meridian,(deg)
ϒ	Vernal equinox of Date

FIGURE 50.- UD-213 PROGRAM COORDINATE SYSTEM

is in the local horizontal plane and is directed along an azimuth of σ_L from true north, and the Z_p axis completes the right-hand system. The X_p, Y_p plane defines the inertial pitch plane.

The equations of motion are solved in this coordinate system.

X_p'', Y_p'', Z_p'' coordinate system. - This inertial coordinate system is parallel to the X_p, Y_p, Z_p system and is located at the center of the earth. It is used to calculate the geocentric radius to the vehicle and the resulting gravity force that is required to integrate the equations of motion.

X, Y, Z coordinate system. - To define the trajectory in a space-fixed coordinate system for possible sun-shadow capability or subsequent interplanetary trajectory studies, the X, Y, Z coordinate system must be developed. This system is an earth-centered inertial rectangular coordinate system. The X axis lies in the equatorial plane and passes through the vernal equinox of date T_0, the Z axis passes through the north pole, and the Y axis lies in the equatorial plane and completes the right-hand system.

X_{GM}, Y_{GM}, Z_{GM} coordinate system.- This coordinate system is an earth-centered inertial coordinate system with the X_{GM} axis in the equatorial plane and passing through the Greenwich (prime) meridian at launch. The Z_{GM} axis passes through the north pole and the Y_{GM} axis lies in the equatorial plane completing the right-hand system.

The above four coordinate systems are the fundamental systems used in describing the equations of motion. The following coordinate systems are used to compute auxiliary information.

X_e, Y_e, Z_e coordinate system. - The X_e, Y_e, and Z_e coordinate system is an auxiliary system used to define the space-fixed velocity components. The system is earth-centered with the X_e axis in the equatorial plane passing through the Greenwich meridian at launch. The Y_e axis lies within the equatorial plane and east of the X_e axis, with the Z_e axis directed north through the spin axis. This coordinate system rotates with the earth.

X_{PF}, Y_{PF}, Z_{PF} coordinate system. - The range safety coordinate system is an earth-fixed, pad-centered, left-handed coordinate system with the X_{PF}, Y_{PF} plane tangent to the earth at the launch pad. The X_{PF} axis is directed at an angle σ_L from the north, and the positive Z_{PF} axis is perpendicular to, and directed outward from, the X_{PF}/Y_{PF} plane. The Y_{PF} axis, directed to the left, and looking downrange, completes the system.

1, 2, 3 Body-centered coordinate system. - For 3-axis simulations, an additional orthogonal coordinate system (1, 2, 3) is body-fixed with its origin at the vehicle center of gravity. The 1-axis corresponds to the roll axis, the 2-axis corresponds to the pitch axis, and the 3-axis corresponds to the yaw axis.

Planet Model

The oblate spheroid is characterized by the semimajor axis, the semiminor axis, the eccentricity of the elliptic section of the oblate spheroid, and the rotational rate about its spin axis (north pole).

The potential function is characterized by the gravitational constant of the attracting body, the equatorial radius, the geocentric latitude, and three potential function terms.

The parameters required to define the atmospheric effects are pressure ratio, density ratio, speed of sound, Mach number, and atmospheric temperature. These parameters are a function of altitude.

Two atmosphere models stored in the program use table lookups to obtain the pressure and temperature. The stored models are the 624A and 1962 standard atmospheres.

In the 1963 Patrick AFB atmosphere, which uses polynomials, the pressure and temperature are calculated as functions of geometric altitude. These parameters are calculated in metric units and converted to English units if required.

Numerical Integration

The numerical integration is performed using any one of the following schemes, which can be selected by input:

1) Predictor-corrector;
2) Adams-Moulton;
3) Second-order Runge-Kutta;
4) Fourth-order Runge-Kutta;
5) Fourth-order modified Runge-Kutta.

External Forces

Vacuum thrust and propellant flow rate may be input directly as a function of time or they may be represented by 6th degree polynomials. An option allows the axial acceleration to be limited to a specific value.

There are two methods for computing normal force, depending on which vehicle option (point mass or 3-axis) is being used. The method for computing axial force is the same for both options with the exception that the axial force coefficient may be input as a bivariant function of total angle of attack and Mach number for the 3-axis option.

When utiliaing the 3-axis mode of simulation, the moment balance option that calculates the engine deflections in pitch and yaw required to balance the aerodynamic normal and side forces to produce zero resultant moment can be requested. The present simulation allows for a cg and cp offset in pitch but no offset in yaw.

Attitude Control Laws

The vehicle attitude may be controlled using various control laws for both the point mass and the 3-axis options. In the point mass option, the vehicle is instantaneously oriented to follow the specified control law, i.e., there are no vehicle rates for this option except for information purposes.

In the 3-axis option, the vehicle is oriented by commanding body rates or gimbal angle (Euler) rates. For this reason, the vehicle orientation lags the commanded orientation slightly due to computational lags. The amount of lag is a function of the step size and, for most simulations, is negligible.

The control laws available for the point mass and 3-axis option are tabulated.

POINT MASS CONTROL LAWS
Vertical flight
Pitch angle of attack, 6th degree polynomial [f(t)]
Yaw angle of attack, 6th degree polynomial [f(t)]
Zero lift (relative gravity turn)
Inertial gravity turn
Inertial pitch angle versus time
Incremental inertial pitch angle
Zero inertial yaw angle
Zero yaw angle of attack
Inertial yaw angle versus time
Incremental inertial yaw angle
Local horizontal pitch angle

THREE-AXIS CONTROL LAWS
Vertical flight
Pitch angle of attack, 6th degree polynomial [f(t)]
Yaw angle of attack, 6th degree polynomial [f(t)]
Slideslip angle, 6th degree polynomial [f(t)]
Zero lift (relative gravity turn)
Inertial gravity turn
Inertial pitch angle versus time
Incremental inertial pitch angle
Inertial yaw angle versus time
Incremental inertial yaw angle
Inertial roll angle versus time
Incremental inertial roll angle
Constant inertial roll, pitch, and yaw rates
Local horizontal pitch angle
Constant platform gimbal angles
Local horizontal roll angle

Guidance Schemes

An open-loop guidance option that calculates pitch and yaw commands based on constant values of pitch and yaw guidance coefficients is available. The coefficients required to achieve the desired end conditions may be iterated on using the simultaneous iteration scheme.

A closed-loop explicit linear guidance option is also available in the 3-axis control option. The pitch and yaw inertial angles are defined as linear functions of time. The linear tangent commands are calculated by integrating from the current stage forward over all stages and burn times. The steering coefficients and time-to-go are determined using a simultaneous iteration scheme within the guidance logic.

Aerodynamic Heating Calculations

Certain aerodynamic heating parameters can be calculated and used as dependent variables for trajectory-shaping purposes. Other calculations are performed only for information purposes. The following heating indicators are calculated:

1) Heating rate for zero total angle of attack;
2) Aerodynamic heating indicator for zero total angle of attack;
3) Heating indicator for nonzero angles of attack;
4) Heating indicator for laminar flow;
5) Heating indicator for turbulent flow.

The temperature of a skin element of area and mass located at a distance from the nose of the vehicle is computed for Mach numbers greater than 1.

Tracking Stations

The program computes information relating to tracking stations located on the reference ellipsoid. The tracking station locations are specified in terms of latitude, longitude, and altitude above the ellipsoid.

The slant range, range rate, and acceleration from the tracker to the vehicle is calculated in addition to the elevation angle and rate, azimuth angle and rate, and look angle.

Conic Parameters

The conic parameters are calculated at the end of the trajectory or whenever they are requested by input. The following calculations pertain to both elliptic and hyperbolic orbits:

1) Energy per unit mass;
2) Eccentricity;
3) Semimajor axis;
4) Semilatus rectum;
5) Perigee radius;
6) Perigee velocity;
7) Angular momentum per unit mass;
8) Escape velocity;
9) Circular velocity;
10) True anomaly;
11) Orbit inclination;
12) Longitude of the ascending node;
13) Argument of perigee.

The following computations are also made if the conic is an ellipse:

1) Apogee radius;
2) Apogee velocity;
3) Eccentric anomaly;
4) Mean anomaly;
5) Period;
6) Time to perigee;
7) Semiminor axis;
8) Delta V required to circularize at apogee;
9) Delta V required to circularize at perigee;
10) Perigee position;
11) Latitude of perigee;
12) Radius to the surface at perigee;
13) Perigee altitude;
14) Apogee altitude;
15) Longitude at perigee.

If the unit is hyperbolic, the following additional parameters are computed:

1) Velocity at infinity;
2) Time from perigee.

APPENDIX C

SPACE TRAJECTORY ERROR ANALYSIS PROGRAM (STEAP)

STEAP II is a series of three computer programs developed by the Martin Marietta Corporation for the mathematical analysis of the navigation and guidance of lunar and interplanetary trajectories. The first series of programs under this name was developed under Contract NAS1-8745 for the Langley Research Center and was documented in two volumes (*STEAP User's Manual, STEAP Analytical Manual*) as NASA Contract Report 66818. Under Contract NAS5-11795, the STEAP series was extensively modified and expanded for the Goddard Space Flight Center. This second-generation series of programs is referred to as STEAP II.

STEAP II is composed of three independent yet related programs -- NOMNAL, ERRAN, and SIMUL. All three programs require the integration of n-body trajectories for both interplanetary and lunar missions. The virtual mass technique is the scheme used for this purpose in all three programs.

The first program named NOMNAL is responsible for the generation of n-body nominal trajectories (either lunar or interplanetary) performing a number of deterministic guidance events. These events include initial or injection targeting, midcourse retargeting, and orbit insertion. A variety of target parameters are available for the targeting events. The actual targeting is done iteratively either by a modified Newton-Raphson algorithm or by a steepest descent-conjugate gradient scheme. Planar and nonplanar strategies are available for the orbit insertion computation. All maneuvers may be executed either by a simple impulsive model or by a pulsing sequence model.

ERRAN, the second program of STEAP II, is used to conduct linear error analysis studies along specific targeted trajectories. The targeted trajectory may however be altered during flight by retargeting events (computed either by linear or nonlinear guidance) and by an orbit insertion event. Knowledge and control covariances are propagated along the trajectory through a series of measurements and guidance events in a totally integrated fashion. The knowledge covariance is processed through measurements using an optimal Kalman-Schmidt filter with arbitrary solve-for/consider augmentation. Execution errors at guidance events may be modeled either by an impulsive approximation or by a pulsing sequence model. The resulting knowledge and control covariances may be analyzed by the program at various events to determine statistical data, including probabilistic midcourse correction sizing and effectiveness, probability of impact, and biased aimpoint requirements.

The third and final program in the STEAP II series is the simulation program SIMUL. SIMUL is responsible for the testing of the mathematical models used in the navigation and guidance process.

APPENDIX D
ISOPROBABILITY CONTOUR PROGRAM

One method of demonstrating mission accuracy is via isoprobability contours. These graphs depict certain orbital parameter deviations for various probabilities. It is possible to predict the boundaries within which errors in radius of perigee and errors in radius of apogee will fall 99.7% of the time if the state covariance matrix is known.

The Martin Marietta approach begins with a radii-tangential-normal (RTN) covariance matrix in position and velocity (6x6) and a nominal XYZ inertial state vector (6x1). The RTN covariance matrix is transformed to its XYZ counterpart via the XYZ state vector. For each trial orbit, a set of six normally distributed random numbers are drawn from a digital random number generator. These basic random numbers are uncorrelated with zero mean and unit variance. Proper scaling and correlating with the XYZ covariance converts them to a (6x1) vector of XYZ perturbations, whereupon they are added algebraically to the nominal XYZ state vector to form a perturbed XYZ state vector.

Apogee and perigee radii are then computed from the nominal and perturbed XYZ state vectors and the differences between the nominal and perturbed radii are formed. The process is repeated an arbitrary number of times to accumulate a sufficient population of perturbed radii for plotting a meaningful scattergram, the outer boundary of which forms the basis for an 0.997 probability contour. Confidence regions are thus contoured for each candidate guidance system, the smallest of which corresponds to the most accurate candidate.

The above method has been implemented on a small IBM 1130 computer with a Cal Comp plotter and runs at roughly a 100 trial/minute computing rate.

APPENDIX E

GUIDANCE STEERING CONCEPTS

This section presents a cross-section survey of guidance equations used to solve various missions. This survey spans a wide complexity of equations and includes present state-of-the-art algorithms.

The guidance logic data sheets give information on basic guidance logic, guidance requirements, guidance equations, and steering and cut off in terms of functional notation. These data sheets are summarized in table 51 and detailed in tables 52 thru 60.

The guidance logic data sheets and associated systems are:

1) Minuteman I;
2) Titan II;
3) Polaris;
4) Pershing;
5) Titan IIIA;
6) Titan IIIC;
7) Saturn;
8) Atlas ICBM;
9) Thor ICBM.

The conclusions that can be drawn from the guidance logic data sheets are:

1) Concepts vary from the simplest Q-guidance to the most complex (Saturn approach);

2) Guidance equations include delta expansion (up to third-order), Q-matrix (time varying), and various explicit formulations. Delta and Q are generally termed implicit. Although Saturn has a very sophisticated explicit formulation, an implicit implementation using a third-order approximating polynomial is being proposed. This suggests that a delta expansion of sufficiently high order could pass as an explicit concept. Q cannot since by definition it is a linear approximation;

3) The highest polynomial expansion appearing in any of these concepts is third order;

4) Steering is generally unsophisticated (attitude program or position and velocity error steering) during early stages, and in some cases even during later stages;

5) There is a difference in approach that appears between equations for ballistic missile applications and orbital injection or space missions. In the ballistic application, $\vec{V}_g$ is derived using the delta expansion or Q-matrix, while in the space applications $\vec{V}_g$ is derived explicitly in almost all cases.

TABLE 51.- GUIDANCE LOGIC SUMMARY

Project	Guidance equations	Steering equations	Thrust-terminate equations	Guidance requirements
Minuteman	$\bar{V}_g$ by delta expansion (second-order)	Pitch steering by velocity polynomials (third-order) in all stages. Yaw null in first and second stages. $\bar{V}_g$ component yaw steering in third stage.	$\bar{V}_g$ component = 0	Range and time of flight
Titan II	$\bar{V}_g$ by delta expansion (third-order)	Pitch and yaw steering by velocity and position polynomial (second-order) in first stage. Pitch and yaw steering by $\bar{V}_g$ components in second and vernier stages	$\bar{V}_g$ component = 0	Range and time of flight
Polaris	$\bar{V}_g$ by Q-matrix (linear time-varying)	Pitch and yaw steering by velocity polynomials in first stage. Pitch and yaw steering by $\bar{V}_g$ components in second stage.	$\bar{V}_g$ component = 0	Range and time of flight
Pershing	$\bar{V}_g$ by Q-matrix (linear)	Pitch and yaw steering by velocity and position errors in both stages.	$\bar{V}_g$ component = 0	Range and time of flight
Titan IIIA	$\bar{V}_g$ and t_g (time-to-go)	Pitch and yaw steering by velocity polynomial and nulling in first stage. Pitch and yaw steering using t_g and explicitly calculated constants in second and third stages.	$\bar{V}_g$ (nonvectorial) = 0	Attitude, velocity, path angle azimuth
Titan IIIC	$\bar{V}_g$ and t_g (time-to-go)	Pitch and yaw steering by attitude program and nulling in zero stage. Pitch and yaw steering using t_g and explicitly calculate constants in first, second, and third stage.	$\bar{V}_g$ (nonvectorial) = 0	Attitude, velocity, path angle azimuth
Saturn	Explicit calculus of variations formulation, with implicit approximating polynomial (third-order) implementation	Pitch and yaw steering by attitude programmer velocity steering in first stage. Pitch and yaw steering by position, velocity, force, time polynomial (third-order).	Use of approximating polynomial function	Variety of space missions with minimum fuel consumption
Atlas ICBM	$\bar{V}_g$ by delta expansion (second-order)	Stage I pitch and yaw by time programmer and stage II vernier - constant pitch attitude. $\bar{V}_g$ component yaw steering.	$\bar{V}_g$ component = 0	Range and time of flight
Thor ICBM	$\bar{V}_g$ by Q-matrix	Atmospheric phase, time-programmed attitude. Closed-loop phase, cross-product steering	$\bar{V}_g$ component = 0	Range and time of flight

TABLE 52.- MINUTEMAN I (THREE STAGES) GUIDANCE LOGIC DATA SHEET

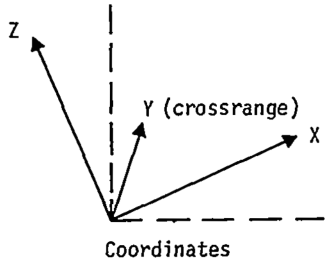

Navigation: Inertial platform

Logic:

Stage I - Velocity and position steering (implicit)
Stage II - Same
Stage III - Delta with $\bar{V}_g$ steering (implicit) and cutoff

Requirements: Total range and time of flight specified

Guidance equations:

$$\dot{X}_g\left[\Delta\dot{X},\ \Delta\dot{Z},\ \Delta X,\ \Delta Y,\ \Delta Z,\ \Delta X\ \Delta\dot{Z},\ \Delta X\ \Delta Z\right]$$

$$\dot{Y}_g\left[\Delta\dot{Y},\ \Delta\dot{Z},\ \Delta X,\ \Delta Y,\ \Delta Z\right]$$

$$\dot{Y}_g\left[\dot{Y},\ \dot{X}_g\right]$$

so $\dot{Y}_g = 0$ at start of third stage on nominal trajectory. Δ's are differences in present condition and nominal condition at burnout.

Steering equations:

Stage I

Yaw $\psi_c\left[\dot{Y},\ Y\right] = 0$,

Pitch $\theta_c\left[\dot{Z},\ \dot{X},\ \dot{X}^2,\ X^3\right]$ to maintain nominal relationship between $\dot{X}$, $\dot{Z}$;

Stage II

Yaw $\psi_c\left[\dot{Y},\ Y\right] = 0$

Pitch $\theta_c\left[\dot{Z},\ \dot{X},\ \dot{X}^2,\ X^3\right]$ same as above;

Stage III

Yaw $\psi_c\left[Y_g^*,\ \int \dot{Y}_g^*\ at\right]$ same as above;

Pitch $\theta_c\left[\dot{Z},\ \dot{X},\ \dot{X}^2,\ \dot{X}^3\right]$ same as above.

Thrust-terminate equation:

$\dot{X}_g = 0$.

TABLE 53.- TITAN II (TWO STAGES AND VERNIER) GUIDANCE LOGIC DATA SHEET

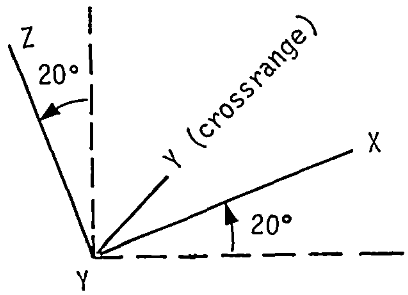

Coordinates

Navigation: Inertial platform

Logic:

Stage I - Velocity and position steering (implicit)

Stage II and V - Delta with $\bar{V}_g$ steering (implicit) and cutoff

Requirements: Total range and time of flight specified

Guidance equations:

$$\dot{X}_g\left[\Delta\dot{X}, \Delta X, \Delta Y, \Delta Z, \Delta t, (\Delta X)^2, \Delta X\ \Delta t, (\Delta t)^2\right]$$
$$\dot{Z}_g\left[\Delta\dot{X}, \Delta X, \Delta Y, \Delta Z, \Delta t, (\Delta X)^2, \Delta X\ \Delta t, (\Delta t)^2\right]$$
$$\dot{Y}_g\left[\Delta\dot{Y}, \Delta X, \Delta Y, \Delta Z, \Delta t\right]$$
$$\dot{Z}_g\left(\dot{Z}_g, \dot{X}_g, \dot{X}_g^2, \dot{X}_g^3\right)$$
$$\dot{Y}_g\left(\dot{Y}_g, \dot{X}_g, \dot{X}_g^2\right).$$

Δ's are differences in present condition and nominal condition at burnout.

Steering equations:

Stage I

$$\text{Yaw } \psi_c\left[\dot{Y}, Y\right] = 0,$$

$$\text{Pitch } \theta_c\left[X, Z, \dot{X}, \dot{X}^2, \dot{Z}\right];$$

Stages II and V

$$\text{Yaw } \psi_c\left[\dot{Y}_g^*, \int \dot{Y}_g^*\ dt\right],$$

$$\text{Pitch } \theta_c\left[\dot{Z}_g^*, \int \dot{Z}_g^*\ dt\right].$$

Thrust-terminate equation:

$$\dot{X}_g = 0.$$

TABLE 54.- POLARIS (TWO SOLID STAGES) GUIDANCE LOGIC DATA SHEET

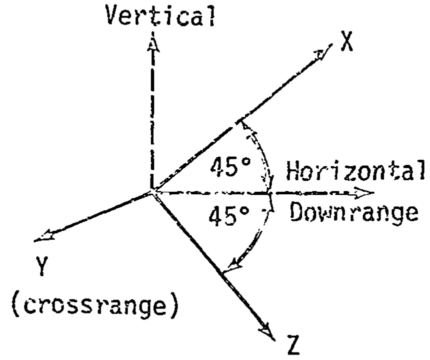

Coordinates

Navigation: Inertial platform

Logic:

Stage I - Velocity steering (implicit)
Stage II - Q-guidance with $\vec{V}_g$ steering (implicit) and cutoff

Requirements: Total range and time of flight specified

Guidance equations:

Velocity-to-be-gained V_g is computed continuously, with a special-purpose DDA, by solution of the equation

$$\dot{\vec{V}}_g + Q\vec{V}_g = -\vec{a}_T,$$

with suitable constraints, where Q is the (3x3) Q matrix. The elements of Q are functions of time, evaluated along the nominal trajectory. By proper orientation of the computational coordinate system and trajectory shaping, they are able to perform each mission by reading in only two elements of the Q-matrix, Q_{xx} and Q_{yx}.

Steering equations:

These drive two components of V_g to zero simultaneously with thrust termination.

Thrust-terminate equation:

$$\dot{X}_g = 0.$$

TABLE 55.- PERSHING (SOLID, TWO STAGES) GUIDANCE LOGIC DATA SHEET

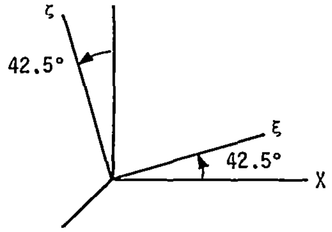

Z, ζ (crossrange)

Coordinates

Navigation: Inertial platform

Logic:

Both stages - Velocity and position steering (implicit) and Q-matrix with $\vec{V}_g$ steering and cutoff (implicit)

Requirements: Total range and time of flight specified

Guidance equations:

$$\dot{\vec{V}}_g + Q\,\vec{V}_g = -\vec{a}_t$$

$$Q = \begin{vmatrix} Q_{xx} & Q_{xy} & Q_{xz} \\ Q_{yx} & Q_{yy} & Q_{yz} \\ Q_{zx} & Q_{zy} & Q_{zz} \end{vmatrix} = \begin{vmatrix} \frac{\partial V_{RX}}{\partial x} & \frac{\partial V_{RX}}{\partial y} & \frac{\partial V_{RX}}{\partial z} \\ \frac{\partial V_{RY}}{\partial x} & \frac{\partial V_{RY}}{\partial y} & \frac{\partial V_{RY}}{\partial z} \\ \frac{\partial V_{RZ}}{\partial x} & \frac{\partial V_{RZ}}{\partial y} & \frac{\partial V_{RZ}}{\partial z} \end{vmatrix}$$

$$-\dot{\xi}_g = \dot{\xi}_p - \dot{\xi} + \frac{1}{T}\left[\xi_p + \int \left(\dot{\xi}_p + \dot{\xi}\right) dt\right]$$

where the p-subscript refers to programmed values.

$$T = t_{imp} - \bar{\bar{t}}_{co}$$

$$\dot{\eta}_g = \left(\dot{\eta}_p - \dot{\eta}\right) + \frac{1}{t_i - t} \int_0^{t_{co}} \left(\dot{\eta}_p - \dot{\eta}\right) dt.$$

Steering equations:

Both stages

Yaw $\psi_c\left[\zeta, \dot{\zeta}\right] = 0$

Pitch $\theta_c\left[\dot{\eta}_p - \dot{\eta} \int \left(\dot{\eta}_p - \eta\right) dt\right].$

Thrust-terminate equation:

$$\dot{\xi}_g = 0.$$

TABLE 56.- TITAN IIIA (THREE STAGES) GUIDANCE CONCEPT LOGIC SHEET

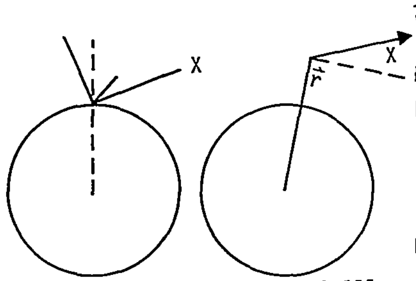

Stage I Stages II & III

Coordinates

Navigation: Inertial platform

Logic:

Stage I - Velocity steering (implicit)
Stage II and III - Explicit, based on rocket equation rather than Kepler's Laws

Requirements: Orbit injection, burnout altitude, velocity, flightpath angle, and azimuth are specified at each aiming point

<u>Guidance equations</u>:

$V_g = V_f - V$ (nonvectorial)

$V_g - V_L$,

where V_L is the predicted velocity loss (gravitational and aerodynamic)

Time-to-go t_g is obtained by solution of the rocket equation

$$V^* = g_o I_{sp} \ln \frac{m}{m + m t_g}.$$

<u>Steering equations</u>:

Stage I

Yaw $\psi_c = .0.$

Pitch $\theta_c \left[X_{gf}, Z_{gf}\right]$

where gf denotes "gravity-free, velocity measurements made by integration of accelerometer outputs, without gravity corrections.

Stages II and III

Yaw $\psi_c = B_1 + B_2 t_g$ (similar to pitch, but a much simpler problem).

Pitch $\theta_c = A_1 + A_2 t_g$,

where A_1 and A_2 are a solution to the two-point boundary value problem of driving present velocity and radial position to their desired burnout values (aiming point), in the predicted t_g.

<u>Thrust-termination equation</u>:

$t_g = 0.$

TABLE 57.- TITAN IIIC (FOUR STAGES) GUIDANCE LOGIC SHEET

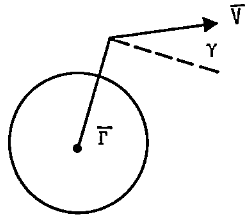

Stages I, II, III

Coordinates

Navigation: Inertial platform

Logic:

Stage 0 - Velocity steering in yaw and open-loop in pitch

Stages I thru III - Explicit, based on rocket equation rather than Kepler's laws

Requirements: Orbit injection burnout altitude, velocity, flightpath angle, and azimuth are specified at each aiming point

Guidance equations:

V_g, from a t_g iteration/integration process.

t_g, from an angular momentum iteration/integration process.

$$\Delta H = H_d - H_o = \int_0^{T_g} \dot{H}(t)\, dt$$

where H_d is the desired, H_o is the derivative of angular momentum. The equation is evolved for t_g in an iterative process for successive predictions of $\dot{H}(t)$. The state is integrated (5 points Simpson) to the target points to get the intermediate value of $\dot{H}(t)$.

Steering equations:

Stage 0

Yaw $\psi_c = 0$.

Pitch $\theta_c = f(t)$

Stages I thru III

Yaw $\psi_c = B_1 + B_2\, t_g$ (similar to pitch, but a much simpler problem).

Pitch $\theta_c = A_1 + A_2\, t_g$,

where A_1 and A_2 are a solution to the two-point boundary value problem of driving present velocity and radial position to their desired burnout values (aiming point) in the predicted t_g.

Thrust-terminate equation:

$t_g = 0$.

TABLE 58.- SATURN (THREE STAGES) GUIDANCE LOGIC DATA SHEET

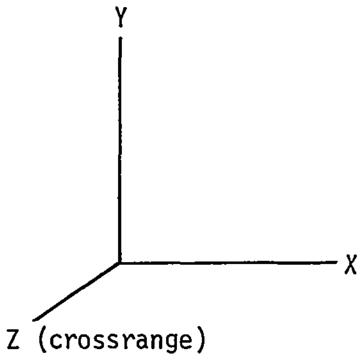

Coordinates

Navigation: Inertial platform

Logic:

Stage I (S-IC) - Time-tilt, minimum-drift program

Stages II, III (S-II, S-IVB) - Path-adaptive guidance mode

Requirements: Minimize flight time (or fuel consumption) for such space missions as lunar impact and orbit injection. Must have one-engine-out capability and must be adaptable to a wide range of missions

Guidance, steering, and thrust-terminate equations:

Stage I

Attitude-time program or velocity steering.

Stages II, III

Periodically along the trajectory, the two-point boundary value problem in the calculus of variations is solved, requiring minimizing the flight time between the present state and the desired state at mission completion. A steering function and a cutoff function are generated numerically by solving a large number of possible nominal and off-nominal trajectories on an IBM 7090. An approximating polynomial is used to represent the family of trajectories. Least-squares technique is used. Polynomials that have been evaluated and shown to give good results for low-orbit inject missions contained terms as high as third order:

$$\theta_c \text{ or } \psi_c \text{ or } t_{co}\left[X, Y, Z, \dot{X}, \dot{Y}, \dot{Z}, \frac{F}{m}, t, \text{and products up to third-order}\right].$$

TABLE 59.- ATLAS ICBM (TWO STAGES AND VERNIER) GUIDANCE LOGIC DATA SHEET

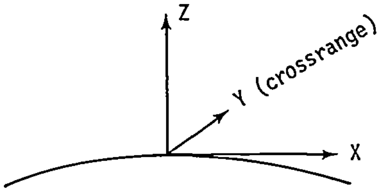

Coordinate system (inertial, launch point-oriented)

Navigation: Inertial platform (Arma)

Logic:

Stage I - Programmed attitude

Stage II - Delta with $\bar{V}_g$ steering (implicit)
Vernier - Same

Requirements: Total range and time-of-flight specified

Guidance equations:

$$V_{gx} = \left[\Delta X, \Delta Y, \Delta Z, \Delta t, \Delta\dot{X}, \Delta\dot{Z}\right]\text{, a second-degree polynomial}$$

$$V_{gy} = \Delta\dot{y}.$$

Δ's are differences between present values and nomial values at VECO.

Steering equations:

Stage I

Yaw $\psi_c = 0$

Pitch $\theta_c = f(t)$- time programmer.

Stage II

Pitch θ_c = constant

Vernier

Yaw $\psi_c = \psi_{nom} + K_1\left(V_{gy} - K_2 V_{gx}\right)$

where gain K_2 is chosen to make $K_2 V_{gx} = V_{gy}$ at initiation of guidance.

Thrust-terminate equation:

Stage II

V_{gx} = A small value compatible with vernier capability,

Vernier

$V_{gx} = 0$.

TABLE 60.- THOR ICBM (ONE STAGE AND VERNIER) GUIDANCE LOGIC DATA SHEET

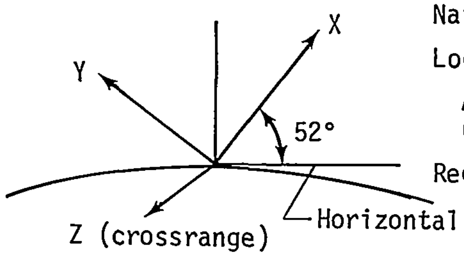

Coordinates

Navigation: Inertial platform (Delco)

Logic:

Atmospheric phase - Programmed attitude
Closed-loop phase - Q-guidance and vernier

Requirements: Total range and time-of-flight specified

Guidance equations:

$\vec{V}_g$ obtained as a solution to the equation

$$\dot{\vec{V}}_g = Q\,\vec{V}_g - \vec{a}_T$$

where elements of the Q-matrix are evaluated as functions of time along the nominal trajectory, and approximated by constants in actual use.

Steering equations:

Atmospheric phase

Yaw $\psi_c = 0$

Pitch $\theta_c = f(t)$ - time programmer.

Closed-loop phase (thru vernier)

$$\left.\begin{aligned} \text{Yaw } \psi_c &= K\left(\dot{V}_{gx} V_{gz} - \dot{V}_{gz} V_{gx}\right) \\ \text{Pitch } \theta_c &= K\left(\dot{V}_{gx} V_{gy} - \dot{V}_{gy} V_{gx}\right) \end{aligned}\right\} \quad \text{cross-product steering}$$

Thrust-terminate equations:

SECO - $\vec{V}_g$ = A small value compatible with vernier capabilities,

VECO - $\vec{V}_g = 0$.

The Scout vehicle and its guidance software considerations should be analyzed in developing a set of guidance algorithms. A Scout-oriented design phase should consider existing logic while solving the Scout-peculiar problems.

APPENDIX F

Centralized Executive System

The onboard computer operates in a complex environment supporting a number and variety of functions. The complex problems associated with the computer's operational environment, such as scheduling the next program for execution, loading the program, and initiating machine components must be handled in an efficient manner. The onboard executive system provides overall supervision and operational control of the computational resources available. The executive system functions during all mission phases to control the execution of application programs as required. Representative computer functions are:

1) Navigation;
2) Guidance;
3) Flight control;
4) Separation and staging;
5) Attitude control;
6) Telemetry;
7) Vehicle status and sequencing.

The environment involves five basic types of programming:

1) Mathematical calculations;
2) Message formulating;
3) Decision making;
4) Data manipulation;
5) Program control.

The basic performance requirements of the executive system are to:

1) Centralize functions that control flow of information between the programs and the external environment;

2) Manage the resources of the system to obtain efficient use of the hardware and to assure the response required by the application, and provide a standardized internal environment that will permit programs to be constructed and executed independently of one another;

3) Minimize impact of hardware changes on application program.

General functional design.- The general functional requirements for the design of an onboard executive system can be categorized as:

1) Program control;
2) Interrupt supervision;
3) Input/output supervision;
4) System services;
5) Environmental interface.

Each function is briefly described in the following subsections.

Program Control.- The function of program control is to govern the initiation, execution, and termination of scheduled programs. The master cycle controls the overall cycle of programs in accordance with the scheduling algorithm employed. Two options may be provided:

1) The basic cycle function is required with a scheduling capability to provide a point of return for the scheduling cycle, and a place to idle if there is no useful work to be done;

2) With cyclic control a limit is placed on the time a program may execute in a given period, so that the master cycle function must be enlarged to handle a program switch.

The basic initiation/termination processes requests for initiation and termination of programs resident in core. A basic scheduler provides the simplest class of scheduling service, in which selection of the next program to receive CPU time is based on a single service priority. A multiplexing scheduler interleaves the execution of programs, thus permitting concurrent execution of a number of programs. Two options may be provided:

1) Time control permits the executive to regain CPU control at specified intervals, either as the result of voluntary return of control by scheduled programs at intervals in their execution, or as the result of a preset clock interrupt. The latter device prevents the monopoly of CPU time by a single program;

2) Additional service classes provide the means of assigning CPU time according to a number of priorities to resolve conflicts among competing processing requirements.

Interrupt supervision.- The function of interrupt supervision is to direct system action at the occurrence of an asynchronous interrupt. The basic purpose is to provide coherent system response to external stimuli by isolating the operation of the programs responding to the interrupts from the operation of scheduled programs. The functions available are described:

1) Primary routines supply the code to perform initial processing of all interrupts. These routines also provide transfer of control to routines performing any additional interrupt processing that might be required;

2) A save mechanism is required to save and restore machine conditions, and to return control properly to the interrupted programs. Fixed areas for storage are required;

3) Reentrance control permits a serially reusable code accessed by interrupt routines to be operated with minimal disabling of interrupts. This ensures that the system response requirements can be met if at all possible.

I/O supervision.- The function of I/O supervision is to provide all services associated with the use of I/O devices. The purpose of centralizing services is not merely to avoid code duplication; it is necessary to achieve correct usage of I/O devices in the presence of concurrent independent requests. The I/O request processor provides device-independent services -- basically queueing requests, initiating I/O transmission, and monitoring the progress of operations by analyzing completion conditions. Program execution is thus coordinated with I/O execution and optimal use of CPU time is achieved while I/O requests are being serviced;

System services.- System services provide a number of functions used in common by application programs and executive routines. The following are two major functions:

1) Timing services are required to synchronize the operation of programs with real time,

   a) The basic timing service provides a programmed real-time clock for use by any programs and, if cyclic control is implemented, a routine to control action when the time interval expires,

   b) A timing queue provides a means for using the single hardware interval timer for multiple-purpose event initiation based on time of day;

2) Message handler services provide for communication between the computer and human sources of control. A basic message handler is required so programs and executive routines may initiate I/O operations to transmit and receive messages.

Environmental interface.- The function of the environmental interface is to provide for orderly initiation and termination of the system, for monitoring its operations, and for recovering from contingencies insofar as is possible. Tables provide residence for system parameters and status information, both as a means of avoiding redundant incorporation of these data in individual routines and as a means of providing centralized access to key information. Centralization of error detection/recovery permits a prescribed response to system and hardware error conditions commonly encountered by executive routines and application programs. Status monitoring is achieved by the collection, and output on demand, of statistics concerning the execution of individual programs and general aspects of system operation. Its purpose is to provide the dual capability of detecting undesirable aspects of system operation during simulation, and of monitoring actual performance.

Use of executives.- To assure efficient use of system resources, an executive system should be tailored to the mission. The tailoring of executives for each mission is simplified if a modular design approach is adopted. Specific requirements can be met by selecting functional subsets from a general executive design.

Scout executive functions.- To determine the applicability of an executive system on a Scout mission, an analysis was made of the typical computer programs required, with emphasis on program control functions. This analysis included an evaluation of functional requirements and identification of performance and design requirements. A typical design for a Scout executive system was established by selecting specific functions from the general functional design just outlined and is listed:

1) Program control,

    a) Master cycle - basic and cyclic control,

    b) Basic initiate/terminate,

    c) Basic scheduler;

2) Interrupt supervision,

    a) Primary routines,

    b) Save mechanism, fixed areas;

3) I/O supervision, including I/O request processor and onboard device support;

4) System services, including timing services;

5) Environmental interface,

    a) Tables,

    b) Error detection recovery,

    c) Status monitoring.

The normal program sequence will be interrupted provided the interrupt function is not being locked out. The real-time interrupt and the external interrupt need to be provided for in the executive system design.

The input/output section of the guidance computer would be basically a general-purpose interface providing the communication paths between the computer and the control system. Although the I/O system will input and output a variety of data types, the majority of data is one word (24 bits) or less in length. This characteristic and the related addressing characteristics dictate a low level of capability in the executive for I/O control.

In a complex computer program with distributed control, a simple change to one segment of the program may involve a major recoding effort. The centralized executive provides a means for minimizing the cost of changes by localizing changes to interactions with the executive. The initial coding effort may also be reduced with a centralized executive by allowing the application programs to be prepared in modular form with a standard interface with executive. Scheduling and timing requirements for all modules would be satisfied in conjunction with the final design of the executive programs.

The primary objection raised in the use of centralized executives in space applications generally concerns the amount of memory and execution time required to support the executive functions. Memory is required to contain the executive functions. However, the overall system size may be reduced by eliminating redundant code for executive functions and common subroutines distributed throughout the application programs.

A centralized executive system also lends itself to optimization of data processing functions so the computer duty cycle can be minimized.

The design effort concentrated on program control and interrupt supervision for an executive system. Program control is described in the following subsection and interrupt handling in the next subsection.

Program Control.- All programs in the system, whether part of the executive or written for an application, obtain central processing unit (CPU) time in one of two ways:

1) An unscheduled program is initiated by the occurrence of an event and receives control directly from an interrupt or during the course of interrupt processing. Its function is to define the system's response to the event;

2) A scheduled program receives control under specified conditions as a result of selection by the program control routines of the executive system.

When an interrupt occurs it is fielded, identified, queued, and a return made to the program currently being executed. Control is passed to the proper program unit to process the interrupt on a time-available basis. These program units are called unscheduled units. Unscheduled programs define system response to asynchronous events, while scheduled programs implement processes that are synchronous within the application requirements.

Interrupts are usually enabled during execution of any program to allow optimal system response to real-time requirements. This may lead to an interrupt stack of predetermined depth. The stack is processed in last in-first out (LIFO) order until the original interrupt processing is complete.

Each program routine is structured so its execution time does not exceed a specified time interval. CPU requirements are expressed in terms of a repetition rate that describes the number of program units per second required for processing.

The algorithm analyzed for Scout missions is of the "preassigned iterative cycle" system-type in which requirements are determined in advance of the mission and the system structure is tailored to the specific mission. It is therefore necessary that the executive allocate CPU time to operating application programs based on cycle requirements of the missile system. The scheduler portion of the executive will guarantee that each program unit will be executed within the time requirements specified by the system designer.

A typical structure for spaceborne flight programs control consists of a major cycle designed to handle the guidance and navigation functions and a minor cycle concerned with vehicle control and stability. Other computational cycles of interest are those concerned with telemetry processing, which usually occurs at a frequency similar to that of the minor cycle. Also typically, the spaceborne computers input and output processing programs operate at the same frequency as the minor cycle.

The minor cycle processing is accomplished at a high frequency consistent with the frequency of the real-time interrupts and vehicle stability. The major cycle is performed on a low-frequency basis, usually being executed once for every 10 to 50 minor cycles. The major cycle calculations are generally computed on a time-available basis. That is, the minor cycle computational requirements are satisfied first, with any time remaining until the next execution of the minor cycle being used for computation of major cycle program elements. In the general case, computation will be completed before the time allocated for one complete cycle. Therefore, the next level of computations will be executed. These may be either self-test programs or a dummy program to cause the CPU to idle.

To illustrate, assume that there are five minor cycles for each major cycle. The number of real-time interrupts that occur at fixed intervals are not shown but are assumed. For example, five real-time interrupt cycles may occur during each minor cycle. It has also been assumed that both the major and minor cycle computations will be completed prior to the end of the respective cycle.

The program control functions govern the scheduling and operation of program units within the spaceborne computer. Program control will comprise the following operations:

1) Initiation of program units;

2) Scheduling of program units leading to the actual transfer of control to the program unit selected to receive CPU time;

3) Termination of program units.

Scheduled programs are organized into a set of interrelated computational cycle loops that reflect the processing time requirements and sequencing relationships of the programs. The computation time allocated to each loop is termed the basic cycle time. Each program has an associated integer, n, that indicates the frequency of loop execution and can also be thought of as representing the relative priority of programs in that loop with respect to programs in other loops.

The introduction of frequency and priority occurs as a natural consequence of the program selection algorithm. At the start of a basic cycle, the first program in the highest frequency loop is given CPU time. When that program completes execution, the next program in the loop is selected. This process continues until the loop program list is exhausted. When that occurs, and when the basic cycle time has not expired, the next highest frequency loop is entered. The program selected is either the first one that has not yet received CPU time for this computation cycle of the loop, or the one whose execution was suspended because of expiration of a basic cycle time. Entry to a loop of given frequency is not made until the CPU requirements for all higher frequency loops are satisfied.

The effect of this algorithm is to distribute CPU time to programs in proportion to their computational requirements, without requiring individual programs to be cognizant of the requirements of other programs, scheduled or unscheduled.

At completion of the major cycle computation during a computational cycle It maybe desirable to start the major cycle over or start another program, such as a diagnostic or system-idle program. At the end of the computation cycle, the system may either ignore programs with suspended execution or complete them in the next available slack period.

The overall functions of the master cycle supervisor can be summarized as:

1) Return sequences are responsible for updating the status of the program previously in execution;

2) The continue subroutine is always executed on reentry to the master cycle. Its function is to alert the system to computation cycle overloads (if they occur) and to initiate the selection of the next program. It also serves as a control point to idle if there is no program to execute;

3) The select level subroutine is responsible for the processes necessary to initiate and to complete a computation cycle loop, and for the selection of the loop from which the current program should be chosen;

4) The select program subroutine selects a program and examines its status flags to determine whether it should be executed. Selection and examination continues until either a program is chosen or it is determined that a new computation cycle loop should be entered;

5) The dispatcher sets up entry conditions for the selected program and turns CPU control over to it.

Program schedule.- Program scheduling is the set of functions employed in selecting a program to receive CPU time. There are two distinct activities:

1) Activation of programs ready for execution;

2) Selection of a particular program to receive CPU time.

The normal action engendered by this scheduling algorithm is to execute all programs in the highest priority computation cycle first. If time remains before the next cycle is to start, the next lower level is begun. This process continues until all levels are exhausted and the scheduled program loop idles, or until the expiration of a basic time cycle, which forces restart again at the highest level. In passing from one level to the next, if the new level has been previously completed, it will not be restarted until the basic cycle count reaches the restart value. Furthermore, a given level will not be reached until all higher levels have completed their current computation cycle.

Interrupt supervision.- The interrupt supervisor is designed to provide a coherent system response to asynchronous interrupts by isolating the operations of programs responding to the interrupt from the operation of scheduled programs.

The primary interrupt routine is entered under unpredictable conditions. To allow this routine to execute freely without sacrificing minimal delay in response under normal circumstances, the interrupt control mechanism should:

1) Minimize the time required to save and restore machine conditions;

2) Run disabled as little as possible;

3) Permit multiple levels of stacked interrupts;

4) Provide routines with a way of restoring any interrupt conditions they may modify.

The following functions are required to meet these requirements:

1) A method of saving and restoring machine conditions;

2) A method of processing interrupt code appropriate to the interrupt type in both primary- and secondary-level routines;

3) A method of controlling multiple access to interrupt routines.

The primary interrupts of interest to the executive system are the real-time interrupt and the external interrupt. Other interrupts available only require a minimum amount of servicing, primarily to enable and disable the interrupts. Program status will be stored in a save area on interruption. Save areas will be chained to form a last in-first out queue.

During an interrupt, machine conditions are saved in, and restored from, an area called an interrupt save area. The interrupt save area contains the contents of any registers or scratchpad memory addresses that will be used in the interrupt routine and whose contents must be saved. In addition, linkages to both the next higher and lower interrupt levels are supplied.